Studies in Systems, Decision and Control 97

Dan Zhang
Qing-Guo Wang
Li Yu

Filtering and Control of Wireless Networked Systems

Springer

Studies in Systems, Decision and Control

Volume 97

Series editor

Janusz Kacprzyk, Polish Academy of Sciences, Warsaw, Poland
e-mail: kacprzyk@ibspan.waw.pl

About this Series

The series "Studies in Systems, Decision and Control" (SSDC) covers both new developments and advances, as well as the state of the art, in the various areas of broadly perceived systems, decision making and control- quickly, up to date and with a high quality. The intent is to cover the theory, applications, and perspectives on the state of the art and future developments relevant to systems, decision making, control, complex processes and related areas, as embedded in the fields of engineering, computer science, physics, economics, social and life sciences, as well as the paradigms and methodologies behind them. The series contains monographs, textbooks, lecture notes and edited volumes in systems, decision making and control spanning the areas of Cyber-Physical Systems, Autonomous Systems, Sensor Networks, Control Systems, Energy Systems, Automotive Systems, Biological Systems, Vehicular Networking and Connected Vehicles, Aerospace Systems, Automation, Manufacturing, Smart Grids, Nonlinear Systems, Power Systems, Robotics, Social Systems, Economic Systems and other. Of particular value to both the contributors and the readership are the short publication timeframe and the world-wide distribution and exposure which enable both a wide and rapid dissemination of research output.

More information about this series at http://www.springer.com/series/13304

Dan Zhang · Qing-Guo Wang
Li Yu

Filtering and Control of Wireless Networked Systems

Springer

Dan Zhang
Department of Automation
Zhejiang University of Technology
Hangzhou
China

Li Yu
Department of Automation
Zhejiang University of Technology
Hangzhou
China

Qing-Guo Wang
Institute for Intelligent Systems
University of Johannesburg
Johannesburg
South Africa

ISSN 2198-4182 ISSN 2198-4190 (electronic)
Studies in Systems, Decision and Control
ISBN 978-3-319-53122-9 ISBN 978-3-319-53123-6 (eBook)
DOI 10.1007/978-3-319-53123-6

Library of Congress Control Number: 2017930955

Printed on acid-free paper

This Springer imprint is published by Springer Nature
The registered company is Springer International Publishing AG
The registered company address is: Gewerbestrasse 11, 6330 Cham, Switzerland

Preface

In the last decades, the rapid developments in the communication, control and computer technologies have had a vital impact on the control system structure. In the traditional control systems, the connections between the sensors, controllers and actuators are usually realized by the port to port wiring. Such a structure has certain drawbacks such as difficult wiring and maintenance, and the low flexibility. The drawbacks have become more severe due to the increasing size and complexity of modern plants. A networked control system (NCS) is a control system in which the control loops are closed through a communication network. It is gaining popularity recently because the utilization of a multipurpose shared network to connect spatially distributed elements results in flexible architectures and it generally reduces installation and maintenance costs. The NCSs have been successfully applied in many practical systems such as the car automation, intelligent building, transportation networks, haptics collaboration over the Internet and unmanned aerial vehicles.

Note that an NCS works over a network through "non-ideal channels". This is the main difference between the traditional control systems and NCSs. In NCSs, phenomena such as communication delays, data dropouts, packet disorder, quantization errors and congestions may occur due to the usage of communication channels. These imperfections would significantly degrade the system performance and may even destabilize the control systems.

The wireless communication becomes more popular recently for its better mobility in locations, more flexibility in system design, lower cost in implementation and greater ease in installation, compared with the wired one. While sharing many common features and issues with the wired one as described above, the wireless one has special issues worth mentioning. In wireless networked control systems (WNCSs), a sensor usually has a limited power from its battery, and replacing the battery during the operation of WSNs is very difficult. In addition, sensor nodes are usually deployed in a wild region and they are easily affected by the disturbances from the environment, which may cause malfunction of the sensor nodes, e.g., the gain variations of the computational unit. However, the networked systems should be robust or non-fragile to these disturbances.

Due to the great challenges for the analysis and design of NCSs, especially for wireless one, the filtering and control of such systems is an emerging research domain of significant importance in both theory and applications. This book addresses these challenging issues. It presents new formulations, methods and solutions for filtering and control of wireless networked networks. It gives a timely, comprehensive and self-contained coverage of the recent advances in a single volume for easy access by the researchers in this domain. Special attention is paid to the wireless one with the energy constraint and filter/controller gain variation problems, and both centralized and distributed solutions are presented.

The book is organized as follows: Chap. 1 presents a comprehensive survey of NCSs, which shows major research approaches to the critical issues and insights of these problems. Chapter 2 gives the fundamentals of the system analysis, which are often used in subsequent chapters. The first part with Chaps. 3–6 deals with the centralized filtering of wireless networked systems, in which different approaches are presented to achieve the energy-efficient goal. The second part with Chaps. 7–10 discusses the distributed filtering of wireless networked systems, where the energy constraint and filter gain variation problems are addressed. The last part with Chaps. 11–14 presents the distributed control of wireless networked systems, where the energy constraint and controller gain variations are the main concerns.

This book would not have been possible without supports from our colleagues. In particular, we are indebted to Prof. Peng Shi at University of Adelaide, Australia, and Dr. Rongyao Ling, Zhejiang University of Technology, China, for their fruitful collaboration with us. The supports from the National Natural Science Foundation of China under Grant 61403341, Zhejiang Provincial Natural Science Foundation under Grant LQ14F030002, LZ15F030003 and Zhejiang Qianjiang Talent Project under Grant Grant QJD1402018 are gratefully acknowledged.

Hangzhou, China — Dan Zhang
Johannesburg, South Africa — Qing-Guo Wang
Hangzhou, China — Li Yu
August 2016

Contents

Symbols and Notations

$\mathbb{R}$	Field of real numbers
$\mathbb{R}^n$	n-dimensional real Euclidean space
$\mathbb{R}^{m\times n}$	Space of all $m \times n$ real matrices
I	Identity matrix
0	Zero matrix
$W > 0$	Positive definite matrix W
$W \geqslant 0$	Positive semi-definite matrix W
$W < 0$	Negative definite matrix W
$W \leqslant 0$	Negative semi-definite matrix W
W^T	Transpose of matrix W
W^{-1}	Inverse of matrix W
$[a_{ij}]$	A matrix composed of elements a_{ij}, $i,j \in N$
$\lambda_{\max}(W)$	Maximum eigenvalue of matrix W
$\lambda_{\min}(W)$	Minimum eigenvalue of matrix W
$\mathrm{Tr}(W)$	Trace of matrix W
$\mathrm{diag}\{\cdots\}$	block-diagonal matrix
$\|\|\cdot\|\|$	Euclidean norm of a vector and its induced norm of a matrix
sup	supremum
inf	infimum
$L_2[0,\infty)$	Space of square integrable functions on $[0,\infty)$
$l_2[0,\infty)$	Space of square summable infinite sequence on $[0,\infty)$
$\Pr ob\{x\}$	Probability of x
$\mathbb{E}\{x\}$	Expectation of x
NCS	Networked control system
WSN	Wireless sensor network
CCL	Cone complementarity linearization
LMI	Linear matrix inequality
LTI	Linear time-invariant

Chapter 1
Introduction

1.1 Networked Control Systems

In the last decades, with the rapid development on the communication, control and computer technologies, the conventional control systems have been evolving to modern networked control systems (NCSs), wherein the control loops are closed through a communication network. The utilization of a multi-purpose shared network to connect spatially distributed elements results in flexible architectures and generally reduces installation and maintenance costs. Nowadays, NCSs have been extensively applied in many practical systems such as the car automation [1], intelligent building [2], transportation networks, haptics collaboration over the Internet [3] and unmanned aerial vehicles [4]. A typical architecture of NCSs is shown in Fig. 1.1, and its estimation/filtering system is depicted in Fig. 1.2. In traditional control systems, each component is connected through "ideal channels", while, in NCSs, the connection of each component is realized via "non-ideal channels". This is the main difference between the traditional control systems and NCSs.

In NCSs, the continuous-time measurement is first sampled and quantized. Then, the measurement is transmitted to remote controller via the communication channel, in which the signal may be delayed, lost or even sometimes not be allowed for transmission due to the communication constraints. In recent years, the modeling, analysis and synthesis of NCSs have received more and more attention, giving a great number of publications in literature. Compared with the conventional point-to-point control systems, the following new problems arise in NCSs:

- Signal sampling: an NCS is a digital control system and a continuous signal is usually sampled at a certain time instant, and then the sampled measurement is utilized for controller design. In the traditional digital control system, the sampling period is usually fixed. However, in NCSs, the measurement packet may not be transmitted when it is sampled since all the packets have to wait in a queue, and then it is not desirable to sample the system with a fixed period.
- Signal quantization: Due to the limited communication bandwidth, the sampled signal has to be quantized and it is a common phenomenon in any digital

D. Zhang et al., *Filtering and Control of Wireless Networked Systems*,
Studies in Systems, Decision and Control 97, DOI 10.1007/978-3-319-53123-6_1

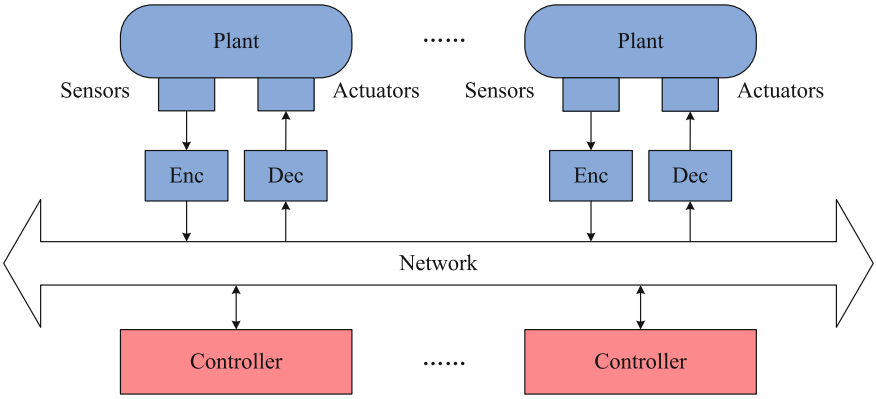

Fig. 1.1 A typical structure of NCS

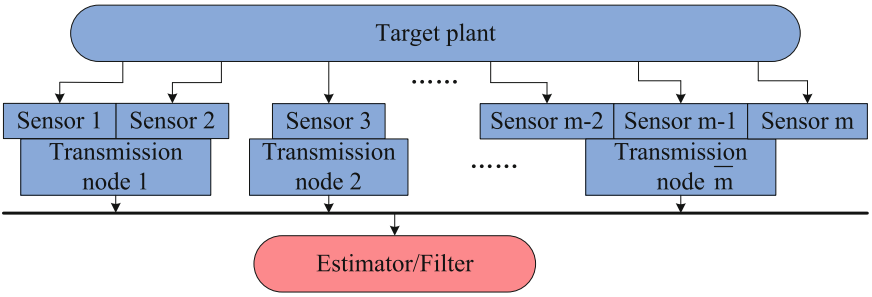

Fig. 1.2 A networked estimation system

control systems. In this scenario, only a finite bit of information is available for the controller design.

- Communication delay: The delay in NCSs includes computation delay in each component due to the finite processing speed of devices, the waiting delay, i.e., the time for a packet waiting before being sent out, and the transmission delay with which the packet goes through the communication channel. Compared with the other two types of delays, the computational delay is usually negligible due to the rapid development on the hardware instrument, while, the waiting delay is determined by the transmission protocol and the impact of this delay can be alleviated by some appropriate protocols. Hence, the transmission delay becomes the main concern in the system analysis and design.
- Packet dropout: Due to network traffic congestions and packet transmission failures, packet dropouts are inevitable in networks, especially in a wireless network. Actually, the propagation of long transmission delay can also be viewed as the packet dropout phenomenon if one ignores the outdated data. In this case, the controller or actuator has to decide what information should be used, the newest data in the buffer or a simple zero signal.

- Medium access constraint: The progress in digital computation and communication has enabled the development of distributed control systems in which multiple sensors and actuators are connected to a centralized controller via a shared communication medium. Due to the limitations on data transmission, it is impossible for all sensors and actuators to access to the communication channel for all the time, leading to a new problem, the medium access constraint problem.

The network-induced problems mentioned above would certainly degrade the control performance and may even destabilize the system [5]. In recent years, much research effort has been devoted onto this area, and issues such as the stability analysis, state estimation, controller design and fault detection for NCSs have been widely investigated. According to the connection nature, we can classify the NCSs into wired and wireless communication ones. To help readers understand some basic modeling and analysis methods for NCSs, we first discuss the NCSs with wired communication in the subsequent sections, and each for one particular network-induced issue. Within each section, we present different approaches to the same issue. After them, we briefly address special issues on the wireless case. This chapter will be concluded with a short overview of the book.

1.2 Signal Sampling

An NCS is a digital control system and a continuous-time signal is usually sampled at a certain time instant, and then the sampled measurement is utilized for controller design. In the traditional digital control system, the sampling period is time-invariant. However, in NCSs, the sampled measurement may not be transmitted immediately since the sampled data has to wait in a queue, and it has been shown that the time-varying sampling period can achieve a better performance than the time-invariant one. Some representative modeling and analysis methods for NCSs with sampled-data are discussed as follows.

Hybrid discrete/continuous approach: This approach is based on the representation of system in the form of a hybrid discrete/continuous model or more precisely, the impulsive system, and the solution was first obtained in terms of differential Riccati equations with jumps [6] and [7]. The hybrid system approach has been recently applied to robust H_∞ filtering with sampled-data [8]. Sampling interval-independent LMI conditions have been derived, which were quite restrictive since the information of sampling period was not utilized in filter design. Recently, the impulsive system modeling of sampled-data system was also used in [9], which introduced a new Lyapunov function with discontinuities at the impulse time. To illustrate the main results in [9], we consider the following LTI system:

$$\dot{x}(t) = Ax(t) + Bu(t), \tag{1.1}$$

where x and u are the state and the input of plant, respectively. Denote the sampling time instant by t_k, and let $\varepsilon \leq t_k - t_{k-1} \leq \tau_{\text{MATI}}$, where ε and τ_{MATI} are some positive scalars. Then, using a linear state feedback controller $u(t) = Kx(t_k)$ and defining a new state $\xi(t) = \left[x^T(t)\ z^T(t)\right]^T$, where $z(t) = x(t_k)$. The dynamics of system (1.1) can be written as

$$\begin{aligned} \dot{\xi}(t) &= F\xi(t), \quad t \neq t_k, \\ \xi(t_k) &= \begin{bmatrix} x(t_k^-) \\ x(t_k^-) \end{bmatrix}, \quad t = t_k, \end{aligned} \tag{1.2}$$

where $F = \begin{bmatrix} A & B_u \\ 0 & 0 \end{bmatrix}$ and $B_u = BK$. Equation (1.2) means that x and z evolve according to the first equation of (1.2) between t_k and t_{k+1}, while, at t_k, the value of x before and after t_k remains unchanged but the value of z is updated by $x(t_k^-)$. The stability condition of system (1.2) was guaranteed if there exist symmetric positive definite matrices P, R, X_1 and a slack matrix N such that the following inequalities

$$M_1 + \tau_{\text{MATI}} M_2 < 0, \tag{1.3}$$

$$\begin{bmatrix} M_1 & \tau_{\text{MATI}} N \\ * & -\tau_{\text{MATI}} R \end{bmatrix} < 0, \tag{1.4}$$

hold, where

$$\begin{aligned} M_1 = &\begin{bmatrix} P \\ 0 \end{bmatrix} \begin{bmatrix} A\ B_u \end{bmatrix} + \begin{bmatrix} A^T \\ B_u^T \end{bmatrix} \begin{bmatrix} P\ 0 \end{bmatrix} - \begin{bmatrix} I \\ -I \end{bmatrix} X_1 \begin{bmatrix} I\ -I \end{bmatrix} \\ &-N \begin{bmatrix} I\ -I \end{bmatrix} - \begin{bmatrix} I \\ -I \end{bmatrix} N^T + \tau_{\text{MATI}} \bar{F}^T R \bar{F}, \\ M_2 = &\begin{bmatrix} I \\ -I \end{bmatrix} X_1 \bar{F} + \bar{F} X_1^T \begin{bmatrix} I\ -I \end{bmatrix}, \bar{F} = \begin{bmatrix} A\ B_u \end{bmatrix}. \end{aligned}$$

The above stability statement can be proved by using the Lyapunov functional approach, and the following candidate Lyapunov function was constructed:

$$\begin{aligned} V = &x^T P x + \xi^T \left(\int_{-\rho}^{0} (s + \tau_{\text{MATI}}) \left(F \exp(Fs)\right)^T \tilde{R} F \exp(Fs) ds \right) \xi \\ &+ (\tau_{\text{MATI}} - \rho)(x - z)^T X_1 (x - z) \end{aligned} \tag{1.5}$$

where $\tilde{R} = \begin{bmatrix} R & 0 \\ 0 & 0 \end{bmatrix}$ and $\rho = t - t_k$.

The improved impulsive system approach for NCSs with time-varying sampling period has recently been proposed in [10], where an NCS was viewed as a interconnected hybrid system composed of an impulsive subsystem and an input delay subsystem. A new type of time-varying discontinuous Lyapunov-Krasovskii functional was introduced to analyze the input-to-state stability (ISS) property of NCSs. More recently, the stability of impulsive systems was studied from the hybrid system

point of view in [11] and [12], and the convex conditions for robust stability analysis and stabilization of linear aperiodic impulsive and sampled-data systems under dwell-time constraints have been presented.

Input delay system approach: Modeling of continuous-time systems with digital control in the form of continuous-time systems with delayed control input was introduced by Mikheev et al. [13] and Astrom et al. [14], and further developed by Fridman et al. [15]. In this approach, the closed-loop system became an infinite-dimensional Delay Differential Equation (DDE) and the stability condition was obtained by using Razumikin or Lyapunov-Krasovskii approach. The control law was represented as the delayed control:

$$u(t) = u_d(t) = u_d(t - (t - t_k)) = u_d(t - \tau(t)), t_k \leq t < t_k + 1, \tag{1.6}$$

where $\tau(t) = t - t_k$. Then, the sampled data control system was transformed to a time-delay system, where the time-varying delay $\tau(t) = t - t_k$ is piecewise linear with derivative 1 for $t = t_k$. For the LTI system (1.1), the closed-loop system can be written as

$$\dot{x}(t) = Ax(t) + Bu_d(t - \tau(t)). \tag{1.7}$$

The recent advances on the time-delay system can be applied for the sampled data system, e.g., the free weighting matrix approach [16] and [17], Jensen's Inequality approach [18] and [19], Wringter Inequality approach [20] and [21] and time-varying Lyapunov functional approach [22]. The input delay system approach has also be applied to the synchronization of complex networks, see [23, 24].

Robust control approach: When a time-varying sampling period is applied in control systems, the discrete-time counterpart would become a time-varying system. For a given continuous time system:

$$\dot{x}(t) = Ax(t) + Bu(t), \tag{1.8}$$

and the control input is

$$u(t) = Kx(t_k), \forall t \in [t_k, t_k + 1). \tag{1.9}$$

The discrete-time system under sampling period $T_k = t_{k+1} - t_k$ becomes

$$x(t_{k+1}) = G(T_k)x(t_k), \tag{1.10}$$

where $G(T_k) = \exp(AT_k) + \int_0^{T_k} \exp(Ar)B\mathrm{d}rK$. It is well known that the sufficient condition for the asymptotic stability of system (1.10) is to find a matrix $P = P^T > 0$ such that $G^T(T)PG(T) < 0$ for all T_k. For a fixed sampling period T, it is easy to find a solution of this inequality, but for any time-varying T_k with $T_{\min} \leq T \leq T_{\max}$, it is however not easy to find the solution since infinity number of LMIs are involved. To

conquer this problem, Suh [25] partitioned the $G(k)$ into $G(T\_\text{nom})+\Delta Q(T\_\text{nom})$, and T_nom is a constant to be chosen. By doing so, $G(T\_\text{nom})$ becomes a constant matrix and the term $\Delta Q(T\_\text{nom})$ caused by the sampling interval variation was treated as an norm bounded uncertainty, which was handled by using the robust control technique. More specifically, they partitioned $G(T)$ as $G(T_{\text{nom}}) + \Delta(\tau)Q(T_{\text{nom}})$, where $\Delta(\tau) = \int_0^\tau \exp(Ar)\mathrm{d}r$. They first show that there exists an upper bound for $\Delta(\tau)$ such that $\|\Delta(\tau)\|_2 \leq \beta$. This bound can be obtained by solving the minimization problem:

$$\bar{\beta} = \min_{T_{\min} \leq T \leq T_{\max}} \max\left\{\beta(T_{\min} - T), \beta(T_{\max} - T)\right\}. \tag{1.11}$$

Moreover, let T_{nom} be the sampling period corresponding to which β reaches its minimum, then $\bar{\beta} = \beta(T_{\text{nom}})$. Based on this treatment, the closed-loop system is stable provided that there exist a symmetric positive definite matrix P and a scalar $\varepsilon > 0$ such that the following inequality holds:

$$\begin{bmatrix} -P & * & * \\ G(T_{\text{nom}})P & -P + \varepsilon I & * \\ \begin{bmatrix} A & B \end{bmatrix} F(T_{\text{nom}}) \begin{bmatrix} I \\ K \end{bmatrix} P & 0 & -\frac{\varepsilon}{\bar{\beta}^2} I \end{bmatrix} < 0 \tag{1.12}$$

where $F(T_{\text{nom}}) = \exp\left(\begin{bmatrix} A & B \\ 0 & 0 \end{bmatrix} T_{\text{nom}}\right)$.

To reduce the conservatism in the above condition, Suh [25] partitioned the uncertainty into N parts. But the main limitation is that the computation is high especially when N is very large. Similar approaches have also been discussed in [26] and [27]. The research in this direction mainly focuses on how to estimate the uncertain term to give a less conservative bound. To overcome the limitation in [25], Oishi et al. [28] proposed three techniques, the delta-operator representation for stability analysis, the parametric uncertainty rather than the matrix uncertainty for the effect of aperiodic sampling, and an adaptive division introduced to reduce the computation. Specifically, they have presented an LMI based sufficient condition for all possible parameter values and they called it as a robust LMI. In Kao et al. [29], the stability of LTI systems with aperiodic sampling devices was tackled from a pure discrete-time point of view, and the system was modeled as the response of a nominal discrete-time LTI system in feedback interconnection with a structured uncertainty. Stability conditions were also derived. Further improvement can also be found in [30] and [31].

Switched system approach: The switched linear system approach was also proposed in [32] to study the sampled data control systems. To show how it works, we consider a simple LTI system:

$$\dot{x}(t) = A_c x(t) + B_c u(t). \tag{1.13}$$

It is assumed that the sampling period $h_k = t_{k+1} - t_k$ only takes a finite number of values. More specifically, let $h_k = n_k T_0$, where $n_k \in \{i_1, \cdots, i_N\}$, i.e., $1 \leq i_1 < i_2 < \cdots < i_N$, and T_0 is termed as the basic sampling period. Then, h_k takes N possible values and $h_k \in \{i_1 T_0, i_2 T_0, \cdots, i_N T_0\}$. The discrete-time counterpart can now be given by

$$x(t_k + 1) = A(h_k)x(t_k) + B(h_k)u(t_k), \tag{1.14}$$

where

$$A(h_k) = e^{A_c h_k} = e^{A_c n_k T_0} = \left(e^{A_c T_0}\right)^{n_k} = A_0^{n_k},$$
$$B(h_k) = \int_0^{n_k T_0} e^{A_c r} \mathrm{d}r B_c = \left(\sum_{i=0}^{n_k - 1} \int_{iT_0}^{(i+1)T_0} e^{A_c r} \mathrm{d}r\right) B_c = \sum_{i=0}^{n_k - 1} A_0^i B_0,$$

with

$$A_0 = e^{A_c T_0}, \ B_0 = \int_0^{T_0} e^{A_c r} \mathrm{d}r B_c.$$

One can see that $A(h_k)$ and $B(h_k)$ are explicitly dependent on n_k, which is varying over different sampling intervals. Thus, the above discrete-time system (1.14) is essentially a switched linear system with finite subsystems. Based on this switched system model, the average dwell time approach from the switched system theory was applied for the stability analysis and controller design, see [32].

In the view of the stochastic evolution of different sampling periods, the Markovian system theory can also be applied to study the stochastic sampling problem. The modeling method is similar to the above switched system approach, but the only difference is that the transition of different subsystems follows the Markovian process. More specifically, Ling et al. [33] considered the distributed H_∞ filtering for NCSs with stochastic sampling, and the sampling period jumps was assumed to be a Markovian process. Then, the well-known Markovian system theory was applied for the stability analysis of the filtering error system. Further developments can be found in [34]. In these results, they are assumed that the transition probabilities are exactly known. However in some scenarios this information may not be available [35]. Therefore, the uncertain sampling problem deserves further investigation.

1.3 Signal Quantization

Signal quantization is a common phenomenon in NCSs. The research on control with quantized feedback is not a new topic and can be traced back to 1956 [36], in which the effect of quantization in a sampled data system was studied. In [37], Delchamps showed that if a linear system is open-loop unstable, there exists a minimum rate for

the coding of the feedback information to achieve stabilization. Since then, various methods have been proposed to study the quantized feedback control problem. The utilization of quantizer will result in two phenomena, i.e., saturation and performance deterioration around the original point, which may destabilize the system. Research on quantized feedback can be categorized, depending on whether the quantizer is static or dynamic. The logarithmic quantizer is a kind of static quantizer and the uniform quantizer is basically a dynamical one.

Logarithmic quantization: This quantizer $Q(\bullet)$ is usually symmetric and time-invariant, i.e., $Q(v) = -Q(-v)$. The set of quantization levels is described as

$$\begin{aligned} U = &\left\{\pm\kappa_i, \kappa_i = \rho^i \kappa_0, i = 0, \pm 1, \pm 2, ...\right\} \\ &\cup \{\pm\kappa_0\} \cup \{0\}, 0 < \rho < 1, \kappa_0 > 0. \end{aligned} \tag{1.15}$$

The quantized output $Q(\bullet)$ is given by:

$$Q(v) = \begin{cases} \kappa_i, & \text{if } \frac{1}{1+\delta}\kappa_i < v < \frac{1}{1-\delta}\kappa_i, v > 0, \\ 0, & \text{if } v = 0, \\ -Q(-v), & \text{if } v < 0, \end{cases} \tag{1.16}$$

where $\delta = \frac{1-\rho}{1+\rho} < 1$, with the quantization density $0 < \rho < 1$. The illustration of logarithmic quantization is depicted in Fig. 1.3.

Elia et al. [38] considered quadratic stabilization problem of a discrete-time single-input single-output (SISO) linear time-invariant systems and it is shown that a logarithmic quantize can achieve the quadratic stabilization. Following this work, Fu and Xie [39] proposed a sector bound approach to quantized feedback control, and

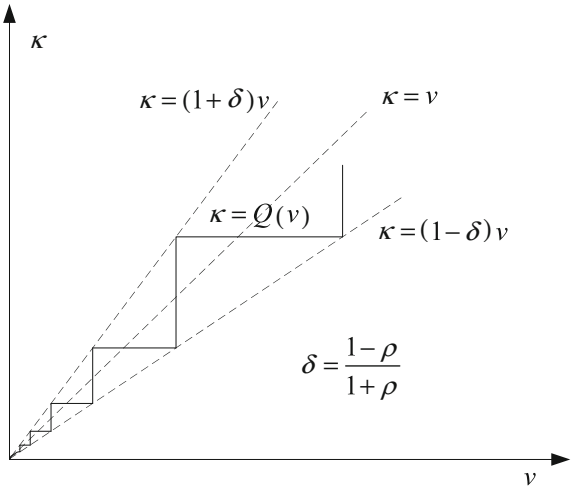

Fig. 1.3 Logarithmic quantizer

presented some interesting results for multiple-input multiple-output (MIMO) linear discrete-time systems. For a given discrete-time LTI system

$$x(k+1) = Ax(k) + Bu(k), \tag{1.17}$$

with the quantized state feedback controller $u(k) = KQ(x(k))$, we can define the quantization error

$$e(k) = x(k) - Q(x(k)) = (I + \Delta(k))x(k), \tag{1.18}$$

where $\|\Delta\| < \delta I$. The closed-loop system now becomes

$$x(k+1) = (A + BK(I + \Delta(k))x(k). \tag{1.19}$$

The robust control approach can then be applied to study the stability and stabilization of closed-loop system since it is essentially an LTI system with norm-bounded uncertainty. Recently, a suboptimal approach for the optimization of the number of quantization levels was proposed in [40] and the design of a corresponding quantized dynamic output feedback controller was also given. The sector bound approach is effective to handle the quantization problem, which enables us to incorporate other network-induced phenomena into the quantized control systems, e.g., the packet dropouts [41, 42], and the communication delay [43, 44].

Uniform quantization: Brokett et al. [45] proposed the uniform quantizers with an arbitrarily shaped quantitative area. Based on these quantizers, the "zooming" theory was used for linear and nonlinear systems, and the sufficient condition for the asymptotical stability was given. The uniform quantizers with an arbitrarily shaped quantitative area have the following properties:

$$\begin{cases} \text{if } \|x\|_2 \leq M\mu, \text{ then } \|Q(x) - x\|_2 \leq \Delta\mu, \\ \text{if } \|x\|_2 > M\mu, \text{ then } \|Q(x)\|_2 > M\mu - \Delta\mu, \end{cases} \tag{1.20}$$

where M is the saturation value and Δ is the sensitivity. The first property gives the upper bound of the quantization error when the quantized measurement is not saturated. The second one provides the approach to test whether the quantized measurement is saturated. The illustration of uniform quantization is depicted in Fig. 1.4.

The stabilization problem was discussed recently in [46] for discrete-time linear systems with multidimensional state and one-dimensional input using quantized feedbacks with a memory structure. They have shown that in order to obtain a control strategy which yields arbitrarily small values of $T/\ln C$, $LN/\ln C$ should be big enough, where C is the contraction rate, T is the time to shrink the state of the plant from a starting set to a target set, L is the number of the controller states, and N is the number of the possible values that the output map of the controller can take at each time. Recently, Liberzon et al. [47] considered the input-to-state stabilization of linear systems with quantized state measurements. They developed a control methodology that counteracts an unknown disturbance by switching between

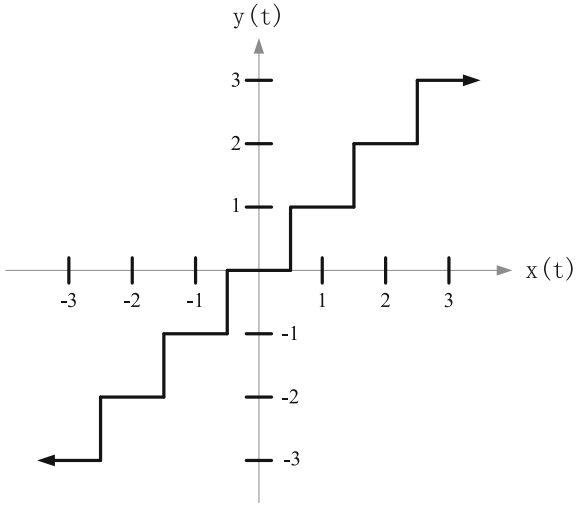

Fig. 1.4 Uniform quantizer

the so-called "zooming out" and "zooming in", that is, when the initial state to be quantized is saturated, the "zooming out" stage is adopted to increase the sensitivity Δ until the state gets unsaturated, while in the "zooming in" stage, the sensitivity Δ is reduced to push the state to zero. If the initial state to be quantized is unsaturated, the "zooming out" stage can be omitted and the "zoom-in" stage is implemented directly.

The "zooming out" and "zooming in" strategy has been widely used in the NCS with quantized measurement. For example, the H_∞ control for NCS with communication delay and state quantization has been studied in [48] and a unified modeling was proposed to capture the delay and quantization. More specifically, they transformed an NCS to a LTI system with input delay, which is the approach we have discussed before. On the other hand, the output feedback control of NCSs with communication delay and quantization has been studied in [49].

1.4 Communication Delay

In this section, we will focus on the transmission delay problem as other delays, e.g., the computation delay can be reduced by using some high performance hardware. In a traditional control system, sensor, controller and actuator usually work based on a fixed sampling period. But in NCSs, the above nodes can work in an event-based mode, i.e., they can work once they have received data. It should be noted that different work modes may lead to different models, and thus different analysis and synthesis results would be obtained.

The communication delay can be constant or time-varying. The constant delay occurs in NCSs when we use a buffer in the controller side and the controller reads

the data periodically. The main limitation of such a treatment leads to much design conservatism as we have introduced man-made delay though the packet has already arrived but it can also be used at some fixed time instant. In other word, the delay may have been enlarged for controller design. The analysis of NCSs with constant delay has been discussed in Zhang et al. [50], in which the stability region was obtained for a given constant delay. On the other hand, the controller and actuator are usually event-driven in the NCSs, which may lead to the time-varying delay in NCSs. Different modeling results may be obtained when different delay cases are considered, i.e., shorter or larger than one sampling period and deterministic or stochastic. Hence, analysis and synthesis of NCSs with time-varying delay becomes a very active research area, and many interesting approaches are proposed.

Input delay system approach: The main idea is to transform the communication delay into the input delay and then the recent results on the delay system approaches are applied for the stability analysis, filter and controller designs. More specifically, Yue et al. [51] considered the following system:

$$\begin{cases} \dot{x}(t) = [A + \Delta A(t)]x(t) + [B + \Delta B(t)]u(t) + B_w w(t), \\ z(t) = Cx(t) + Du(t). \end{cases} \tag{1.21}$$

When the state information is transmitted via a communication channel, which is subject to communication delay, system (1.21) becomes

$$\begin{cases} \dot{x}(t) = [A + \Delta A(t)]x(t) + [B + \Delta B(t)]u(t) + B_w w(t), \\ z(t) = Cx(t) + Du(t), \\ u(t) = Kx(i_k h), \\ t \in [i_k h + \tau_k, i_{k+1} h + \tau_{k+1}), \end{cases} \tag{1.22}$$

where τ_k is the time delay at the k-th sampling time instant, and h is the sampling period. Then let $i_k h = t - (t - i_k h)$, and define $\tau(t) = t - i_k h$, (1.22) can be re-written as

$$\begin{cases} \dot{x}(t) = [A + \Delta A(t)]x(t) + [B + \Delta B(t)]u(t) + B_w w(t), \\ z(t) = Cx(t) + Du(t), \\ u(t) = Kx(t - \tau(t)), \\ t \in [i_k h + \tau_k, i_{k+1} h + \tau_{k+1}). \end{cases} \tag{1.23}$$

Then, the H_∞ stabilization conditions have been presented by using the time-delay system approach. Recently, Lam et al. [52] proposed a new NCS model, which has two additive delays. The intention of Lam et al. was to expose a new delay model and to give a preliminary result on its stability analysis. It is worth pointing out that the above stability conditions have left much room for improvement. The same problem was then considered in [53] and some less conservative stability and H_∞ controller design conditions have been obtained. More recently, Gao et. al also proposed a modified model for the NCS with time-delay, in which the H_∞ filtering and output tracking problems were investigated, respectively, see [54] and [55].

In Xiong et al. [56], the stabilization problem of NCSs was studied by using a logical zero-order hold (ZOH), which was assumed to be both time-driven and event-driven, and has the logical capability of comparing the time stamps of the arrived control input packets and choosing the newest one to control the process. Based on the packet time sequence analysis, the overall NCS was then discretized as a linear discrete-time system with input delay. Till now, there are still growing papers on the input delay system approach, and the results are extended to other complex systems such as T-S fuzzy system [57], Markovian systems [58] and singular systems [59].

Robust control approach: The sampled system is usually modeled as a discrete-time system, and the network-induced delay is treated as a variation parameter of the system. Here, we discuss the scenario where the time-varying delay is smaller than one sampling period. Specifically, for an LTI system

$$\dot{x}(t) = Ax(t) + Bu(t), \tag{1.24}$$

assuming that $0 \leq \tau_m \leq \tau(k) \leq \tau_M \leq h$, the discrete-time system is obtained as

$$x(k+1) = (A_d + B_{d0}(\tau(k))K)x(k) + B_{d0}(\tau(k))Kx(k-1), \tag{1.25}$$

where

$$A_d = e^{Ah}, B_{d0}(\tau(k)) = \left(\int_0^{h-\tau(k)} e^{As}ds\right)B, B_{d1}(\tau(k)) = \left(\int_{h-\tau(k)}^{h} e^{As}ds\right)B.$$

This system can be transformed into

$$x(k+1) = G(\tau(k))\begin{bmatrix} x(k) \\ x(k-1) \end{bmatrix}, \tag{1.26}$$

where $G(\tau(k)) = \begin{bmatrix} A_d + B_{d0}(\tau(k))K & B_{d1}(\tau(k))K \end{bmatrix}$.

Now by partitioning $G(\tau(k))$ as a constant term and an uncertain term, the robust control approach can be applied to estimate the bound of the latter uncertain term, see [60, 61] for the different bounding techniques.

Switched system approach: Although the uncertain system approach is effective, complicated numerical algorithms or parameters tuning are usually required to guarantee that the uncertain matrix is unit norm-bounded. Unlike the above robust control approach, Zhang et al. [62] proposed a new modeling method, where the actuator is assumed to be time-driven, and it reads the buffer periodically at a higher frequency than the sampling frequency, i.e., $T_0 = T/N$, where T is the sampling period, and $N \geq 2$ is a large integer. Denote the time-varying delay τ_k, which was assumed to be $\tau_k < T$. Then, at most two control signals can be involved in the control task during one sampling period, i.e., $u(k)$ and $u(k-1)$. Let the activation time of $u(k)$ and $u(k-1)$ during one sampling period be $n_0(k)T_0$ and $n_1(k)T_0$, it is easy to see that $n_0(k) + n_1(k) = N$. Then for a simple LTI system:

$$\dot{x}(t) = A_p x(t) + B_p u(t), \tag{1.27}$$

we can define $A = e^{A_p T}$, $A_0 = e^{A_p T_0}$, and $B_0 = \int_0^{T_0} e^{A_p r} B_p \mathrm{d}r$. Then the closed-loop system is written as

$$\begin{aligned}
&x(k+1)\\
&= Ax(k) + \textstyle\int_{n_0(k)T_0}^{T} e^{A_p r} B_p \mathrm{d}r \times u(k-1)\\
&\quad + \textstyle\int_0^{n_0(k)T_0} e^{A_p r} B_p \mathrm{d}r \times u(k)\\
&= Ax(k) + \textstyle\int_{n_0(k)T_0}^{(n_0(k)+n_1(k))T_0} e^{A_p r} B_p \mathrm{d}r \times u(k-1)\\
&\quad + \textstyle\int_0^{n_0(k)T_0} e^{A_p r} B_p \mathrm{d}r \times u(k)\\
&= Ax(k) + \left(e^{A_p T_0}\right)^{n_0(k)} \textstyle\int_0^{n_1(k)T_0} e^{A_p r} B_p \mathrm{d}r \times u(k-1)\\
&\quad + \textstyle\int_0^{n_0(k)T_0} e^{A_p r} B_p \mathrm{d}r \times u(k)\\
&\vdots\\
&= Ax(k) + \sum_{i=0}^{n_1(k)-1} A_0^{i+n_0(k)} B_0 u(k-1) + \sum_{i=0}^{n_0(k)-1} A_0^i B_0 u(k).
\end{aligned} \tag{1.28}$$

The above system becomes a switched system as it depends on the values of $n_0(k)$ and $n_1(k)$. Then the average dwell time switching scheme was applied for the exponential stability of the closed-loop system. The above modeling idea can be tracked back to [63], where the same working mode was firstly introduced for the NCS with time-varying delay and packet dropout. A switched system modeling was also obtained in [64] and the NCS is presented as a discrete-time switched system with arbitrary switching. More related results on this approach are can found in [65, 66].

Stochastic system approach: When the statistical information of delay is available for system design, the stochastic system approach can be applied. To model the random delay, the independent identically distributed case (i.i.d) and Markovian system approach have been widely used. For the i.i.d case, a delay distribution based stability analysis and synthesis approach for NCSs with non-uniform distribution characteristics of network communication delays was firstly considered in [67], where the delay was partitioned into multiple different time-varying delays and each delay has a certain bound. More specifically,

$$u(t) = \alpha(t) K x(t - \tau_1(t)) + (1 - \alpha(t)) K x(t - \tau_2(t)), \tag{1.29}$$

where $\tau_1(t) = \delta(t)\tau(t)$, $\tau_2(t) = (1 - \delta(t))\tau(t)$, $0 < \tau_1(t) \leq \tau_1$, $0 < \tau_2(t) \leq \tau_2$, and $\delta(t) = 0$ or 1. They showed that a less conservative stability condition can be obtained when the distribution information of time delay is used. The same delay distribution based analysis method has been extended to fuzzy systems [68] and [69]. To reduce the conservative of the results in [67], an improved Lyapunov-Krasovskii method was proposed in [70] and a new bounding technique is introduced to estimate the cross-product integral terms of the Lyapunov functional.

Recently, the Markovian system approach was proposed under the assumption that the delay is correlated and the transition of different delays obey the Markovian process. In [71] and [72], the network-induced random delays were modeled as Markov chains such that the closed-loop system is a jump linear system with one

mode. More specifically, let the delay $r_s(k)$ satisfy $0 \leq r_s(k) \leq d_s < \infty$. Then, the controller becomes

$$u(k) = K_{r_s}(k)x(k - r_s(k)). \tag{1.30}$$

By the lifting technique, we obtain the closed-loop system:

$$\bar{x}(k+1) = (\bar{A} + \bar{B}K_{r_s}(k)\bar{C}_{r_s}(k))\bar{x}(k), \tag{1.31}$$

where

$$\bar{A} = \begin{bmatrix} A & 0 & \cdots & 0 & 0 \\ I & 0 & \cdots & 0 & 0 \\ 0 & I & \cdots & 0 & 0 \\ \vdots & \vdots & \ddots & \vdots & \vdots \\ 0 & 0 & \cdots & I & 0 \end{bmatrix}, \ \bar{B} = \begin{bmatrix} B \\ 0 \\ 0 \\ \vdots \\ 0 \end{bmatrix},$$

$$C_{r_s}(k) = \begin{bmatrix} 0 & \cdots & 0 & I & 0 & \cdots & 0 \end{bmatrix}.$$

The above augmented system is a Markovian jump system and $r_s(k)$ is a Markovian chain. It should be noted that the state-feedback gain was mode-independent in [71] and [72], the state-feedback gain only depends on the delay from sensor to controller. Later in [73], the two random delays (sensor-to-controller and controller-to-sensor) were modeled as two different Markov chains, and the closed-loop system was described as a Markovian jump linear system with two modes characterized by two Markov chains. There are also some newly reported results on the NCSs with two random delays based on the Markovian system approach and the main concerns are the design of a new mode-dependent controller with more information, see [74, 75].

1.5 Packet Dropouts

In NCSs, the packet dropout is also inevitable, especially in a wireless networked system. In NCSs, different transmission protocols are used, i.e., user datagram protocol (UDP) and transmission control protocol (TCP). Most results on the packet dropouts are implicitly based on the UDP, while transmission delay may occur when the TCP protocol is applied. The research of this area is fruitful, and the main focus is how to model the packet dropout phenomenon and then carry out the stability and stabilization studies based on these models. In NCSs when the packet dropout occurs, the controller can either use the zero signal or the newest signal available in the buffer to update the control signal, which are usually called as the zero-input and hold-input schemes. Schenato et al. [76] discussed these schemes over a lossy link. The expressions for computing the optimal static gain for both strategies have been

derived and they compared their LQG performance on some numerical examples. It is interesting to see that none of the two schemes is superior to the other. Later in [77], a simple compensation scheme has been proposed such that the filter used the newest signal to update the state, and the determination of optimal weighting factor was also given. Other efforts are also devoted on how to compensate for the effect induced by the packet dropouts, see [78, 79] and the reference therein.

We now discuss how to model and analyze the NCSs when a packet dropout occurs.

Switched system approach: A typical work was studied by Zhang et al. [80], where the plant was described by the following discrete-time LTI model:

$$\begin{cases} x(k+1) = Ax(k) + Bu(k), \\ y(k) = Cx(k). \end{cases} \tag{1.32}$$

Their purpose was to design the following controller:

$$\begin{aligned} &\text{Observer}: \begin{cases} \hat{x}(k+1) = A\hat{x}(k) + Bu(k) + L[w(k) - \hat{y}(k)], \\ \hat{y}(k) = C\hat{x}(k), \end{cases} \\ &\text{Controller}: v(k) = K\hat{x}(k). \end{aligned} \tag{1.33}$$

Zhang et al. [80] used two switches T_1 and T_2 to describe the states of the forward channel and the backward channel, e.g., when T_1 is closed, then the packet transmission from the controller to actuator is successful and $u(k) = v(k)$, otherwise, the hold-input compensation scheme is used when the packet dropout occurs in this channel and $u(k) = u(k-1)$, see Fig. 1.5. Define the estimation error by

$$e(k) = x(k) - \hat{x}(k), \tag{1.34}$$

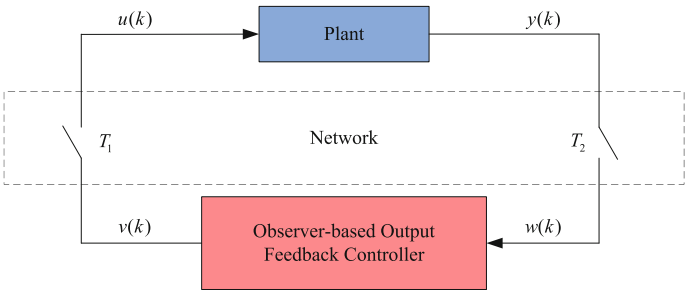

Fig. 1.5 NCS with packet dropouts

and let

$$z(k) = [x^T(k)\ e^T(k)\ \ u^T(k-1)\ w^T(k-1)]^T, \tag{1.35}$$

we have the following four cases:

(1) There is no packet dropout in either the backward channel or the forward channel;

(2) Packet dropout only occurs in the backward channel;

(3) Packet dropout only occurs in the forward channel;

(4) There are packet dropouts in both the backward channel and the forward channel.

For the above four different cases, the following closed-loop systems are obtained, respectively,:

$$S_1\colon z(k+1) = A_1 z(k), A_1 = \begin{bmatrix} A+BK & -BK & 0 & 0 \\ 0 & A-LC & 0 & 0 \\ K & -K & 0 & 0 \\ C & 0 & 0 & 0 \end{bmatrix}.$$

$$S_2\colon z(k+1) = A_2 z(k), A_2 = \begin{bmatrix} A+BK & -BK & 0 & 0 \\ LC & A-LC & 0 & -L \\ K & -K & 0 & 0 \\ 0 & 0 & 0 & I \end{bmatrix}.$$

$$S_3\colon z(k+1) = A_3 z(k), A_3 = \begin{bmatrix} A & 0 & B & 0 \\ 0 & A-LC & 0 & 0 \\ 0 & 0 & I & 0 \\ C & 0 & 0 & 0 \end{bmatrix}.$$

$$S_4\colon z(k+1) = A_4 z(k), A_4 = \begin{bmatrix} A & 0 & B & 0 \\ LC & A-LC & 0 & -L \\ 0 & 0 & I & 0 \\ 0 & 0 & 0 & I \end{bmatrix}.$$

It can be seen from the above analysis that the closed-loop system is essentially a switched system with four subsystems, i.e., $z(k+1) = A_{\sigma(k)} z(k)$, where $\sigma(k) = 1, 2, 3, 4$. Based on this modeling, the switched linear system theory can be applied for the stability and controller design. The extension to the filter design has recently been reported in [81]. For the switched system approach, the packet dropout phenomenon is usually modeled as a switch, and then different scenarios are considered under different switch status. More recent works can also be found in [82, 83]. The main merit is that one can find some explicit conditions on the packet dropout bound which guarantees the stability of closed-loop system. For example, the NCS with sampled-data and packet dropouts was modeled as a switched time-delay

system in [84], and several quantitative relations among some system parameters were obtained, such as the sampling period and the exponential decay rate, the actual data dropout rate, and the admissible data dropout rate bound.

Stochastic system approach: If the packet dropout phenomenon occurs randomly, a stochastic binary variable taking values in {0, 1} is used to model the transmission process, where "1" for successful transmission and "0" for packet dropout. The main results can be divided into two scenarios depending on whether the packet dropout process is correlated or not. Then we will have the i.i.d. packet dropout and Markovian packet dropout, respectively.

Consider the following discrete-time LTI system:

$$x(k+1) = Ax(k) + Bu(k). \tag{1.36}$$

When the zero-input compensation scheme is applied, the inputs of controller and actuator become

$$u_c(k) = \alpha(k)x(k),\ u(k) = \beta(k)u_c(k), \tag{1.37}$$

where $\alpha(k)$ and $\beta(k)$ are independent Bernoulli processes, and $\alpha(k)$, $\beta(k) = 1$ means that the packet transmission is successfully, while $\alpha(k)$, $\beta(k) = 0$ indicates that the packet is lost. Usually, the probabilities of two stochastic variables are required to be known for system analysis, i.e., $\Pr ob\{\alpha(k) = 1\} = \mathbb{E}\{\alpha(k)\} = \bar{\alpha}$, and $\Pr ob\{\beta(k) = 1\} = \mathbb{E}\{\beta(k)\} = \bar{\beta}$ are known. Then, the closed-loop system can be written as

$$x(k+1) = (A + \alpha(k)\beta(k)BK)x(k). \tag{1.38}$$

Let $\gamma(k) = \alpha(k)\beta(k)$, the closed-loop system becomes $x(k+1) = (A + \gamma(k)BK)$ $x(k)$, where $\Pr ob\{\gamma(k) = 1\} = \mathbb{E}\{\gamma(k)\} = \bar{\alpha}\bar{\beta}$. The stability analysis and controller design are then carried out by using some stochastic system analysis. This i.i.d modeling is simple and it has been widely used in the analysis and synthesis of NCSs with packet dropouts, see the control problem [85] and [86], the filtering problem [87] and [88], and the fault detection problem [89]. More recently, the above modeling method has been extended to study the fuzzy-model-based nonlinear NCSs, see [90, 91].

The above modeling only considers the scenario whether the packet is lost or not, but the information on the number of successive packet dropouts has not been discussed. The ignorance of this information may lead to some design conservatism. Very recently, the optimal guaranteed cost stabilizing controller design problem for a class of NCSs with random packet losses was considered in [92]. The number of successive packet losses was assumed to be upper bounded, and the closed-loop NCS was modeled as a discrete-time stochastic delay system with a time-varying input delay and a stochastic parameter:

$$x(k+1) = (A + (1 - \alpha(k))BK)x(k) + \alpha(k)BKx(k - d(k)), \tag{1.39}$$

where $\alpha(k)$ is a binary variable, taking the values in $\{0, 1\}$. $d(k)$ is the number of successive packet dropouts and it is bounded as $1 \leq d(k) \leq d$. By this modeling, the closed-loop system (1.39) is a stochastic time-delay systems. The theory of time-delay system would be applied to analyze such a system.

When the packet dropout process is correlated, a Markov chain can be used to model such a packet dropout process [93] and Poisson processes can be used to model stochastic dropouts in continuous-time [94]. This is usually called as the Gilbert-Elliott channel model. One can simply introduce two Markovian chains to model the packet dropouts in the backward and forward channels, then the closed-loop system is modeled as a Markovian jump linear system with two Markovian chains, i.e.,

$$x(k+1) = (A + \alpha(k)\beta(k)BK)x(k), \tag{1.40}$$

where $\alpha(k), \beta(k) \in \{0, 1\}$ are two Markovian chains with transition probabilities $\Pi_1 = \begin{bmatrix} 1-p_1 & p_1 \\ q_1 & 1-q_1 \end{bmatrix}$, and $\Pi_2 = \begin{bmatrix} 1-p_2 & p_2 \\ q_2 & 1-q_2 \end{bmatrix}$. Finally, the Markovian system approach is applied onto the analysis and synthesis of such NCSs.

1.6 Medium Access Constraint

Due to the limitations on data transmission, it is impossible for all sensors and actuators to have access to the communication channel for all the time, leading to a new problem, medium access constraint problem. Such a constraint has been handled via the well-known time-multiplexing mechanism which has been implemented in a variety of Fieldbus and CAN-based networks. In the time-multiplexing mechanism, time on the shared medium is divided into many slots, and only some nodes are allowed to access the network according to a specified media access control (MAC) protocol. In the last decades, various MAC protocols have been proposed, which may be random or deterministic [95]. Hence, the results on this area can also be divided into the deterministic and stochastic ones. A typical NCS including multiple sensor-controller and controller-actuator pairs can be found in Fig. 1.6.

In the analysis and synthesis of NCSs with medium access constraint, a so-called "communication sequence" [96] is usually used. The earlier research in this area is to find a stabilizing constant feedback controller when a periodical communication sequence has been chosen [96]. But it has been shown that the determination on whether there exists such a controller is an NP-hard problem [97]. Later the attention has been paid on how to design the communication sequence if the controller is given in advance. Various scheduling methods have been proposed, see the Lyapunov-based theory [98] and rate monotonic scheduling theory [99]. Very recently, Zhang et al. [100] discussed the communication and control co-design for NCSs, where the access process to communication medium is governed by a pair of periodic communication sequences. The zero-input compensation scheme is applied when the corresponding

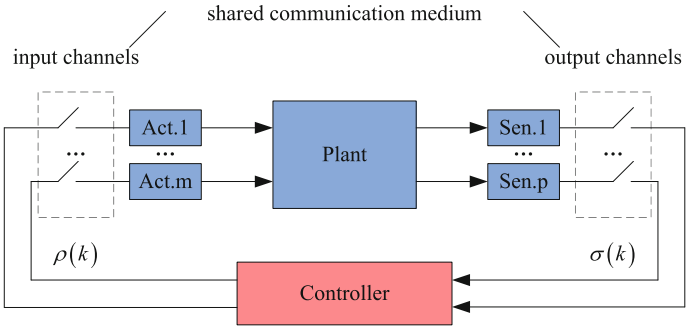

Fig. 1.6 NCS with shared a communication medium

sensors and actuators are not actively communicating. The communication sequence is usually a diagonal matrix and each element is a binary-valued function.

Consider a discrete-time LTI system:

$$\begin{cases} x(k+1) = Ax(k) + Bu(k), \\ y(k) = Cx(k), \end{cases} \tag{1.41}$$

with p sensor nodes and m actuator nodes and suppose that at any one time, only partial sensor and actuator nodes are allowed to access to communication channels. The node accessing process can be modeled by introducing two diagonal matrices, i.e., $M = \text{diag}\{\sigma_1(k), \cdots, \sigma_p(k)\}$, $N = \text{diag}\{\rho_1(k), \cdots, \rho_m(k)\}$, where $\sigma_i(k) = \{0, 1\}, \rho_i(k) = \{0, 1\}, i \in \{1, 2, \cdots, p\}, j \in \{1, 2, \cdots, m\}$. Zhang et al. [100] showed that when A is invertible, and the pair (A, B) is reachable, the pair (A, C) is observable, there do exist a periodic communication sequence pairs such that the closed-loop system is l-step reachable and l-step observable. By resorting to the linear time-varying (LTV) system theory [101], the observer-based output feedback controller design algorithm has been given. Based on the periodical communication sequence in [100], the problem of fault detection was addressed for NCSs subject to both access constraints and random packet dropout in [102].

In NCSs, a specified media access control (MAC) protocol could be random, e.g., Carrier Sense Multiple Access (CSMA) is a probabilistic MAC protocol in which a node verifies the absence of other traffic before transmitting on a shared transmission medium [95]. Hence, much effort has been devoted to the NCSs with stochastic MAC. The results can also be divided into the i.i.d and the Markovian case.

The optimal linear estimation for networked systems with communication constraints was firstly discussed in [103], where one network node is allowed to gain access to a shared communication channel, and channel accessing processes of those network nodes are modeled by Bernoulli processes. The input signal to filter is described as

$$y_e(k) = \left(\sum_{i=0}^{\bar{m}} \sigma_i(k)\Pi_i\right) y(k) + R\left(I - \sum_{i=0}^{\bar{m}} \sigma_i(k)\Pi_i\right) y_e(k-1), \qquad (1.42)$$

where

$$\sigma_i(k) \in \{0, 1\}, \begin{cases} \Pi_i = \text{diag}\{\delta(i-1), \cdots \delta(i-m)\}, \\ \Pi_0 = 0, \\ R = \text{diag}\{r, \cdots, r\}. \end{cases}$$

and $\delta \in \{0, 1\}$ is the Kronecker delta function, R is a slack matrix introduced to compensate for the effect of the sensors that are not accessing to the network. The optimal linear filters were then designed by using the orthogonal projection principle. The similar modeling was later extended to T-S fuzzy-model-based stabilization of nonlinear NCSs with medium access constraint [104]. In [105], the stochastic observability of discrete-time linear stochastic systems with stochastic accessing constraint was investigated. The observability condition for both time-varying and time-invariant systems were presented.

The NCSs with medium access constraint is also studied from the Markovian jump system point of view. The H_∞ filtering for NCS with stochastic protocol was firstly considered in [106], where the accessing process of multiple sensors is governed by a Markovian chain. In their work, the filter input signal is $\bar{y}(k) = \Pi_{\rho(k)} y(k)$, and for each $\rho(k) = i$, $\Pi_{\rho(k)} = \text{diag}\{\delta(i-1), \cdots \delta(i-m)\}$. The variation of the time-varying signal $\rho(k)$ is assumed to obey the Markovian process. Guo et al. [107] considered the stability analysis and controller design for linear systems, where the sensors and actuators are triggered in groups by two independent Markovian chains. In their work, the time-varying communication delay is also incorporated into the closed-loop system. Very recently, the H_∞ control problem for a class of linear time-varying NCSs with stochastic communication protocol was investigated in [108], where the Markovian jump system approach was used to model the accessing process of sensors and actuators. The controller parameters can be determined by solving two coupled backward recursive Riccati difference equations. By using the similar modeling, the H_∞ filtering for nonlinear networked systems with various networked-induced stochastic uncertainties has been investigated in [109], where the accessing process was also modeled by a Markovian chain.

1.7 Wireless Communication

In the preceding sections, we have discussed network-induced issues such as signal sampling, quantization, communication delay, packet dropouts and medium access constraint. They are common for both wired and wireless network ones. This section attempts to discuss some special issues in wireless network control systems (WNCSs).

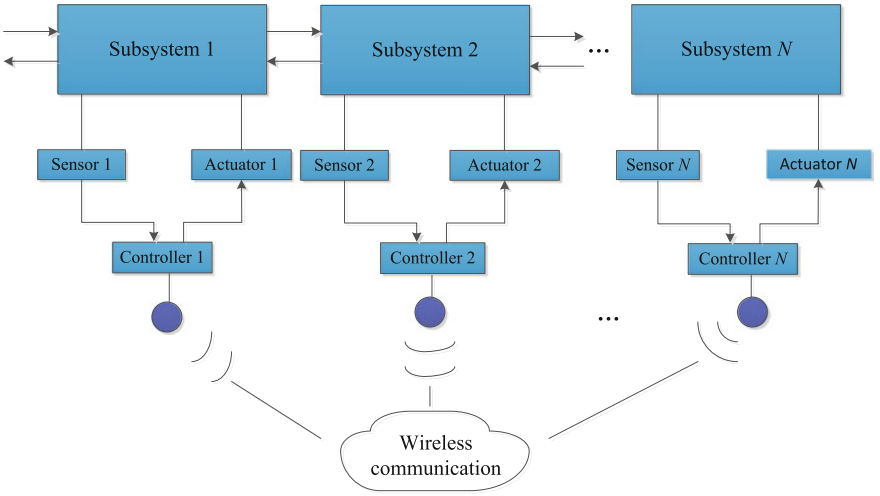

Fig. 1.7 Distributed control systems

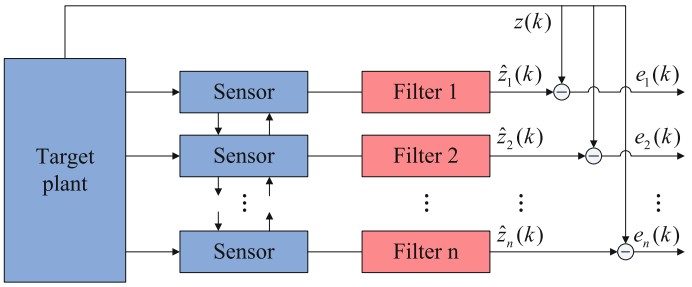

Fig. 1.8 Distributed estimation/filtering systems

Compared with the wired networks, the wireless communication and networks have gained rapid development and adaptation over recent years due to its more mobility and flexibility compared with wired one. One popular example is the wireless sensor networks (WSNs). The applications of WNCSs can be also found in target tracking, condition monitoring, smart factory and so on. Various system structures have been studied in this area, see, e.g., Figs. 1.7 and 1.8. In WNCSs, a sensor usually has a limited power from the battery, and replacing the battery during the operation of system is very difficult. Furthermore, sensor nodes are usually deployed in a wild region and are thus much easier to be affected by the disturbance from environment, causing malfunction of the sensor nodes, e.g., the possible gain variations. Naturally, the networked systems should be robust or non-fragile to these disturbances. Compared with the NCSs with wired communication, the analysis and synthesis of NCSs with wireless communication are more difficult because one needs to simultaneously consider the common imperfections encountered in wired networked

systems together with the other two new issues, i.e., the *energy constraint* and system *gain variations*. Substantial publications can be found in the literature but they scatter over diverse journals and conferences with different approaches, see e.g., references [110] and [111]. This book attempts to unify their major contributions in a single volume for easy access for the researchers.

1.8 Oview of the Book

The rest of this book is organized as follows.

Chapter 2 presents some fundamental knowledge on the system stability, filtering and control in framework of the Lyapunov stability theory. It also gives some useful lemmas on matrix inequalities.

Chapter 3 studies the filtering of wireless networked systems with scheduled transmission and random packet dropouts. First, a new time-varying transmission protocol is introduced to reduce the communication rates of the network, which may be helpful on reducing the communication load. Then, a set of stochastic variables are used to model the random packet dropout phenomenon. Based on the switched system theory and the stochastic system approach, a sufficient condition is presented in terms of linear matrix inequality, which guarantees the mean-square exponential stability and H_∞ performance of the estimation error system. The determination of the filter gains is also given.

Chapter 4 studies the filtering of wireless networked systems with energy constraint, where a nonuniform sampling is firstly used to reduce the communication rate and then a measurement size reduction is introduced to reduce the packet size. Both techniques are helpful to reduce the communication load. By some simple modeling and manipulation, we show that the filtering error system can be modeled as a switched system. The stability condition and the determination of filter gain parameters are proposed from the switched system approach. The effectiveness of the proposed filter design is illustrated by a simulation study.

Chapter 5 deals with the filtering of networked systems with energy constraints, where a stochastic transmission protocol is proposed. More specifically, a set of stochastic variables are introduced to set the transmission rate at the sensor side. Then, a new sufficient condition is obtained such that the filtering error system is mean-square stable and the optimal filter gain parameters are determined by solving an optimization problem subject to some LMI constraints. The determination of the transmission rate and the filter gain parameters are finally illustrated by a simulation study on the CSTR system.

Chapter 6 discusses the filtering of wireless networked system with energy constraint and a stochastic sampling and transmission scheme is presented to achieve this goal. First, a Markovian chain is introduced to model the stochastic sampling and then the sampled measurements are selected such that only a finite element is transmitted. A useful measurement size reduction scheme is proposed and different selection schemes are assumed to follow the Markovian process. Under our design,

the transmission rate and the packet size are both reduced, which can save a certain amount of transmission power. Then, based on the Markovian system approach and the Lyapunov stability theory, a sufficient condition is obtained for the stability analysis and the filter gain parameter design procedure is also presented.

Chapter 7 deals with the distributed filtering of wireless networked systems with energy constraint, and a unified switched system approach is proposed. Firstly, the wireless sensor collects the measurement by a nonuniform sampling rate and then only one element of each measurement is selected for transmission. To reduce the communication rate, each sensor is regulated for transmission at each time instant, leading to the topology switching phenomenon. Based on the switched system approach, the filtering error system is exponentially stable provided that the above scheduling is not so frequently. A simulation study is given to demonstrate the energy efficiency of the proposed schemes.

Chapter 8 considers the distributed filtering of wireless networked systems with energy constraint, and a stochastic Markovian-based approach is proposed to achieve this goal. In this chapter, the sensor collects the measurement under a nonuniform sampling framework, and the sampling process is assumed to follow the Markovian variation. A sufficient condition is obtained such that the filtering error system is stochastic stable with a desired H_∞ performance level. The filter gains can be determined by solving a set of LMIs.

Chapter 9 investigates the distributed filtering for a class of wireless networked systems with filter gain variations. A set of stochastic variables are introduced to model the random filter gain variation phenomenon. The filtering error system is shown to be asymptotically stable in the mean-square sense with a desired H_∞ disturbance attenuation level. The relations on the gain variation bounds and the filtering performance are also obtained.

Chapter 10 discusses how to design the distributed filters for the wireless networked systems with gain variations and energy constraint. The measurement size reduction technique and the stochastic signal transmission technique are both used to save the transmission power. Meanwhile, the exponential stability condition is obtained based on the switched system approach and the Lyapunov stability theory. The optimal filter gain parameters are determined by solving an optimization problem. The advantages and effectiveness of the proposed filter design algorithm is verified by a simulation study.

Chapter 11 studies the distributed stabilization of large-scale networked system with controller gain variations and controller failure. The so-called distributed nonfragile control problem is firstly studied and a set of random variables are introduced to model the controller failure phenomenon. Based on the Lyapunov stability theory and some stochastic system analysis method, a sufficient condition is obtained such that the closed-loop system is asymptotically stable in the mean-square sense with a prescribed H_∞ performance level. A simulation study on the interconnected inverted pendulums is given to show the effectiveness of the proposed controller design method.

Chapter 12 is concerned with distributed stabilization of nonlinear large-scale systems with energy constraints and random sensor faults. Due to the limited power

in sensors, techniques such as reduction of times and size of the transmission packet are utilized to save the energy. While a set of binary variables is introduced to model the sensor failure phenomenon. Based on the switched system theory, the Lyapunov stability technique and some stochastic system analysis, a sufficient condition is established under which the closed-loop system is exponentially stable in the mean-square sense with a prescribed H_∞ disturbance attenuation level. The controller gain design algorithm is presented with help of the cone complementarity linearization (CCL) method.

Chapter 13 investigates the distributed control of large-scale networked systems with energy constraints, and a unified switched system approach is utilized to achieve this goal. The techniques proposed in the above, i.e., nonuniform sampling, measurement size reduction and communication rate scheduling are all used such that the communication load has been reduced effectively. A sufficient condition is obtained which can guarantee the exponential stability of the closed-loop system and the controller gain parameters are determined by using the CCL method. The effectiveness of the proposed controller design algorithm is demonstrated by a case study on the CSTR system.

Chapter 14 is concerned with the distributed control for a class of large-scale networked control systems with energy constraints and topology switching. The event-based communication protocol is first employed to reduce the unnecessary communications between the plant network and controller network. Then, the selected measurement signal is quantized by a logarithmic quantizer for transmission. A group of asynchronous controllers are designed to tackle the problem when the real time information about the topology is not available in such a networked environment. A stochastic switched system model with sector bound uncertainties is proposed to capture the communication constraints and topology switching phenomena. A sufficient condition is developed that guarantees the globally exponential stability of the overall system by using the Lyapunov direct method and the controller gains are determined by using the CCL algorithm. Finally, a simulation study on the CSTR systems is performed and the effectiveness of controller design algorithm is verified.

References

1. K.H. Johansson, M. Trngren, L. Nielsen, Vehicle applications of controller area network, in *Handbook of Networked and Embedded Control Systems, Part of the series Control Engineering* (2005), pp. 741–765
2. J.K.W. Wong, H. Li, S.W. Wang, Intelligent building research: a review. Autom. Constr. **14**, 143–159 (2005)
3. R.J. Anderson, M.W. Spong, Bilateral control of teleoperators with time delay. IEEE Trans. Autom. Control **34**(5), 494–501 (1989)
4. Y. Eun, H. Bang, Cooperative control of multiple unmanned aerial vehicles using the potential field theory. J. Aircr. **43**(6), 1805–1814 (2006)
5. R.M. Murray, K.J. Astrom, S.P. Boyd, R.W. Brockett, G. Stein, Control in an information rich world. IEEE Control Syst. Mag. **23**(2), 20–33 (2003)

6. N. Sivashankar, P. Khargonekar, Characterization of the L_2-induced norm for linear systems with jumps with applications to sampled-data systems. SIAM J. Control Optim. **32**, 1128–1150 (1994)
7. T. Basar, P. Bernard, H_∞ optimal control and related minimax design problems. A dynamic game approach, in *Systems and Control: Foundation and Applications* (Birkhauser, Boston, 1995)
8. S. Xu, T.W. Chen, Robust H_∞ filtering for uncertain impulsive stochastic systems under sampled measurements. Automatica **39**(3), 509–516 (2003)
9. P. Naghshtabrizi, J.P. Hespanha, A.R. Teel, Exponential stability of impulsive systems with application to uncertain sampled-data systems. Syst. Control Lett. **57**(5), 378–385 (2008)
10. W.H. Chen, W.X. Zheng, Input-to-state stability for networked control systems via an improved impulsive system approach. Automatica **47**(4), 789–796 (2011)
11. C. Briat, A. Seuret, Convex dwell-time characterizations for uncertain linear impulsive systems. IEEE Trans. Autom. Control **57**(12), 3241–3246 (2012)
12. C. Briat, Convex conditions for robust stability analysis and stabilization of linear aperiodic impulsive and sampled-data systems under dwell-time constraints. Automatica **49**(11), 3449–3457 (2013)
13. Y. Mikheev, V. Sobolev, E. Fridman, Asymptotic analysis of digital control systems. Autom. Remote Control **49**, 1175–1180 (1988)
14. K. Astrom, B. Wittenmark, *Adaptive Control* (Addison-Wesley, Reading, MA, 1989)
15. E. Fridman, Use of models with aftereMect in the problem of design of optimal digital control. Autom. Remote Control **53**(10), 1523–1528 (1992)
16. M. Wu, Y. He, J.H. She, G.P. Liu, Delay-dependent criteria for robust stability of time-varying delay systems. Automatica **40**(8), 1435–1439 (2004)
17. Y. He, Q.G. Wang, C. Lin, M. Wu, Delay-range-dependent stability for systems with time-varying delay. Automatica **43**(2), 371–376 (2007)
18. H.Y. Shao, New delay-dependent stability criteria for systems with interval delay. Automatica **45**(3), 744–749 (2009)
19. P. Park, J.W. Ko, C. Jeong, Reciprocally convex approach to stability of systems with time-varying delays. Automatica **47**(1), 235–238 (2011)
20. A. Seureta, F. Gouaisbaut, Wirtinger-based integral inequality: application to time-delay systems. Automatica **49**(9), 2860–2866 (2013)
21. K. Liu, E. Fridman, Wirtinger's inequality and Lyapunov-based sampled-data stabilization. Automatica **48**(1), 102–108 (2012)
22. E. Fridman, A refined input delay approach to sampled-data control. Automatica **46**(2), 421–427 (2010)
23. Z.G. Wu, P. Shi, H.Y. Su, J. Chu, Local synchronization of chaotic neural networks with sampled-data and saturating actuators. IEEE Trans. Cybern. **44**(12), 2635–2645 (2014)
24. Y. Liu, S.M. Lee, Stability and stabilization of Takgsi-Sugeno fuzzy systems via sampled-data and state quantized controller. IEEE Trans. Fuzzy Syst. (2016)
25. Y.S. Suh, Stability and stabilization of nonuniform sampling systems. Automatica **44**(12), 3222–3226 (2008)
26. H. Fujioka, Stability analysis for a class of networked/embedded control systems: output feedback case, in *Proceedings of the 17th IFAC World Congress*, Seoul, Korea, 2008, pp. 4210–4215
27. H. Fujioka, A discrete-time approach to stability analysis of systems with aperiodic sample-and-hold devices. IEEE Trans. Autom. Control **54**(10), 2440–2445 (2009)
28. Y. Oishi, H. Fujioka, Stability and stabilization of aperiodic sampled-data control systems using robust linear matrix inequalities. Automatica **46**(8), 1327–1333 (2010)
29. C.Y. Kao, H. Fujioka, On stability of systems with aperiodic sampling devices. IEEE Trans. Autom. Control **58**(8), 2085–2090 (2013)
30. D.H. Lee, Y.H. Joo, A note on sampled-data stabilization of LTI systems with aperiodic sampling. IEEE Trans. Autom. Control **60**(10), 2746–2751 (2015)

31. A. Seuret, M.M. Peet, Stability analysis of sampled-data systems using sum of squares. IEEE Trans. Autom. Control **58**(6), 1620–1625 (2013)
32. W.A. Zhang, A.D. Liu, K.X. Xing, Stability analysis and stabilization of aperiodic sampled-data systems based on a switched system approach. J. Frankl. Inst. **353**, 955–970 (2016)
33. R.Y. Ling, L. Yu, D. Zhang, W.A. Zhang, A Markovian system approach to distributed H_∞ filtering for sensor networks with stochastic sampling. J. Frankl. Inst. **351**(11), 4998–5014 (2014)
34. R.Y. Ling, J.T. Chen, W.A. Zhang, D. Zhang, Energy-efficient H_∞ filtering over wireless networked systems-a Markovian system approach. Signal Process. **120**, 495–502 (2016)
35. L.X. Zhang, E.K. Boukas, Stability and stabilization of Markovian jump linear systems with partly unknown transition probabilities. Automatica **45**(2), 463–468 (2009)
36. R. Kalman, Nonlinear aspects of sampled-data control systems, in *Proceedings of the Symposium on Nonlinear Circuit Analysis*, vol. 6 (1956), pp. 273–313
37. D.F. Delchamps, Stabilizing a linear system with quantized state feedback. IEEE Trans. Autom. Control **35**(8), 916–924 (1990)
38. N. Elia, S. Mitter, Stabilization of linear systems with limited information. IEEE Trans. Autom. Control **46**(9), 1384–1400 (2001)
39. M.Y. Fu, L.H. Xie, The sector bound approach to quantized feedback control. IEEE Trans. Autom. Control **50**(11), 1698–1711 (2005)
40. M.Y. Fu, L.H. Xie, Finite-level quantized feedback control for linear systems. IEEE Trans. Autom. Control **54**(5), 1165–1170 (2009)
41. Y. Ishido, K. Takaba, D.E. Quevedo, Stability analysis of networked control systems subject to packet-dropouts and finite-level quantization. Syst. Control Lett. **60**(5), 325–332 (2011)
42. Y.G. Niu, T.G. Jia, X.Y. Wang, F.W. Yang, Output-feedback control design for NCSs subject to quantization and dropout. Inf. Sci. **179**(21), 3804–3813 (2009)
43. F. Rasool, S.K. Nguang, D. Huang, L.X. Zhang. Quantized robust H_∞ control of discrete-time systems with random communication delays, in *Joint 48th IEEE Conference on Decision and Control and 28th Chinese Control Conference*, Shanghai, P.R. China, 16–18 December 2009
44. M.S. Mahmoud, M.H. Baig, Networked feedback control for systems with quantization and non-stationary random delays. IMA J. Math. Control Inf. **32**, 119–140 (2015)
45. R.W. Brockett, D. Liberzon, Quantized feedback stabilization of linear systems. IEEE Trans. Autom. Control **45**(7), 1279–1289 (2000)
46. F. Fagnani, S. Zampieri, Quantized stabilization of linear systems-complexity versus performance. IEEE Trans. Autom. Control **49**(9), 1534–1548 (2004)
47. D. Liberzon, D. Nesic, Input-to-state stabilization of linear systems with quantized state measurements. IEEE Trans. Autom. Control **52**(5), 767–781 (2007)
48. C. Peng, Y.C. Tian, Networked H_∞ control of linear systems with state quantization. Inf. Sci. **177**(24), 5763–5774 (2007)
49. E.G. Tian, D. Yue, C. Peng, Quantized output feedback control for networked control systems. Inf. Sci. **178**(12), 2734–2749 (2008)
50. W. Zhang, M.S. Branicky, S.M. Phillips, Stability of networked control systems stability of networked control system. IEEE Control Syst. **21**(1), 84–99 (2001)
51. D. Yue, Q.L. Han, J. Lam, Network-based robust H_∞ control of systems with uncertainty. Automatica **41**(6), 999–1007 (2005)
52. J. Lam, H.J. Gao, C.H. Wang, Stability analysis for continuous systems with two additive time-varying delay components. Syst. Control Lett. **56**(1), 16–24 (2007)
53. H.J. Gao, T.W. Chen, J. Lam, A new delay system approach to network-based control. Automatica **44**(1), 39–52 (2008)
54. H.J. Gao, T.W. Chen, H_∞ estimation for uncertain systems with limited communication capacity. IEEE Trans. Autom. Control **52**(11), 2070–2084 (2007)
55. H.J. Gao, T.W. Chen, Network-based H_∞ output tracking control. IEEE Trans. Autom. Control **53**(3), 655–667 (2008)
56. J.L. Xiong, J. Lam, Stabilization of networked control systems with a logic ZOH. IEEE Trans. Autom. Control **54**(2), 358–363 (2009)

57. H. Zhang, J. Yang, C.Y. Su, T-S fuzzy-model-based robust H_∞ design for networked control systems with uncertainties. IEEE Trans. Ind. Inform. **3**(4), 289–301 (2007)
58. E.G. Tian, D. Yue, Z. Gu, Robust H_∞ control for nonlinear systems over network: a piecewise analysis method. Fuzzy Sets Syst. **161**(21), 2731–2745 (2010)
59. R.Q. Lu, Y. Xu, A.K. Xue, H_∞ filtering for singular systems with communication delays. Signal Process. **90**(4), 1240–1248 (2010)
60. W.H. Fan, H. Cai, Q.W. Chen, W.L. Hu, Stability of networked control systems with time-delay. Control Theory Appl. **21**(6), 880–884 (2004)
61. M.B.G. Cloosterman, N. van de Wouw, W.P.M.H. Heemels, H. Nijmeijer, Stability of networked control systems with uncertain time-varying delays. IEEE Trans. Autom. Control **54**(7), 1575–1580 (2009)
62. W.A. Zhang, L. Yu, S. Yin, A switched system approach to H_∞ control of networked control systems with time-varying delays. J. Frankl. Inst. **348**(2), 165–178 (2011)
63. H. Lin, P.J. Antsaklis, Persistent disturbance attenuation properties for networked control systems, in *Proceeding of the 43rd IEEE Conference on Decision and Control*, 2004, pp. 953–958
64. H. Lin, P.J. Antsaklis, Stability and persistent disturbance attenuation properties for a class of networked control systems: switched system approach. Int. J. Control **78**(18), 1447–1458 (2005)
65. Y.L. Wang, G.H. Yang, H_∞ control of networked control systems with time delay and packet disordering. IET Control Theory Appl. **1**(5), 1344–1354 (2007)
66. W.A. Zhang, L. Yu, New approach to stabilization of networked control systems with time-varying delays. IET Control Theory Appl. **2**(12), 1094–1104 (2008)
67. C. Peng, D. Yue, E.G. Tian, Z. Gu, A delay distribution based stability analysis and synthesis approach for networked control systems. J. Frankl. Inst. **346**(4), 349–365 (2009)
68. C. Peng, T.C. Yang, Communication-delay-distribution-dependent networked control for a class of T-S fuzzy systems. IEEE Trans. Fuzzy Syst. **18**(2), 326–335 (2010)
69. S.L. Hu, Y.N. Zhang, Z.P. Du, Robust H_∞ control for T-S fuzzy systems with probabilistic interval time varying delay. Nonlinear Anal. Hybrid Syst. **6**(3), 871–884 (2012)
70. B. Tang, J. Wang, Y. Zhang, A delay-distribution approach to stabilization of networked control systems. IEEE Trans. Control Netw. Syst. **2**(4), 382–392 (2015)
71. R. Krtolica, U. Ozguner, H. Chan, H. Goktas, J. Winkelman, M. Liubakka, Stability of linear feedback systems with random communication delays. Int. J. Control **59**(4), 925–953 (1994)
72. L. Xiao, A. Hassibi, J.P. How, Control with random communication delays via a discrete-time jump linear system approach, in *The Proceeding of 2000 American Control Conference*, Chicago, IL (2000), pp. 2199–2204
73. L.Q. Zhang, Y. Shi, T.W. Chen, B. Huang, A new method for stabilization of networked control systems with random delays. IEEE Trans. Autom. Control **50**(8), 1177–1181 (2005)
74. Y. Shi, B. Yu, Output feedback stabilization of networked control systems with random delays modeled by Markov chains. IEEE Trans. Autom. Control **54**(7), 1668–1674 (2009)
75. M.X. Liu, X.T. Liu, Y. Shi, S.Q. Wang, T-S fuzzy-model-based H_2 and H_∞ filtering for networked control systems with two-channel Markovian random delays. Digit. Signal Process. **27**, 167–174 (2014)
76. L. Schenato, To zero or to hold control inputs with lossy links? IEEE Trans. Autom. Control **54**(5), 1093–1099 (2009)
77. D. Zhang, L. Yu, W.A. Zhang, Exponential H_∞ filtering for nonlinear discrete-time switched stochastic systems with mixed time delays and random missing measurements. Asian J. Control **14**(3), 807–816 (2012)
78. Y.C. Tian, D. Levy, Compensation for control packet dropout in networked control systems. Inf. Sci. **178**(5), 1263–1278 (2008)
79. J.T. Yu, L.C. Fu, An optimal compensation framework for linear quadratic Gaussian control over lossy networks. IEEE Trans. Autom. Control **60**(10), 2692–2697 (2015)
80. W.A. Zhang, L. Yu, Output feedback stabilization of networked control systems with packet dropouts. IEEE Trans. Autom. Control **52**(9), 1705–1710 (2007)

81. S. Yin, L. Yu, W.A. Zhang, A switched system approach to networked H_∞ filtering with packet losses. Circuits Syst. Signal Process. **30**(6), 1341–1354 (2011)
82. J.Y. Yu, L. Wang, G.F. Zhang, M. Yu, Output feedback stabilisation of networked control systems via switched system approach. Int. J. Control **82**(9), 1665–1677 (2009)
83. M. Wang, J. Qiu, M. Chadli, M. Wang, A switched system approach to exponential stabilization of sampled-data T-S fuzzy systems with packet dropouts. IEEE Trans. Cybern. (2016)
84. W.A. Zhang, L. Yu, Stabilization of sampled-data control systems with control inputs missing. IEEE Trans. Autom. Control **55**(2), 447–452 (2010)
85. Z. Wang, F. Yang, D.W.C. Ho, X. Liu, Robust H_∞ control for networked systems with random packet losses. IEEE Trans. Syst. Man Cybern. Part B (Cybern.) **37**(4), 916–924 (2007)
86. Z. Wang, D.W.C. Ho, Y. Liu, X. Liu, Robust H_∞ control for a class of nonlinear discrete time-delay stochastic systems with missing measurements. Automatica **45**(3), 685–691 (2009)
87. B. Sinopoli, L. Schenato, M. Franceschetti, K. Poolla, M.I. Jordan, S.S. Sastry, Kalman filtering with intermittent observations. IEEE Trans. Autom. Control **49**(9), 1453–1464 (2004)
88. G. Wei, Z. Wang, H. Shu, Robust filtering with stochastic nonlinearities and multiple missing measurements. Automatica **45**(3), 836–841 (2009)
89. X. He, Z. Wang, Y.D. Ji, D.H. Zhou, Robust fault detection for networked systems with distributed sensors. IEEE Trans. Aerosp. Electron. Syst. **47**(1), 166–177 (2011)
90. H.J. Gao, Y. Zhao, J. Lam, K. Chen, H_∞ fuzzy filtering of nonlinear systems with intermittent measurements. IEEE Trans. Fuzzy Syst. **17**(2), 291–300 (2009)
91. H. Li, C. Wu, L. Wu, H.K. Lam, Y. Gao, Filtering of interval type-2 fuzzy systems with intermittent measurements. IEEE Trans. Cybern. **46**(3), 668–678 (2016)
92. W.A. Zhang, L. Yu, Optimal guaranteed cost stabilization of networked systems with bounded random packet losses. Optim. Control Appl. Methods **33**(1), 81–99 (2012)
93. S.C. Smith, P. Seiler, Estimation with lossy measurements: jump estimators for jump systems. IEEE Trans. Autom. Control **48**(12), 2163–2171 (2003)
94. Y. Xu, J.P. Hespanha, Estimation under uncontrolled and controlled communications in networked control systems, in *Proceeding of the 44th Conference on Decision and Control* (2005), pp. 842–847
95. A.L. Garcia, I. Widjaja, *Communication Networks: Fundamental Concepts and Key Architectures* (McGraw-Hill, Boston, 2001)
96. R.W. Brockett, Stabilization of motor networks, in *Proceedings of the 34th IEEE Conference on Decision and Control* (1995), pp. 1484–1488
97. V. Blondell, J. Tsitsiklis, NP hardness of some linear control design problem. SIAM J. Control Optim. **35**(6), 2118–2127 (1997)
98. D.H. Varsakelis, Feedback control systems as users of a shared network: communication sequences that guarantee stability, in *Proceedings of the 40th IEEE Conference on Decision and Control* (2001), pp. 3631–3636
99. M.S. Branicky, S.M. Phillips, W. Zhang, Scheduling and feedback co-design for networked control systems, in *Proceedings of the 41st IEEE Conference on Decision and Control* (2002), pp. 1211–1217
100. L. Zhang, D.H. Varsakelis, Communication and control co-design for networked control systems. Automatica **42**(6), 953–958 (2006)
101. W.J. Rugh, *Linear System Theory* (Prentice Hall, New Jersey, 1996)
102. Y.Q. Wang, H. Ye, S.X. Ding, G.Z. Wang, Fault detection of networked control systems subject to access constraints and random packet dropout. Acta Autom. Sin. **35**(9), 1235–1239 (2009)
103. W.A. Zhang, L. Yu, G. Feng, Optimal linear estimation for networked systems with communication constraints. Automatica **47**(9), 1992–2000 (2011)
104. H. Zhang, Y. Tian, L.X. Gao, Stochastic observability of linear systems under access constraints. Asian J. Control **17**(1), 64–73 (2015)
105. C.Z. Zhang, G. Feng, J.B. Qiu, W.A. Zhang, T-S fuzzy-model-based piecewise H_∞ output feedback controller design for networked nonlinear systems with medium access constraint. Fuzzy Sets Syst. **248**, 86–105 (2014)

106. P.D. Zhou, L. Yu, H.B. Song, L.L. Ou, H-infinity filtering for network-based systems with stochastic protocols. Control Theory Appl. **27**(12), 1711–1716 (2010)
107. G. Guo, Z.B. Lu, Q.L. Han, Control with Markov sensors/actuators assignment. IEEE Trans. Autom. Control **57**(7), 1799–1804 (2012)
108. L. Zou, Z.D. Wang, H. Gao, Observer-based H_∞ control of networked systems with stochastic communication protocol: the finite-horizon case. Automatica **63**, 366–373 (2016)
109. D. Zhang, H.Y. Song, L. Yu, Robust fuzzy-model-based filtering for nonlinear cyber-physical systems with multiple stochastic incomplete measurements. IEEE Trans. Syst. Man Cybern. Syst. 1–13 (2016). doi:10.1109/TSMC.2016.2551200
110. D. Zhang, P. Shi, Q.G. Wang, Energy-efficient distributed control of large-scale systems: a switched system approach. Int. J. Robust Nonlinear Control **26**(14), 3101–3117 (2016). doi:10.1002/rnc.3494
111. D. Zhang, P. Shi, W.A. Zhang, L. Yu, Energy-efficient distributed filtering in sensor networks: a unified switched system approach. IEEE Trans. Cybern. doi:10.1109/TCYB.2016.2553043

Chapter 2
Fundamentals

In analysis and synthesis of NCSs and WNCSs, various approaches have been proposed, such as stochastic systems, Markovian jump systems, switched systems and time-delay systems. To help readers understand the book well, some fundamentals on stability analysis, controller and filter design are first presented for linear time-invariant (LTI) systems, Markovian jump systems and switched systems. Several lemmas are introduced, and some of them will be used in this chapter. The proof of these lemmas can be found in the literature and thus are omitted in this book.

2.1 Mathematical Preliminaries

Some basic mathematical preliminaries relevant to this book are given in this section.

Lemma 2.1 ([1]) *For a given matrix* $S = \begin{bmatrix} S_{11} & S_{12} \\ * & S_{22} \end{bmatrix}$, *the following three statements are equivalent:*

(1) $S < 0$;
(2) $S_{11} < 0$, $S_{22} - S_{12}^T S_{11}^{-1} S_{12} < 0$;
(3) $S_{22} < 0$, $S_{11} - S_{12} S_{22}^{-1} S_{12}^T < 0$.

Lemma 2.2 ([2]) *For given matrices* K_1, K_2 *and* K_3 *with appropriate dimensions, and* K_1 *satisfying* $K_1 = K_1^T$, *then there holds*

$$K_1 + K_2 \Delta(k) K_3^T + K_3 \Delta^T(k) K_2^T < 0 \tag{2.1}$$

for all $\Delta^T(k)\Delta(k) \leq I$ *if and only if there exists a scalar* $\varepsilon > 0$ *such that*

$$K_1 + \varepsilon K_2 K_2^T + \varepsilon^{-1} K_3 K_3^T < 0. \tag{2.2}$$

D. Zhang et al., *Filtering and Control of Wireless Networked Systems*,
Studies in Systems, Decision and Control 97, DOI 10.1007/978-3-319-53123-6_2

Lemma 2.3 ([3]) *For matrices A, $Q = Q^T$ and $P > 0$, the following matrix inequality,*

$$A^T P A - Q < 0, \tag{2.3}$$

holds if and only if there exists a matrix W of appropriate dimensions such that

$$\begin{bmatrix} -Q & A^T W \\ * & P - W - W^T \end{bmatrix} < 0. \tag{2.4}$$

2.2 LTI Systems

A dynamic system is usually modeled as a differential or difference equation. A continuous-time linear time-invariant system is usually described by

$$\dot{x}(t) = Ax(t) + Bu(t), \tag{2.5}$$

and a discrete-time system is

$$x(k+1) = Ax(k) + Bu(k). \tag{2.6}$$

where $x \in \mathbb{R}^n$ is the state vector and $u \in \mathbb{R}^m$ is the state vector. $A \in \mathbb{R}^{n\times n}$ and $B \in \mathbb{R}^{n\times m}$ are two constant matrices. It follows from the Lyapunov stability theory that the above systems are asymptotically sable if the state $x(t)$ or $x(k)$ tends to its equilibrium point when the time goes to infinity. The above system is exponentially stable if the state $x(t)$ or $x(k)$ tends to its equilibrium point with an exponential decay rate. Taking the discrete-time system (2.6) as an illustration, it is said to be exponentially stable if there exist some scalars $\delta > 0$ and $0 < \beta < 1$, such that the state of (2.6) satisfies $\|x(k)\| < \delta\beta^{k-k_0} \|x(k_0)\|, \forall k \geq k_0$.

There are various ways to check whether an LTI system is stable or not. We focus on the Lyapunov stability theory and linear matrix inequality based conditions. We first discuss the scenario when system (2.5) and (2.6) are in the absence of input, i.e., $u = 0$.

Proposition 2.1 *The continuous-time LTI system (2.5) with u=0 is said to be asymptotically sable if there exists a positive definite matrix $P > 0$ such that the following inequality is true:*

$$A^T P + PA < 0. \tag{2.7}$$

Proof Consider the Lyapunov function candidate $V(x(t)) = x^T(t)Px(t)$. The derivative of this Lyapunov function is

$$\begin{aligned}\dot{V}(x(t)) &= \dot{x}^T(t)Px(t) + x^T(t)P\dot{x}(t)\\ &= (Ax(t))^T Px(t) + x^T(t)P\left(Ax(t)\right)\\ &= x^T(t)\left(A^T P + PA\right)x(t).\end{aligned} \tag{2.8}$$

One can see that $\dot{V}(x(t)) < 0$ if (2.7) holds. It follows from the Lyapunov stability theory, the system (2.5) with $u = 0$ is asymptotically stable.

Proposition 2.2 *The discrete-time LTI system (2.6) with $u = 0$ is said to be asymptotically sable if there exists a positive definite matrix $P > 0$ such that the following inequality is true:*

$$A^T PA - P < 0. \tag{2.9}$$

Proof Use the Lyapunov function $V(x(k)) = x^T(k)Px(k)$. The difference of Lyapunov function is

$$\begin{aligned}\Delta V(x(k)) &= V(x(k+1)) - V(x(k))\\ &= x^T(k+1)Px(k+1) - x^T(k)Px(k)\\ &= (Ax(k))^T P\left(Ax(k)\right) - x^T(k)Px(k)\\ &= x^T(k)\left(A^T PA - P\right)x(k).\end{aligned} \tag{2.10}$$

One can see that $\Delta V(x(k)) < 0$ if (2.9) holds. It follows from the Lyapunov stability theory, the system (2.6) with $u = 0$ is asymptotically stable.

For the control system (2.5) and (2.6), the state feedback controller is a simple and effective method to adjust the dynamic of systems. The overall control system is given by

$$\begin{cases}\dot{x}(t) = Ax(t) + Bu(t),\\ u(t) = -Kx(t),\end{cases} \tag{2.11}$$

where $K \in \mathbb{R}^{m\times n}$ is the controller gain to be determined.

Proposition 2.3 *The closed-loop system (2.11) is asymptotically stable if there exist positive definite matrix X and an appropriate matrix Y such that the following inequalities*

$$\begin{cases}AX + XA^T - Y^T B^T - BY < 0,\\ X > 0,\end{cases} \tag{2.12}$$

hold. Moreover, the controller gain is determined by $K = YX^{-1}$.

Proof The closed-loop system can be described as $\dot{x}(t) = (A - BK)x(t)$. By replacing A in (2.7) by $A - BK$, it is easy to see that the closed-loop system is stable when the following inequality,

$$(A - BK)^T P + P(A - BK) < 0, \tag{2.13}$$

holds. Since $P = P^T > 0$, then P is invertible. Left- and right- multiplying the above inequality by P^{-1} yields

$$AP^{-1} + P^{-1}A^T - \left(P^{-1}K^T\right)B^T - B\left(KP^{-1}\right) < 0, \tag{2.14}$$

which is (2.12) by assigning $X = P^{-1}$ and $Y = KP^{-1}$.

The following proposition deals with stabilization of a discrete-time system:

$$\begin{cases} x(k+1) = Ax(k) + Bu(k), \\ u(k) = -Kx(k). \end{cases} \tag{2.15}$$

Proposition 2.4 *The closed-loop system (2.15) is asymptotic stable if there exist positive definite matrix X and an appropriate matrix Y such that the following inequality,*

$$\begin{bmatrix} -X & XA^T - YB^T \\ * & -X \end{bmatrix} < 0, \tag{2.16}$$

holds. Moreover, the controller gain is determined by $K = YX^{-1}$.

Proof The closed-loop system can be described as $x(k+1) = (A - BK)x(k)$. By replacing A in (2.9) by $A - BK$, it is easy to see that the closed-loop system is stable when the following inequality holds:

$$(A - BK)^T P (A - BK) < 0. \tag{2.17}$$

By using Lemma 2.1, (2.17) is equivalent to

$$\begin{bmatrix} -P & (A - BK)^T P \\ * & -P \end{bmatrix} < 0. \tag{2.18}$$

Since $P = P^T > 0$, then P is invertible. Left- and right- multiplying the above inequality by $\mathrm{diag}\{P^{-1}, P^{-1}\}$ gives

$$\begin{bmatrix} -P^{-1} & P^{-1}(A - BK)^T \\ * & -P^{-1} \end{bmatrix} < 0. \tag{2.19}$$

which is (2.16) by assigning $X = P^{-1}$ and $Y^T = P^{-1}K^T$.

2.3 Markovian Jump Systems

A useful category of system models is those in which the system operates in multiple modes. The switching between these modes introduces non-linearity into the overall system description even though each individual mode is linear. A general theory of such systems is presented by the hybrid systems community. However, much tighter results can be developed if some further assumptions are made, for example the mode switches are governed by a stochastic process that is statistically independent from the state values. In the case when the stochastic process can be described by a Markov chain, the system is called a Markovian jump linear system. The Markovian jump system has been applied to the modeling of networked systems, and we focus on the discrete-time system.

Consider a discrete-time Markovian jump system:

$$x(k+1) = A_{r(k)}x(k), \tag{2.20}$$

where $x(k)$ is the state vector, $r(k) \in \Theta = \{1, 2, \ldots, m\}$ is the switching law and the transition probability is denoted as $\Pr ob\,(r_{k+1} = j \,|\, r_k = i) = q_{ij}$, and $0 \leq q_{ij} \leq 1$, which constitutes the transition matrix Q. Such a system has been studied for a long time in the fault isolation community, and received new impetus with the adventure of networked control systems. For example, as mentioned in Chap. 1, the packet dropouts process can be modeled as a two state Markovian jump system. The stochastic access constraint phenomena can also be modeled as a Markovian jump system. Then, it is necessary to introduce some basic knowledge of this system.

Since the Markovian jump linear system is a stochastically varying system, numerous notions of stability may be defined. We will primarily be interested in mean-square stability, that is the state of a Markovian system tends to its equilibrium point in the mean-square sense when the time goes to infinity. Mathematically, $\mathbb{E}\left\{\sum_{k=0}^{\infty} \|x(k)\|^2 | \chi(0)\right\} < \infty$, where $\chi(0)$ is the initial condition.

A sufficient stability condition for the Markovian jump system (2.20) is given as follows.

Proposition 2.5 *The discrete-time Markovian jump system (2.20) is said to be mean-square sable if there exist positive definite matrices $P_i > 0$, such that the following inequalities are all true:*

$$A_i^T \left(\sum_{j=1}^{m} q_{ij} P_j \right) A_i - P_i < 0, \quad i, j \in \Theta. \tag{2.21}$$

Proof Let $V(x(k)) = x^T(k) P_{r(k)} x(k)$, $r(k) = i$ and $r(k+1) = j$, it follows from that

$$\begin{aligned}\mathbb{E}\{\Delta V(x(k))\} &= \mathbb{E}\{V(x(k+1)) - V(x(k))\} \\ &= \mathbb{E}\left\{x^T(k+1)\left(\sum_{j=1}^{m} q_{ij}P_j\right)x(k+1) - x^T(k)P_i x(k)\right\} \\ &= \mathbb{E}\left\{(A_i x(k))^T\left(\sum_{j=1}^{m} q_{ij}P_j\right)(A_i x(k)) - x^T(k)P_i x(k)\right\} \\ &= \mathbb{E}\left\{x^T(k)\left[A_i^T\left(\sum_{j=1}^{m} q_{ij}P_j\right)A_i - P_i\right]x(k)\right\}.\end{aligned} \tag{2.22}$$

One can see that $\mathbb{E}\{\Delta V(x(k))\} < 0$ if (2.21) holds. It follows from the Lyapunov stability theory, the system (2.20) is asymptotically stable in the mean-square sense.

Proposition 2.5 gives a sufficient condition for the asymptotically stability of system (2.20). We now consider a system with the input, and the overall system is described by

$$\begin{cases} x(k+1) = A_{r(k)}x(k) + B_{r(k)}u(k), \\ u(k) = K_{r(k)}x(k), \end{cases} \tag{2.23}$$

where $u(k)$ is the control input and $K_{r(k)}$ is the feedback gain, which is to be determined. The following algorithm can be used to determine the controller gain.

Proposition 2.6 *For the discrete-time Markovian jump system (2.23), it is mean-square stable if there exist positive-definite matrices $Q_i > 0$ and matrices $\bar{K}_i, i = 1, 2, \ldots, m$, such that the following inequalities,*

$$\begin{bmatrix} -Q_i & \sqrt{q_{i1}}\left(Q_1 A_i^T + \bar{K}_i^T B_i^T\right) & \cdots & \sqrt{q_{im}}\left(Q_m A_i^T + \bar{K}_i^T B_i^T\right) \\ * & -Q_1 & \cdots & 0 \\ \vdots & * & \ddots & \vdots \\ * & * & \cdots & -Q_m \end{bmatrix} < 0, \tag{2.24}$$

hold. Moreover, the controller gain can be determined by $K_i = \bar{K}_i Q_i^{-1}$.

Proof By replacing A_i in (2.21) by $A_i + B_i K_i$, the system (2.23) is stable if

$$(A_i + B_i K_i)^T\left(\sum_{j=1}^{m} q_{ij}P_j\right)(A_i + B_i K_i) - P_i < 0, \quad i, j \in \Theta, \tag{2.25}$$

which is equivalent to

$$\begin{bmatrix} -P_i & \sqrt{q_{i1}}\left(A_i^T + K_i^T B_i^T\right) P_1 & \cdots & \sqrt{q_{im}}\left(A_i^T + K_i^T B_i^T\right) P_m \\ * & -P_1 & \cdots & 0 \\ \vdots & * & \ddots & \vdots \\ * & * & \cdots & -P_m \end{bmatrix} < 0. \tag{2.26}$$

By left- and right- multiplying $\text{diag}\{P_i^{-1}, P_1^{-1}, \ldots, P_m^{-1}\}$ and its transpose to (2.26), respectively, we have

$$\begin{bmatrix} -P_i^{-1} & \sqrt{q_{i1}}P_1^{-1}\left(A_i^T + K_i^T B_i^T\right) & \cdots & \sqrt{q_{im}}P_m^{-1}\left(A_i^T + K_i^T B_i^T\right) \\ * & -P_1^{-1} & \cdots & 0 \\ \vdots & * & \ddots & \vdots \\ * & * & \cdots & -P_m^{-1} \end{bmatrix} < 0. \quad (2.27)$$

Let $P_i^{-1} = Q_i$ and $\bar{K}_i^T = Q_i K_i^T$. We see that (2.27) is the same as (2.24).

Apart from stability and control problems, the state estimation problem, also called as the filtering is another important research topic. The main purpose is to estimate the plant state by using the available measurement signals. The estimated state can be used for state monitoring when the state is not measurable. It can also be used for controller design when full state information is not available. In the last decades, many filtering approaches have been proposed such as Kalman filtering, H_2 filtering, H_∞ filtering and l_2-l_∞. It is well known that the standard Kalman filter is sensitive to modeling errors and the distribution of noise should be Gaussian white noise. In practice, the modeling error is inevitable and one may not always have the distribution of noise. We focus on the H_∞ filtering approach in this book as it requires less information than the Kalman filtering approach. To start, we consider the following system:

$$\begin{cases} x(k+1) = A_i x(k) + B_i w(k), \\ z(k) = L_i x(k), \end{cases} \quad (2.28)$$

where $x(k) \in \mathbb{R}^n$ is the state vector, $w(k) \in \mathbb{R}^m$ is the unknown disturbance and usually assumed to belong to $l_2[0, \infty)$ in the H_∞ filtering framework. $z(k) \in \mathbb{R}^p$ is the signal to be estimated, which can be a partial state vector. The measurement signal $y(k)$ is usually described by

$$y(k) = C_i x(k) + D_i w(k). \quad (2.29)$$

To estimate $z(k)$ in (2.28), one uses the following filter:

$$\begin{cases} \hat{x}(k+1) = A_{fi}\hat{x}(k) + B_{fi} y(k), \\ z_f(k) = C_{fi}\hat{x}(k), \end{cases} \quad (2.30)$$

where $\hat{x}(k) \in \mathbb{R}^n$ is the state of the filter, and $z_f \in \mathbb{R}^p$ is the estimation of $z(k)$ in (2.28). A_{fi}, B_{fi} and C_{fi} are the filter gains to be determined. Based on (2.28)–(2.30), we have the filtering error system described by

$$\begin{cases} \eta(k+1) = \tilde{A}_i \eta(k) + \tilde{B}_i w(k), \\ e(k) = \tilde{C}_i \eta(k), \end{cases} \quad (2.31)$$

where

$$\eta(k) = \begin{bmatrix} x(k) \\ \hat{x}(k) \end{bmatrix}, e(k) = z(k) - z_f(k),$$
$$\tilde{A}_i = \begin{bmatrix} A_i & 0 \\ B_{fi}C_i & A_{fi} \end{bmatrix}, \tilde{B}_i = \begin{bmatrix} B_i \\ B_{fi}D_i \end{bmatrix}, \tilde{C}_i = \begin{bmatrix} L_i & -C_{fi} \end{bmatrix}.$$

The purpose of the estimation problem is to design the filter in the form of (2.30) such that the filtering error system (2.31) is mean-square stable and achieves a prescribed H_∞ filtering performance level. That is

- system (2.31) is stochastically stable with $w(k) = 0$;
- under the zero initial conditions, $\mathbb{E}\left\{\sum_{s=0}^{t}\left[e^T(s)e(s)\right]\right\} < \gamma^2 \sum_{s=0}^{t}\left[w^T(s)w(s)\right]$ holds.

The following proposition gives a sufficient condition for the existence of such a filter.

Proposition 2.7 *The filtering error system (2.31) is asymptotically stable in the mean-square sense and with a prescribed H_∞ performance level γ, if there exist positive-definite matrices P_i such that the following inequalities are true,*

$$\begin{bmatrix} -P_i & 0 & \tilde{A}_i^T\bar{P}_i & \tilde{C}_i^T \\ * & -\gamma^2 I & \tilde{B}_i^T\bar{P}_i & 0 \\ * & * & -\bar{P}_i & 0 \\ * & * & * & -I \end{bmatrix} < 0, \tag{2.32}$$

where $\bar{P}_i = \sum_{j=1}^{m} q_{ij}P_j$.

Proof Let $V(x(k)) = x^T(k)P_{r(k)}x(k)$, $r(k) = i$ and $r(k+1) = j$, then

$$\begin{aligned} &\mathbb{E}\left\{V(x(k+1)) - V(x(k)) + e^T(k)e(k) - \gamma^2 w(k)w(k)\right\} \\ &\quad = \mathbb{E}\left\{\eta^T(k+1)\bar{P}_i\eta(k+1) - \eta^T(k)P_i\eta(k)\right\} \\ &\qquad + \mathbb{E}\left\{\left(\tilde{C}_i x(k)\right)^T\left(\tilde{C}_i x(k)\right) - \gamma^2 w(k)w(k)\right\} \\ &\quad = \mathbb{E}\left\{\left[\tilde{A}_i\eta(k) + \tilde{B}_i w(k)\right]^T\bar{P}_i\left[\tilde{A}_i\eta(k) + \tilde{B}_i w(k)\right]\right\} \\ &\qquad - \eta^T(k)P_i\eta(k) \\ &\qquad + \mathbb{E}\left\{\left(\tilde{C}_i x(k)\right)^T\left(\tilde{C}_i x(k)\right) - \gamma^2 w(k)w(k)\right\} \\ &\quad = \mathbb{E}\left\{\bar{\eta}^T(k)\left(\Omega + \Omega_1\bar{P}_i\Omega_1^T + \Omega_2\Omega_2^T\right)\bar{\eta}(k)\right\}, \end{aligned} \tag{2.33}$$

where

$$\bar{\eta}(k) = \begin{bmatrix} \eta(k) \\ w(k) \end{bmatrix}, \Omega = \begin{bmatrix} -P_i & 0 \\ * & -\gamma^2 I \end{bmatrix},$$
$$\Omega_1 = \begin{bmatrix} \tilde{A}_i^T \\ \tilde{B}_i^T \end{bmatrix}, \Omega_2 = \begin{bmatrix} \tilde{C}_i^T \\ 0 \end{bmatrix}.$$

By Lemma 2.1, it is easy to see that (2.32) guarantees $\Omega + \Omega_1 \bar{P}_i \Omega_1^T + \Omega_2 \Omega_2^T < 0$. Then, $\mathbb{E}\left\{V(x(k+1)) - V(x(k)) + e^T(k)e(k) - \gamma^2 w(k)w(k)\right\}$. By summing both sides of this inequality, we have

$$\mathbb{E}\left\{\sum_{s=0}^{t}\left[V(x(s+1)) - V(x(s)) + e^T(s)e(s) - \gamma^2 w(s)w(s)\right]\right\} < 0. \tag{2.34}$$

It follows from $V(x(0)) = 0$ and $V(x(s+1)) \geq 0$ that

$$\mathbb{E}\left\{\sum_{s=0}^{t}\left[e^T(s)e(s) - \gamma^2 w(s)w(s)\right]\right\} < 0, \tag{2.35}$$

that is

$$\mathbb{E}\left\{\sum_{s=0}^{t}\left[e^T(s)e(s)\right]\right\} < \gamma^2 \sum_{s=0}^{t}[w(s)w(s)]. \tag{2.36}$$

We can conclude that system (2.31) is mean-square stable and also has a prescribed H_∞ performance γ.

With the help of Proposition 2.7, we can determine the filter gain parameters by using the following proposition.

Proposition 2.8 *The H_∞ filtering problem is solvable if there exist positive definite matrices P_i and some matrices W_i with appropriate dimensions such that the following inequalities,*

$$\begin{bmatrix} -P_i & 0 & \Xi_1 & \Xi_3 \\ * & -\gamma^2 I & \Xi_2 & 0 \\ * & * & \tilde{P}_i & 0 \\ * & * & * & -I \end{bmatrix} < 0, \tag{2.37}$$

hold for all $i \in \Theta$. Then the filter gains can be determined by $A_{fi} = W_{3i}^{-T} A_{Fi}$, $B_{fi} = W_{3i}^{-T} B_{Fi}$, and $C_{fi} = C_{Fi}$, where

$$\Xi_1 = \begin{bmatrix} A_i^T W_{1i} + C_i^T B_{Fi}^T & A_i^T W_{2i} + C_i^T B_{Fi}^T \\ A_{Fi}^T & A_{Fi}^T \end{bmatrix},$$
$$\Xi_2 = \begin{bmatrix} B_i^T W_{1i} + D_i^T B_{Fi}^T & B_i^T W_{2i} + D_i^T B_{Fi}^T \end{bmatrix},$$
$$\Xi_3 = \begin{bmatrix} L_i^T \\ -C_{Fi}^T \end{bmatrix}, \tilde{P}_i = \sum_{j=1}^{m} q_{ij} P_j - W_i - W_i^T,$$
$$P_i = \begin{bmatrix} P_{1i} & P_{2i} \\ * & P_{3i} \end{bmatrix}, W_i = \begin{bmatrix} W_{1i} & W_{2i} \\ W_{3i} & W_{3i} \end{bmatrix}.$$

Proof By Lemma 2.3, (2.32) holds if and only if there exist matrices W_i such that

$$\begin{bmatrix} -P_i & 0 & \tilde{A}_i^T W_i & \tilde{C}_i^T \\ * & -\gamma^2 I & \tilde{B}_i^T W_i & 0 \\ * & * & \tilde{P}_i & 0 \\ * & * & * & -I \end{bmatrix} < 0. \tag{2.38}$$

Let $A_{Fi} = W_{3i}^T A_{fi}$, $B_{Fi} = W_{3i}^T B_{fi}$, $C_{Fi} = C_{fi}$, $P_i = \begin{bmatrix} P_{1i} & P_{2i} \\ * & P_{3i} \end{bmatrix}$ and $W_i = \begin{bmatrix} W_{1i} & P_{2i} \\ W_{3i} & W_{3i} \end{bmatrix}$. One sees that (2.38) is equivalent to (2.37). The proof is completed.

When the Markovian jump system approach is applied to the modeling and analysis of the NCSs, the transition probabilities should be known a prior. In some scenarios, the transition probabilities may be too expensive or even impossible to find. Then, the following switched linear system is more appropriate for such a situation.

2.4 Switched Systems

Since the switched system approach will be used to model and analyze the wireless networked systems in this book, some discussions on the switched systems are necessary. A switched system is a dynamical system that consists of a finite number of subsystems and a logical rule that orchestrates switching between these subsystems. These subsystems are usually described by a group of differential or difference equations. Unlike the Markovian jump systems in Sect. 2.2, the probabilities of the switching here are completely unknown. A simple way to classify switched systems is based on the dynamics of their subsystems, for example continuous-time or discrete-time, linear or nonlinear and so on. see Fig. 2.1.

In this book, we only consider the discrete-time switched linear systems as follows

$$x(k+1) = A_{\rho(k)} x(k), \tag{2.39}$$

where $\rho(k)$ is a switching signal and $\rho(k) \in \Omega = \{1, 2, \ldots, M\}$. The switching signal is usually piecewise constant and the subsystems are finite.

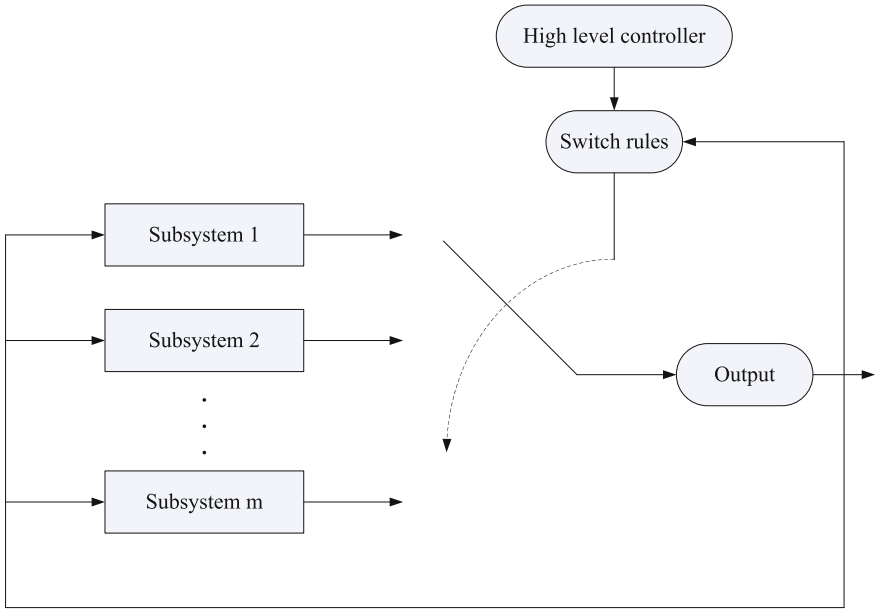

Fig. 2.1 An illustrative example of switched system

The stability analysis of a switched system is more difficult than the traditional LTI system as the dynamics of a switched system is not only determined by its continuous-time or discrete-time dynamics but also by the switching signal. The interaction of continuous-time or discrete-time dynamics with the switching signal makes the research of switched system an attractive research direction. It is interesting to see that even all subsystems are stable, the overall switched system may be unstable [4]. In the last decades, many results have been reported in literature, and three basic problems are studied: (1) Stability analysis of switched systems under arbitrary switching; (2) Stability analysis of switched systems under some useful switching signal; (3) Constructing some switching signals such that the switched systems are stable. Among them, research of Problem 2 have been recently used to analyze the networked systems when they are modeled as a switched system. For problem 2, special attention has been paid on the stability analysis of switched systems under some special switching signals. For example, Morse [5] proposed a switching signal called as the dwell time switching signal for the switched system. They showed that the system is stable provided that the system dwell on each subsystem for a fixed time interval, called as the dwell time, i.e., the switching should be slow enough. Recently, Hespanha [6] relaxed the dwell time to the average dwell time such that only the average dwell time is required to be satisfied. More specifically, for any $k > k_0$, and a given switching signal $\rho(\tau)$, $k_0 \leq \tau \leq k$, let N_ρ denote the number of switching of $\rho(\tau)$ over time interval (k_0, k). If $N_\rho \leq N_0 + (k - k_0)/T_a$ holds for $T_a > 0$ and $N_0 \geq 0$, then T_a is called the average dwell time and N_0 is the chatter

bound, which is usually set to be zero. Hespanha [6] showed that the switched system is exponentially stable if the average dwell time of the successive switching is larger than a constant value. In this book, the average dwell time approach will be used in some chapters. Now some fundamental analysis and synthesis results are presented for discrete-time switched systems.

Proposition 2.9 *For given scalars* $0 < \lambda < 1$ *and* $\mu \geq 1$, *the discrete-time switched linear system (2.39) is exponentially stable under the switching signal* $\rho(k)$, *if there exist a set of positive definite matrices* P_i, *such that the following inequalities*

$$\begin{bmatrix} -\lambda P_i & A_i^T P_i \\ * & -P_i \end{bmatrix} < 0, \tag{2.40}$$

$$P_i \leq \mu P_j, i \neq j, \tag{2.41}$$

$$T_a > T_a^* = -\frac{\ln \mu}{\ln \lambda}. \tag{2.42}$$

are true for all $i, j \in \Omega$.

Proof The switched system with average dwell time switching is known as a slowly switching system. We can define the switching time instant as $k_0 < k_1 < \cdots k_l < \cdots$. Then we construct the following piecewise Lyapunov function:

$$V_{\rho(k)}(x(k)) = x^T(k) P_{\rho(k)} x(k). \tag{2.43}$$

Then, it follows that for each $i = \rho(k)$,

$$\begin{aligned} & V_i(k+1) - \lambda V_i(k) \\ & \quad = x^T(k+1) P_i x(k+1) - \lambda x^T(k) P_i x(k) \\ & \quad = [A_i x(k)]^T P_i [A_i x(k)] - \lambda x^T(k) P_i x(k) \\ & \quad = x^T(k) \left[A_i^T P_i A_i - \lambda P_i \right] x(k). \end{aligned} \tag{2.44}$$

By (2.40), we have $A_i^T P_i A_i - \lambda P_i < 0$, which implies that $V_i(k+1) - \lambda V_i(k) < 0$. It is easy to see that

$$V_{\rho(k)}(k) \leq \lambda^{k-k_l} V_{\rho(k_l)}(k_l). \tag{2.45}$$

According to (2.41) and (2.45), and the switching sequence, we have

$$\begin{aligned} V_{\rho(k)}(k) &\leq \lambda^{k-k_l} V_{\rho(k_l)}(k_l) \\ &\leq \lambda^{k-k_l} \mu V_{\rho(k_{l-1})}(k_l) \\ &= \lambda^{k-k_l} \mu V_{\rho(k_l-1)}(k_l) \\ &\leq \cdots \\ &\leq \lambda^{k-k_0} \mu^{(k-k_0)/T_a} V_{\rho(k_0)}(k_0) \\ &= \left(\lambda \mu^{1/T_a}\right)^{(k-k_0)} V_{\rho(k_0)}(k_0). \end{aligned} \tag{2.46}$$

In addition, it follows from (2.43) that $V_{\rho(k)}(k) \geq \beta_1 \|x(k)\|^2$ and

$$V_{\rho(k)}(k) \leq \left(\lambda \mu^{1/T_a}\right)^{(k-k_0)} V_{\rho(k_0)}(k_0) \leq \left(\lambda \mu^{1/T_a}\right)^{(k-k_0)} \beta_2 \|x(k_0)\|^2, \tag{2.47}$$

which yields $\|x(k)\| \leq \sqrt{\beta_2/\beta_1}\beta^{(k-k_0)}\|x(k_0)\|^2$, where $\beta_1 = \min_{i\in\Omega} \lambda_{\min}(P_i)$, $\beta_2 = \max_{i\in\Omega} \lambda_{\max}(P_i)$ and $\beta = \lambda\mu^{1/T_a}$. Condition (2.42) guarantees $0 < \beta < 1$. Thus, the system (2.39) is exponentially stable.

Remark 2.1 we have presented an exponential stability condition for system (2.39) in Proposition 2.9. Actually, there are also some other exponential stability conditions reported in recent literature, see [7]. In this book, however, Proposition 2.9 will play an important role in the sequential analysis.

For the controller design problem, we consider the following system:

$$\begin{cases} x(k+1) = A_{\rho(k)}x(k) + B_{\rho(k)}u(k), \\ u(k) = K_{\rho(k)}x(k), \end{cases} \tag{2.48}$$

where $u(k)$ is the control input and $K_{\rho(k)}$ is the feedback gain, which is to be determined. The following algorithm can be used to determine the controller gain.

Proposition 2.10 *The discrete-time switched system (2.48) is exponentially stable if there exist positive definite matrices Q_i and matrices $\bar{K}_i$ with appropriate dimensions, such that the (2.42) and following inequalities,*

$$\begin{bmatrix} -\lambda Q_i & Q_i A_i^T + \bar{K}_i^T B_i^T \\ * & -Q_i \end{bmatrix} < 0, \tag{2.49}$$

$$Q_j \leq \mu Q_i, i \neq j, \tag{2.50}$$

hold for all $i \in \Omega$, moreover, the controller gain can be determined by $K_i = \bar{K}_i Q_i^{-1}$.

Proof By replacing the A_i by $A_i + B_i K_i$, (2.40) is written as

$$\begin{bmatrix} -\lambda P_i & (A_i + B_i K_i)^T P_i \\ * & -P_i \end{bmatrix} < 0. \tag{2.51}$$

By left- and right- multiplying diag$\{P_i^{-1}, P_i^{-1}\}$ and its transpose to (2.51), respectively, one sees that (2.51) is (2.49) by assigning $P_i^{-1} = Q_i$ and $\bar{K}_i^T = Q_i K_i^T$. By using similar manipulation, one can also have (2.50). The proof is completed.

Based on the filter design results in Sect. 2.2, one can also have the corresponding results for the switched systems, and the details are omitted. The fundamentals presented in this chapter will play an important role in the sequential chapters. Readers are encouraged to read this chapter and get to know how to analyze a Markovian jump system and a switched linear system.

2.5 Linear Matrix Inequalities

In the last decades, the linear matrix inequalities (LMIs) have emerged as a powerful tool to solve control and estimation problems that appear hard or even impossible to solve in an analytic way. Currently, several commercial or non-commercial software packages are available, with which an LMI problem can be easily solved by a simple coding. Since the main results of this book are given in terms of LMIs, some basic information is presented in this section. For more details on the LMI, we refer the readers to [1].

A typical LMI has the following form:

$$F(x) = F_0 + \sum_{i=1}^{m} x_i F_i > 0, \tag{2.52}$$

where $x_i \in \mathbb{R}^1$ is the scalar, and the symmetric matrices $F_i = F_i^T \in \mathbb{R}^{q\times q}$ are given. We call (2.52) is a strict LMI, while a non-strict LMI is $F(x) \geq 0$. In this section, we consider the strict LMI only. In the control system design, we will often encounter problems in which the variables are matrices, rather than the scalar in (2.52). We recall the results in Proposition 2.1, i.e., a continuous-time LTI system is asymptotic stable if the following inequality is true: $A^T P + PA < 0$, where $A \in \mathbb{R}^{n\times n}$ is the system matrix, and $P = P^T > 0$ is the unknown variable. The problem now is how to find a required matrix P such that the inequality is true. Here, an illustrative example is first given to show how an LMI can be described by using the Matlab LMI toolbox.

For the above system, we can use "lmivar" and "lmiterm" to describe an LMI as follows:

```
setlmis([ ])
P=lmivar(1,[4 1]);
lmiterm([1 1 1 P],A',1);
lmiterm([1 1 1 P],1,A);
lmiterm([-2 1 1 P],1,1);
lmisys=getlmis
```

Discussions: An LMI usually starts by "setlmis" and ends by "getlmis". "setlmis" is a function, which is used to start a description of LMI. The function "lmivar" is used to define the unknown matrix variable P, and the function "lmiterm" is used to describe the detail of each LMI. "getlmis" returns to the internal LMI description of "lmisys", where it is also a name stored inside the computer.

Special attention should be paid on the "lmivar". A common description of this function is

$$P = \text{lmivar(type, struct)},$$

where "type" confirms the type of the matrix P, "struct" gives the structure of this variable. Usually it has three types:

- symmetric or diagonal.
- rectangular. Then, struct=(m,n) describes the dimension.
- others.

Example 2.1 Consider an LMI with three unknown matrices P_1, P_2 and P_3, where

- P_1 is a symmetric matrix, with dimension 4×4.
- P_2 is a rectangular matrix, with dimension 3×4.
- $P_3 = \begin{bmatrix} \Delta & 0 & 0 \\ 0 & \chi_1 & 0 \\ 0 & 0 & \chi_2 I_3 \end{bmatrix}$, where Δ is a symmetric matrix with dimension 3×3, χ_1 and χ_2 are two scalars, I_3 is an identity matrix with dimension 3×3.

The above matrices can be defined by the using "lmivar" as follows:

```
setlmis([ ])
P1=lmivar(1,[4 1]);
P2=lmivar(2,[3 4]);
P3=lmivar(1,[3 1;1 0;3 0]);
```

It should be pointed out that one needs to describe the LMI with the upper-triangular part only. For example, the following LMI,

$$\begin{bmatrix} A^T X + XA & XB \\ B^T X & -I \end{bmatrix} < 0, \tag{2.53}$$

can be described by

```
lmiterm([1 1 1 X],A',1);
lmiterm([1 1 1 X],1,A);
lmiterm([1 1 2 X],1,B);
lmiterm([1 2 2 0],-1);
```

Next we discuss how to determine whether such an LMI admit a solution. The LMI toolbox provides some solvers for LMI related problems such as

- Feasibility problem.
- Minimization problem subject to LMI constraint.
- Minimization problem of generalized eigenvalue.

In this book, we deal with the first two problems. Readers are referred to [1] for the third case. We now discuss how to solve the first two problems by the LMI toolbox.

The "feasp" solver is usually described by

$$[\text{tmin, xfeas}] = \text{feasp (lmisys, options, target)}.$$

The feasibility problem is solvable, i.e., "lmisys" is feasible, provided that tmin < 0. When it is feasible, the "xfeas" gives a feasible solution to the decision variable. "target" is introduced for the target value of "tmin" such that "tmin $<$ target", then the searching process ends. Usually, target $= 0$ is used.

Consider an LTI system $\dot{x}(t) = Ax(t) + Bu(t)$ with the state matrices as

$$A = \begin{bmatrix} 0 & 1 & 0 & 0 \\ 0 & 0 & -1 & 0 \\ 0 & 0 & 0 & 1 \\ 0 & 0 & 11 & 0 \end{bmatrix}, B = \begin{bmatrix} 0 \\ 1 \\ 0 \\ 1 \end{bmatrix}.$$

We first check the stability of this system when $u = 0$. By running the following code:

```
A=[0 1 0 0;0 0 -1 0;0 0 0 1;0 0 11 0];
setlmis([ ])
P=lmivar(1,[4 1]);
lmiterm([1 1 1 P],A',1);
lmiterm([1 1 1 P],1,A);
lmiterm([-2 1 1 P],1,1);
lmisys=getlmis;
[tmin, xfeas] = feasp(lmisys)
PP=dec2mat(lmisys,xfeas,P)
```

we have

$$\text{tmin} = 1.1659e - 15,$$

which means that it is not stable. Now we use Proposition 2.3 to determine the feedback controller gain K. Based on the following code:

```
A=[0 1 0 0;0 0 -1 0;0 0 0 1;0 0 11 0];
B=[0;1;0;1];
X=lmivar(1,[4 1]);
Y=lmivar(2,[1 4]);
lmiterm([1 1 1 X],A,1);
lmiterm([1 1 1 X],1,A');
lmiterm([1 1 1 Y],B,-1);
lmiterm([1 1 1 -Y],-1,B');
lmiterm([-2 1 1 X],1,1);
lmisys=getlmis;
[tmin, xfeas] = feasp(lmisys)
XX=dec2mat(lmisys,xfeas,X);
YY=dec2mat(lmisys,xfeas,Y);
K=YY*inv(XX)
```

We obtain

$$K = \begin{bmatrix} -3.0056 & -5.8780 & 61.8612 & 13.0596 \end{bmatrix}.$$

In control system design, we may encounter some optimization problem, e.g., the disturbance attenuation level should be minimized in the H_∞ control and estimation problem. The "mincx" solver is usually adopted to the optimization problem. For example, the following optimization problem:

$$\begin{aligned} &\min c^T x \\ &s.t.\ A(x) < B(x). \end{aligned} \tag{2.54}$$

The "mincx" solver is described by

$$\left[\text{copt, xopt}\right] = \text{mincx (lmisys, } c\text{, options, xinit, target)}.$$

As in the "feasp" solver, "mincx" returns the optimal value to "xopt", which can be outputted by using the "dec2mat" function. Traditionally, "lmisys" and "c" are compulsory for the "mincx" solver, while the rest is not. We now take a numerical example to illustrate how to use the "mincx" solver.

Example 2.2 Consider the following optimization problem:

$$\begin{aligned} &\min \text{Tr(P)} \\ &s.t.\ A^T P + PA + PBB^T P + Q < 0, \end{aligned} \tag{2.55}$$

where $P = P^T$ is a unknown matrix and

$$A = \begin{bmatrix} -1 & -2 & 1 \\ 1 & 2 & 1 \\ 1 & -2 & -1 \end{bmatrix}, B = \begin{bmatrix} 1 \\ 0 \\ 1 \end{bmatrix},$$
$$Q = \begin{bmatrix} 1 & -1 & 0 \\ -1 & -3 & -12 \\ 0 & -12 & -36 \end{bmatrix}.$$

Solution: With Lemma 2.1, we formulate the following optimization problem:

$$\begin{aligned} &\min \mathrm{Tr}(P) \\ s.t. &\begin{bmatrix} A^T P + PA + Q & PB \\ B^T P & -I \end{bmatrix} < 0. \end{aligned} \tag{2.56}$$

A possible coding is given by:

```
A=[-1 -2 1;1 2 1;1 -2 -1];
B=[1;0;1];
Q=[1 -1 0;-1 -3 -12;0 -12 -36];
setlmis([ ])
P=lmivar(1,[3 1]);
lmiterm([1 1 1 P],A',1);
lmiterm([1 1 1 P],1,A);
lmiterm([1 1 1 0],Q);
lmiterm([1 1 2 P],1,B);
lmiterm([1 2 2 0],-1);
LMIs=getlmis;
c=mat2dec(LMIs,eye(3));
options=[le-5,0,0,0,0];
[copt, xopt]=mincx(LMIs,c,options);
xopt1=dec2mat(LMIs,xopt,P)
```

It gives the obtained optimal P as

$$\begin{aligned} &\text{xopt1} = \\ &\begin{matrix} -3.9278 & -12.3556 & -0.0722 \\ -12.3556 & -39.5667 & 1.5000 \\ -0.07221 & 1.5000 & -4.7834 \end{matrix} \end{aligned}$$

References

1. S. Boyd, L. Ghaoui, E. Feron, V. Balakrishnan, *Linear Matri Inequalities in Systems and Control Theory* (SIAM, Philadelphia, 1994)

2. L.H. Xie, C.E. de. Souza, Y.Y. Wang, Robust control of discrete-time uncertain dynamical systems. Automatica. **29**(4), 1133–1137 (1993)
3. M.C. de Oliveira, J. Bernussou, J.C. Geromel, A new discrete-time robust stability condition. Syst. Control lett. **37**(4), 261–265 (1999)
4. D. Liberzon, *Switching in Systems and Control* (Birkhauser, Boston, 2003)
5. A.S. Morse, Supervisory control of families of linear set-point controllers-part 1: exact matching. IEEE Trans. Autom. Control **41**(10), 1413–1431 (1996)
6. J. Hespanha, A. Morse, Stability of switched systems with average dwell time, in *Proceedings of the 38th IEEE Conference on Decision and Control* (1999), pp. 2655–2660
7. H. Lin, P.J. Antsaklis, Stability and stabilizability of switched linear systems: a survey of recent results. IEEE Trans. Autom. Control **54**(2), 308–322 (2009)

Chapter 3
H_∞ Filtering with Time-Varying Transmissions

3.1 Introduction

In this chapter, we consider the H_∞ filtering of wireless networked systems with a time-varying transmission protocol and random packet dropout. First, a switched system approach is employed to model the time-varying transmission process of each sensor. Then, the packet dropout phenomenon is modeled by a set of Bernoulli stochastic variables. The filtering error system is finally modeled as a switched system with multiple stochastic variables. With helps of the switched system approach and the Lyapunov stability theory, a sufficient condition is derived for the existence of the filter such that the filtering error system is exponentially stable in the mean-square sense with a prescribed H_∞ disturbance attenuation level. The filter gains are determined by solving an optimization problem. Two numerical examples are given to demonstrate the effectiveness of the proposed design.

3.2 Problem Statement

Consider a networked filtering system shown in Fig. 3.1. The plant is described by the following discrete-time linear time-invariant (LTI) model:

$$\begin{cases} x(k+1) = Ax(k) + Bw(k), \\ y(k) = Cx(k) + Dw(k), \end{cases} \tag{3.1}$$

where $x(k) \in \mathbb{R}^n$ is the state, $y(k) = [y_1(k) \quad y_2(k) \quad \cdots \quad y_p(k)]^T \in \mathbb{R}^p$ is the measured output, and $w(k) \in \mathbb{R}^q$ is the unknown disturbance or noise but assumed to be in $l_2[0, \infty)$. A, B, C and D are some constant matrices.

The communication procedure between the plant and the filter has two stages: local signal processing and network transfer. Local signal processing is to transmit the measurements obtained by a set of distributed sensors, which have the ability to

D. Zhang et al., *Filtering and Control of Wireless Networked Systems*,
Studies in Systems, Decision and Control 97, DOI 10.1007/978-3-319-53123-6_3

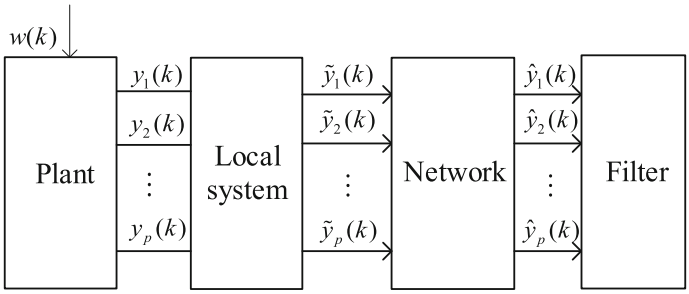

Fig. 3.1 Networked H_∞ filtering system

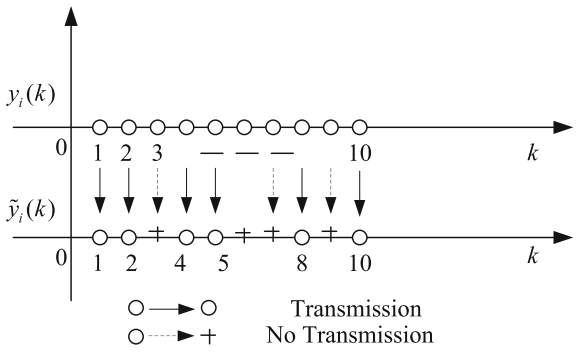

Fig. 3.2 Transmission process

measure the physical plant and to decide when to transmit the data. The transmission process is illustrated in Fig. 3.2, where $y_i(k)$, $i = 1, 2, \ldots, p$, is the measurement of a physical variable. And $\tilde{y}_i(k)$ is the output signal after the local transmission process and it can be described as

- transmitted. Then, the signal to the network is given by $\tilde{y}_i(k) = y_i(k)$; or
- not transmitted. Then, there is no signal to network. $\tilde{y}_i(k)$ is empty.

In this chapter, we assume that the largest transmission time interval is N time steps, that is, there must be one transmission for each output over N time steps.

The second stage of communication is the signal transfer through the wireless communication network. Once the transmission occurs, $\tilde{y}_i(k) = y_i(k)$ is sent to the network. There are two possible situations for network transfer:

- the transfer succeeds. Then, the input to the filter is given by $\hat{y}_i(k) = \tilde{y}_i(k) = y_i(k)$; or
- the transfer fails. This is called the packet dropout. Then, the signal is lost due to the unreliability of the network and the measurement signal will not be received by the filter. There is no input to the filter. $\hat{y}_i(k)$ is empty.

Figure. 3.3 shows this network transfer process.

A filter works at each time instant and it must be fed with some non-empty input, $\bar{y}(k) = [\,\bar{y}_1(k)\ \bar{y}_2(k)\ \cdots\ \bar{y}_p(k)\,]^T$. This input should never have any empty element.

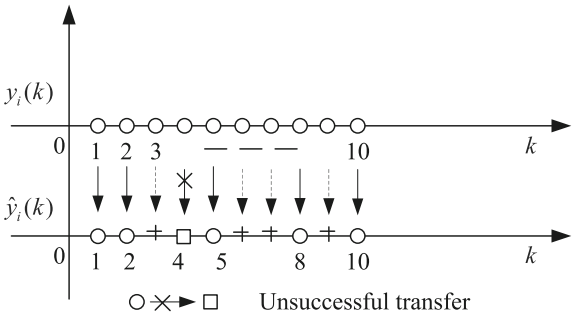

Fig. 3.3 Packet dropout

Obviously, if there is no measurement transmission or the network transfer fails, no signal comes to the filter and the input to the filter has to be pre-defined by some rules, and in such a case, $\bar{y}_i(k)$ is not same as $\hat{y}_i(k)$. It is reasonable to assume that the filter can store the last-received signal in its buffer. Our filter pre-processing will generate $\bar{y}_i(k)$ as follows:

- if there is a measurement transmission and network transfer is successful, there is non-empty $\hat{y}_i(k)$ and $\bar{y}_i(k) = \hat{y}_i(k) = \tilde{y}_i(k) = y_i(k)$;
- otherwise, the input to the filter is assigned as $\bar{y}_i(k) = \bar{y}_i(k-1)$, or as the stored last-received signal, that is, one possible element in this set of $\{y_i(k-1), \ldots y_i(k-N+1)\}$.

To model all possible cases described above, we first determine the latest signal received and stored in the filter, assuming that network is perfect, and then incorporate the networked packet dropout phenomenon. In the case of perfect networking, the network block acts as a transfer function with identity matrix, or equivalently, the network block can be removed, and Fig. 3.1 reduces to Fig. 3.4. Then, when the measurement is transmitted, the signal always arrives at the filter successfully. Let $\breve{y}_i(k)$ be the signal stored in the filter. Since the largest transmission interval is limited to be N time steps, it is easy to see that the signal $\breve{y}_i(k)$ in buffer must be one member of $\{y_i(k), y_i(k-1), \cdots y_i(k-N+1)\}$, $i = 1, 2, \ldots p$. Define

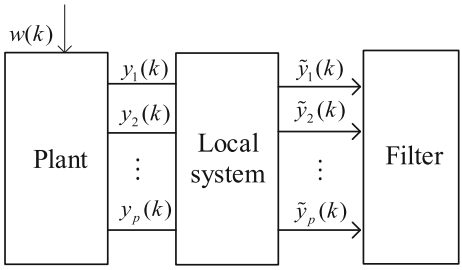

Fig. 3.4 Filtering system without network

$$X(k) = [\, x^T(k)\ x^T(k-1) \cdots x^T(k-N+1)\,]^T,$$
$$W(k) = [\, w^T(k)\ w^T(k-1) \cdots w^T(k-N+1)\,]^T,$$

we have

$$\breve{y}_i(k) = C_i E_{ij}(k) X(k) + D_i H_{ij}(k) W(k), \tag{3.2}$$

where C_i and D_i are the i-th row of matrix C and D, respectively. $E_{ij}(k)$ is an $n \times nN$ matrix with its j-th n by n sub-matrix being an identity matrix and the rest being zero, and $H_{ij}(k)$ a q by qN matrix with its j-th q by q sub-matrix being an identity matrix and the rest being zero, $j = 1, 2, \ldots, N$. Let

$$\begin{aligned}
&\sigma_i(k) \in \{1, 2, \ldots, N\}, i = 1, 2, \ldots, p,\\
&\sigma(k) = [\, \sigma_1(k)\ \sigma_2(k) \cdots \sigma_p(k)\,]^T,\\
&\tilde{E}_{\sigma(k)} = [\, E^T_{1,\sigma_1(k)}\ E^T_{2,\sigma_2(k)} \cdots E^T_{p,\sigma_p(k)}\,]^T,\\
&\tilde{H}_{\sigma(k)} = [\, H^T_{1,\sigma_1(k)}\ H^T_{2,\sigma_2(k)} \cdots H^T_{p,\sigma_p(k)}\,]^T.
\end{aligned}$$

We have the following augmented measurement signal:

$$\breve{y}(k) = \tilde{C} \tilde{E}_{\sigma(k)} X(k) + \tilde{D} \tilde{H}_{\sigma(k)} W(k), \tag{3.3}$$

where $\tilde{C} = \mathrm{diag}\{C_1, C_2, \ldots, C_p\}$ and $\tilde{D} = \mathrm{diag}\{D_1, D_2, \ldots, D_p\}$. Note that the total number of possible numerical realizations of $\sigma(k)$ is N^p, which corresponds to the total combinations of N values of each of p variable $\sigma_i(k)$. Defining the set $\Lambda = \{1, 2, \ldots, N^p\}$, we can view $\sigma(k)$ as the signal which takes one combination from the set Λ and specify one particular case of $(\tilde{E}_{\sigma(k)}, \tilde{H}_{\sigma(k)})$ and thus one case of (3.3). Therefore, the system (3.3) becomes a switched system, where $\sigma(k)$ is viewed as the switching signal.

We now model the process with both time-varying transmission rates and random packet dropout. In this paper, the binary stochastic variable method is adopted to model the random packet dropout phenomenon. Let p stochastic variables, $\alpha_i(k)$, $i = 1, 2, \ldots, p$, be mutually uncorrelated. In this chapter, $\alpha_i(k) \in \{1, 0\}$, and $\alpha_i(k) = 1$ mean that a successful transfer, while $\alpha_i(k) = 0$ otherwise. For filter design, the successful transmission rate $Prob\{\alpha_i(k) = 1\} = \mathbb{E}\{\alpha_i(k)\} = \bar{\alpha}_i$ is assumed to be known. Define

$$\Pi_{\sigma(k)}(k) = \mathrm{diag}\{\alpha_1(k - \sigma_1(k) + 1), \ldots, \alpha_p(k - \sigma_p(k) + 1)\},$$

and let $\bar{\Pi}_l = \mathbb{E}\{\Pi_l(k)\}, l \in \Lambda$. Then, taking the filter pre-processing into consideration under possible packet dropouts, the actual input to the filter is given by

$$\bar{y}(k) = \Pi_{\sigma(k)}(k) \breve{y}(k) + (I - \Pi_{\sigma(k)}(k)) \bar{y}(k-1), \tag{3.4}$$

which by (3.3), becomes

$$\bar{y}(k) = \Pi_{\sigma(k)}(k)\left[\tilde{C}\tilde{E}_{\sigma(k)}X(k) + \tilde{D}\tilde{H}_{\sigma(k)}W(k)\right] + (I - \Pi_{\sigma(k)}(k))\bar{y}(k-1). \tag{3.5}$$

In this chapter, we aim to estimate the signal:

$$z(k) = Lx(k), \tag{3.6}$$

where L is a constant matrix. To this end, we construct the following filter:

$$\begin{cases} x_f(k+1) = A_f x_f(k) + B_f \bar{y}(k), \\ z_f(k) = C_f x_f(k), \end{cases} \tag{3.7}$$

where $x_f(k) \in \mathbb{R}^n$ is the state of filter, $\bar{y}(k) \in \mathbb{R}^p$ is the filter input defined as before and $z_f(k) \in \mathbb{R}^l$ is the estimated signal. A_f, B_f and C_f are filter gains to be determined.

By the lifting technique, the state equation (3.1) can be augmented as

$$\begin{cases} X(k+1) = \tilde{A}X(k) + \tilde{B}W(k), \\ z(k) = \tilde{L}X(k), \end{cases} \tag{3.8}$$

where $\tilde{A} = \begin{bmatrix} A & 0 \\ I_{(N-1)\times(N-1)} & 0 \end{bmatrix}$, $\tilde{B} = \text{diag}\{B, 0, \ldots, 0\}$, and $\tilde{L} = [\, L \; 0 \cdots 0 \,]$.

Denote $\eta(k) = [\, X^T(k) \; x_f^T(k) \; \bar{y}^T(k-1) \,]^T$ and $e(k) = z(k) - z_f(k)$. We have the following filtering error system for each $l \in \Lambda$:

$$\begin{cases} \eta(k+1) = (\breve{A}_l + \breve{C}_l)\eta(k) + (\breve{B}_l + \breve{D}_l)W(k), \\ e(k) = \bar{L}\eta(k), \end{cases} \tag{3.9}$$

where

$$\breve{A}_l = \begin{bmatrix} \tilde{A} & 0 & 0 \\ B_f\bar{\Pi}_l\tilde{C}\tilde{E}_l & A_f & B_f(I - \bar{\Pi}_l) \\ \bar{\Pi}_l\tilde{C}\tilde{E}_l & 0 & (I - \bar{\Pi}_l) \end{bmatrix}, \tilde{B}_l = \begin{bmatrix} \tilde{B} \\ B_f\bar{\Pi}_l\tilde{D}\tilde{H}_l \\ \bar{\Pi}_l\tilde{D}\tilde{H}_l \end{bmatrix},$$

$$\breve{C}_l = \begin{bmatrix} 0 & 0 & 0 \\ B_f(\Pi_l(k) - \bar{\Pi}_l)\tilde{C}\tilde{E}_l & 0 & B_f(\bar{\Pi}_l - \Pi_l(k)) \\ (\Pi_l(k) - \bar{\Pi}_l)\tilde{C}\tilde{E}_l & 0 & (\bar{\Pi}_l - \Pi_l(k)) \end{bmatrix},$$

$$\breve{D}_l = \begin{bmatrix} 0 \\ B_f(\Pi_l(k) - \bar{\Pi}_l)\tilde{D}\tilde{H}_l \\ (\Pi_l(k) - \bar{\Pi}_l)\tilde{D}\tilde{H}_l \end{bmatrix}, \bar{L} = [\, \tilde{L} \; -C_f \; 0 \,].$$

The system (3.9) is a switched system with some stochastic parameters, where $\sigma(k)$ serves as the switching signal. In this chapter, the average dwell time approach will be utilized to analyze such a system. For simplicity but without loss of generality, the chatter bound N_0 is set to 0 in the subsequent development. We recall the following definitions.

Definition 3.1 The system (3.9) with $w(k) = 0$ is said to be exponentially stable in the mean-square sense under switching signal $\sigma(k)$, if there exist some scalars $K > 0$ and $0 < \chi < 1$, such that the solution $\eta(k)$ of system (3.9) satisfies $\mathbb{E}\{\|\eta(k)\|\} < K\chi^{(k-k_0)}\|\eta(k_0)\|, \forall k \geq k_0$.

Definition 3.2 The system (3.9) is said to be exponentially stable in the mean-square sense with an exponential H_∞ performance $\tilde{\gamma}$, if it is exponentially stable and under zero initial condition, $\sum_{s=0}^{+\infty}\mathbb{E}\{e^T(s)e(s)\} \leq \sum_{s=0}^{+\infty}\tilde{\gamma}^2 w^T(s)w(s)$ holds for all nonzero $w(k) \in l_2[0,\infty)$.

3.3 Filter Analysis and Design

In this section, a novel sufficient condition for the exponential stability and H_∞ performance of system (3.9) is presented as follows.

Theorem 3.1 *For given scalars $0 < \lambda < 1, \mu > 1, 1 < \bar{\lambda} < 1/\lambda$, the filtering error system (3.9) is mean-square exponentially stable with a prescribed H_∞ performance level $\tilde{\gamma} = \tau\sqrt{\frac{N(1-\lambda)}{1-\lambda\bar{\lambda}}}$, if there exists a matrix $P_l > 0$ such that the following inequalities*

$$\begin{aligned}\Omega_l = &\begin{bmatrix} -\lambda P_l + \bar{L}^T\bar{L} & 0 \\ 0 & -\tau^2 I \end{bmatrix} + \begin{bmatrix} \bar{A}_l^T \\ \bar{B}_l^T \end{bmatrix} P_l[\,\bar{A}_l \;\; \bar{B}_l\,] \\ &+ \sum_{i=1}^{p}\theta_i^2\begin{bmatrix} W_{2l}^T\Phi_i W_1^T \\ \tilde{H}_l^T\tilde{D}^T\Phi_i W_1^T \end{bmatrix} P_l[\,W_1\Phi_i W_{2l} \;\; W_1\Phi_i\tilde{D}\tilde{H}_l\,] < 0,\end{aligned} \tag{3.10}$$

$$P_l \leq \mu P_v, \tag{3.11}$$

$$T_a > T_a^* = \frac{\ln\mu}{\ln\bar{\lambda}}, \tag{3.12}$$

hold for all $l, v \in \Lambda, l \neq v$, where

$$\begin{aligned}&\bar{A}_l = \begin{bmatrix} \tilde{A} & 0 & 0 \\ B_f\bar{\Pi}\tilde{C}\tilde{E}_l & A_f & B_f(I-\bar{\Pi}) \\ \bar{\Pi}\tilde{C}\tilde{E}_l & 0 & (I-\bar{\Pi}) \end{bmatrix}, \bar{B}_l = \begin{bmatrix} \tilde{B} \\ B_f\bar{\Pi}\tilde{D}\tilde{H}_l \\ \bar{\Pi}\tilde{D}\tilde{H}_l \end{bmatrix}, \\ &W_1 = \begin{bmatrix} 0 \\ B_f \\ I \end{bmatrix}, W_{2l} = [\,\tilde{C}\tilde{E}_l \; 0 \; -I\,], \\ &\Phi_i = \mathrm{diag}\{\underbrace{0, 0, \cdots 0}_{i-1}, 1, 0, \ldots 0\}, \theta_i = \sqrt{\bar{\alpha}_i(1-\bar{\alpha}_i)}, \\ &\bar{\Pi} = \mathrm{diag}\{\bar{\alpha}_1, \bar{\alpha}_2, \ldots \bar{\alpha}_p\}.\end{aligned}$$

Proof We first consider the exponential stability of the filtering error system with $W(k) = 0$. To do so, we choose the Lyapunov functional $V_l(k) = \eta^T(k) P_l \eta(k)$. Then, one sees that

$$\begin{aligned}
&\mathbb{E}\{V_l(k+1) - \lambda V_l(k)\} \\
&= \mathbb{E}\left\{\eta^T(k+1) P_l \eta(k+1) - \lambda \eta^T(k) P_l \eta(k)\right\} \\
&= \mathbb{E}\left\{[(\breve{A}_l + \breve{C}_l)\eta(k)]^T P_l [(\breve{A}_l + \breve{C}_l)\eta(k)] - \lambda \eta^T(k) P_l \eta(k)\right\} \\
&= \eta^T(k)\left[\breve{A}_l^T P_l \breve{A}_l - \lambda P_l\right]\eta(k) + \mathbb{E}\left\{\eta^T(k)\left[\breve{C}_l^T P_l \breve{C}_l\right]\eta(k)\right\}.
\end{aligned} \tag{3.13}$$

It follows from the definition of the stochastic variables $\alpha_i(k)$ that $\mathbb{E}\{\Pi_l(k)\} = \mathbb{E}\{\Pi(k)\} = \bar{\Pi}$. We obtain

$$\mathbb{E}\{\breve{A}_l^T P_l \breve{A}_l\} = \mathbb{E}\{\bar{A}_l^T P_l \bar{A}_l\}, \tag{3.14}$$

$$\mathbb{E}\{\breve{C}_l^T P_l \breve{C}_l\} = \sum_{i=1}^{p} \theta_i^2 (W_1 \Phi_i W_{2l})^T P_l (W_1 \Phi_i W_{2l}). \tag{3.15}$$

Then, it follows that

$$\begin{aligned}
&\mathbb{E}\{V_l(k+1) - \lambda V_l(k)\} \\
&\le \eta^T(k)\left(\bar{A}_l^T P_l \bar{A}_l - \lambda P_l + \sum_{i=1}^{p} \theta_i^2 (W_1 \Phi_i W_{2l})^T P_l (W_1 \Phi_i W_{2l})\right)\eta(k).
\end{aligned} \tag{3.16}$$

It is easy to see that (3.10) guarantees $\mathbb{E}\{V_l(k+1) - \lambda V_l(k)\} < 0$. For any arbitrary switching signal $\sigma(k)$, and any integer $k > 0$, let $0 = k_0 < k_1 < \cdots k_m < k$, be the switching points over the time interval $[k_0, k)$. Then, we obtain

$$\mathbb{E}\{V_{\sigma(k)}(k)\} \le \lambda^{k-k_m} \mathbb{E}\{V_{\sigma(k_m)}(k_m)\}. \tag{3.17}$$

By (3.11) and (3.17), one has

$$\begin{aligned}
\mathbb{E}\{V_{\sigma(k)}(k)\} &\le \lambda^{k-k_m} \mathbb{E}\{V_{\sigma(k_m)}(k_m)\} \\
&\le \lambda^{k-k_m} \mu \mathbb{E}\{V_{\sigma(k_{m-1})}(k_m)\} \\
&= \lambda^{k-k_m} \mu \mathbb{E}\{V_{\sigma(k_m-1)}(k_m)\} \\
&\le \cdots \le \lambda^{k-k_0} \mu^{(k-k_0)/T_a} \mathbb{E}\{V_{\sigma(k_0)}(k_0)\} \\
&= (\lambda \mu^{1/T_a})^{(k-k_0)} \mathbb{E}(V_{\sigma(k_0)}(k_0)).
\end{aligned} \tag{3.18}$$

In addition, for the constructed Lyapunov functional, one can easily see that $\mathbb{E}\{V_{\sigma(k)}(k)\} \ge \beta_1 \mathbb{E}\{\|\eta(k)\|^2\}$ and

$$\begin{aligned}\mathbb{E}\{V_{\sigma(k)}(k)\} &\le (\lambda\mu^{1/T_a})^{(k-k_0)}\mathbb{E}\{V_{\sigma(k_0)}(k_0)\}\\ &\le (\chi^2)^{(k-k_0)}\beta_2\,\|\eta(k_0)\|^2,\end{aligned} \tag{3.19}$$

which yields $\mathbb{E}\{\|\eta(k)\|^2\} \le \frac{\beta_2}{\beta_1}\chi^{2(k-k_0)}\,\|\eta(k_0)\|^2$, where $\beta_1 = \min_{l\in\Lambda}\lambda_{\min}(P_l)$, $\beta_2 = \max_{l\in\Lambda}\lambda_{\max}(P_l)$, and $\chi = \sqrt{\lambda\mu^{1/T_a}}$. Therefore, one can readily obtain $\chi < 1$ from condition (3.12). According to Definition 3.1, the filtering error system (3.9) is exponentially stable in the mean-square sense with $W(k) = 0$.

We now consider the H_∞ performance of system (3.9). With a similar argument to the above, we have

$$\mathbb{E}\{V_l(k+1) - \lambda V_l(k) + \Gamma(k)\} = \xi^T(k)\Omega_l\xi(k), \tag{3.20}$$

where $\Gamma(k) = e^T(k)e(k) - \tau^2 W^T(k)W(k)$ and $\xi(k) = [\,\eta^T(k)\ \ W^T(k)\,]^T$. Condition (3.10) guarantees

$$\mathbb{E}\{V_l(k+1) - \lambda V_l(k) + \Gamma(k)\} < 0. \tag{3.21}$$

Applying (3.21) recursively gives

$$\mathbb{E}\{V_l(k)\} \le \mathbb{E}\{\lambda^{k-k_0}V_l(k_0)\} - \sum_{s=k_0}^{k-1}\lambda^{k-s-1}\mathbb{E}\{\Gamma(s)\}, \tag{3.22}$$

where $\Gamma(k) = e^T(k)e(k) - \tau^2 W^T(k)W(k)$. It follows from (3.11) and (3.22), that

$$\begin{aligned}&\mathbb{E}\{V_{\sigma(k)}(k)\}\\ &\le \lambda^{k-k_m}\mathbb{E}\{V_{\sigma(k)}(k_m)\} - \sum_{s=k_m}^{k-1}\lambda^{k-s-1}\mathbb{E}\{\Gamma(s)\}\\ &\le \lambda^{k-k_m}\mu\mathbb{E}\{V_{\sigma(k_{m-1})}(k_m)\} - \sum_{s=k_m}^{k-1}\lambda^{k-s-1}\mathbb{E}\{\Gamma(s)\}\\ &+ \lambda^{k-k_m}\mu[\lambda^{k_m-k_{m-1}}\mathbb{E}\{V_{\sigma(k_{m-1})}(k_{m-1})\} - \sum_{s=k_{m-1}}^{k_m-1}\lambda^{k_m-s-1}\mathbb{E}\{\Gamma(s)\}]\\ &- \sum_{s=k_m}^{k-1}\lambda^{k-s-1}\mathbb{E}\{\Gamma(s)\}\\ &\le \cdots \le \lambda^{k-k_0}\mu^{N_\sigma(k_0,k)}V_{\sigma(k_0)}(k_0) - \lambda^{k-k_m}\mu^{N_\sigma(k_0,k)}\sum_{s=k_0}^{k_1-1}\lambda^{k_1-s-1}\mathbb{E}\{\Gamma(s)\}\\ &- \lambda^{k-k_2}\mu^{N_\sigma(k_1,k)}\sum_{s=k_1}^{k_2-1}\lambda^{k_2-s-1}\mathbb{E}\{\Gamma(s)\}\cdots - \sum_{s=k_m}^{k-1}\lambda^{k-s-1}\mathbb{E}\{\Gamma(s)\}\end{aligned}$$

$$= \lambda^{k-k_0}\mu^{N_\sigma(k_0,k)}V_{\sigma(k_0)}(k_0) - \sum_{s=k_0}^{k-1}\mu^{N_\sigma(s,k-1)}\lambda^{k-s-1}\mathbb{E}\{\Gamma(s)\}. \tag{3.23}$$

Under the zero initial condition, we have

$$\sum_{s=k_0}^{k-1}\mu^{N_\sigma(s,k-1)}\lambda^{k-s-1}\mathbb{E}\{\Gamma(s)\} \le 0. \tag{3.24}$$

With the average dwell time condition (3.12), it is easy to see

$$\frac{N_\sigma(s,k-1)}{k-s-1} < \frac{\ln\bar{\lambda}}{\ln\mu}. \tag{3.25}$$

Since $\mu > 1$, we have $\ln\mu^{N_\sigma(s,k-1)} < \ln\bar{\lambda}^{k-s-1}$, and

$$1 < \mu^{N_\sigma(s,k-1)} < \bar{\lambda}^{k-s-1}. \tag{3.26}$$

It follows from (3.26) that

$$\sum_{s=k_0}^{k-1}\mu^{N_\sigma(s,k-1)}\lambda^{k-s-1}\mathbb{E}\{e^T(s)e(s)\} \le \tau^2\sum_{s=k_0}^{k-1}\mu^{N_\sigma(s,k-1)}\lambda^{k-s-1}W^T(s)W(s). \tag{3.27}$$

By (3.27), one can see that

$$\begin{aligned}
&\textstyle\sum_{s=k_0}^{k-1}\lambda^{k-s-1}\mathbb{E}\{e^T(s)e(s)\} \\
&\quad < \textstyle\sum_{s=k_0}^{k-1}\mu^{N_\sigma(s,k-1)}\lambda^{k-s-1}\mathbb{E}\{e^T(s)e(s)\} \\
&\quad \le \tau^2\textstyle\sum_{s=k_0}^{k-1}\mu^{N_\sigma(s,k-1)}\lambda^{k-s-1}W^T(s)W(s) \\
&\quad < \tau^2\sum_{s=k_0}^{k-1}(\bar{\lambda}\lambda)^{k-s-1}W^T(s)W(s).
\end{aligned} \tag{3.28}$$

Summing (3.28) from $k = k_0 + 1$ to $k = \infty$ and changing the order of summation yield

$$\sum_{s=k_0}^{+\infty}\mathbb{E}\{e^T(s)e(s)\}\sum_{k=s+1}^{+\infty}\lambda^{k-s-1} < \tau^2\sum_{s=k_0}^{+\infty}W^T(s)W(s)\sum_{k=s+1}^{+\infty}(\lambda\bar{\lambda})^{k-s-1}. \tag{3.29}$$

Since $\sum_{k=s+1}^{+\infty} \lambda^{k-s-1} = \frac{1}{1-\lambda}$ and $\sum_{k=s+1}^{+\infty} (\lambda\bar{\lambda})^{k-s-1} = \frac{1}{1-\lambda\bar{\lambda}}$, we have

$$\sum_{s=k_0}^{+\infty} \mathbb{E}\{e^T(s)e(s)\} < \gamma^2 \sum_{s=k_0}^{+\infty} W^T(s)W(s), \tag{3.30}$$

where $\gamma = \tau\sqrt{\frac{(1-\lambda)}{1-\lambda\bar{\lambda}}}$. It is noted that $\bar{\lambda} < \frac{1}{\lambda}$, which ensures $\gamma > 0$. Thus, one has $\sum_{s=0}^{+\infty} \mathbb{E}\{e^T(s)e(s)\} \le \gamma^2 \sum_{s=0}^{+\infty} W^T(s)W(s) = \tilde{\gamma}^2 \sum_{s=0}^{+\infty} w^T(s)w(s)$, where $\tilde{\gamma}^2 = N\gamma^2$. This completes the proof.

Remark 3.1 The condition (3.12) implies that the variation rate of different transmissions should be bounded by $\frac{\ln\bar{\lambda}}{\ln\mu}$. Note that the decay rate of the filtering error system, χ, is explicitly determined by the variation rate, and thus, relation between the filtering performance and the variation rate of different scheduling is established. It should be pointed out that the transmission scheduling can be arbitrary if one chooses some appropriate μ and $\bar{\lambda}$ such that $T_a^* < 1$, which enables us to use our method for the event-driven transmission.

Remark 3.2 In Theorem 3.1, the H_∞ performance level is given by $\tilde{\gamma} = \tau\sqrt{\frac{N(1-\lambda)}{1-\lambda\bar{\lambda}}}$. It is interesting to see that the larger N is, the worse H_∞ performance is. This relation is practical as the larger N is, the less data arrive at the remote filter.

Based on Theorem 3.1, we now discuss how to determine the filter gains. The main procedure is presented in the following theorem.

Theorem 3.2 *For given scalars $0 < \lambda < 1, \mu > 1, 1 < \bar{\lambda} < 1/\lambda$, if there exist a matrix $P_l > 0$ and any matrix G_l of appropriate dimensions, such that the following inequalities,*

$$\begin{bmatrix} -\lambda P_l & 0 & \Psi_{1l} & \hat{L}^T & \theta_1\Omega_{1l} & \cdots & \theta_p\Omega_{pl} \\ * & -\tau^2 I & \Psi_{2l} & 0 & \theta_1\Gamma_{1l} & \cdots & \theta_p\Gamma_{pl} \\ * & * & T_l & 0 & 0 & \cdots & 0 \\ * & * & * & -I & 0 & \cdots & 0 \\ * & * & * & * & T_l & \cdots & 0 \\ * & * & * & * & * & \ddots & \vdots \\ * & * & * & * & * & \cdots & T_l \end{bmatrix} < 0, \tag{3.31}$$

(3.11) and (3.12) hold for all $l, v \in \Lambda, l \neq v$, then, the filtering problem is solvable, and the filter gains are given by $A_f = G_4^{-T} A_F$, $B_f = G_4^{-T} B_F$ and $C_f = C_F$, where,

$$\Psi_{1l} = \begin{bmatrix} \tilde{A}^T G_{1l} + \tilde{E}_l^T \tilde{C}^T \bar{\Pi}(B_F^T + G_{5l}) F_l \\ A_F^T F_l \\ (I - \bar{\Pi})(B_F^T + G_{5l}) F_l \end{bmatrix}$$

$$\begin{bmatrix} \tilde{A}^T G_{2l} + \tilde{E}_l^T \tilde{C}^T \bar{\Pi}(B_F^T + G_{6l}) & \tilde{A}^T G_{3l} + \tilde{E}_l^T \tilde{C}^T \bar{\Pi} G_{7l} \\ A_F^T & 0 \\ (I - \bar{\Pi})(B_F^T + G_{6l}) & (I - \bar{\Pi}) G_{7l} \end{bmatrix},$$

$$\Psi_{2l} = \begin{bmatrix} \tilde{B}^T G_{1l} + \tilde{H}_l^T \tilde{D}^T \bar{\Pi}(B_F^T + G_{5l}) F_l \\ \tilde{B}^T G_{2l} + \tilde{H}_l^T \tilde{D}^T \bar{\Pi}(B_F^T + G_{6l}) \quad \tilde{B}^T G_{3l} + \tilde{H}_l^T \tilde{D}^T \bar{\Pi} G_{7l} \end{bmatrix},$$

$$\Omega_{il} = \begin{bmatrix} \tilde{E}_l^T \tilde{C}^T \Phi_i (B_F^T + G_{5l}) F_l & \tilde{E}_l^T \tilde{C}^T \Phi_i (B_F^T + G_{6l}) & \tilde{E}_l^T \tilde{C}^T \Phi_i G_{7l} \\ 0 & 0 & 0 \\ -\Phi_i (B_F^T + G_{5l}) F_l & -\Phi_i (B_F^T + G_{6l}) & -\Phi_i G_{7l} \end{bmatrix},$$

$$\Gamma_{il} = \begin{bmatrix} \tilde{H}_l^T \tilde{D}^T \Phi_i (B_F^T + G_{5l}) F_l & \tilde{H}_l^T \tilde{D}^T \Phi_i (B_F^T + G_{6l}) & \tilde{H}_l^T \tilde{D}^T \Phi_i G_{7l} \end{bmatrix},$$

$$T_l = P_l - G_l - G_l^T, \hat{L} = [\tilde{L} \ -C_F \ 0],$$

$$P_l = \begin{bmatrix} P_{1l} & P_{2l} & P_{3l} \\ * & P_{4l} & P_{5l} \\ * & * & P_{6l} \end{bmatrix}, G_l = \begin{bmatrix} G_{1l} & G_{2l} & G_{3l} \\ G_4 F_l & G_4 & 0 \\ G_{5l} F_l & G_{6l} & G_{7l} \end{bmatrix},$$

and F_l is the last n row elements of $\tilde{E}_l$.

Proof By Lemma 2.2, an equivalent form of matrix inequality (3.10) is given by introducing the variable G_l as

$$\begin{bmatrix} \Theta_{11l} & \Theta_{12l} \\ * & \Theta_{22l} \end{bmatrix} < 0, \tag{3.32}$$

where

$$\Theta_{11l} = \begin{bmatrix} -\lambda P_l & 0 & \bar{A}_l^T G_l & \bar{L}^T \\ * & -\tau^2 I & \bar{B}_l^T G_l & 0 \\ * & * & T_l & 0 \\ * & * & * & -I \end{bmatrix},$$

$$\Theta_{12l} = \begin{bmatrix} \theta_1 W_{2l}^T \Phi_1 W_1^T G_l & \cdots & \theta_p W_{2l}^T \Phi_p W_1^T G_l \\ \theta_1 \tilde{H}_{2l}^T \tilde{D}^T \Phi_1 W_1^T G_l & \cdots & \theta_1 \tilde{H}_{2l}^T \tilde{D}^T \Phi_p W_1^T G_l \\ 0 & \cdots & 0 \\ 0 & \cdots & 0 \end{bmatrix},$$

$$\Theta_{22l} = \text{diag}\{\underbrace{T_l, T_l, \ldots, T_l}_{p}\}.$$

Construct P_l and G_l in (3.32) with the ones in Theorem 3.2, one can easily obtain Theorem 3.2. This completes the proof.

Remark 3.3 In order to obtain the minimum H_∞ performance $\tilde{\gamma}^*$, one can solve the following optimization problem:

$$\begin{array}{c} \min \quad \rho \\ \text{s.t. (3.11), (3.12) and (3.31) with } \rho{=}\tau^2 \end{array} \tag{3.33}$$

and find the minimum H_∞ performance $\tilde{\gamma}^*$ by $\tilde{\gamma}^* = \sqrt{\frac{\rho^* N(1-\lambda)}{1-\lambda\bar{\lambda}}}$.

3.4 Illustrative Examples

Example 3.1 Consider a spring-mass system, which was studied in [1]. Its structure is shown in Fig. 3.5, where m_1 and m_2, x_1 and x_2 are the weights and positions of mass 1 and mass 2, respectively. k_1 and k_2 are the spring constants of spring 1 and spring 2, respectively. c denotes the viscous friction coefficient between the masses and the horizontal surface. The plant noise is denoted by v_1. It is assumed that x_1 and x_2 are measured with noise v_2. By denoting $x(t) = [\, x_1(t)\ x_2(t)\ \dot{x}_1(t)\ \dot{x}_2(t)\,]^T$ and $w(t) = [\, v_1(t)\ v_2(t)\,]^T$, we obtain the following state-space model for this spring-mass system:

$$\begin{cases} \dot{x}(t) = \begin{bmatrix} 0 & 0 & 1 & 0 \\ 0 & 0 & 0 & 1 \\ -\frac{k_1+k_2}{m_1} & \frac{k_2}{m_1} & -\frac{c}{m_1} & 0 \\ \frac{k_2}{m_2} & -\frac{k_2}{m_2} & 0 & -\frac{c}{m_2} \end{bmatrix} x(t) + \begin{bmatrix} 0 & 0 \\ 0 & 0 \\ \frac{1}{m_1} & 0 \\ \frac{1}{m_2} & 0 \end{bmatrix} w(t), \\ y(t) = \begin{bmatrix} 1 & 0 & 0 & 0 \\ 0 & 1 & 0 & 0 \end{bmatrix} x(t) + \begin{bmatrix} 0 & d \\ 0 & d \end{bmatrix} w(t), \end{cases} \tag{3.34}$$

where d is constant. Our objective is to estimate the signal $z = x_1 + x_2$ with $m_1 = 1, m_2 = 0.5, k_1 = k_2 = 1, c = 0.5, d = 0.1$. The above dynamic system can be described by the following continuous-time LTI system:

$$\dot{x}(t) = A_c x(t) + B_c w(t), \tag{3.35}$$

where

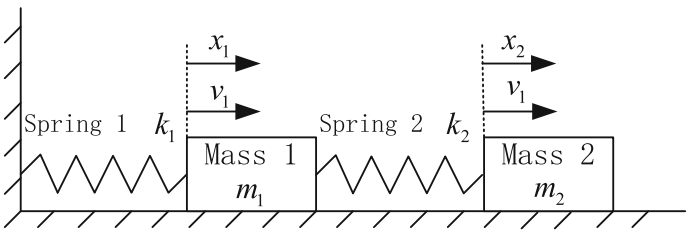

Fig. 3.5 Spring mass system

$$A_c = \begin{bmatrix} 0 & 0 & 1 & 0 \\ 0 & 0 & 0 & 1 \\ -2 & 1 & -0.5 & 0 \\ 2 & -2 & 0 & -1 \end{bmatrix}, B_c = \begin{bmatrix} 0\ 0 \\ 0\ 0 \\ 1\ 0 \\ 2\ 0 \end{bmatrix}.$$

Let the sampling period be $h = 0.2s$, we obtain the following discrete-time system:

$$A = \begin{bmatrix} 0.9617 & 0.0191 & 0.1878 & 0.0012 \\ 0.0370 & 0.9629 & 0.0025 & 0.1789 \\ -0.3732 & 0.1853 & 0.8678 & 0.0179 \\ 0.3528 & -0.3553 & 0.0357 & 0.7840 \end{bmatrix},$$
$$B = \begin{bmatrix} 0.0193\ 0 \\ 0.0373\ 0 \\ 0.1903\ 0 \\ 0.3602\ 0 \end{bmatrix}, C = \begin{bmatrix} 1\ 0\ 0\ 0 \\ 0\ 1\ 0\ 0 \end{bmatrix},$$
$$D = \begin{bmatrix} 0\ 0.1 \\ 0\ 0.1 \end{bmatrix}, L = \begin{bmatrix} 1\ 1\ 0\ 0 \end{bmatrix}.$$

It is seen that $p = 2$. We assume that y_1 and y_2 are measured by two sensors, which are not located together and thus the outputs should be transmitted by sensors 1 and 2 via two communication channels. In this example, we assume that sensor 1 is full of power and the transmission of this sensor is always available. But sensor 2 has less energy and sensor 2 should not transmit the data for all the time. We do simulation for 50 time steps for brevity. Here we suppose that sensor 2 is only measuring the target plant but not transmitting data at the following time instants: $4th$, $6th$, $8th$, $9th$, $13th$, $15th$, $16th$, $21th$, $22th$, $33th$, $34th$, $41th$, $47th$, and $48th$.

From the transmissions of sensors 1 and 2, we have $\sigma(k) \in \{1, 2, 3\}$. It is assumed that the packet dropout rate of the first channel is 20% and the second one is 10%. From the transmission process discussed above, it is easy to verify that $T_a = 50/14$. We choose $\lambda = 0.97$, $\mu = 1.1$ and $\bar{\lambda} = 1.028$, such that $T_a > T_a^* = 3.4514$ holds. The exponential decay rate can be determined as $\chi = \sqrt{\lambda \mu^{1/T_a}} = 0.9981$. By solving the optimization problem (3.33), the optimal H_∞ performance level is obtained as $\tilde{\gamma}^* = 6.4427$. The corresponding filter gains are

$$A_f = \begin{bmatrix} 0.3538 & -0.1756 & -0.0571 & 0.1231 \\ -0.3208 & 0.2567 & -0.3318 & 0.3158 \\ -1.3938 & 0.5738 & 0.8427 & 0.0067 \\ -1.0000 & 0.1480 & -0.0778 & 0.8549 \end{bmatrix},$$
$$B_f = \begin{bmatrix} -0.5772 & -0.2132 \\ -0.7750 & -0.4044 \\ -0.8822 & 0.2859 \\ -1.1941 & 0.3888 \end{bmatrix}, C_f = \begin{bmatrix} -0.9843 \\ -0.9984 \\ -0.3195 \\ -0.1060 \end{bmatrix}^T.$$

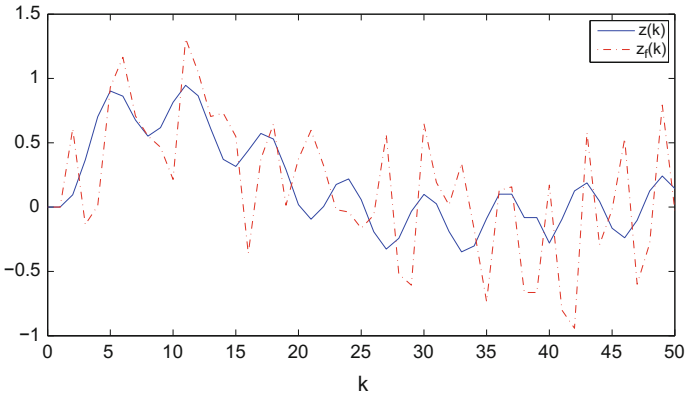

Fig. 3.6 The trajectories of $z(k)$ and $z_f(k)$

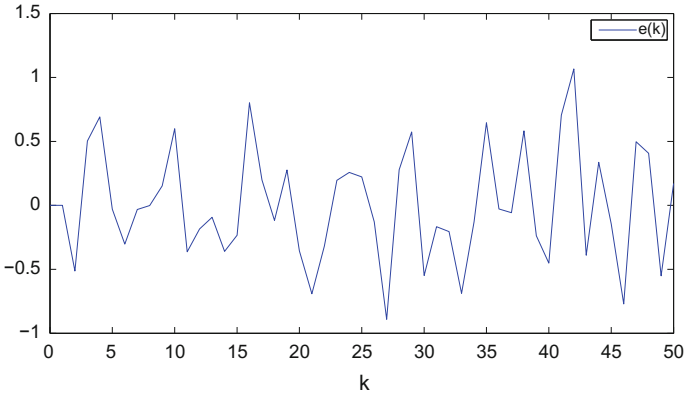

Fig. 3.7 The trajectories of estimation error $e(k)$

In the simulation setup, we choose the following noise signal:

$$\begin{cases} v_1(k) = 2\sin(k), \\ v_2(k) = 3\sin(2k). \end{cases}$$

The packet dropout process is randomly generated according to the given rates. The initial condition of system (3.34) is assumed to be $[\,0\ 0\ 0\ 0\,]^T$. The trajectories of $z(k)$ and $z_f(k)$ are depicted in Fig. 3.6. The trajectory of estimation error $e(k)$ is shown in Fig. 3.7. By simple calculation, we have $\tilde{\gamma} = \sqrt{\frac{\|e(k)\|^2}{\|w(k)\|^2}} = \sqrt{\frac{9.8267}{325.7185}} = 0.1737 < \tilde{\gamma}^*$, which shows the effectiveness of the proposed design method.

Now, we show how to use our method to the event-driven transmission. We assume that multiple sensors are allowed to transmit data via their own channels simultaneously, and no communication constraint or channel occupation occurs.

Example 3.2 We consider the system in [2] with some modification on the output matrices C and D as follows:

$$A = \begin{bmatrix} 0.2 & 0.05 \\ -0.02 & 0.3 \end{bmatrix}, B = \begin{bmatrix} 0.1 \\ -0.2 \end{bmatrix},$$
$$C = \begin{bmatrix} 0.5 & -0.7 \\ 0 & 1 \end{bmatrix}, D = \begin{bmatrix} 0.3 \\ 0.2 \end{bmatrix}, L = [1\ 0.6].$$

We here aim to transmit the measurement signals of y_1 and y_2 based on the event-driven transmission protocol proposed in [3], where the new measurement value will be sent to the estimator if one of the following two conditions is satisfied:

$$\left| y_i(k) - y_{last,i} \right| > \delta_{y,i}, \tag{3.36}$$

$$k - k_{last,i} > \delta_{k,i}, \tag{3.37}$$

where $y_{last,i}$, $i = 1, 2$, is the last transmitted value of the i-th sensor at time instant $k_{last,i}$, $\delta_{y,i}$ and $\delta_{k,i}$ are the given magnitude and time threshold values respectively at the i-th sensor node. These two threshold values are embedded into the sensors.

In this example, we set $\delta_{y,1} = 0.05$, $\delta_{y,2} = 0.1$, and $\delta_{k,1} = \delta_{k,2} = 1$. Then, we have four subsystems for system (3.9). It is assumed that the packet dropout rate of the first channel is 20% and the second one is 10%. We now choose $\lambda = 0.97$, $\mu = 1.03$ and $\bar{\lambda} = 1.0301$, which yields $T_a^* = 0.9967$. It follows from $T_a^* < 1$ that the scheduling can be arbitrary. By solving the optimization problem (3.33), the optimal H_∞ performance level is obtained as $\tilde{\gamma}^* = 0.4468$. The corresponding filter gains are

$$A_f = \begin{bmatrix} 0.7258 & 0.4497 \\ -1.4667 & -0.8980 \end{bmatrix},$$
$$B_f = \begin{bmatrix} -0.1199 & -0.0951 \\ 0.3830 & 0.0303 \end{bmatrix}, C_f = \begin{bmatrix} -0.6473 \\ -0.3790 \end{bmatrix}^T.$$

In the simulation setup, we take the noise signal as $w(k) = 1.1e^{-0.1k}\sin(k)$. The packet dropout process is randomly generated according to the given probability. The initial condition of target plant is assumed to be $[0\ 0]^T$. The trajectories of $z(k)$ and $z_f(k)$ are depicted in Fig. 3.8 by the event-driven transmission protocol. By simple calculation, we have $\tilde{\gamma} = \sqrt{\frac{\|e(k)\|^2}{\|w(k)\|^2}} = \sqrt{\frac{0.0014}{2.9925}} = 0.0216 < \tilde{\gamma}^*$, which indicates that our design method can also be applied to the event-driven transmission protocol. On the other hand, for given $\bar{\alpha}_1 = 0.5$, the relation between the successful transfer probability $\bar{\alpha}_2$ and the minimal H_∞ performance is established in Table 3.1, from which, we see that the more data successfully transferred to the filter is, the better H_∞ performance is.

In the scenario where no packet dropout occurs, we set $\bar{\alpha}_1 = 1$ and $\bar{\alpha}_2 = 1$. The optimal H_∞ performance level is obtained as $\tilde{\gamma}^* = 0.4383$, which is smaller than the ones in Table 3.1. When all packets are dropped, it is seen that the optimization

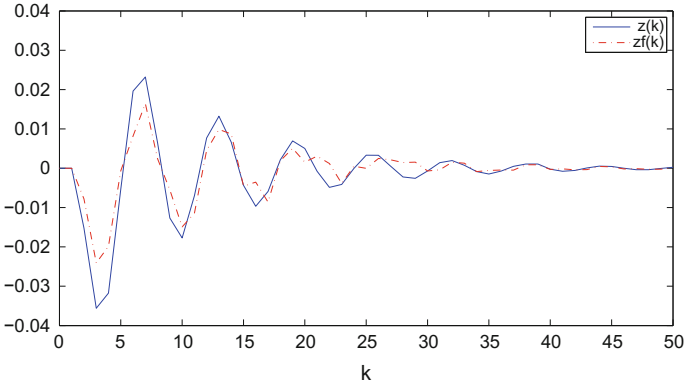

Fig. 3.8 The trajectories of $z(k)$ and $z_f(k)$

Table 3.1 Relations between $\bar{\alpha}_2$ and the minimal H_∞ index $\tilde{\gamma}^*$

$\bar{\alpha}_2$	0.9	0.7	0.5	0.3	0.1
$\tilde{\gamma}^*$	0.4732	0.4801	0.4907	0.4996	0.5017

problem (3.33) has no solution. This is because one of the eigenvalues of $\breve{A}_l + \breve{C}_l$ in (3.9) is 1, which is not stable. This is intuitively correct since one cannot design an estimator to guarantee the estimation performance, if all packets are dropped and thus all information is lost.

3.5 Conclusions

In this chapter, the H_∞ filtering problem is addressed for the wireless networked systems with energy constraint, and a time-varying transmission protocol has been proposed to reduce the power consumption. A switched system approach is employed to model the time-varying transmission process and a diagonal stochastic matrix is introduced to model the random packet dropout phenomenon. The filter gains are determined by solving a set of LMIs, which can be easily found in the existing software, e.g., Matlab LMI toolbox. Two numerical examples have been given to show the effectiveness of the proposed design method. The main results can also be applied to the event-based communication transmission scenario. In the next chapter, some other energy-efficient transmission protocols will be presented and the corresponding filter design will be addressed.

References

1. H.J. Gao, T.W. Chen, H_∞ estimation for uncertain systems with limited communication capacity. IEEE Trans. Autom. Control **52**(11), 2070–2084 (2007)
2. H. Song, L. Yu, W. Zhang, H_∞ filtering of networked-based systems with random delay. Signal Process. **89**(4), 615–622 (2010)
3. V.H. Nguyen, Y.S. Suh, Networked estimation for event-based sampling systems with packet droputs. Sensor **9**(4), 3078–3089 (2009)

Chapter 4
H_∞ Filtering with Energy Constraint and Stochastic Gain Variations

4.1 Introduction

The filter gain variation and energy constraints are frequently encountered in wireless networked systems. In this chapter, these two issues are discussed in a unified framework. New techniques for the nonuniform sampling and the measurement size reduction are presented. In the filter design, the so-called random filter gain variation problem is discussed. A stochastic switched system approach is first proposed to capture the nonuniform sampling, the measurement size reduction and the random filter gain variation phenomena. Based on the average dwell time scheme and the Lyapunov stability theory, a sufficient condition is established such that the filtering error system is exponentially stable in the mean-square sense with a prescribed H_∞ disturbance attenuation level. The filter gain parameters are determined by solving an optimization problem. Finally, the effectiveness of the proposed new filter design method is demonstrated by a simulation study.

4.2 Problem Formulation

The filtering system structure under consideration is shown in Fig. 4.1, where the plant is firstly sampled under time-varying sampling periods, and then only one element of the sampled measurement is chosen to be transmitted to the remote filter. The plant is described by the following continuous-time system:

$$\begin{cases} \dot{x}(t) = Ax(t) + Bw(t), \\ z(t) = Lx(t), \end{cases} \tag{4.1}$$

where $x(t) \in \mathbb{R}^{n_x}$ is the system state, $z(t) \in \mathbb{R}^{n_z}$ is the signal to be estimated, and $w(t) \in \mathbb{R}^{n_w}$ is the disturbance signal, which belongs to $L_2[0, +\infty)$. A, B and L are

D. Zhang et al., *Filtering and Control of Wireless Networked Systems*,
Studies in Systems, Decision and Control 97, DOI 10.1007/978-3-319-53123-6_4

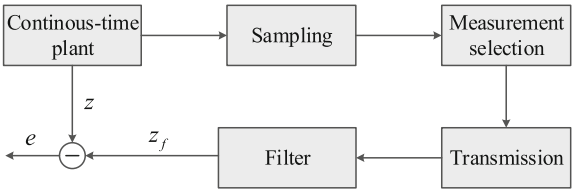

Fig. 4.1 Structure of the filtering system

some constant matrices with appropriate dimensions. The local measurement signal is assumed to be

$$y(t_k) = Cx(t_k) + Dw(t_k), \tag{4.2}$$

where $y(t_k) \in \mathbb{R}^{n_y}$ is the observation collected by the sensor at the discrete time instants t_k, $k = 0, 1, 2, \ldots$, C and D are constant matrices.

Let the sampling period be $h_k = t_{k+1} - t_k$. Then h_k is a time-varying value for nonuniform sampling. In this chapter, we assume that h_k takes a value from a given set, that is, $h_k = n_k T_0$, where $n_k \in \{i_1, i_2, \ldots, i_{n_1}\}$, i_j, $j = 1, 2, \ldots, n_1$ are positive integers, and T_0 is defined as a basic sampling period.

By discretizing the system (4.1) with the sampling period h_k and applying a zero-order-hold, the following discrete-time system is obtained:

$$\begin{cases} x(t_{k+1}) = A_k x(t_k) + B_k w(t_k), \\ z(t_k) = Lx(t_k), \end{cases} \tag{4.3}$$

where $A_k = e^{Ah_k}$ and $B_k = \int_0^{h_k} e^{A\tau} d\tau$. Let $A_0 = e^{AT_0}$ and $B_0 = B \int_0^{T_0} e^{A\tau} d\tau$. Then $A_k = {A_0}^{n_k}$ and $B_k = \sum_{i=0}^{n_k - 1} {A_0}^i B_0$. It is seen that the values of A_k and B_k are explicitly dependent on the sampling period h_k. We now define a piecewise constant signal, $s(k) \in \Omega_1 = \{1, 2, \ldots, n_1\}$. Then the system (4.3) can be re-written as

$$\begin{cases} x(t_{k+1}) = A_{s(t_k)} x(t_k) + B_{s(t_k)} w(t_k), \\ z(t_k) = Lx(t_k), \end{cases} \tag{4.4}$$

where $A_{s(t_k)} = {A_0}^{i_{s(t_k)}}$ and $B_{s(t_k)} = \sum_{l=1}^{i_{s(t_k)}} A_0^{l-1} B_0$.

It has been shown in [1] that more power is needed if we want to transmit more packets. Hence, if the packet size can be reduced, power can be saved. Here, only one element of the sampled-data is selected and transmitted to the remote filter. Thus, the selected signal is described as

$$\bar{y}(t_k) = \Pi_{\sigma(t_k)} y(t_k), \tag{4.5}$$

where $\Pi_{\sigma(t_k)}$ is a structured matrix used to choose an element for transmission, and $\sigma(t_k)$ is a piecewise signal belonging to $\Omega_{p2} = \{1, 2, \ldots, n_y\}$. Specifically,

$\Pi_{\sigma(t_k)} = [1\ 0 \cdots 0]$ when the first element is selected, $\Pi_{\sigma(t_k)} = [0\ 1 \cdots 0]$ when the second element is selected, and so on. It is seen that $\sigma(t_k)$ is a switching signal such that $\sigma(k) \in \Omega_2 = \{1, 2, \ldots, n_y\}$.

Remark 4.1 In the above measurement size reduction method, we assume that only one element of the sampled data can be transmitted to the remote filter. One may also extend the above to other general case. As we try to reduce the energy consumption of the wireless network, the less information we transmit, the less energy are consumed.

Due to the fact that the uncertainty may occur in the filter implementation even though the filter is well designed, we propose the following filter:

$$\begin{cases} x_f(t_{k+1}) = \left(A_f + \alpha(t_k)\Delta A_f\right) x_f(t_k) + \left(B_f + \alpha(t_k)\Delta B_f\right) \bar{y}(t_k), \\ z_f(t_k) = \left(C_f + \alpha(t_k)\Delta C_f\right) x_f(t_k), \end{cases} \tag{4.6}$$

where $x_f(t) \in \mathbb{R}^{n_x}$ is the filter's state and $z_f(t) \in \mathbb{R}^{n_z}$ is the estimation signal from the filter. A_f, B_f and L_f are the filter gain parameters to be determined. The stochastic variable $\alpha(t_k)$ is a binary variable. $\alpha(t_k)) = 1$ means the uncertainty in the filter gain occurs, while $\alpha(t_k)) = 0$ means that no uncertainty occurs in the filter gain. ΔA_f, ΔB_f, and ΔC_f are the uncertainties in the filter gain, and they are assumed to satisfy the following structure:

$$\begin{cases} \Delta A_f = M_1 \Delta_1(t_k) N_1, \\ \Delta B_f = M_2 \Delta_2(t_k) N_2, \\ \Delta C_f = M_3 \Delta_3(t_k) N_3, \end{cases} \tag{4.7}$$

where M_i and N_i, $i = 1, 2, 3$ are some constant matrices with appropriate dimensions. $\Delta_1(t_k)$, $\Delta_2(t_k)$ and $\Delta_3(t_k)$ are the uncertainties with $\|\Delta_i(t_k)\| \leq \delta_i I$, where δ_i are positive scalars. In this chapter, the occurrence probability of the uncertainty is assumed to be available for filter design, i.e., $\Pr ob\{\alpha(t_k) = 1\} = \bar{\alpha}$ is a known scalar.

Remark 4.2 The filter uncertainty described above is an additive type, which can be found in [2]. Recently, the multiplicative type filter gain variation has also been addressed in [3]. Based on the main results proposed in this chapter, one may obtain the corresponding filter design results for the multiplicative type uncertainty.

Based on the above discussions, for each $s(t_k) \in \Omega_1$ and $\sigma(t_k) \in \Omega_2$, the following filtering error system is obtained:

$$\begin{cases} \eta(t_{k+1}) = \left(\tilde{A}_{s(t_k),\sigma(t_k)} + \bar{\alpha}\bar{M}\bar{\Delta}_1(t_k)\bar{N}_{1,\sigma(t_k)}\right)\eta(t_k) \\ \qquad\quad + \left(\tilde{B}_{s(t_k),\sigma(t_k)} + \bar{\alpha}\bar{M}\bar{\Delta}_1(t_k)\bar{N}_{2,\sigma(t_k)}\right) w(t_k) \\ \qquad\quad + (\alpha(t_k) - \bar{\alpha})\left(\bar{M}\bar{\Delta}_1(t_k)\bar{N}_{1,\sigma(t_k)}\eta(t_k) + \bar{M}\bar{\Delta}_1(t_k)\bar{N}_{2,\sigma(t_k)}w(t_k)\right) \\ e(t_k) = \left(\tilde{L} + \bar{\alpha}M_3\Delta_3(t_k)\bar{N}_3\right)\eta(t_k) + (\alpha(t_k) - \bar{\alpha})M_3\Delta_3(t_k)\bar{N}_3\eta(t_k), \end{cases} \tag{4.8}$$

where

$$\eta(t_k) = \left[x^T(t_k)\ x_f^T(t_k) \right]^T, e(t_k) = z_f(t_k) - z(t_k),$$
$$\tilde{A}_{s(t_k),\sigma(t_k)} = \begin{bmatrix} A_{s(t_k)} & 0 \\ B_f \Pi_{\sigma(t_k)} C & A_f \end{bmatrix}, \tilde{B}_{\rho(t_k),\sigma(t_k)} = \begin{bmatrix} B_{s(t_k)} \\ B_f \Pi_{\sigma(t_k)} D \end{bmatrix},$$
$$\bar{M} = \begin{bmatrix} 0 & 0 \\ M_2 & M_1 \end{bmatrix}, \bar{N}_{1,\sigma(t_k)} = \begin{bmatrix} N_2 \Pi_{\sigma(t_k)} C & 0 \\ 0 & N_1 \end{bmatrix},$$
$$\bar{\Delta}_1(t_k) = \begin{bmatrix} \Delta_2(t_k) & 0 \\ 0 & \Delta_1(t_k) \end{bmatrix}, \bar{N}_2(t_k) = \begin{bmatrix} N_2 \Pi_{\sigma(t_k)} D \\ 0 \end{bmatrix},$$
$$\tilde{L} = \left[-L\ C_f \right], \bar{N}_3 = \left[0\ N_3 \right].$$

The system (4.8) has two switching signals, and it is usually not easy to analyze such a complex system directly. As in Chap. 3, we define a mapping: $(s(t_k), \sigma(t_k)) \to \rho(t_k)$, and we can see that $\rho(t_k) \in \Omega = \{1, 2, \ldots, n_1 \times n_y\}$. Then, for each $\rho(t_k) = i$, we revise the system (4.8) as

$$\begin{cases} \eta(t_{k+1}) = \left(\tilde{A}_i + \bar{\alpha} \bar{M} \bar{\Delta}_1(t_k) \bar{N}_{1,i} \right) \eta(t_k) + \left(\tilde{B}_i + \bar{\alpha} \bar{M} \bar{\Delta}_1(t_k) \bar{N}_{2,i} \right) w(t_k) \\ \qquad + (\alpha(t_k) - \bar{\alpha}) \left(\bar{M} \bar{\Delta}_1(t_k) \bar{N}_{1,i} \eta(t_k) + \bar{M} \bar{\Delta}_1(t_k) \bar{N}_{2,i} w(t_k) \right), \\ e(t_k) = \left(\tilde{L} + \bar{\alpha} M_3 \Delta_3(t_k) \bar{N}_3 \right) \eta(t_k) + (\alpha(t_k) - \bar{\alpha}) M_3 \Delta_3(t_k) \bar{N}_3 \eta(t_k). \end{cases} \tag{4.9}$$

The system (4.9) now becomes a stochastic switched system with uncertainty and the average dwell time approach will be utilized to derive the main results. Our filtering purpose is to design the filter in form of (4.6) such that the system (4.9) has some certain performance.

Definition 4.1 The system (4.9) is called exponentially stable in the mean-square sense, if there exist some scalars $\pi > 0$ and $0 < \chi < 1$, such that the solution η of system (4.9) satisfies $\mathbb{E}\{\|\eta(t_k)\|\} < \pi \chi^{(k-k_0)} \|\eta(t_0)\|,\ \forall t_k \geq t_0$.

Definition 4.2 For a given scalar $\gamma > 0$, the system (4.9) is said to be robustly exponentially stable in the mean-square sense and achieves a prescribed H_∞ performance γ, if it is exponentially stable and under zero initial condition, $\sum_{k=0}^{+\infty} \mathbb{E}\{e^T(t_k) e(t_k)\} \leq \sum_{k=0}^{+\infty} \gamma^2 w^T(t_k) w(t_k)$ holds for all nonzero $w(t_k) \in l_2[0, \infty)$.

4.3 Filter Analysis and Design

In this section, a sufficient condition is obtained such that the filtering error system (4.9) is exponentially stable in the mean-square sense with a prescribed H_∞ performance level.

Theorem 4.1 For some given scalars $\lambda_i > 0, \bar{\alpha} > 0, \mu \geq 1$, and $\tau > 0$, if there exist positive-definite matrices P_i and a positive scale $\varepsilon > 0$ such that the following inequalities,

$$\begin{bmatrix} \Psi_1 & \Psi_2 & 0 & \Psi_3 & 0 & \Psi_4 & 0 \\ * & -P_i^{-1} & 0 & 0 & 0 & 0 & \Psi_5 \\ * & * & -P_i^{-1} & 0 & 0 & 0 & \Psi_6 \\ * & * & * & -I & 0 & 0 & \Psi_7 \\ * & * & * & * & -I & 0 & \Psi_8 \\ * & * & * & * & * & \bar{\varepsilon} & 0 \\ * & * & * & * & * & * & \bar{\varepsilon} \end{bmatrix} < 0, \tag{4.10}$$

$$P_i \leq \mu P_j, \ i \neq j, \tag{4.11}$$

$$T_a > T_a^* = -\frac{\ln \mu}{\ln \lambda}, \tag{4.12}$$

hold for all $i, j \in \Omega$, then the filtering error system (4.9) is exponentially stable in the mean-square sense with a decay rate $\chi = \sqrt{\lambda_b \mu^{1/T_a}}$ and achieves a prescribed H_∞ performance level $\gamma = \tau \sqrt{\frac{(1-\lambda_a)}{1-\lambda_b/\lambda}}$, where, $\lambda_a = \min_{i \in \Omega}\{\lambda_i\}$, $\lambda_b = \max_{i \in \Omega}\{\lambda_i\}$, $\lambda > \lambda_b$, and

$$\Psi_1 = \begin{bmatrix} -P_{i,s} & 0 \\ 0 & -\gamma^2 I \end{bmatrix}, \Psi_2 = \begin{bmatrix} \widetilde{A}_i & \widetilde{B}_i \end{bmatrix}^T, \Psi_3 = \begin{bmatrix} \tilde{L} & 0 \end{bmatrix}^T,$$
$$\Psi_4 = \begin{bmatrix} \varepsilon \bar{N}_1^T \bar{\Lambda}_1 & \varepsilon \bar{N}_3^T \Lambda_3 \\ \varepsilon \bar{N}_2^T \bar{\Lambda}_1 & 0 \end{bmatrix}, \Psi_5 = \begin{bmatrix} \bar{\alpha} \bar{M} & 0 \end{bmatrix}, \Psi_6 = \begin{bmatrix} \theta \bar{M} & 0 \end{bmatrix},$$
$$\Psi_7 = \begin{bmatrix} 0 & \bar{\alpha} \bar{M} \end{bmatrix}, \Psi_8 = \begin{bmatrix} 0 & \theta \bar{M} \end{bmatrix}, \bar{\varepsilon} = \begin{bmatrix} -\varepsilon I & 0 \\ * & -\varepsilon I \end{bmatrix}, \theta = \sqrt{\bar{\alpha}(1-\bar{\alpha})}.$$

Proof For easy presentation, we use k to stand for t_k. In order to derive the stability condition for the system (4.9), we choose the following Lyapunov functional:

$$V_{\rho(k)}(k) = \eta^T(k) P_{\rho(k)} \eta(k). \tag{4.13}$$

Then for each $\rho(k) = i$ and $\forall i \in \Omega$, it follows that

$$
\begin{aligned}
&\mathbb{E}\{V_i(k+1)-\lambda_i V_i(k)+\Upsilon(k)\}\\
&=\Big[\Big(\tilde{A}_i+\bar{\alpha}\bar{M}\bar{\Delta}_1(t_k)\bar{N}_{1,i}\Big)\eta(t_k)+\Big(\tilde{B}_i+\bar{\alpha}\bar{M}\bar{\Delta}_1(t_k)\bar{N}_{2,i}\Big)w(t_k)\Big]^T\\
&\quad\times P_i\Big[\Big(\tilde{A}_i+\bar{\alpha}\bar{M}\bar{\Delta}_1(t_k)\bar{N}_{1,i}\Big)\eta(t_k)+\Big(\tilde{B}_i+\bar{\alpha}\bar{M}\bar{\Delta}_1(t_k)\bar{N}_{2,i}\Big)w(t_k)\Big]\\
&\quad+\theta\big[\bar{M}\bar{\Delta}_1(t_k)\bar{N}_{1,i}\eta(t_k)+\bar{M}\bar{\Delta}_1(t_k)\bar{N}_{2,i}w(t_k)\big]^T\\
&\quad\times P_i\big[\bar{M}\bar{\Delta}_1(t_k)\bar{N}_{1,i}\eta(t_k)+\bar{M}\bar{\Delta}_1(t_k)\bar{N}_{2,i}w(t_k)\big]\\
&\quad+\Big[\Big(\tilde{L}+\bar{\alpha}M_3\Delta_3(t_k)\bar{N}_3\Big)\eta(t_k)\Big]^T\Big[\Big(\tilde{L}+\bar{\alpha}M_3\Delta_3(t_k)\bar{N}_3\Big)\eta(t_k)\Big]\\
&\quad+\theta\big[\big(M_3\Delta_3(t_k)\bar{N}_3\big)\eta(t_k)\big]^T\big[\big(M_3\Delta_3(t_k)\bar{N}_3\big)\eta(t_k)\big]\\
&\quad-\lambda_i\eta^T(t_k)P_i\eta(t_k)-\tau^2w^T(t_k)w(t_k),
\end{aligned}
\tag{4.14}
$$

where $\Upsilon(k)=e^T(t_k)e(t_k)-\tau^2w^T(t_k)w(t_k)$. By Lemma 2.1, one sees that

$$
\mathbb{E}\{V_i(k+1)-\lambda_i V_i(k)+\Upsilon(k)\}<0 \tag{4.15}
$$

is equivalent to

$$
\Theta_1+\Theta_2\Delta(k)\Theta_3^T+\Theta_3\Delta(k)\Theta_2^T<0, \tag{4.16}
$$

where

$$
\Theta_1=\begin{bmatrix}\Psi_1 & \Psi_2 & 0 & \Psi_3 & 0\\ * & -P_i^{-1} & 0 & 0 & 0\\ * & * & -P_i^{-1} & 0 & 0\\ * & * & * & -I & 0\\ * & * & * & * & -I\end{bmatrix},\ \Theta_2=\begin{bmatrix}\bar{\Psi}_4\\ 0\\ 0\\ 0\\ 0\end{bmatrix},\ \Theta_3=\begin{bmatrix}0\\ \Psi_5\\ \Psi_6\\ \Psi_7\\ \Psi_8\end{bmatrix}^T,
$$

with

$$
\bar{\Psi}_4=\begin{bmatrix}\bar{N}_1^T & \bar{N}_3^T\\ \bar{N}_2^T & 0\end{bmatrix},\ \Delta(k)=\begin{bmatrix}\bar{\Delta}_1(t_k) & 0\\ 0 & \Delta_3(t_k)\end{bmatrix}.
$$

By some manipulations, (4.16) can be rewritten as

$$
\Theta_1+\Theta_2\Lambda\bar{\Delta}(k)\Theta_3^T+\Theta_3^T\Lambda\bar{\Delta}(k)\Theta_2<0, \tag{4.17}
$$

where $\bar{\Delta}(k)=\frac{\Delta(k)}{\Lambda}$. It follows that $\left\|\frac{\Delta(k)}{\Lambda}\right\|\le I$. Based on Lemma 2.2, one sees that (4.17) holds if and only if (4.10) holds. Hence, we have

$$
\mathbb{E}\{V_i(k+1)-\lambda_i V_i(k)+\Upsilon(k)\}<0. \tag{4.18}
$$

For the switching time instant $k_0<k_1<\cdots<k_l<\cdots<k_t$, $l=1,2,\ldots,t$, we define the switching number of $\rho(k)$ over (k_0,k) by $N_\rho(k_0,k)$. Thus one has

$$\mathbb{E}\{V_l(k)\} \le \mathbb{E}\{\lambda_l^{k-k_l} V_l(k_l)\} - \sum_{s=k_l}^{k-1} \lambda_l^{k-s-1} \mathbb{E}\{\Upsilon(s)\}. \tag{4.19}$$

It follows from (4.11) and (4.19) that

$$\begin{aligned}
&\mathbb{E}\{V_{\rho(k_l)}(k)\} \\
&\le \lambda_{\rho(k_l)}^{k-k_l} \mathbb{E}\{V_{\rho(k_l)}(k_l)\} - \sum_{s=k_l}^{k-1} \lambda_{\rho(k_l)}^{k-s-1} \mathbb{E}\{\Upsilon(s)\} \\
&\le \lambda_{\rho(k_l)}^{k-k_l} \mu \mathbb{E}\{V_{\rho(k_{l-1})}(k_l)\} - \sum_{s=k_l}^{k-1} \lambda_{\rho(k_l)}^{k-s-1} \mathbb{E}\{\Upsilon(s)\} \\
&\le \lambda_{\rho(k_l)}^{k-k_l} \mu \left[\lambda_{\rho(k_{l-1})}^{k_l-k_{l-1}} \mathbb{E}\{V_{\rho(k_{l-1})}(k_l-1)\} - \sum_{s=k_{l-1}}^{k_l-1} \lambda_{\rho(k_{l-1})}^{k-s-1} \mathbb{E}\{\Upsilon(s)\} \right] \\
&\quad - \sum_{s=k_l}^{k-1} \lambda_{\rho(k_l)}^{k-s-1} \mathbb{E}\{\Upsilon(s)\} \\
&\le \cdots \le \mu^{N_\rho(k_0,k)} \lambda_{\rho(k_l)}^{k-k_l} \lambda_{\rho(k_{l-1})}^{k_l-k_{l-1}} \cdots \lambda_{\rho(k_0)}^{k_1-k_0} V_{\rho(k_0)}(k_0) - \Theta(\Upsilon),
\end{aligned} \tag{4.20}$$

where

$$\begin{aligned}
\Theta(\Upsilon) &= \mu^{N_\varpi(k_0,k-1)} \lambda_{\rho(k_l)}^{k-k_l} \prod_{s=1}^{l-1} \lambda_{\rho(k_s)}^{k_{s+1}-k_s} \sum_{s=k_0}^{k_1-1} \lambda_{\rho(k_0)}^{k_1-1-s} \mathbb{E}\{\Upsilon(s)\} \\
&\quad + \mu^{N_\varpi(k_0,k-1)-1} \lambda_{\rho(k_l)}^{k-k_l} \prod_{s=2}^{l-1} \lambda_{\rho(k_j)}^{k_{j+1}-k_j} \sum_{s=k_1}^{k_2-1} \lambda_{\rho(k_1)}^{k_2-1-s} \mathbb{E}\{\Upsilon(s)\} \\
&\quad + \cdots + \mu^0 \prod_{s=k_l}^{k-1} \lambda_{\rho(k_l)}^{k-1-s} \mathbb{E}\{\Upsilon(s)\}.
\end{aligned}$$

Now, we consider the exponential stability of system (4.9) with $w(k) = 0$. One has

$$\begin{aligned}
&\mathbb{E}\{V_{\rho(k_l)}(k)\} \\
&\le \mu^{N_\rho(k_0,k)} \lambda_{\rho(k_l)}^{k-k_l} \lambda_{\rho(k_{l-1})}^{k_l-k_{l-1}} \cdots \lambda_{\rho(k_0)}^{k_1-k_0} V_{\rho(k_0)}(k_0) \\
&\le \mu^{N_\rho(k_0,k)} \lambda_b^{k-k_0} V_{\rho(k_0)}(k_0) \\
&\le \left(\mu^{1/T_a} \lambda_b\right)^{k-k_0} V_{\rho(k_0)}(k_0) \\
&= \chi^{2(k-k_0)} V_{\rho(k_0)}(k_0),
\end{aligned} \tag{4.21}$$

which yields $\mathbb{E}\left\{\|\eta(k)\|^2\right\} \le \frac{\varphi_2}{\varphi_1} \chi^{2(k-k_0)} \|\eta(k_0)\|^2$, where $\varphi_1 = \min_{i\in\Omega} \sigma_{\min}(P_i)$, $\varphi_2 = \max_{i\in\Omega} \sigma_{\max}(P_i)$, $\chi = \sqrt{\lambda_b \mu^{1/T_a}}$. Therefore, one can readily obtain $\chi < 1$ from (4.14). According to Definition 4.1, the filtering error system (4.9) is exponentially stable in the mean-square sense with $w(k) = 0$.

For the H_∞ performance level, we consider $w(k) \neq 0$. Under the zero initial condition, it follows from (4.20) that

$$\sum_{s=k_0}^{k-1}\mu^{N_\rho(s,k-1)}\lambda_a^{k-s-1}\mathbb{E}\{e^T(s)e(s)\}\le\tau^2\sum_{s=k_0}^{k-1}\mu^{N_\rho(s,k-1)}\lambda_b^{k-s-1}w^T(s)w(s). \quad (4.22)$$

Based on the average dwell time condition (4.12), it is easy to see $\frac{N_\rho(s,k-1)}{k-s-1}<-\frac{\ln\lambda}{\ln\mu}$. Since $\mu>1$, we obtain $\ln\mu^{N_\rho(s,k-1)}<\ln\lambda^{-(k-s-1)}$ and $1<\mu^{N_\rho(s,k-1)}<\lambda^{-(k-s-1)}$. Then, it can be readily seen that

$$\sum_{s=k_0}^{k-1}\lambda_a^{k-s-1}\mathbb{E}\{e^T(s)e(s)\}<\tau^2\sum_{s=k_0}^{k-1}(\lambda_b/\lambda)^{k-s-1}\,\lambda^{k-s-1}w^T(s)w(s). \quad (4.23)$$

Summing (4.23) from $k=k_0+1$ to $k=\infty$ and changing the order of summation yield

$$\sum_{s=k_0}^{+\infty}\mathbb{E}\{e^T(s)e(s)\}\sum_{k=s+1}^{+\infty}\lambda_a^{k-s-1}<\tau^2\sum_{s=k_0}^{+\infty}w^T(s)w(s)\sum_{k=s+1}^{+\infty}(\lambda_b/\lambda)^{k-s-1}. \quad (4.24)$$

Since $\sum_{k=s+1}^{+\infty}\lambda_a^{k-s-1}=\frac{1}{1-\lambda_a}$ and $\sum_{k=s+1}^{+\infty}(\lambda_b/\lambda)^{k-s-1}=\frac{1}{1-(\lambda_b/\lambda)}$, we have

$$\sum_{s=k_0}^{+\infty}\mathbb{E}\{e^T(s)e(s)\}<\gamma^2\sum_{s=k_0}^{+\infty}w^T(s)w(s), \quad (4.25)$$

where $\gamma=\tau\sqrt{\frac{1-\lambda_a}{1-\lambda}}$. It is noted that $\lambda_b<\lambda$, which ensures $\gamma>0$. Let $k_0=0$, the filtering error system (4.9) is exponentially stable in the mean-square sense and achieves a prescribed H_∞ performance level γ. This completes the proof.

The sufficient condition in Theorem 4.1 guarantees the existence of the filter if certain conditions are satisfied but it does not give the filter gains. The filter gain is given in the following theorem.

Theorem 4.2 For some given scalars $\lambda_i>0,\bar{\alpha}>0,\mu\ge1$, and $\tau>0$, if there exist positive-definite matrices P_i, any matrices G_i, and a positive scale $\varepsilon>0$ such that (4.11), (4.12) and the following inequalities,

$$\begin{bmatrix}\Psi_1 & \tilde{\Psi}_2 & 0 & \tilde{\Psi}_3 & 0 & \tilde{\Psi}_4 & 0\\ * & P_i-G_i-G_i^T & 0 & 0 & 0 & 0 & \tilde{\Psi}_5\\ * & * & P_i-G_i-G_i^T & 0 & 0 & 0 & \tilde{\Psi}_6\\ * & * & * & -I & 0 & 0 & \tilde{\Psi}_7\\ * & * & * & * & -I & 0 & \tilde{\Psi}_8\\ * & * & * & * & * & \bar{\varepsilon} & 0\\ * & * & * & * & * & * & \bar{\varepsilon}\end{bmatrix}<0, \quad (4.26)$$

hold for all $i, j \in \Omega$, then the filtering problem is solvable. Moreover, the filter gains are determined by $A_f = G_3^{-T} A_F$, $B_f = G_3^{-T} B_F$ and $C_f = C_F$, where

$$\tilde{\Psi}_2 = \begin{bmatrix} \tilde{\Psi}_{21} \\ \tilde{\Psi}_{22} \end{bmatrix}, \tilde{\Psi}_3 = \begin{bmatrix} \tilde{\Psi}_{31} \\ 0 \end{bmatrix}, \tilde{\Psi}_4 = \begin{bmatrix} \tilde{\Psi}_{41} & \tilde{\Psi}_{42} \\ \tilde{\Psi}_{43} & 0 \end{bmatrix},$$
$$\tilde{\Psi}_5 = \begin{bmatrix} \tilde{\Psi}_{51} & 0 \end{bmatrix}, \tilde{\Psi}_6 = \begin{bmatrix} \tilde{\Psi}_{61} & 0 \end{bmatrix}, \tilde{\Psi}_7 = \begin{bmatrix} 0 & \bar{\alpha} M_3 \end{bmatrix}, \tilde{\Psi}_8 = \begin{bmatrix} 0 & \theta M_3 \end{bmatrix},$$

with

$$\tilde{\Psi}_{21} = \begin{bmatrix} A_i^T G_{1i} + C^T \Pi_i^T B_F^T & A_i^T G_{2i} + C^T \Pi_i^T B_F^T \\ A_F^T & A_F^T \end{bmatrix},$$
$$\tilde{\Psi}_{22} = \begin{bmatrix} B_i^T G_{1i} + D^T \Pi_i^T B_F^T & B_i^T G_{2i} + D^T \Pi_i^T B_F^T \end{bmatrix},$$
$$\tilde{\Psi}_{31} = \begin{bmatrix} -L & C_F \end{bmatrix}^T, \tilde{\Psi}_{41} = \begin{bmatrix} \varepsilon C^T \Pi_i^T N_2^T \Lambda_2 & 0 \\ 0 & \varepsilon N_1^T \Lambda_1 \end{bmatrix},$$
$$\tilde{\Psi}_{42} = \begin{bmatrix} 0 \\ \varepsilon N_3^T \Lambda_3 \end{bmatrix}, \tilde{\Psi}_{43} = \begin{bmatrix} \varepsilon D^T \Pi_i^T N_2^T \Lambda_2 & 0 \end{bmatrix},$$
$$\tilde{\Psi}_{51} = \begin{bmatrix} \bar{\alpha} G_3^T M_2 & \bar{\alpha} G_3^T M_1 \\ \bar{\alpha} G_3^T M_2 & \bar{\alpha} G_3^T M_1 \end{bmatrix}, \tilde{\Psi}_{61} = \begin{bmatrix} \theta G_3^T M_2 & \theta G_3^T M_1 \\ \theta G_3^T M_2 & \theta G_3^T M_1 \end{bmatrix}.$$

Proof By left- and right- multiplying (4.10) with $\mathrm{diag}\{I, G^T, I, G^T, I, I, I\}$ and its transpose, (4.10) is equivalent to

$$\begin{bmatrix} \Psi_1 & \Psi_2 G_i & 0 & \Psi_3 & 0 & \Psi_4 & 0 \\ * & -G_i^T P_i^{-1} G & 0 & 0 & 0 & 0 & G_i^T \Psi_5 \\ * & * & -G_i^T P_i^{-1} G_i & 0 & 0 & 0 & G_i^T \Psi_6 \\ * & * & * & -I & 0 & 0 & \Psi_7 \\ * & * & * & * & -I & 0 & \Psi_8 \\ * & * & * & * & * & \bar{\varepsilon} & 0 \\ * & * & * & * & * & * & \bar{\varepsilon} \end{bmatrix} < 0. \tag{4.27}$$

On the other hand, it is easy to see that the inequality $-G_i^T P_i^{-1} G_i \le P_i - G_i - G_i^T$ always holds for any matrix G_i. Then, (4.27) holds if

$$\begin{bmatrix} \Psi_1 & \Psi_2 G_i & 0 & \Psi_3 & 0 & \Psi_4 & 0 \\ * & P_i - G_i - G_i^T & 0 & 0 & 0 & 0 & G_i^T \Psi_5 \\ * & * & P_i - G_i - G_i^T & 0 & 0 & 0 & G_i^T \Psi_6 \\ * & * & * & -I & 0 & 0 & \Psi_7 \\ * & * & * & * & -I & 0 & \Psi_8 \\ * & * & * & * & * & \bar{\varepsilon} & 0 \\ * & * & * & * & * & * & \bar{\varepsilon} \end{bmatrix} < 0, \tag{4.28}$$

which is the same as (4.26) with

$$P_i = \begin{bmatrix} P_{1i} & P_{2i} \\ * & P_{3i} \end{bmatrix}, G = \begin{bmatrix} G_{1i} & G_{2i} \\ G_3 & G_3 \end{bmatrix},$$
$$A_F = G_3^T A_f, B_F = G_3^T B_f, L_F = L_f.$$

This completes the proof.

Remark 4.3 In Theorem 4.2, the existence condition for the filters is given in terms of LMIs which is convex in the scalar τ^2. Therefore, one may solve the following optimization problem:

$$\begin{aligned} &\min \rho, \\ &\text{s.t. (4.11), (4.12), (4.26) with } \rho = \tau^2 \end{aligned} \tag{4.29}$$

to obtain the filter gain parameters such that the H_∞ disturbance attenuation level is minimized. When the optimal ρ is obtained from the above optimization problem, the designed filter guarantees that the filtering error system is exponentially stable and achieves a prescribed H_∞ performance level $\gamma = \tau\sqrt{\frac{(1-\lambda_a)}{1-\lambda_b/\lambda}}$.

4.4 An Illustrative Example

In this section, a simulation study is given to show the effectiveness of our new design. We consider a satellite yaw angles control system with noise, which has been studied in [4]. The state-space model of this system is given by

$$\begin{bmatrix} 1 & 0 & 0 & 0 \\ 0 & 1 & 0 & 0 \\ 0 & 0 & J_1 & 0 \\ 0 & 0 & 0 & J_2 \end{bmatrix} \begin{bmatrix} \dot{\theta}_1(t) \\ \dot{\theta}_2(t) \\ \dot{\delta}_1(t) \\ \dot{\delta}_2(t) \end{bmatrix} = \begin{bmatrix} 0 & 0 & 1 & 0 \\ 0 & 0 & 0 & 1 \\ -k & k & -f & f \\ k & -k & f & -f \end{bmatrix} \begin{bmatrix} \theta_1(t) \\ \theta_2(t) \\ \delta_1(t) \\ \delta_2(t) \end{bmatrix} + \begin{bmatrix} 0 \\ 0 \\ 1 \\ 0 \end{bmatrix} u(t) + \begin{bmatrix} 0 \\ 0.1 \\ 0 \\ 0.1 \end{bmatrix} w(t). \tag{4.30}$$

The satellite yaw angles control system consists of two rigid bodies jointed by a flexible link. This link is modeled as a spring with torque constant k and viscous damping f. $\theta_1(t)$ and $\theta_2(t)$ are the yaw angles for the main body and the instrumentation module of the satellite. Moreover, $\delta_1(t) = \dot{\theta}_1(t)$ and $\delta_2(t) = \dot{\theta}_2(t)$. $u(t)$ is the control torque, while J_1 and J_2 are the moments of the main body and the instrumentation module, respectively.

Suppose that $J_1 = J_2 = 1, k = 0.3, f = 0.004$, the sampling period is $T \in \{0.05\,\text{s}, 0.1\,\text{s}\}$ and the controller is

$$u(k) = 10^3 \begin{bmatrix} -0.1591 & -5.9343 & -0.0172 & -2.8604 \end{bmatrix} x(k).$$

The resulting discrete-time satellite yaw angles closed-loop system is given by

$$A_1 = \begin{bmatrix} 0.8008 & -7.4165 & 0.0285 & -3.5750 \\ 0.0003 & 0.9887 & 0 & 0.0495 \\ -7.9682 & -296.6333 & 0.1396 & -142.9873 \\ 0.0132 & -0.0817 & 0.0004 & 0.9673 \end{bmatrix}, B_1 = \begin{bmatrix} 0 \\ 0.0051 \\ 0 \\ 0.0050 \end{bmatrix},$$

$$A_2 = \begin{bmatrix} 0.2033 & -29.6586 & 0.0140 & -14.2964 \\ 0.0012 & 0.9871 & 0 & 0.0944 \\ -15.9288 & -592.9849 & -0.7207 & -285.8380 \\ 0.0188 & -0.4451 & 0.0007 & 0.7980 \end{bmatrix}, B_2 = \begin{bmatrix} 0 \\ 0.0105 \\ 0.002 \\ 0.0098 \end{bmatrix},$$

and $x(k) = \begin{bmatrix} \theta_1(k) & \theta_2(k) & \delta_1(k) & \delta_2(k) \end{bmatrix}^T$.

Suppose that the remote filter is designed to estimate the signal

$$z(t) = Lx(t), \tag{4.31}$$

where $L = \begin{bmatrix} 1 & 1 & 0 & 0 \end{bmatrix}$. Two sensors are deployed to measure the target plant and the local measurements are described by

$$y(t) = Cx(t) + Dw(t), \tag{4.32}$$

where $C = \begin{bmatrix} 1 & 0 & 0 & 0 \\ 0 & 1 & 0 & 0 \end{bmatrix}$, $D = \begin{bmatrix} 0.8 \\ 1.0 \end{bmatrix}$.

For estimation purpose, the measurement size of sampled data is then reduced by using the above scheme with $\Pi_{\sigma(t_k)} \in \left\{ \begin{bmatrix} 1 & 0 \end{bmatrix}, \begin{bmatrix} 0 & 1 \end{bmatrix} \right\}$. The probability of the filter gain variation is taken as $\bar{\alpha} = 0.5$ and the uncertainties are $\Delta_i(t_k) = rand$, where

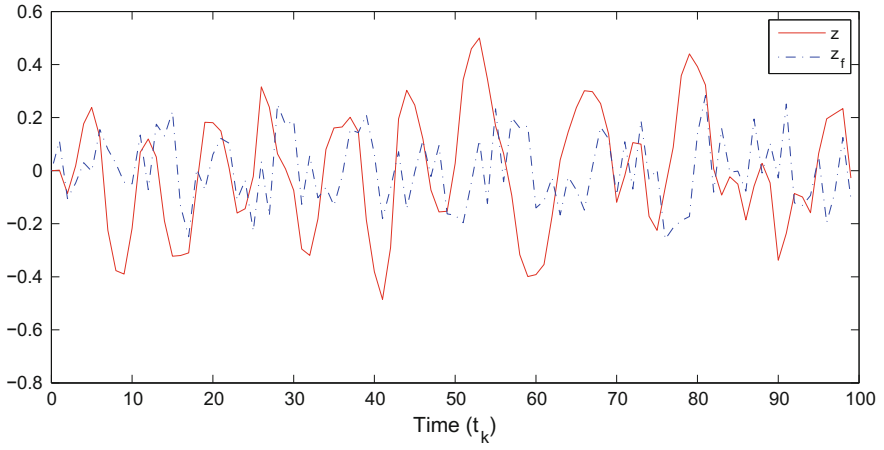

Fig. 4.2 Trajectories of z and its estimates z_f

"*rand*" is a random function, generating a value between 0 and 1. Such a function will also be applied in the subsequent chapters. The uncertainty related matrices are

$$M_1 = \begin{bmatrix} 0.1 & 0.2 & 0.1 & 0.1 \end{bmatrix}^T, M_2 = \begin{bmatrix} 0.1 & 0.1 & 0.2 & 0.1 \end{bmatrix}^T, M_2 = 0.2,$$
$$N_1 = \begin{bmatrix} 0.2 & 0.1 & 0.2 & 0.1 \end{bmatrix}, N_2 = 0.1, N_3 = \begin{bmatrix} 0.1 & -0.1 & -0.1 & 0.05 \end{bmatrix}.$$

The mode jumping of two switching signals are assumed to be periodical and synchronized. Each mode is activating for two time steps. Then, we have two subsystems for (4.9), and $T_a = 2$. By choosing $\lambda_1 = 0.92$, $\lambda_1 = 0.94$, and $\mu = 1.05$, we have $\lambda_a = 0.92$ and $\lambda_b = 0.94$. It is seen that $T_a^* = 0.9512 < T_a$, which means

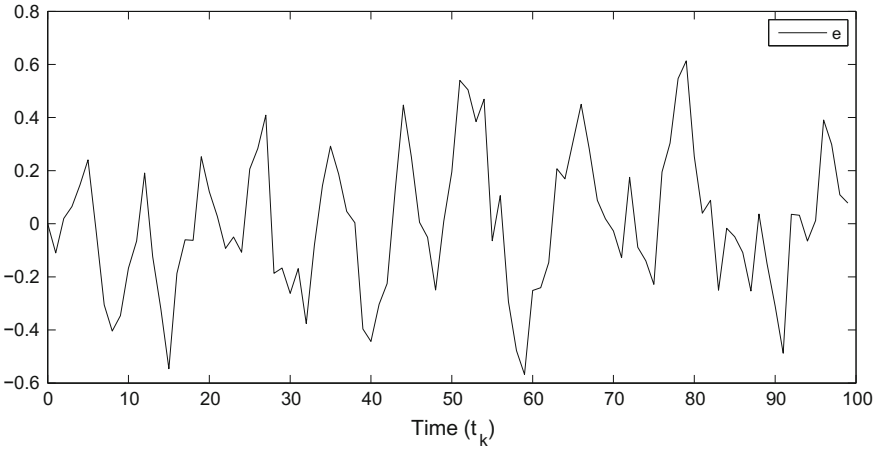

Fig. 4.3 Trajectory of estimation error e

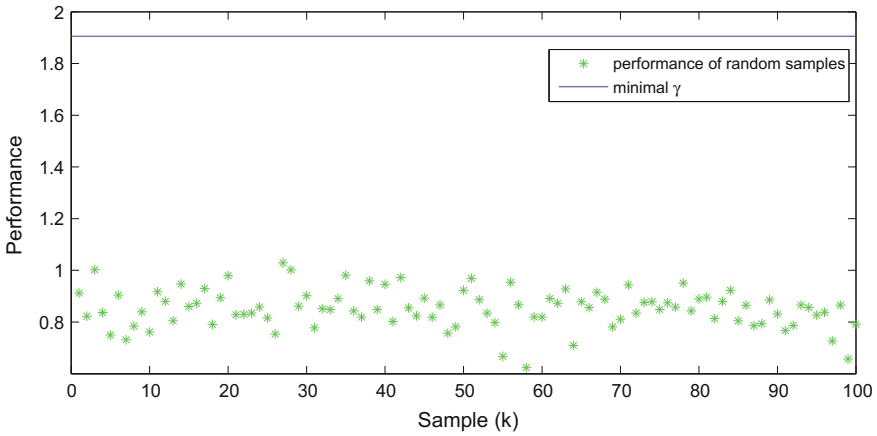

Fig. 4.4 100 samples for the performance level γ

that (4.12) holds. By solving the optimization problem (4.29), we have H_∞ level $\gamma = 1.9054$. To illustrate the filtering performance, we take the disturbance signal as $w(t_k) = rand - 0.5$. Figure 4.2 shows the trajectories of z and its estimate z_f. The trajectory of estimation error e is depicted in Fig. 4.3. 100 samples on the H_∞ performance level γ are also depicted in Fig. 4.4. One sees that the performance of the filtering error system is guaranteed.

4.5 Conclusions

We have discussed the H_∞ filtering problem for a class of wireless networked systems with random filter gain variations and energy constraint. Techniques such as time-varying sampling and measurement size reduction are proposed to reduce the energy consumption. In order to capture the stochastic filter gain variations, a binary stochastic variable is introduced. Based on the switched system theory, a sufficient condition has been presented to guarantee the exponential stability of the filtering error system and a prescribed H_∞ performance level is also ensured. The filter gain parameters are then determined by solving an optimization problem. Finally, a simulation study has been given to show the effectiveness of the new design method. It is noted that in this chapter and Chap. 3, the transmission process is designed to be deterministic. In NCSs, a stochastic scheme may help improve the filtering performance. The stochastic protocol will be discussed in the next chapter.

References

1. I. Akyildiz, W. Su, Y. Sankarasubramaniam, E. Cayirci, A survey on sensor networks. IEEE Commun. Mag. **40**(8), 102–114 (2002)
2. X. Chang, Robust nonfragile H_∞ filtering for fuzzy systems with linear fractional parameteric uncertainties. IEEE Trans. Fuzzy Syst. **20**(6), 1001–1011 (2012)
3. X. Chang, G. Yang, Non-fragile H_∞ filter design for discrete-time fuzzy systems with multiplicative gain variations. Inf. Sci. **266**, 171–185 (2014)
4. W.A. Zhang, L. Yu, H.B. Song, H_∞ filtering of networked discrete-time systems with random packet losses. Inf. Sci. **179**(22), 3944–3955 (2009)

Chapter 5
H_∞ Filtering with Stochastic Signal Transmissions

5.1 Introduction

In this chapter, the H_∞ filtering problem is addressed for a class of networked systems, where the measurement signal is transmitted to the remote filter stochastically. Unlike the last chapter, where the transmission process is deterministic, a new stochastic strategy is proposed here. Based on the stochastic system analysis, a sufficient condition is obtained such that the filtering error system is asymptotically stable in the mean-square sense and achieves a prescribed H_∞ performance level. A case study on a continuous stirred-tank reactors (CSTR) system is given to show the effectiveness of the proposed design.

5.2 Problem Formulation

Consider the following discrete-time system:

$$x(k+1) = Ax(k) + Bw(k), \tag{5.1}$$

where $x(k) \in \mathbb{R}^{n_x}$ is the state, $w(k) \in \mathbb{R}^{n_w}$ is the unknown disturbance signal belonging to $l_2[0, +\infty)$, and A and B are the constant matrices with appropriate dimensions. Suppose that there are m distributed sensors for the system and the p-th sensor produces its measurement as

$$y_p(k) = C_p x(k) + D_p w(k), \tag{5.2}$$

where $y_p \in \mathbb{R}^{n_p}$ is the output signal, C_p and D_p are the constant matrices with appropriate dimensions. To save energy, the measurement may not be transmitted to the remote filter at each time instant. On the other hand, to estimate the state reasonably well, the filter needs recent measurements. Thus, a reasonable communication

D. Zhang et al., *Filtering and Control of Wireless Networked Systems*,
Studies in Systems, Decision and Control 97, DOI 10.1007/978-3-319-53123-6_5

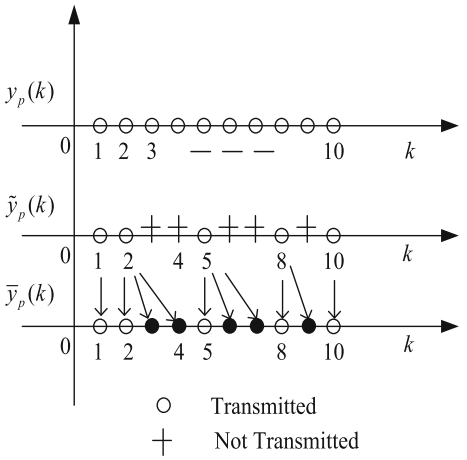

Fig. 5.1 Transmission process

protocol is that the measurement signal is transmitted at least once over N_p time steps, where $N_p > 0$ is an integer. No other restrictions are made on the protocol, implying that the transmission can happen at any time in these N_p steps and is random. One possible transmission scenario is depicted in Fig. 5.1, where $y_p(k)$ is the measurement signal sequence and $\tilde{y}_p(k)$ is the transmitted one with $N_p = 3$.

It follows from the transmission mechanism that there could be no transmission at some time instants. In the case where no transmission occurs, the filter has to use the last transmitted measurement signal as its input. Then, at each time instant k, the filter input, $\bar{y}_p(k)$, will be the most recent member of the transmitted subset of $\{y_p(k), y_p(k-1), \ldots, y_p(k-N_p+1)\}$. To reflect this random selection of one member, a set of stochastic variables, $\alpha_{p,s}(k) \in \{0, 1\}$, $s = 0, 1, \ldots, N_p - 1$, is introduced such that $\alpha_{p,s}(k) = 1$ if $y_p(k-s)$ is selected at k as the filter input, which happens when there is transmission at $k-s$ but none at $k-s+1$, $k-s+2, \ldots, k$; $\alpha_{p,s}(k) = 0$, otherwise. For the scenario considered before, the selected $\bar{y}_p(k)$ is shown in Fig. 5.1 as the 3rd line. The above filter input selection rule implies that at each k, there is one and only one measurement point (most recent one) is selected as the filter input, and equivalently, there is one and only one $\alpha_{p,s}(k) = 1$ with all other variables being zero, so that $\sum_{s=0}^{N_p-1} \alpha_{p,s}(k) = 1$. In this chapter, the probabilities $\Pr ob\{\alpha_{p,s}(k) = 1\} = \mathbb{E}\{\alpha_{p,s}(k) = 1\} = \bar{\alpha}_{p,s}$ are assumed to be known, which is reasonable as the data on actual transmissions could be collected on any given system and the estimates of these probabilities can be obtained with their frequencies. Obviously, $\sum_{s=0}^{N_p-1} \bar{\alpha}_{p,s} = 1$ is true. Moreover, different sensors are assumed to operate independently of each other and their transmission sequences are then also independent.

It follows from the above transmission protocol and input selection rule that the filter input can be expressed as

$$\bar{y}_p(k) = \alpha_{p,0}(k)y_p(k) + \alpha_{p,1}(k)y_p(k-1) + \cdots + \alpha_{p,N_p-1}(k)y_p(k-N_p+1). \tag{5.3}$$

The analysis is similar to the one in Chap. 3.

Remark 5.1 It is seen that (5.3) reduces to measurement models in [1–3] when $\alpha_{p,s}(k) = 0$ for all $s = 1, \ldots, N_p - 1$. Incorporating these statistics information to our new filter design can achieve a better estimation performance than that of [1–3], as will be shown in simulation later.

Remark 5.2 In this chapter, our attention is focused on the stochastic transmission issue, but the packet may be lost under the networked environment. It should be pointed out that the proposed modelling (5.3) has also captured the successive packet dropout phenomenon. When one further considers the packet dropout problem, one may replace N_p in (5.3) by $M_p + \bar{N}_p$, where M_p is the upper bound of successive packet dropout and $\bar{N}_p$ is the largest transmission span.

Let $N = \max\limits_{p=1,2,\ldots,m}\{N_p\}$. As in Chap. 3, we define

$$\begin{aligned} X(k) &= \left[\, x^T(k)\ x^T(k-1)\ \cdots\ x^T(k-N+1)\,\right]^T, \\ W(k) &= \left[\, w^T(k)\ w^T(k-1)\ \cdots\ w^T(k-N+1)\,\right]^T. \end{aligned}$$

Substituting (5.2)–(5.3) yields

$$\bar{y}_p(k) = \sum_{s=0}^{N_p-1} \alpha_{p,s}(k)\left\{C_p E_{ps} X(k) + D_p H_{ps} W(k)\right\}, \tag{5.4}$$

where $E_{ps} = \left[\, 0 \cdots 0\ I_{n_x}\ 0 \cdots 0\,\right]$ and $H_{ps} = \left[\, 0 \cdots 0\ I_{n_w}\ 0 \cdots 0\,\right]$, in which all elements are zeros except that they are I_{n_x} and I_{n_w} in the $(s+1)$-th block, respectively.

Let $\alpha_p(k) = \left[\alpha_{p,0}(k), \alpha_{p,1}(k), \ldots, \alpha_{p,N_p-1}(k)\right]$. The the stochastic vector $\alpha_p(k)$ has N_p possible realizations as

$$\alpha_p(k) \in \{[1, 0, 0, \ldots, 0], \ldots [0, 0, 0, \ldots, 1]\}. \tag{5.5}$$

Define $\alpha(k) = [\alpha_1(k), \alpha_2(k), \ldots, \alpha_m(k)]$. Then the total number of possible realizations of $\alpha(k)$ is $N = N_1 \times N_2 \times \cdots \times N_m$. Let

$$\begin{aligned} \bar{E}_{\alpha(k)} &= [\ E^T_{1,\alpha_1(k)}\ E^T_{2,\alpha_2(k)}\ \cdots\ E^T_{m,\alpha_m(k)}\ ]^T, \\ \bar{H}_{\alpha(k)} &= [\ H^T_{1,\alpha_1(k)}\ H^T_{2,\alpha_2(k)}\ \cdots\ H^T_{m,\alpha_m(k)}\ ]^T. \end{aligned}$$

One particular realization of $\alpha(k)$ means one sequence of $\alpha(k)$, which is a particular case of $(\bar{E}_{\alpha(k)}, \bar{H}_{\alpha(k)})$. For ease of discussion, we define an integer set $\Gamma = \{1, 2, \ldots, N\}$, and introduce a new set of stochastic variables, $\beta_i(k) \in \{1, 0\}, i \in \Gamma$, one variable for one possible realization of $\alpha(k)$, such that $\beta_1(k) = 1$ if and only if $\alpha_p(k) = [1, 0, \ldots, 0]$, $p = 1, 2, \ldots, m$; $\beta_2(k) = 1$ if and only if

$\alpha_p(k) = [1, 0, \ldots, 0]$, $p = 1, 2, \ldots, m-1$, $\alpha_m(k) = [0, 1, \ldots, 0]$; and so on. By our construction, there is one and only one realization of $\alpha(k)$ at any time instant, so that $\sum_{i=1}^{N} \beta_i(k) = 1$.

The probability, Pr $ob\{\beta_i(k) = 1\} = \mathbb{E}\{\beta_i(k)\} = \bar{\beta}_i$, can be computed by the probabilities of sensor transmissions, $\bar{\alpha}_{p,s}$. For example, we have two sensors and each sensor transmits the measurement within two time steps stochastically with their probabilities being $\bar{\alpha}_{1,0}$, $\bar{\alpha}_{1,1}$ and $\bar{\alpha}_{2,0}$, $\bar{\alpha}_{2,1}$, respectively. Then, it follows from simple probability rules that $\bar{\beta}_1 = \bar{\alpha}_{1,0}\bar{\alpha}_{2,0}$, $\bar{\beta}_2 = \bar{\alpha}_{1,0}\bar{\alpha}_{2,1}$, $\bar{\beta}_3 = \bar{\alpha}_{1,1}\bar{\alpha}_{2,0}$ and $\bar{\beta}_4 = \bar{\alpha}_{1,1}\bar{\alpha}_{2,1}$.

Based on the above development, we can express the filter input vector as

$$\bar{y}(k) = \sum_{i=1}^{N} \beta_i(k) \left\{ \bar{C}\bar{E}_i X(k) + \bar{D}\bar{H}_i W(k) \right\}, \tag{5.6}$$

where $\bar{C} = \text{diag}\{C_1, C_2, \ldots, C_m\}$ and $\bar{D} = \text{diag}\{D_1, D_2, \ldots, D_m\}$.

In this chapter, we aim to estimate the following signal:

$$z(k) = Lx(k), \tag{5.7}$$

where $z(k) \in \mathbb{R}^{n_z}$ and L is a constant matrix with appropriate dimension. In order to estimate the signal in (5.7), we propose the following filter:

$$\begin{cases} x_f(k+1) = A_f x_f(k) + B_f \bar{y}(k), \\ z_f(k) = C_f x_f(k), \end{cases} \tag{5.8}$$

where $x_f(k) \in \mathbb{R}^{n_x}$ is the state of the filter and $z_f(k) \in \mathbb{R}^{n_z}$ is the estimate of $z(k)$. A_f, B_f, and C_f are the filter parameters to be designed.

In order to derive the filtering error system, we rewrite state equation in (5.1) and the estimation equation in (5.7) as

$$\begin{cases} X(k+1) = \bar{A}X(k) + \bar{B}W(k), \\ z(k) = \bar{L}X(k), \end{cases} \tag{5.9}$$

where

$$\bar{A} = \begin{bmatrix} A & 0 \\ I_{nN} & 0 \end{bmatrix}, \bar{B} = \begin{bmatrix} B & 0 \\ 0 & 0 \end{bmatrix}, \bar{L} = \begin{bmatrix} L & 0 \end{bmatrix}.$$

Define the augmented state $\eta(k) = \begin{bmatrix} X^T(k) & x_f^T(k) \end{bmatrix}^T$ and let the estimation error be $e(k) = z(k) - z_f(k)$. Then the filtering error system is given by

$$\begin{cases} \eta(k+1) = \tilde{A}\eta(k) + \tilde{B}W(k) + \sum_{i=1}^{N} \left(\beta_i(k) - \bar{\beta}_i\right) \left[\hat{A}_i \eta(k) + \hat{B}_i W(k) \right], \\ e(k) = \tilde{L}\eta(k), \end{cases} \tag{5.10}$$

where

$$\tilde{A} = \begin{bmatrix} \bar{A} & 0 \\ B_f \bar{C} \bar{E} & A_f \end{bmatrix}, \tilde{B} = \begin{bmatrix} \bar{B} \\ B_f \bar{D} \bar{H} \end{bmatrix}, \tilde{L} = \begin{bmatrix} \bar{L} & -C_f \end{bmatrix},$$
$$\hat{A}_i = \begin{bmatrix} 0 & 0 \\ B_f \bar{C} \bar{E}_i & 0 \end{bmatrix}, \hat{B}_i = \begin{bmatrix} 0 \\ B_f \bar{D} \bar{H}_i \end{bmatrix}, \bar{E} = \sum_{i=1}^{N} \bar{\beta}_i \bar{E}_i, \bar{H} = \sum_{i=1}^{N} \bar{\beta}_i \bar{H}_i.$$

Definition 5.1 The system (5.10) with $w(k) = 0$ is said to be asymptotically stable in the mean-square sense, if the solution $\eta(k)$ of system (5.10) satisfies $\lim_{k\to\infty} \mathbb{E}\{\|\eta(k)\|\} = \eta(0)$ for any initial condition.

Definition 5.2 For given scalars $\gamma > 0$, the system (5.10) is said to be asymptotically stable in the mean-square sense and achieves a prescribed H_∞ performance $\gamma > 0$, if it is asymptotically stable and under zero initial condition, $\sum_{s=0}^{+\infty} \mathbb{E}\{e^T(s)e(s)\} \leq \sum_{s=0}^{+\infty} \gamma^2 w^T(s)w(s)$ holds for all nonzero $w(k) \in l_2[0, \infty)$.

The filtering problem is stated as follows:

Filtering Problem: Design a filter in form of (5.8) such that the filtering error system (5.10) is asymptotically stable in the mean-square sense and achieves a prescribed H_∞ performance level in the presence of stochastic transmissions.

5.3 Filter Analysis and Design

Based on the stochastic analysis method, a sufficient condition is established for the solvability of considered filtering problem in the following theorem.

Theorem 5.1 *For given scalars τ and $\bar{\beta}_i$, $i = 1, 2, \ldots, N$, the filtering error system (5.10) is asymptotically stable in the mean-square sense and achieves a prescribed H_∞ performance level $\gamma = \tau\sqrt{N}$, if there exists a positive-definite matrix P such that the following inequality,*

$$\begin{bmatrix} \Phi_1 & \Phi_2 & \sqrt{\bar{\beta}_1}\Xi_1 & \cdots & \sqrt{\bar{\beta}_N}\Xi_N & \Phi_3 \\ * & -P^{-1} & 0 & 0 & 0 & 0 \\ * & * & -P^{-1} & 0 & 0 & 0 \\ * & * & * & \ddots & 0 & 0 \\ * & * & * & * & -P^{-1} & 0 \\ * & * & * & * & * & -I \end{bmatrix} < 0, \tag{5.11}$$

holds, where

$$\Phi_1 = \begin{bmatrix} -P & 0 \\ 0 & -\tau^2 I \end{bmatrix}, \Phi_2 = \begin{bmatrix} \tilde{A} & \tilde{B} \end{bmatrix}^T, \Xi_i = \begin{bmatrix} \hat{A}_i & \hat{B}_i \end{bmatrix}^T, \Phi_3 = \begin{bmatrix} \tilde{L} & 0 \end{bmatrix}^T.$$

Proof We first show the stability of the filtering error system (5.10) with $w(k) = 0$. Suppose the following Lyapunov function for system (5.10):

$$V(k) = \eta^T(k) P \eta(k). \tag{5.12}$$

Then, one sees that

$$\begin{aligned} &\mathbb{E}\{V(k+1) - V(k)\} \\ &= \left[\tilde{A}\eta(k)\right]^T P \left[\tilde{A}\eta(k)\right] - \eta^T(k) P \eta(k) \\ &+ \mathbb{E}\left\{\left[\sum_{i=1}^{N} \phi_i(k)\hat{A}_i\eta(k)\right]^T P \left[\sum_{i=1}^{N} \phi_i(k)\hat{A}_i\eta(k)\right]\right\}, \end{aligned} \tag{5.13}$$

where $\phi_i(k) = \beta_i(k) - \bar{\beta}_i$. On the other hand, we have

$$\begin{aligned} &\mathbb{E}\left\{\left[\sum_{i=1}^{N} \phi_i(k)\hat{A}_i\eta(k)\right]^T P \left[\sum_{i=1}^{N} \phi_i(k)\hat{A}_i\eta(k)\right]\right\} \\ &= \mathbb{E}\left\{\begin{array}{l} \sum_{i=1}^{N} (\phi_i(k))^2 \left[\hat{A}_i\eta(k)\right]^T P \left[\hat{A}_i\eta(k)\right] \\ + \sum_{i=1}^{N} \sum_{j=1, j\neq i}^{N} \phi_i(k)\phi_j(k) \left[\hat{A}_i\eta(k)\right]^T P \left[\hat{A}_j\eta(k)\right] \end{array}\right\} \\ &= \sum_{i=1}^{N} \bar{\beta}_i \left[\hat{A}_i\eta(k)\right]^T P \left[\hat{A}_i\eta(k)\right] \\ &- \left[\sum_{i=1}^{N} \bar{\beta}_i \hat{A}_i\eta(k)\right]^T P \left[\sum_{i=1}^{N} \bar{\beta}_i \hat{A}_i\eta(k)\right] \\ &\leq \sum_{i=1}^{N} \bar{\beta}_i \left[\hat{A}_i\eta(k)\right]^T P \left[\hat{A}_i\eta(k)\right]. \end{aligned} \tag{5.14}$$

Hence, we have

$$\begin{aligned} &\mathbb{E}\{V(k+1) - V(k)\} \\ &\leq \left[\tilde{A}\eta(k)\right]^T P \left[\tilde{A}\eta(k)\right] \\ &-\eta^T(k) P \eta(k) + \sum_{i=1}^{N} \bar{\beta}_i \left[\hat{A}_i\eta(k)\right]^T P \left[\hat{A}_i\eta(k)\right]. \end{aligned} \tag{5.15}$$

It is seen that the right hand side of (5.15) is negative under (5.11), and then system (5.10) is asymptotically stable in the mean-square sense.

Now we consider the H_∞ performance of the filtering error system (5.10). It follows from the above analysis method that

$$
\begin{aligned}
&\mathbb{E}\left\{V(k+1)-V(k)+e^T(k)e(k)-\tau^2 W^T(k)W(k)\right\}\\
&=\left[\tilde{A}\eta(k)+\tilde{B}W(k)\right]^T P\left[\tilde{A}\eta(k)+\tilde{B}W(k)\right]-\eta^T(k)P\eta(k)\\
&+\mathbb{E}\left\{\begin{array}{l}\left[\sum\limits_{i=1}^{N}\left(\beta_i(k)-\bar{\beta}_i\right)\left(\hat{A}_i\eta(k)+\hat{B}_iW(k)\right)\right]^T\\ \quad\times P\left[\sum\limits_{i=1}^{N}\left(\beta_i(k)-\bar{\beta}_i\right)\left(\hat{A}_i\eta(k)+\hat{B}_iW(k)\right)\right]\end{array}\right\}\\
&+\left[\tilde{L}\eta(k)\right]^T\left[\tilde{L}\eta(k)\right]-\tau^2W^T(k)W(k)\\
&\le\bar{\eta}^T(k)\left[\Phi_1+\Phi_2P\Phi_2^T+\sum_{i=1}^{N}\bar{\beta}_i\Xi_iP\Xi_i^T+\Phi_3\Phi_3^T\right]\bar{\eta}(k),
\end{aligned}
\tag{5.16}
$$

where $\bar{\eta}(k)=\left[\bar{\eta}^T(k)\ W^T(k)\right]^T$. By Lemma 2.1, it is easy to see

$$
\mathbb{E}\left\{V(k+1)-V(k)+e^T(k)e(k)-\tau^2W^T(k)W(k)\right\}<0. \tag{5.17}
$$

Summing both side of (5.17) from $k=0$ to $k=T$ leads to

$$
\mathbb{E}\left\{V(k+1)-V(0)+\sum_{k=0}^{T}\left\{e^T(k)e(k)-\tau^2W^T(k)W(k)\right\}\right\}<0, \tag{5.18}
$$

which implies, by the zero initial condition and positiveness of $V(k+1)$, that

$$
\mathbb{E}\left\{\sum_{k=0}^{T}\left\{e^T(k)e(k)-\tau^2W^T(k)W(k)\right\}\right\}<0. \tag{5.19}
$$

Letting $T\to+\infty$ gives

$$
\sum_{k=0}^{+\infty}\mathbb{E}\left\{e^T(k)e(k)\right\}\le\tau^2W^T(k)W(k)=\gamma^2w^T(k)w(k). \tag{5.20}
$$

Hence, the system (5.10) achieves a prescribed H_∞ performance level as well. This completes the proof.

Remark 5.3 In the filtering of stochastic transmitted systems, one of the main difficulties is how to relate the transmission parameters to the filtering performance. In Theorem 5.1, it is interesting to see that the filtering performance level is a monotonic function of the largest transmission span N.

It should be pointed out that theorem 1 can not be used to determine the filter gain directly due to the co-existence of P and P^{-1}. In the following theorem, we present the filter gain design algorithm.

Theorem 5.2 *For given scalars τ and $\bar{\beta}_i, i = 1, 2, \ldots, N$, if there exist a positive-definite matrix P and a matrix G with appropriate dimensions, such that the following inequality,*

$$\begin{bmatrix} \Phi_1 & \bar{\Phi}_2 & \sqrt{\bar{\beta}_1}\bar{\Xi}_1 & \cdots & \sqrt{\bar{\beta}_N}\bar{\Xi}_N & \bar{\Phi}_3 \\ * & \bar{P} & 0 & 0 & 0 & 0 \\ * & * & \bar{P} & 0 & 0 & 0 \\ * & * & * & \ddots & 0 & 0 \\ * & * & * & * & \bar{P} & 0 \\ * & * & * & * & * & -I \end{bmatrix} < 0, \tag{5.21}$$

holds, then the filtering performance is solvable. Moreover, the filter gains are determined by $A_f = G_3^{-T} A_F$, $B_f = G_3^{-T} B_F$ and $C_f = C_F$, where

$$\bar{\Phi}_2 = \begin{bmatrix} \bar{\Phi}_2^1 \\ \bar{\Phi}_2^2 \end{bmatrix}, \bar{\Xi}_i = \begin{bmatrix} \bar{\Xi}_i^1 \\ \bar{\Xi}_i^2 \end{bmatrix}, \bar{\Phi}_3 = \begin{bmatrix} \bar{\Phi}_3^1 \\ 0 \end{bmatrix}, \bar{P} = P - G - G^T,$$

with

$$\begin{aligned}
\bar{\Phi}_2^1 &= \begin{bmatrix} \bar{A}^T G_1 + E^T B_F^T M & \bar{A}^T G_2 + E^T B_F^T \\ A_F^T M & A_F^T \end{bmatrix}, \\
\bar{\Phi}_2^2 &= \begin{bmatrix} \bar{B}^T G_1 + \bar{H}^T B_F^T M & \bar{B}^T G_2 + \bar{H}^T B_F^T \end{bmatrix}, \\
\bar{\Xi}_i^1 &= \begin{bmatrix} \bar{E}_i^T \bar{C}^T B_F^T M & \bar{E}_i^T \bar{C}^T B_F^T \\ 0 & 0 \end{bmatrix}, \\
\bar{\Xi}_i^2 &= \begin{bmatrix} \bar{H}_i^T \bar{D}^T B_F^T M & \bar{H}_i^T \bar{D}^T B_F^T \end{bmatrix}, \\
\bar{\Phi}_3^1 &= \begin{bmatrix} \bar{L}^T \\ -C_F^T \end{bmatrix}, P = \begin{bmatrix} P_1 & P_2 \\ * & P_3 \end{bmatrix}, \\
G &= \begin{bmatrix} G_1 & G_2 \\ G_3 M & G_3 \end{bmatrix}, M = \begin{bmatrix} I & \cdots & I \end{bmatrix}.
\end{aligned}$$

Proof By pre and post multiplying (5.11) with diag $\left\{ I, G^T, \underbrace{G^T, \cdots G^T}_{N}, I \right\}$ and its transpose, respectively, (5.11) is equivalent to

$$\begin{bmatrix} \Phi_1 & \Phi_2 G & \sqrt{\bar{\beta}_1}\Xi_1 G & \cdots & \sqrt{\bar{\beta}_N}\Xi_N G & \Phi_3 \\ * & \tilde{P} & 0 & 0 & 0 & 0 \\ * & * & \tilde{P} & 0 & 0 & 0 \\ * & * & * & \ddots & 0 & 0 \\ * & * & * & * & \tilde{P} & 0 \\ * & * & * & * & * & -I \end{bmatrix} < 0, \tag{5.22}$$

where $\tilde{P} = -G^T P^{-1} G$. On other hand, it is easy to see that the inequality $-G^T P^{-1} G^T \leq P - G - G^T$, always hold for any matrix G. Then, (5.22) holds if

$$\begin{bmatrix} \Phi_1 & \Phi_2 G & \sqrt{\bar{\beta}_1}\Xi_1 G & \cdots & \sqrt{\bar{\beta}_N}\Xi_N G & \Phi_3 \\ * & \bar{P} & 0 & 0 & 0 & 0 \\ * & * & \bar{P} & 0 & 0 & 0 \\ & & & \ddots & & \\ * & * & * & 0 & 0 & 0 \\ * & * & * & * & \bar{P} & 0 \\ * & * & * & * & * & -I \end{bmatrix} < 0, \tag{5.23}$$

which is the same as (5.21) with

$$P = \begin{bmatrix} P_1 & P_2 \\ * & P_3 \end{bmatrix}, G = \begin{bmatrix} G_1 & G_2 \\ G_3 M & G_3 \end{bmatrix},$$
$$A_F = G_3^T A_f, B_F = G_3^T B_f, C_F = C_f.$$

This completes the proof.

Remark 5.4 In order to obtain the minimum H_∞ performance γ^*, one can solve the following optimization problem:

$$\begin{array}{c} \min \quad \nu \\ \text{s.t. (5.21) with } \nu = \tau^2 \end{array} \tag{5.24}$$

and find the minimum H_∞ performance γ^* by $\gamma^* = \sqrt{\nu^* N}$.

5.4 An Illustrative Example

In this section, a modified CSTR system [4] is used to show the usefulness of the proposed filter design. The CSTR is depicted in Fig. 5.2, and there is the following series-parallel reactions:

$$\begin{array}{l} \mathbb{A} \to \mathbb{B} \to \mathbb{C} \\ 2\mathbb{A} \to \mathbb{D} \end{array} \tag{5.25}$$

where $\mathbb{A}$ = cyclopentadiene, $\mathbb{B}$ = cyclopentenol, $\mathbb{C}$ = cyclopentanediol and $\mathbb{D}$ = dicyclopentadiene. The reactor inflow contains only the educt $\mathbb{A}$ in low concentration $c_{\mathbb{A}0}$. The desired product is the component $\mathbb{B}$, the intermediate component in the series reaction. Assuming constant density and an ideal residence time distribution within the reactor, the balance equations are given in [4] as follows:

$$\begin{array}{l} \frac{dc_{\mathbb{A}}}{dt} = \frac{\dot{V}}{V_R}(c_{\mathbb{A}0} - c_{\mathbb{A}}) - k_1 c_{\mathbb{A}} - k_3 c_{\mathbb{A}}^2, \\ \frac{dc_{\mathbb{B}}}{dt} = -\frac{\dot{V}}{V_R} c_{\mathbb{B}} + k_1 c_{\mathbb{A}} - k_2 c_{\mathbb{B}}, \\ \frac{d\vartheta}{dt} = \frac{\dot{V}}{V_R}(\vartheta_0 - \vartheta) + \frac{k_w A_R}{\zeta C_p V_R}(\vartheta_{\mathrm{K}} - \vartheta) \\ \qquad - \frac{k_1 c_{\mathbb{A}} \Delta H_{\mathrm{R}}^{\mathbb{AB}} + k_2 c_{\mathbb{B}} \Delta H_{\mathrm{R}}^{\mathbb{BC}} + k_3 c_{\mathbb{A}}^2 \Delta H_{\mathrm{R}}^{\mathbb{AD}}}{\zeta C_p}, \end{array} \tag{5.26}$$

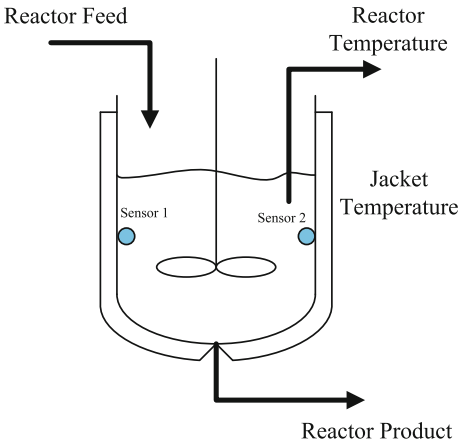

Fig. 5.2 Continuous stirred tank reactor

where $c_{\mathbb{A}}$ and $c_{\mathbb{B}}$ are the concentrations of educt $\mathbb{A}$ and the desired product $\mathbb{B}$ within the reactor and ϑ denotes the reactor temperature. The rate factors k_1, k_2 and k_3 depend exponentially on the reactor temperature ϑ via Arrhenius' law,

$$k_i(\vartheta) = k_{0i} \exp\left(\frac{-E_{\mathrm{A}i}}{R\vartheta}\right). \tag{5.27}$$

For the reaction system at hand, we let $k_1 = k_2$. The values of model parameters and the steady-state values of the main operating point of the reactor are listed in Table 5.1.

Linearizing (5.26) at the operating point yields the following state space model:

$$\dot{x}(t) = A_p x(t) + B_p u(t), \tag{5.28}$$

Table 5.1 Model parameters and main operating point

Model parameters	$A_R = 0.215\,\mathrm{m}^2$
$k_{01,2} = 1.287 \times 10^{12}\,\mathrm{h}^{-1}$	$V = 10.01$
$k_{03} = 9.043 \times 10^9\,\mathrm{l/mol\,h}^{-1}$	$\vartheta_0 = 403.15\,\mathrm{K}$
$E_{A1,2}/R = 9758.3\,\mathrm{K}$	$k_w = 4032\,\mathrm{kJ/h\,m}^2\,\mathrm{K}$
$E_{A3}/R = 8560.0\,\mathrm{K}$	Main operating point
$\Delta H_R^{\mathbb{AB}} = 4.2\,\mathrm{kJ/mol}$	$C_{\mathbb{A}s} = 1.235\mathrm{mol/l}$
$\Delta H_R^{\mathbb{BC}} = -11\,\mathrm{kJ/mol}$	$C_{\mathbb{B}s} = 0.9\mathrm{mol/l}$
$\Delta H_R^{\mathbb{AD}} = -41.85\,\mathrm{kJ/mol}$	$\vartheta_s = 407.29\mathrm{K}$
$\rho = 0.9342\,\mathrm{kg/l}$	$\dot{V}/V_R = 18.83\,\mathrm{h}^{-1}$
$C_P = 3.01\,\mathrm{kJ/kg\,K}$	$C_{\mathbb{A}0s} = 5.1\,\mathrm{mol/l}$

where

$$x = \begin{bmatrix} x_1 \\ x_2 \\ x_3 \end{bmatrix} = \begin{bmatrix} c_{\mathbb{A}} - c_{\mathbb{A}s} \\ c_{\mathbb{B}} - c_{\mathbb{B}s} \\ \vartheta - \vartheta_{\mathrm{s}} \end{bmatrix}, u = \begin{bmatrix} u_1 \\ u_2 \end{bmatrix} = \begin{bmatrix} \dot{V} - \dot{V}_{\mathrm{s}} \\ c_{\mathbb{A}0} - c_{\mathbb{A}0s} \end{bmatrix},$$

A_p and B_p are Jacobian matrices with

$$A_p = \begin{bmatrix} -86.0962 & 0 & 4.2077 \\ 50.6146 & -69.4446 & -0.9974 \\ 172.2263 & 197.9985 & -65.5149 \end{bmatrix},$$
$$B_p = \begin{bmatrix} 0.3861 & 18.83 \\ -0.0899 & 0 \\ -0.4136 & 0 \end{bmatrix}.$$

In the state estimation problem, one may also treat the control input as the unknown input signal. It is seen that the CSTR system is open loop stable, we choose $u = 0$ in the simulation. By further considering the unknown disturbance in CSTR, we have the following discrete-time state space model with sampling period $T_0 = 1$ min:

$$x(k+1) = Ax(k) + Bw(k), \tag{5.29}$$

where

$$A = \begin{bmatrix} 0.2747 & 0.0345 & 0.0206 \\ 0.2323 & 0.3152 & 0.0033 \\ 1.2566 & 1.1042 & 0.3671 \end{bmatrix}, B = \begin{bmatrix} 1 \\ 1 \\ 1 \end{bmatrix}.$$

In practice, it may be necessary for one to know the product concentration $c_{\mathbb{B}}$ for other use, but the direct measure of concentration $c_{\mathbb{B}}$ by traditional chemical approaches is usually expensive. An alternative yet non-expensive approach is to use signal processing approaches to estimate the concentration. In this example, we deploy two sensors to measure the educt concentration $c_{\mathbb{A}}$ and the reactor temperature ϑ. Our purpose is to estimate the product concentration $c_{\mathbb{B}}$. Hence, $C_1 = \begin{bmatrix} 1 & 0 & 0 \end{bmatrix}$, $C_2 = \begin{bmatrix} 0 & 0 & 1 \end{bmatrix}$, $D_1 = 0.3$, $D_2 = 0.2$ and $L = \begin{bmatrix} 0 & 1 & 0 \end{bmatrix}$. Suppose the noise varies in $w(k) \in [-1, 1]$. Note that this assumption is only for simulation purpose. One may obtain the statistical information about the noise in real industrial fields. In this example, we run the estimation task for 100 min.

Suppose that the transmission occurs if one of the following events happens:

$$\left\| y_p(k) - y_{last,p} \right\| \geq \delta_{y,p}, \tag{5.30}$$

$$k - k_{last,p} > \theta_{k,p}, \tag{5.31}$$

where $y_{last,p}$ is the last transmitted signal of sensor p and $k_{last,p}$ is the last transmitted time instant of sensor p. $\delta_{y,p}$ and $\theta_{k,p}$ are the measurement threshold and time

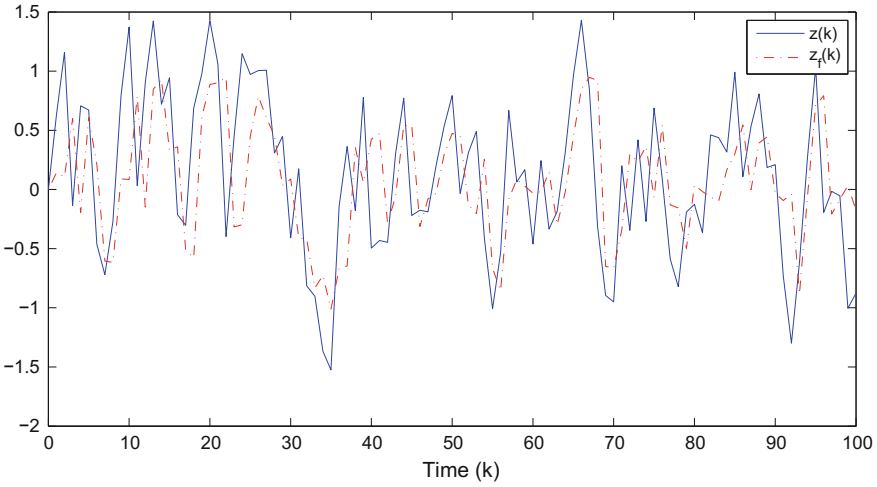

Fig. 5.3 Trajectories of $z(k)$ and $z_f(k)$

threshold, respectively. In this example, we assume that no packet dropout occurs for simulation simplicity. We set $\delta_{y,1} = 0.1$, $\delta_{y,2} = 0.2$; $\theta_{k,1} = \theta_{k,2} = 1$. It implies that $N_1 = N_2 = 2$. By doing 200 random samples for the transmissions, we have $\bar{\alpha}_{1,0} = 0.69$, $\bar{\alpha}_{1,1} = 0.31$; $\bar{\alpha}_{2,0} = 0.44$, $\bar{\alpha}_{2,1} = 0.56$.

With all information available, we solve the optimization problem (5.24) to get $\gamma^* = 1.9069$. The corresponding filter gains are

$$A_f = \begin{bmatrix} 0.2171 & 0.0420 & 0.0167 \\ 0.4788 & -0.0179 & 0.0159 \\ 6.0850 & -4.3532 & 0.6279 \end{bmatrix}, B_f = \begin{bmatrix} -1.2479 & 0.1254 \\ -1.4373 & 0.1444 \\ -4.2860 & 0.4305 \end{bmatrix},$$
$$C_f = \begin{bmatrix} -1.5297 & 0.7602 & 0.0040 \end{bmatrix}.$$

One sample trajectories of $z(k)$ and $z_f(k)$ are shown in Fig. 5.3. By simple calculation, we have $\sqrt{\sum_{k=0}^{100} e^T(k)e(k) \Big/ \sum_{k=0}^{100} w^T(k)w(k)} = 0.9342 < \gamma^* = 1.9069$. In order to see how robust our method is, we run 500 simulations. In each simulation, the transmission process is randomly generated and the transmission probabilities of each simulation are different (also different from the statistical one). It is shown in Fig. 5.4 that the true performance levels are smaller than the optimal one γ^*. Hence, the estimator design is robust to the probability uncertainties from the simulation point of view. Please note that if the transmission protocol in [1–3] is used, the optimal H_∞ performance is $\gamma^* = 2.0362$, which is much larger than that of our ones.

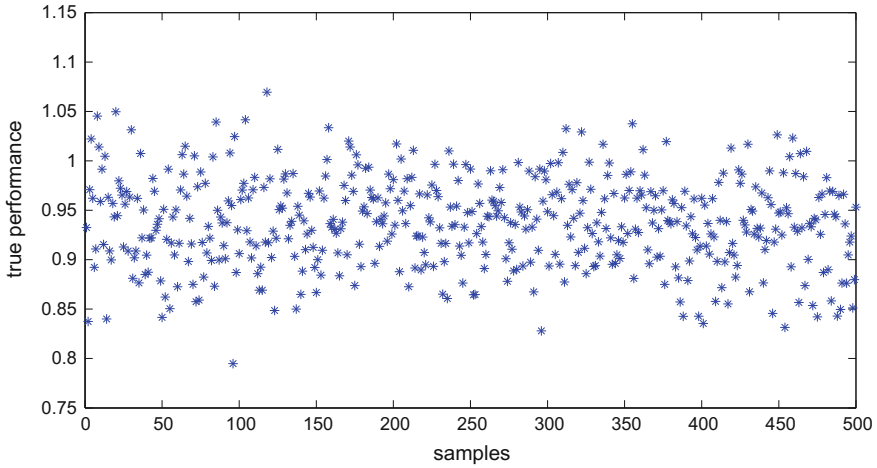

Fig. 5.4 True performance level of 500 samples

Table 5.2 Relation between $\bar{\alpha}_{1,0}$ and γ^*

$\delta_{y,1}$	0.1	0.15	0.2	0.25	0.3
$\bar{\alpha}_{1,0}$	0.69	0.58	0.49	0.43	0.39
γ^*	1.9069	2.0926	2.1378	2.1670	2.1859

We are now on the position to see how the transmission parameters affect the filtering performance. Here, we increase the measurement threshold $\delta_{y,1}$. The relation between transmission probability and the filtering performance is listed in the Table 5.2. It is seen that the more frequently the measurement is transmitted, the better filtering performance one obtains. In this scenario, more energy would be consumed by the sensors. The tradeoff between the energy consumption and the filtering performance should be considered in design of the WSNs, for example, if one requires that the filtering performance level is below 2.1, then, one may set $\delta_{y,1} = 0.15$ but not necessary to choose $\delta_{y,1} = 0.1$.

5.5 Conclusions

In this chpater, the energy-efficient filtering for a class of networked systems has been investigated, and a new stochastic transmission protocol is proposed and formulated. A sufficient condition has been given such that the filtering error system is asymptotically stable in the mean-square sense and achieves a prescribed H_∞ performance level. A filter design has been presented and the effectiveness has been illustrated by a case study of CSTR system. The relations between the transmission parameters, e.g.,

the transmission interval, the transmission probability and the filtering performance have been established.

References

1. E. Fridman, Use of models with aftereMect in the problem of design of optimal digital control. Autom. Remote Control. **53**(10), 1523–1528 (1992)
2. M. Wu, Y. He, J.H. She, G.P. Liu, Delay-dependent criteria for robust stability of time-varying delay systems. Automatica **40**(8), 1435–1439 (2004)
3. Y. He, Q.G. Wang, C. Lin, M. Wu, Delay-range-dependent stability for systems with time-varying delay. Automatica **43**(2), 371–376 (2007)
4. K.U. Klatt, S. Engell, Gain-scheduling trajectory control of a continuous stirred tank reactor. Comput. Chem. Eng. **22**(4–5), 491–502 (1998)

Chapter 6
H_∞ Filtering with Stochastic Sampling and Measurement Size Reduction

6.1 Introduction

In this chapter, a new approach is proposed for the H_∞ filtering over wireless networks. Firstly, the local measurement is sampled under a nonuniform sampling scheme. Then, one dimension of the measurement, which is selected and quantized for transmission. Finally, each quantized measurement is transmitted to the remote filter under a stochastic transmission protocol. A discrete-time stochastic Markovian system model with uncertainty is presented to model the above network-induced issues. Sufficient conditions are obtained such that the filtering error system is exponentially stable in the mean-square sense and achieves a prescribed H_∞ performance level. The filter gain parameters are determined by solving an optimization problem. The effectiveness of the proposed design is illustrated via a simulation study. The similar aperiodic sampling and measurement size reduction schemes have been proposed in Chap. 4, in which a deterministic one was addressed, but these two schemes are stochastically triggered in this chapter.

6.2 Problem Formulation

The structure of the filtering system is shown in Fig. 6.1 The continuous-time plant is described by the following linear time-invariant system:

$$\begin{cases} \dot{x}(t) = Ax(t) + Bw(t), \\ z(t) = Lx(t), \end{cases} \tag{6.1}$$

where $x(t) \in \mathbb{R}^{n_x}$ is the system state, $z(t) \in \mathbb{R}^{n_z}$ is the signal to be estimated, and $w(t) \in \mathbb{R}^{n_w}$ is the disturbance signal, which belongs to $L_2[0, +\infty)$. A, B and L are some constant matrices with appropriate dimensions. The local measurement signal is assumed to be

D. Zhang et al., *Filtering and Control of Wireless Networked Systems*,
Studies in Systems, Decision and Control 97, DOI 10.1007/978-3-319-53123-6_6

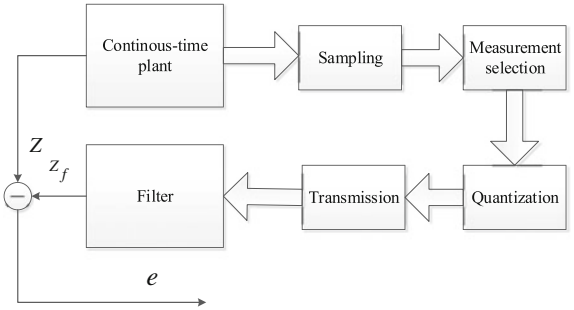

Fig. 6.1 Structure of the filtering system

$$y(t_k) = C_p x(t_k) + D_p w(t_k), \tag{6.2}$$

where $y(t_k) \in \mathbb{R}^{n_y}$ is the observation collected by the sensor at the discrete time instants t_k, $k = 0, 1, 2, \cdots$. C_p and D_p are constant matrices.

Define the measurement sampling period as $h_k = t_{k+1} - t_k$. Then h_k is a time-varying value. In this chapter, we assume that h_k takes a value from a given set. Specifically, let $h_k = n_k T_0$, where $n_k \in \{i_1, i_2, \cdots, i_{n_1}\}$, i_j, $j = 1, 2, \cdots, n_1$, are positive integers, and T_0 is a basic sampling period.

We now discretize the system (6.1) with the sampling period h_k and applying a zero-order-holder, the following discrete-time system is obtained:

$$\begin{cases} x(t_{k+1}) = A_k x(t_k) + B_k w(t_k), \\ z(t_k) = L x(t_k), \end{cases} \tag{6.3}$$

where $A_k = e^{Ah_k}$, and $B_k = B\int_0^{h_k} e^{A\tau} d\tau$. Let $A_0 = e^{AT_0}$ and $B_0 = B\int_0^{T_0} e^{A\tau} d\tau$. Then $A_k = {A_0}^{n_k}$ and $B_k = \sum_{i=0}^{n_k-1} {A_0}^i B_0$. It is seen that the values of A_k and B_k are determined by the sampling period h_k. Define a piecewise constant signal $\rho(k) \in \Omega_1 = \{1, 2, \cdots, n_1\}$. Then we have the following switched system model for (6.3):

$$\begin{cases} x(t_{k+1}) = A_{\rho(t_k)} x(t_k) + B_{\rho(t_k)} w(t_k), \\ z(t_k) = L x(t_k), \end{cases} \tag{6.4}$$

where $A_{\rho(t_k)} = {A_0}^{i_{\rho(t_k)}}$ and $B_{\rho(t_k)} = \sum_{l=1}^{i_{\rho(t_k)}} A_0^{l-1} B_0$.

In this chapter, the piece-wise constant signal $\rho(t_k)$ is assumed to satisfy a Markovian process, with the transition probabilities $\Theta_1 = [\rho_{ij}]$:

$$\begin{cases} \rho_{ij} = \Pr\ ob\{\rho(t_{k+1}) = j \,|\, \rho(t_k) = i\}, \\ \sum_{j=1}^{n_1} \rho_{ij} = 1, \quad \rho_{ij} \geq 0. \end{cases} \tag{6.5}$$

Due to the fact that the size of measurement signal $y_p(t_k)$ is n_{y_p}, when such a measurement is directly transmitted to the estimator, the sensor may still consume much power. As in Chap. 4, we also choose one dimension for transmission at each time instant. Hence, the selected signal is described as

$$\bar{y}(t_k) = \Pi_{\sigma(t_k)} y(t_k), \tag{6.6}$$

where $\Pi_{\sigma(t_k)}$ is a structured matrix used to choose one element for transmission, and $\sigma(t_k)$ is a piecewise signal belonging to $\Omega_2 = \{1, 2, \cdots, n_y\}$. Specifically, when the first element is selected, then $\Pi_{\sigma(t_k)} = [\,1\ 0 \cdots 0\,]$, when the second element is selected, then $\Pi_{\sigma(t_k)} = [\,0\ 1 \cdots 0\,]$, and so on. It is seen that $\sigma(t_k)$ is a switching signal, and it is also assumed to be a Markovian process with the transition probabilities $\Theta_2 = [\lambda_{ij}]$:

$$\begin{cases} \lambda_{ij} = \Pr\ ob\,\{\lambda(t_{k+1}) = t \,|\, \lambda(t_k) = s\}, \\ \sum\limits_{t=1}^{n_y} \lambda_{st} = 1, \quad \lambda_{st} \geq 0. \end{cases} \tag{6.7}$$

Remark 6.1 The above nonuniform sampling and measurement size reduction are performed in a stochastic way, which are different from the ones in Chap. 4. The stochastic modeling approach may help obtain a better estimation performance.

The measurement size reduction technique introduced above is an effective method to reduce the measurement size. Another effective way to reduce the packet size is the quantization scheme. In this chapter, the logarithmic quantizer $Q(\bullet)$ is used to further reduce the packet size. The quantizer is assumed to be symmetric and time-invariant, i.e., $Q(v) = -Q(-v)$. The set of quantization levels is described as

$$\begin{aligned} U = &\{\pm\kappa_i, \kappa_i = \rho_i \kappa_0, i = 0, \pm 1, \pm 2, ...\} \\ &\cup \{\pm\kappa_0\} \cup \{0\}, 0 < \rho < 1, \kappa_0 > 0. \end{aligned} \tag{6.8}$$

The quantized output $Q(\bullet)$ is given by

$$Q(v) = \begin{cases} \kappa_i, & \text{if } \frac{1}{1+\delta}\kappa_i < v < \frac{1}{1-\delta}\kappa_i, v > 0, \\ 0, & \text{if } v = 0, \\ -Q(-v), & \text{if } v < 0, \end{cases} \tag{6.9}$$

where $\delta = \frac{1-\rho}{1+\rho} < 1$, with the quantization density $0 < \rho < 1$. The quantized measurement signal is described by

$$\hat{y}(t_k) = Q(\bar{y}(t_k)). \tag{6.10}$$

Define the quantization error $\tilde{e} = \hat{y}(t_k) - \bar{y}(t_k)$. Then $\hat{y}(t_k) = (I + \Delta(t_k))\bar{y}(t_k)$, where $\|\Delta(t_k)\| \leq \Lambda$. The transmission of quantized measurement is finally scheduled by a stochastic transmission protocol, i.e., the final measurement signal used by

the filter is

$$\tilde{y}(t_k) = \alpha(t_k) Q(\bar{y}(t_k)), \tag{6.11}$$

where $\alpha(t_k) \in \{0, 1\}$ is a binary stochastic variable, and Pr $ob\{\alpha(t_k) = 1\} = \bar{\alpha}$ is called the transmission rate, which can be set by the designer. It is easy to see that more energy can be saved if a coarser quantizer is chosen, and more energy is saved if one sets a smaller transmission rate.

We are now on the stage to design the following filter:

$$\begin{cases} x_f(t_{k+1}) = A_f \hat{x}_f(t_k) + B_f \tilde{y}(t_k), \\ z_f(t_k) = L_f \hat{x}_f(t_k), \end{cases} \tag{6.12}$$

where $x_f(t) \in \mathbb{R}^{n_x}$ is the filter's state, and $z_f(t) \in \mathbb{R}^{n_z}$ is the estimation signal from the filter. A_f, B_f and L_f are the filter gain parameters to be determined. Based on the above discussions, for each $i \in \Omega_1$ and $s \in \Omega_2$, the following filtering error system is obtained:

$$\begin{cases} \eta(t_{k+1}) = \tilde{A}_{i,s}\eta(t_k) + \tilde{B}_{i,s} w(t_k) \\ \qquad\quad +(\alpha(t_k) - \bar{\alpha}) \left\{ \tilde{A}_s \eta(t_k) + \tilde{B}_s w(t_k) \right\}, \\ e(t_k) = \tilde{L}\eta(t_k), \end{cases} \tag{6.13}$$

where

$$\begin{aligned} &\eta(t_k) = \left[x^T(t_k)\ x_f^T(t_k) \right]^T, e(t_k) = z_f(t_k) - z(t_k), \\ &\tilde{A}_{i,s} = A_{i,s} + \bar{\alpha} M \Delta(t_k) N_{1s}, \tilde{B}_{i,s} = B_{i,s} + \bar{\alpha} M \Delta(t_k) N_{2s}, \\ &\tilde{A}_s = \bar{A}_s + M \Delta(t_k) N_{1s}, \tilde{B}_s = \bar{B}_s + M \Delta(t_k) N_{2s}, \\ &A_{i,s} = \begin{bmatrix} A_i & 0 \\ \bar{\alpha} B_f \Pi_s C & A_f \end{bmatrix}, B_{i,s} = \begin{bmatrix} B_i \\ \bar{\alpha} B_f \Pi_s D \end{bmatrix}, \\ &\bar{A}_s = \begin{bmatrix} 0 & 0 \\ B_f \Pi_s C & 0 \end{bmatrix}, \bar{B}_s = \begin{bmatrix} 0 \\ B_f \Pi_s D \end{bmatrix}, \tilde{L} = \begin{bmatrix} -L & C_f \end{bmatrix}, \\ &M = \begin{bmatrix} 0 \\ B_f \end{bmatrix}, N_{1s} = \begin{bmatrix} \Pi_s C & 0 \end{bmatrix}, N_{2s} = \Pi_s D. \end{aligned}$$

The System (6.13) is an uncertain Markovian jump system with two Markovian chains, and the following useful definitions are needed in the derivation of the main results.

Definition 6.1 The filtering error system (6.13) with $w(t_k) = 0$ is said to be mean-square exponentially stable if there exist constants $c > 0$ and $\beta > 1$ such that, for every initial condition $\chi(0) = (\eta(0), \sigma(0), \rho(0))$, the corresponding solution satisfies $\mathbb{E}\left\{ \|\eta(t_k)\|^2 \middle| \chi(0) \right\} \leq c\beta^{-k} \|\eta(0)\|^2, \forall k \geq 0$, where β is the decay rate.

Definition 6.2 For given a scalar $\gamma > 0$, the filtering error system (6.13) is said to be mean-square exponentially stable with an H_∞ noise attenuation level γ if it is mean-square exponentially stable and under zero initial condition, $\sum_{k=0}^{\infty} \mathbb{E}\left\{ e^T(t_k) e(t_k) \middle| \chi(0) \right\} < \gamma^2 \sum_{k=0}^{\infty} w^T(t_k) w(t_k)$ holds.

The filtering problem is formulated as follows.

Filtering Problem: design the filter in form of (6.12) such that the filtering error system (6.13) is exponentially stable in the mean-square sense and achieves a prescribed H_∞ performance level in the presence of stochastic sampling, stochastic measurement size reduction, signal quantization and stochastic signal transmission.

6.3 Filter Analysis and Design

In this section, a sufficient condition is firstly established such that the filtering error system (6.13) is exponentially stable in the mean-square sense with a prescribed H_∞ performance level.

Theorem 6.1 *For the given scalars $\rho_{ij} \geq 0$, $\lambda_{ij} \geq 0$, $\bar{\alpha} > 0$, $\delta \geq 1$, and $\gamma > 0$, the filtering error system (6.13) is exponentially stable in the mean-square sense with the decay rate δ^2, and achieves a prescribed H_∞ performance level γ, if there exist positive-definite matrices $P_{i,s}$ and a positive scale $\varepsilon > 0$ such that the following inequalities,*

$$\begin{bmatrix} \Psi_1 & \Psi_2 & \Psi_3 & \Psi_4 & \Psi_5 & 0 \\ * & -\bar{P}^{-1} & 0 & 0 & 0 & \bar{\alpha} M \\ * & * & -\bar{P}^{-1} & 0 & 0 & \theta M \\ * & * & * & -I & 0 & 0 \\ * & * & * & * & -\varepsilon I & 0 \\ * & * & * & * & * & -\varepsilon I \end{bmatrix} < 0 \tag{6.14}$$

hold for all $i \in \Omega_1$, $s \in \Omega_2$, where

$$\Psi_1 = \begin{bmatrix} -P_{i,s} & 0 \\ 0 & -\gamma^2 I \end{bmatrix}, \Psi_2 = \delta \begin{bmatrix} A_{i,s} & B_{i,s} \end{bmatrix}^T, \Psi_3 = \theta\delta \begin{bmatrix} \bar{A}_s & \bar{B}_s \end{bmatrix}^T,$$
$$\Psi_4 = \begin{bmatrix} \tilde{L} & 0 \end{bmatrix}^T, \Psi_5 = \delta \begin{bmatrix} N_{1s} \Lambda\varepsilon & N_{2s} \Lambda\varepsilon \end{bmatrix}^T,$$
$$\bar{P} = \sum_{j=1}^{n_1} \sum_{t=1}^{n_2} \rho_{ij} \lambda_{st} P_{j,t}, \theta = \sqrt{\bar{\alpha}(1-\bar{\alpha})}.$$

Proof Let $\psi(t_k) = \delta^k \eta(t_k)$ and $v(t_k) = \delta^k w(t_k)$. Choose the following Lyapunov function:

$$V(t_k) = \psi^T(t_k) P(\rho(t_k), \sigma(t_k))\psi(t_k). \tag{6.15}$$

We have

$$\begin{aligned}
&\mathbb{E}\{\Delta V(t_k)\} \\
&= \mathbb{E}\{V(t_{k+1}) | \psi(t_k), \rho(t_k), \sigma(t_k)\} - V(t_k) \\
&= \mathbb{E}\left\{\delta^{2(k+1)} \eta^T(t_{k+1}) P(\rho(t_{k+1}), \sigma(t_{k+1}))\eta(t_{k+1}) \middle| \psi(t_k), \rho(t_k), \sigma(t_k)\right\} \\
&\quad - \psi^T(t_k) P(\rho(t_k), \sigma(t_k))\psi(t_k) \\
&= \left\{\delta\tilde{A}_{i,s}\psi(t_k) + \delta\tilde{B}_{i,s}v(t_k)\right\}^T \bar{P} \left\{\delta\tilde{A}_{i,s}\psi(t_k) + \delta\tilde{B}_{i,s}v(t_k)\right\} \\
&\quad + \theta^2 \left\{\delta\tilde{A}_s\psi(t_k) + \delta\tilde{B}_s v(t_k)\right\}^T \bar{P} \left\{\delta\tilde{A}_s\psi(t_k) + \delta\tilde{B}_s v(t_k)\right\} \\
&\quad - \psi^T(t_k) P(\rho(t_k), \sigma(t_k))\psi(t_k) \\
&= \begin{bmatrix} \psi(t_k) \\ v(t_k) \end{bmatrix}^T \begin{bmatrix} \delta\left(\tilde{A}_{i,s}\right)^T \\ \delta\left(\tilde{B}_{i,s}\right)^T \end{bmatrix} \bar{P} \begin{bmatrix} \delta\left(\tilde{A}_{i,s}\right) & \delta\left(\tilde{B}_{i,s}\right) \end{bmatrix} \begin{bmatrix} \psi(t_k) \\ v(t_k) \end{bmatrix} \\
&\quad + \begin{bmatrix} \psi(t_k) \\ v(t_k) \end{bmatrix}^T \begin{bmatrix} \theta\delta\left(\tilde{A}_s\right)^T \\ \theta\delta\left(\tilde{B}_s\right)^T \end{bmatrix} \bar{P} \begin{bmatrix} \theta\delta\left(\tilde{A}_s\right) & \theta\delta\left(\tilde{B}_s\right) \end{bmatrix} \begin{bmatrix} \psi(t_k) \\ v(t_k) \end{bmatrix} \\
&\quad + \begin{bmatrix} \psi(t_k) \\ v(t_k) \end{bmatrix}^T \begin{bmatrix} -P_{i,s} + \tilde{L}^T\tilde{L} & 0 \\ 0 & -\gamma^2 I \end{bmatrix} \begin{bmatrix} \psi(t_k) \\ v(t_k) \end{bmatrix} \\
&\quad - \begin{bmatrix} \psi(t_k) \\ v(t_k) \end{bmatrix}^T \begin{bmatrix} \tilde{L}^T\tilde{L} & 0 \\ 0 & 0 \end{bmatrix} \begin{bmatrix} \psi(t_k) \\ v(t_k) \end{bmatrix} \\
&\quad + \gamma^2 v^T(t_k) v(t_k) \\
&= \begin{bmatrix} \psi(t_k) \\ v(t_k) \end{bmatrix}^T \left\{ \Xi - \begin{bmatrix} \tilde{L}^T\tilde{L} & 0 \\ 0 & 0 \end{bmatrix} \right\} \begin{bmatrix} \psi(t_k) \\ v(t_k) \end{bmatrix} + \gamma^2 v^T(t_k) v(t_k),
\end{aligned} \tag{6.16}$$

where

$$\begin{aligned}
\Xi &= \begin{bmatrix} \delta\left(\tilde{A}_{i,s}\right)^T \\ \delta\left(\tilde{B}_{i,s}\right)^T \end{bmatrix} \bar{P} \begin{bmatrix} \delta\left(\tilde{A}_{i,s}\right) & \delta\left(\tilde{B}_{i,s}\right) \end{bmatrix} \\
&\quad + \begin{bmatrix} \theta\delta\left(\tilde{A}_s\right)^T \\ \theta\delta\left(\tilde{B}_s\right)^T \end{bmatrix} \bar{P} \begin{bmatrix} \theta\delta\left(\tilde{A}_s\right) & \theta\delta\left(\tilde{B}_s\right) \end{bmatrix} \\
&\quad + \begin{bmatrix} -P_{i,s} + \tilde{L}^T\tilde{L} & 0 \\ 0 & -\gamma^2 I \end{bmatrix}.
\end{aligned}$$

It is seen that $\Xi < 0$ guarantees $\mathbb{E}\{\Delta V(t_k)\} < 0$ when $v(t_k) = 0$. By Lemma 2.1, $\Xi < 0$ is equivalent to

$$\begin{bmatrix} \Psi_1 & \Psi_2 & \Psi_3 & \Psi_4 \\ * & -\bar{P}^{-1} & 0 & 0 \\ * & * & -\bar{P}^{-1} & 0 \\ * & * & * & -I \end{bmatrix} + \begin{bmatrix} \tilde{\Psi}_5 \\ 0 \\ 0 \\ 0 \end{bmatrix} \frac{\Delta}{\Lambda} \begin{bmatrix} 0 \\ \bar{\alpha}M \\ \theta M \\ 0 \end{bmatrix}^T + \begin{bmatrix} 0 \\ \bar{\alpha}M \\ \theta M \\ 0 \end{bmatrix} \frac{\Delta}{\Lambda} \begin{bmatrix} \tilde{\Psi}_5 \\ 0 \\ 0 \\ 0 \end{bmatrix}^T < 0, \tag{6.17}$$

where $\tilde{\Psi}_5 = \delta\begin{bmatrix} N_{1s}\Lambda & N_{2s}\Lambda \end{bmatrix}^T$. It follows from Lemma 2.2 that (6.17) holds if and only if there exists a scalar $\varepsilon > 0$ such that

$$\begin{bmatrix} \Psi_1 & \Psi_2 & \Psi_3 & \Psi_4 \\ * & -\bar{P}^{-1} & 0 & 0 \\ * & * & -\bar{P}^{-1} & 0 \\ * & * & * & -I \end{bmatrix} + \varepsilon \begin{bmatrix} \tilde{\Psi}_5 \\ 0 \\ 0 \\ 0 \end{bmatrix} \begin{bmatrix} \tilde{\Psi}_5 \\ 0 \\ 0 \\ 0 \end{bmatrix}^T + \varepsilon^{-1} \begin{bmatrix} 0 \\ \bar{\alpha}M \\ \theta M \\ 0 \end{bmatrix} \begin{bmatrix} 0 \\ \bar{\alpha}M \\ \theta M \\ 0 \end{bmatrix}^T < 0. \tag{6.18}$$

By Lemma 2.1, we have that (6.14) guarantees (6.18), i.e., $\mathbb{E}\{\Delta V(t_k)\} < 0$ holds. Then

$$\mathbb{E}\{V(t_{k+1})|\,\psi(t_k), \rho(t_k), \sigma(t_k)\} < V(t_k). \tag{6.19}$$

By deduction, it follows from (6.19) that

$$\mathbb{E}\{V(t_k)|\,\psi(0), \rho(0), \sigma(0)\} < V(0). \tag{6.20}$$

Let $\beta_1 = \min\left\{\lambda_{\min}(P_{i,s})\right\}$ and $\beta_2 = \lambda_{\max}(P(\rho(0), \sigma(0)))$. Then it follows from (20) and the fact $\psi(0) = \eta(0)$ that $\mathbb{E}\left\{\|\eta(t_k)\|^2 \middle|\, \eta(0), \rho(0), \sigma(0)\right\} \leq \frac{\beta_2}{\beta_1}\left(\delta^2\right)^{-k}\|\eta(0)\|$. By Definition 6.1, the filtering error system (6.13) is mean-square exponentially stable and achieves a decay rate $\beta = \delta^2 \geq 1$.

Now, to establish the H_∞ performance of the filtering error system, we consider the following performance index:

$$J = \mathbb{E}\left\{\sum_{k=0}^{N}\left[e^T(t_k)e(t_k) - \gamma^2 w^T(t_k)w(t_k)\right]\middle|\, \chi(0)\right\}, \tag{6.21}$$

where $\chi(0) = \{\eta(0), \rho(0), \sigma(0)\}$. Under the zero initial condition, we have

$$
\begin{aligned}
J &= \mathbb{E}\left\{\sum_{k=0}^{N}\left[e^T(t_k)e(t_k)-\gamma^2 w^T(t_k)w(t_k)+\delta^{-2k}\Delta V(t_k)\right]\Big|\,\chi(0)\right\}\\
&\quad -\mathbb{E}\left\{\sum_{k=0}^{N}\left[\delta^{-2k}\Delta V(t_k)\right]\Big|\,\chi(0)\right\}\\
&= \mathbb{E}\left\{\sum_{k=0}^{N}\left[\eta^T(t_k)\tilde{L}^T\tilde{L}\eta(t_k)-\gamma^2 w^T(t_k)w(t_k)+\delta^{-2k}\gamma^2 v^T(t_k)v(t_k)\right]\Big|\,\chi(0)\right\}\\
&\quad +\mathbb{E}\left\{\sum_{k=0}^{N}\left[\delta^{-2k}\begin{bmatrix}\psi(t_k)\\ v(t_k)\end{bmatrix}^T\left\{\Xi-\begin{bmatrix}\tilde{L}^T\tilde{L} & 0\\ 0 & 0\end{bmatrix}\right\}\begin{bmatrix}\psi(t_k)\\ v(t_k)\end{bmatrix}\right]\Big|\,\chi(0)\right\}\\
&\quad -\mathbb{E}\left\{\delta^{-2N}V(t_{N+1})+\sum_{k-1}^{N}\delta^{-2(k-1)}(1-\delta^{-2})V(t_k)\Big|\,\chi(0)\right\}+V(0)\\
&\le \left\{\sum_{k=0}^{N}\begin{bmatrix}\eta(t_k)\\ w(t_k)\end{bmatrix}^T\Xi\begin{bmatrix}\eta(t_k)\\ w(t_k)\end{bmatrix}\Big|\,\chi(0)\right\}.
\end{aligned}
$$

Therefore, $\Xi < 0$ guarantees $J < 0$. Let $N \to \infty$, and we have

$$
\mathbb{E}\left\{\sum_{k=0}^{\infty}\left[e^T(t_k)e(t_k)\right]\Big|\,\chi(0)\right\} \le \gamma^2\sum_{k=0}^{\infty}w^T(t_k)w(t_k). \tag{6.22}
$$

Thus, the filtering error system (6.13) is exponentially stable in the mean-square sense and achieves a prescribed H_∞ performance level γ.

One also sees that it is difficult to obtain the filter gains from Theorem 6.1 due to the fact that (6.14) is not an LMI. We now propose the filter gain design algorithm in the following theorem.

Theorem 6.2 *For the given scalars $\rho_{ij} \ge 0$, $\lambda_{ij} \ge 0$, $\bar{\alpha} > 0$, $\delta \ge 1$, and $\gamma > 0$, if there exist positive-definite matrices P_{is}, any matrices G of appropriate dimensions, and a positive scale $\varepsilon > 0$ such that the following inequalities,*

$$
\begin{bmatrix}
\Psi_1 & \tilde{\Psi}_2 & \tilde{\Psi}_3 & \tilde{\Psi}_4 & \tilde{\Psi}_5 & 0\\
* & \bar{T} & 0 & 0 & 0 & \tilde{\Psi}_6\\
* & * & \bar{T} & 0 & 0 & \tilde{\Psi}_7\\
* & * & * & -I & 0 & 0\\
* & * & * & * & -\varepsilon I & 0\\
* & * & * & * & * & -\varepsilon I
\end{bmatrix} < 0, \tag{6.23}
$$

hold for all $i \in \Omega_1$, $s \in \Omega_2$, then our filtering problem is solvable, and the filter gains are determined by $A_f = G_3^{-T}A_F$, $B_f = G_3^{-T}B_F$ and $L_f = L_F$, where

$$
\begin{aligned}
&\tilde{\Psi}_2 = \begin{bmatrix}\tilde{\Psi}_{21}\\ \tilde{\Psi}_{22}\end{bmatrix}, \tilde{\Psi}_3 = \begin{bmatrix}\tilde{\Psi}_{31}\\ \tilde{\Psi}_{32}\end{bmatrix}, \tilde{\Psi}_4 = \begin{bmatrix}\tilde{\Psi}_{41}\\ 0\end{bmatrix}, \tilde{\Psi}_5 = \begin{bmatrix}\tilde{\Psi}_{51}\\ \tilde{\Psi}_{52}\end{bmatrix},\\
&\tilde{\Psi}_6 = \bar{\alpha}\begin{bmatrix}B_F\\ B_F\end{bmatrix}, \tilde{\Psi}_7 = \theta\begin{bmatrix}B_F\\ B_F\end{bmatrix}, T = \bar{P} - G - G^T,
\end{aligned}
$$

with

$$\tilde{\Psi}_{21} = \delta \begin{bmatrix} A_i^T G_1 + \bar{\alpha} C^T \Pi_s^T B_F^T & A_i^T G_2 + \bar{\alpha} C^T \Pi_s^T B_F^T \\ A_F^T & A_F^T \end{bmatrix},$$

$$\tilde{\Psi}_{22} = \delta \begin{bmatrix} B_i^T G_1 + \bar{\alpha} \bar{D}^T \Pi_s^T B_F^T & B_i^T G_2 + \bar{\alpha} \bar{D}^T \Pi_s^T B_F^T \end{bmatrix},$$

$$\tilde{\Psi}_{31} = \theta\delta \begin{bmatrix} C^T \Pi_s^T B_F^T & C^T \Pi_s^T B_F^T \\ 0 & 0 \end{bmatrix},$$

$$\tilde{\Psi}_{32} = \theta\delta \begin{bmatrix} \bar{D}^T \Pi_s^T B_F^T & \bar{D}^T \Pi_s^T B_F^T \end{bmatrix},$$

$$\tilde{\Psi}_{41} = \begin{bmatrix} -L^T \\ C_F^T \end{bmatrix}, \tilde{\Psi}_{51} = \delta \begin{bmatrix} C^T \Pi_s^T \Lambda\varepsilon \\ 0 \end{bmatrix}, \tilde{\Psi}_{52} = \delta D^T \Pi_s^T \Lambda\varepsilon,$$

$$P_{i,s} = \begin{bmatrix} P_{1i,s} & P_{2i,s} \\ * & P_{3i,s} \end{bmatrix}, G = \begin{bmatrix} G_1 & G_2 \\ G_3 & G_3 \end{bmatrix}.$$

Proof By left- and right- multiplying (6.14) with $\mathrm{diag}\{I, I, G^T, G^T, I, I, I\}$ and its transpose, (6.14) is equivalent to

$$\begin{bmatrix} \Psi_1 & \Psi_2 G & \Psi_3 G & \Psi_4 & \Psi_5 & 0 \\ * & -G^T \bar{P}^{-1} G & 0 & 0 & 0 & \bar{\alpha} G^T M \\ * & * & -G^T \bar{P}^{-1} G & 0 & 0 & \theta G^T M \\ * & * & * & -I & 0 & 0 \\ * & * & * & * & -\varepsilon I & 0 \\ * & * & * & * & * & -\varepsilon I \end{bmatrix} < 0. \tag{6.24}$$

On the other hand, the inequality, $-G^T \bar{P}^{-1} G \le \bar{P} - G - G^T$, always holds for any matrix G. Then, (6.24) holds if

$$\begin{bmatrix} \Psi_1 & \Psi_2 G & \Psi_3 G & \Psi_4 & \Psi_5 & 0 \\ * & \bar{P} - G - G^T & 0 & 0 & 0 & \bar{\alpha} G^T M \\ * & * & \bar{P} - G - G^T & 0 & 0 & \theta G^T M \\ * & * & * & -I & 0 & 0 \\ * & * & * & * & -\varepsilon I & 0 \\ * & * & * & * & * & -\varepsilon I \end{bmatrix} < 0, \tag{6.25}$$

which is the same as (6.23) with

$$P_{i,s} = \begin{bmatrix} P_{1i,s} & P_{2i,s} \\ * & P_{3i,s} \end{bmatrix}, G = \begin{bmatrix} G_1 & G_2 \\ G_3 & G_3 \end{bmatrix},$$
$$A_F = G_3^T A_f, B_F = G_3^T B_f, L_F = L_f.$$

This completes the proof.

Remark 6.2 In Theorem 6.2, the existence condition for the filters is given in terms of LMIs which is convex in the scalar γ^2. Therefore, one may solve the following optimization problem:

$$\begin{aligned} &\min \rho, \\ &\text{s.t. (6.23)} \quad \text{with} \quad \rho = \gamma^2 \end{aligned} \tag{6.26}$$

to obtain the filter gain parameters such that the H_∞ disturbance attenuation level is minimized. When the optimal ρ is obtained from the above optimization problem, the designed filter ensures that the filtering error system is exponentially stable and achieves a prescribed H_∞ performance level ρ.

6.4 An Illustrative Example

Consider a satellite yaw angles control system with noise, which has been discussed in Chap. 4. The state-space model is described as follows:

$$\begin{aligned} \begin{bmatrix} 1 & 0 & 0 & 0 \\ 0 & 1 & 0 & 0 \\ 0 & 0 & J_1 & 0 \\ 0 & 0 & 0 & J_2 \end{bmatrix} \begin{bmatrix} \dot{\theta}_1(t) \\ \dot{\theta}_2(t) \\ \dot{\delta}_1(t) \\ \dot{\delta}_2(t) \end{bmatrix} &= \begin{bmatrix} 0 & 0 & 1 & 0 \\ 0 & 0 & 0 & 1 \\ -k & k & -f & f \\ k & -k & f & -f \end{bmatrix} \begin{bmatrix} \theta_1(t) \\ \theta_2(t) \\ \delta_1(t) \\ \delta_2(t) \end{bmatrix} \\ &+ \begin{bmatrix} 0 \\ 0 \\ 1 \\ 0 \end{bmatrix} u(t) + \begin{bmatrix} 0 \\ 0.1 \\ 0 \\ 0.1 \end{bmatrix} w(t). \end{aligned} \tag{6.27}$$

The satellite yaw angles control system consists of two rigid bodies jointed by a flexible link. This link is modeled as a spring with torque constant k and viscous damping f. $\theta_1(t)$ and $\theta_2(t)$ are the yaw angles for the main body and the instrumentation module of the satellite. Moreover, $\delta_1(t) = \dot{\theta}_1(t)$ and $\delta_2(t) = \dot{\theta}_2(t)$. $u(t)$ is the control torque, while J_1 and J_2 are the moments of the main body and the instrumentation module, respectively.

Suppose that $J_1 = J_2 = 1, k = 0.3$, $f = 0.004$, the sampling period is $T \in \{0.05s, 0.1s\}$ and the controller is

$$u(k) = 10^3 \left[-0.1591 \ -5.9343 \ -0.0172 \ -2.8604 \right] x(k).$$

The resulting discrete-time satellite yaw angles closed-loop system is given by

$$A_1 = \begin{bmatrix} 0.8008 & -7.4165 & 0.0285 & -3.5750 \\ 0.0003 & 0.9887 & 0 & 0.0495 \\ -7.9682 & -296.6333 & 0.1396 & -142.9873 \\ 0.0132 & -0.0817 & 0.0004 & 0.9673 \end{bmatrix}, B_1 = \begin{bmatrix} 0 \\ 0.0051 \\ 0 \\ 0.0050 \end{bmatrix},$$

$$A_2 = \begin{bmatrix} 0.2033 & -29.6586 & 0.0140 & -14.2964 \\ 0.0012 & 0.9871 & 0 & 0.0944 \\ -15.9288 & -592.9849 & -0.7207 & -285.8380 \\ 0.0188 & -0.4451 & 0.0007 & 0.7980 \end{bmatrix}, B_2 = \begin{bmatrix} 0 \\ 0.0105 \\ 0.002 \\ 0.0098 \end{bmatrix},$$

and $x(k) = \left[\theta_1(k)\ \theta_2(k)\ \delta_1(k)\ \delta_2(k)\right]^T$.

Suppose that the remote filter is designed to estimate the signal

$$z(t) = Lx(t), \tag{6.28}$$

by using the measurements

$$y(t) = Cx(t) + Dw(t), \tag{6.29}$$

where $L = \left[1\ 1\ 0\ 0\right]$, $C = \begin{bmatrix} 1 & 0 & 0 & 0 \\ 0 & 1 & 0 & 0 \end{bmatrix}$ and $D = \begin{bmatrix} 0.2 \\ 0.3 \end{bmatrix}$.

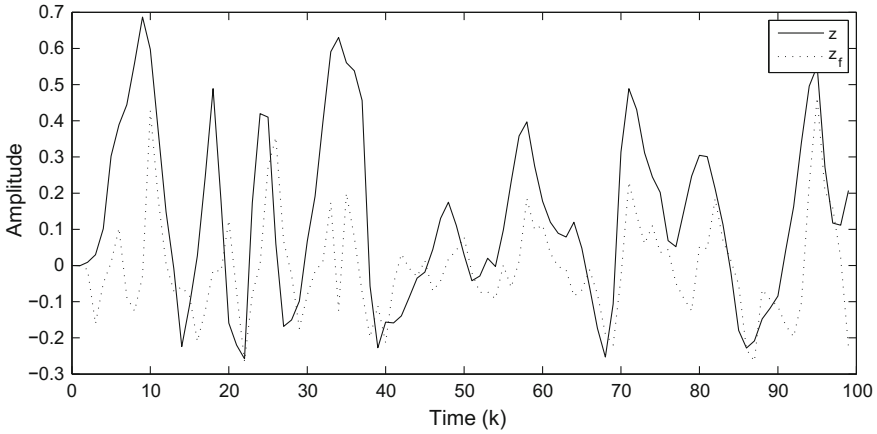

Fig. 6.2 Trajectories of z and its estimates z_f

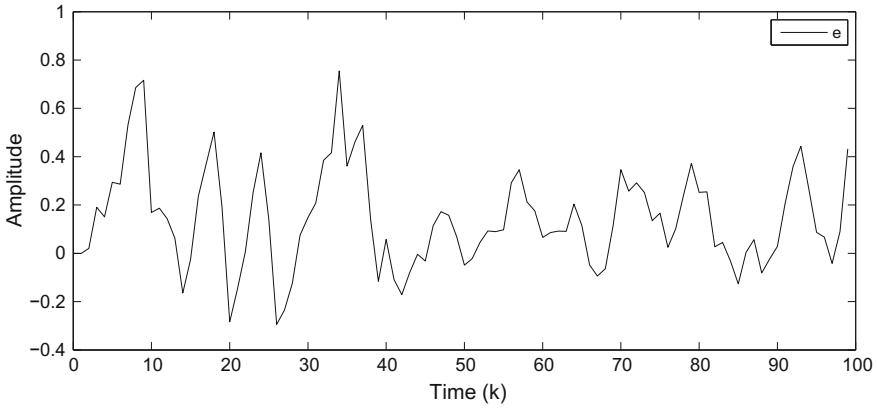

Fig. 6.3 Trajectory of estimation error e

In this example, the transition probability of the above two sampling periods is assumed to be $\Theta_1 = \begin{bmatrix} 0.6 & 0.4 \\ 0.4 & 0.6 \end{bmatrix}$. For estimation purpose, the measurement size of sampled data is then reduced by using a stochastic scheme, and $\Pi_{\sigma(t_k)} \in \{[1\ 0], [0\ 1]\}$. The transition probability of the measurement reduction policy is taken as $\Theta_2 = \begin{bmatrix} 0.5 & 0.5 \\ 0.7 & 0.3 \end{bmatrix}$. The selected measurement is further quantized by a quantization density level $\rho = 0.9$. The transmission rate is set to be $\bar{\alpha} = 0.7$. By solving the optimization problem (6.26), we have $\gamma^* = 2.3016$. We only run 100 time steps for the sequential simulation. The unknown disturbance signal is chosen as $w(t_k) = rand - 1$, where $rand$ is a random function generating a value between

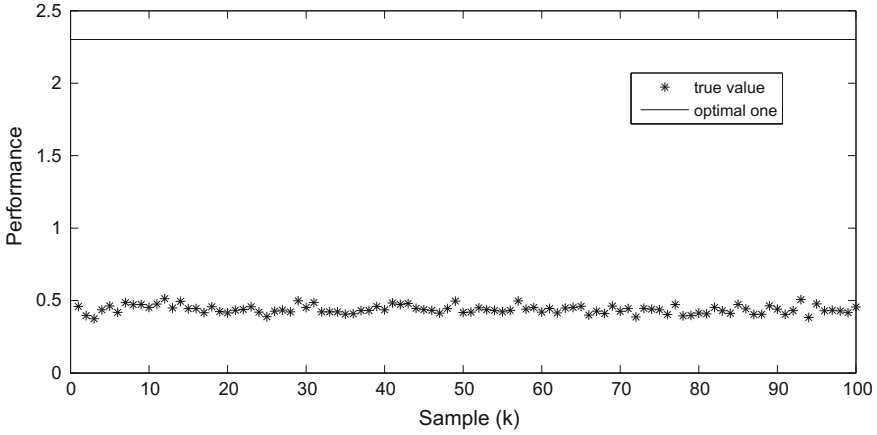

Fig. 6.4 100 samples for the performance level γ

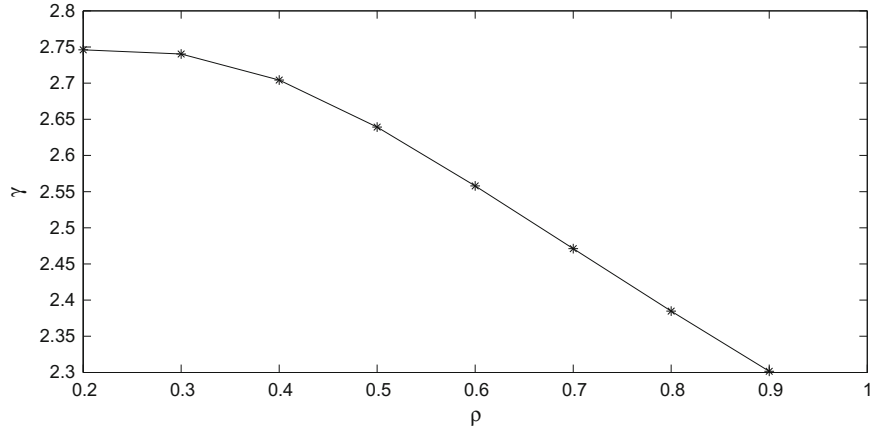

Fig. 6.5 The relation between the quantizer parameter ρ and the filtering performance level γ

[0, 1]. Figure 6.2 shows the trajectories of z and its estimates z_f. The trajectory of estimation error e is depicted in Fig. 6.3. 100 samples on the H_∞ performance level γ are also depicted in Fig. 6.4. One sees that the performance of the filtering error system is guaranteed. The relation between the quantizer parameter ρ and the filtering performance level γ is depicted in Fig. 6.5. One can see that the filtering performance becomes worse when the quantizer parameter ρ is small.

6.5 Conclusions

We have studied the energy-efficient H_∞ filtering for a class of wireless networked systems with energy constraint. Due to the limited power in sensors, the techniques such as stochastic sampling, measurement size reduction, signal quantization and stochastic signal transmission have been used simultaneously. A new Markovian system approach has been proposed to model the above issues and sufficient conditions have been obtained such that the filtering error system is exponentially stable in the mean-square sense and achieves a prescribed H_∞ performance level. The filter gain parameters have been determined by solving an optimization problem. Finally, a simulation study has been given to show the effectiveness of the new design method.

Chapter 7
Distributed Filtering with Communication Reduction

7.1 Introduction

Chapters 3–6 present several filter designs for the wireless networked control systems with energy constraints in a centralized framework. In the last a few years, the distributed filtering in wireless sensor networks (WSNs) has received a tremendous attention due to its potential applications in various areas such as target surveillance, information collection and environment monitoring [1]. In such a distributed filtering system, each sensor has the ability to measure, communicate and compute. Compared with the centralized filtering system, the distributed filters can share their measurements and local estimates with each other. Such a cooperative way can achieve a better estimation performance. Nevertheless, the sensor nodes are usually deployed in a large area, and replacing the sensor battery is very difficult. Hence, the power limitation should also be considered in the distributed filtering problem. The main difficulties arise from the complicated coupling among different sensors due to information sharing.

In this chapter, a new energy-efficient distributed filtering algorithm is proposed. Firstly, a nonuniform sampling approach is used such that the measurements of the target plant are sampled with a time-varying sampling period taking a finite number of values. Secondly, only one element of each sampled measurements is selected and then quantized for transmission. Finally, the quantized measurement is transmitted to the estimator intermittently to further save the constrained power in sensors. Based on the switched system approach, a sufficient condition is presented to guarantee that the filtering error system is exponentially stable in the mean-square sense with a prescribed H_∞ performance level. It is shown that the filter gain parameters can be determined by a set of linear matrix inequalities (LMIs), which are numerically efficient. A simulation example is given to verify the effectiveness of the proposed design. Moreover, a detailed energy consumption study is performed for various energy saving schemes.

D. Zhang et al., *Filtering and Control of Wireless Networked Systems*,
Studies in Systems, Decision and Control 97, DOI 10.1007/978-3-319-53123-6_7

7.2 Problem Formulation

A sensor network is deployed to monitor the plant, and there is no centralized estimation center in this network, see the filtering structure in Fig. 7.1. Standard definitions for the sensor networks are given as follows. Let the topology of a given sensor network be represented by a direct graph $\pi(k) = (\upsilon, \chi, \mathbb{A}^{\sigma(k)})$ of order n with the set of sensors $\upsilon = \{1, 2, \ldots, n\}$, set of edges $\chi \subseteq \upsilon \times \upsilon$, and a weighted adjacency matrix $\mathbb{A}^{\sigma(k)} = [a_{pq}^{\sigma(k)}]$ with nonnegative adjacency elements $a_{pq}^{\sigma(k)}$. The edge of π is denoted by (p, q). The adjacency elements associated with the edges of the graph are $a_{pq}^{\sigma(k)} = 1 \Leftrightarrow (p, q) \in \upsilon$, when sensor p can receive information from sensor q. On the other hand, $a_{pq}^{\sigma(k)} = 0$ if sensor p can not receive information from sensor q, which may be out of sensing range or the q-th sensor does not broadcast information. Moreover, we assume $a_{pp}^{\sigma(k)} = 1$ for all $p \in \upsilon$. The set of neighbors of node $p \in \upsilon$ plus the node itself are denoted by $N_p = \{q \in \delta : (p, q) \in \upsilon\}$. $\sigma(k) : [0, \infty) \to \Omega_3 = \{1, 2, \ldots, N\}$ is a switching signal. For each $l \in \Omega_3$, $\mathbb{A}^l = [a_{ij}^l]$ is a square matrix representing the topology of the sensor network. The number of the topologies is determined directly by how one regulates the working mode of the sensors.

Consider the following continuous-time system as our target plant:

$$\begin{cases} \dot{x}(t) = Ax(t) + Bw(t), \\ z(t) = Lx(t), \end{cases} \tag{7.1}$$

where $x(t) \in \mathbb{R}^{n_x}$ is the system state, $z(t) \in \mathbb{R}^{n_z}$ is the signal to be estimated, and $w(t) \in \mathbb{R}^{n_w}$ is the disturbance signal, which belongs to $L_2[0, +\infty)$. A, B and L are some constant matrices with appropriate dimensions. A typical sensor network has n sensor nodes deployed to monitor the plant (7.1) according to the following observation model:

$$y_p(t_k) = C_p x(t_k), \quad p = 1, 2, \ldots, n, \tag{7.2}$$

where $y_p(t_k) \in \mathbb{R}^{n_p}$ is the local measurement collected by the p-th sensor at the discrete time instants t_k, $k = 0, 1, 2, \ldots$. C_p are constant matrices. Define the measurement sampling period as $h_k = t_{k+1} - t_k$. Then h_k is a time-varying value. In this

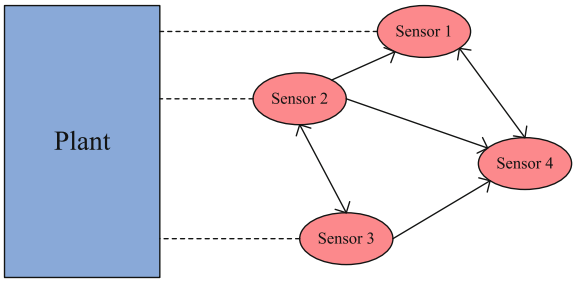

Fig. 7.1 A structure of distributed filtering in sensor networks

chapter, we assume that h_k takes a value from a given set. Specifically, let $h_k = n_k T_0$, where $n_k \in \{i_1, i_2, \ldots, i_t\}$, i_j, $j = 1, 2, \ldots, t$ are positive integers, and T_0 is the so-called basic sampling period.

We now discretize the system (7.1) with the sampling period h_k and applying a zero-order-holder to have the following discrete-time system:

$$\begin{cases} x(t_{k+1}) = A_k x(t_k) + B_k w(t_k), \\ z(t_k) = Lx(t_k), \end{cases} \tag{7.3}$$

where $A_k = e^{Ah_k}$ and $B_k = \int_0^{h_k} e^{A\tau} B d\tau$. Let $A_0 = e^{AT_0}$ and $B_0 = B\int_0^{T_0} e^{A\tau} d\tau$. Then $A_k = {A_0}^{n_k}$, $B_k = \sum_{i=0}^{n_k-1} {A_0}^i B_0$. It is seen that the values of A_k and B_k are determined by the sampling period h_k. Define a piecewise constant signal $s(k) \in \Omega_1 = \{1, 2, \ldots, t\}$. Then we have the following switching system model for (7.3):

$$\begin{cases} x(t_{k+1}) = A_{s(t_k)} x(t_k) + B_{s(t_k)} w(t_k), \\ z(t_k) = Lx(t_k), \end{cases} \tag{7.4}$$

where $A_{s(t_k)} = {A_0}^{i_{s(t_k)}}$ and $B_{s(t_k)} = \sum_{l=1}^{i_{s(t_k)}} A_0^{l-1} B_0$.

Since the major power consumption in sensor nodes comes from the communication process, energy can be saved by reducing the transmitted information size at the sampling time instant t_k. One sees that size of measurement signal $y_p(t_k)$ in (7.2) is n_{y_p}, when such a measurement is directly transmitted to the estimator, much energy may still be consumed. Now, a useful measurement size reduction protocol is introduced. Without loss of generality, only one dimension of the measurement is selected for transmission at each time, and the remaining measurement elements will be selected and transmitted at the rest of time. Hence, the signal after selection is

$$\bar{y}_p(t_k) = \Pi_{\rho_{p(t_k)}} y_p(t_k), \tag{7.5}$$

where $\Pi_{\rho_{p(t_k)}}$ is a matrix introduced to choose one element for transmission, and $\rho_{p(t_k)}$, $p = 1, 2, \ldots, n$, are piecewise signals belonging to $\Omega_{p2} = \{1, 2, \ldots, n_p\}$. Specifically, $\Pi_{\rho_{p(t_k)}} = [\,1\ 0 \cdots 0\,]$ when the first element is selected, $\Pi_{\rho_{p(t_k)}} = [\,0\ 1 \cdots 0\,]$ if the second element is selected, and so on. It is seen that $\Pi_{\rho_{p(t_k)}}$ are a set of switching signals.

It it well known that the quantization technique is also an important method to reduce the packet size. In this chapter, the selected measurement is then quantized before transmission, and the logarithmic quantizer is used. The quantizer $Q^p(\bullet)$ is assumed to be symmetric and time-invariant, i.e., $Q^p(-v_p) = -Q^p(-v_p)$. For any $p = 1, 2, \ldots, n$, the set of quantization levels are described as

$$\begin{aligned} U^p = &\left\{\pm\kappa_i^p,\ \kappa_i^p = \rho_i^p \kappa_0^p,\ i = 0, \pm 1, \pm 2, \ldots\right\} \\ &\cup \left\{\pm\kappa_0^p\right\} \cup \{0\},\ 0 < \rho^p < 1,\ \kappa_0^p > 0. \end{aligned} \tag{7.6}$$

The quantized output of $Q^p(\bullet)$ is given by

$$Q^p(v_p) = \begin{cases} \kappa_i^p, & \text{if } \frac{1}{1+\delta^p}\kappa_i^p < v_p < \frac{1}{1-\delta^p}\kappa_i^p, v_p > 0, \\ 0, & \text{if } v_p = 0, \\ -Q^p(-v_p), & \text{if } v_p < 0, \end{cases} \tag{7.7}$$

where $\delta_p = \frac{1-\rho_p}{1+\rho_p} < 1$ with the quantization density $0 < \rho_p < 1$. The quantized measurement is described by

$$\hat{y}_p(t_k) = Q_p(\bar{y}_p(t_k)). \tag{7.8}$$

Define the quantization error $e_p = \hat{y}_p(t_k) - \bar{y}_p(t_k)$. Then $\hat{y}_p(t_k) = (I + \Delta_p(t_k))\bar{y}_p(t_k)$, where $\|\Delta_p(t_k)\| \leq \delta_p$. By further considering the possible measurement missing phenomenon and disturbance signal from the environment, the final measurement signal used by the filter is given by

$$\tilde{y}_p(t_k) = \alpha_p(k)Q_p(\bar{y}_p(t_k)) + D_p w(t_k), \tag{7.9}$$

where $\alpha_p(k)$ is a binary stochastic variable taking the values in $\{0, 1\}$. The occurrence probability, $\Pr ob\{\alpha_p(k) = 1\} = \bar{\alpha}_p$ is known as the successful transmission rate of the local measurement and is assumed to be known for filter design.

We are now on the stage to propose the filter. Traditionally, the p-th filter is designed as

$$\begin{cases} \hat{x}_p(t_{k+1}) = \sum\limits_{q\in N_p} a_{pq}K_{pq}\hat{x}_q(t_k) + \sum\limits_{q\in N_p} a_{pq}H_{pq}\tilde{y}_q(t_k), \\ \hat{z}_p(t_k) = L_p\hat{x}_p(t_k), \end{cases} \tag{7.10}$$

where $\hat{x}_p(t_k) \in \mathbb{R}^{n_x}$ is the filter's state, $\hat{z}_p(t_k) \in \mathbb{R}^{n_z}$ is the estimation from the p-th sensor, and $\tilde{y}_p(t_k)$ is the input signal of filter. It is seen that the above filter is designed based on the assumption that the sampled data is transmitted to other filter at each sampling time instant. If the sensors do not frequently communicate with each other at each sampling time instant, power will be saved. In the scenario where the sensors do not communicate with each other, the topology will change. Hence, we design the following filter:

$$\begin{cases} \hat{x}_p(t_{k+1}) = \sum\limits_{q\in N_p} a_{pq}^{\sigma(t_k)}K_{pq}^{\sigma(t_k)}\hat{x}_q(t_k) + \sum\limits_{q\in N_p} a_{pq}^{\sigma(t_k)}H_{pq}^{\sigma(t_k)}\tilde{y}_q(t_k), \\ \hat{z}_p(t_k) = L_p^{\sigma(t_k)}\hat{x}_p(t_k), \end{cases} \tag{7.11}$$

where $\sigma(k) \in \Omega_3 = \{1, 2, \ldots, N\}$ is a piecewise signal, and N is an integer.

Remark 7.1 In order to save energy in WSNs, sensors are not required to communicate with other ones at each sampling instant t_k. It follows that the topology changes when the sensors communicate with each other at some time instant but sometimes

they do not. Clearly, the most energy-efficient case is the scenario where the sensors do not communicate with each other, but the corresponding filtering performance is the worst. A tradeoff should be made between the filtering performance and the energy consumption.

To simplify the presentations, we define the following notations:

$$
\begin{aligned}
&\bar{x}(t_k) = [\, x^T(t_k)\ x^T(t_k)\ \cdots\ x^T(t_k)\,]^T,\ \hat{x}(t_k) = [\, \hat{x}_1^T(t_k)\ \hat{x}_2^T(t_k)\ \cdots\ \hat{x}_n^T(t_k)\,]^T,\\
&\bar{z}(t_k) = [\, z^T(t_k)\ z^T(t_k)\ \cdots\ z^T(t_k)\,]^T,\ \hat{z}(t_k) = [\, \hat{z}_1^T(t_k)\ \hat{z}_2^T(t_k)\ \cdots\ \hat{z}_n^T(t_k)\,]^T,\\
&\bar{A}_{s(t_k)} = \mathrm{diag}\{A_{s(t_k)}, A_{s(t_k)}, \ldots, A_{s(t_k)}\},\ \bar{B}_{s(t_k)} = [\, B_{s(t_k)}^T\ B_{s(t_k)}^T\ \cdots\ B_{s(t_k)}^T\,]^T,\\
&\bar{C} = \mathrm{diag}\{C_1, C_2, \ldots, C_n\},\ \bar{D} = [\, D_1^T\ D_2^T\ \cdots\ D_n^T\,]^T,\\
&\Delta(t_k) = \mathrm{diag}\{\Delta_1(t_k), \Delta_2(t_k), \ldots, \Delta_n(t_k)\},\ \bar{L} = \mathrm{diag}\{L, L, \ldots, L\},\\
&\mathrm{T}_\alpha = \mathrm{diag}\{\bar{\alpha}_1, \bar{\alpha}_2, \ldots, \bar{\alpha}_n\},\ \Phi_p = \mathrm{diag}\{0, \ldots, \underbrace{1}_{p-th}, \ldots, 0\},\\
&\Pi_{\rho(t_k)} = \mathrm{diag}\{\Pi_{\rho_1(t_k)}, \Pi_{\rho_2(t_k)}, \ldots, \Pi_{\rho_n(t_k)}\},\\
&\bar{H}_{\sigma(t_k)} = \begin{bmatrix} a_{11}^{\sigma(t_k)} H_{11}^{\sigma(t_k)} & \cdots & a_{1n}^{\sigma(t_k)} H_{1n}^{\sigma(t_k)} \\ \vdots & \ddots & \ddots \\ a_{n1}^{\sigma(t_k)} H_{n1}^{\sigma(t_k)} & \cdots & a_{nn}^{\sigma(t_k)} H_{nn}^{\sigma(t_k)} \end{bmatrix},\\
&\bar{K}_{\sigma(t_k)} = \begin{bmatrix} a_{11}^{\sigma(t_k)} K_{11}^{\sigma(t_k)} & \cdots & a_{1n}^{\sigma(t_k)} K_{1n}^{\sigma(t_k)} \\ \vdots & \ddots & \ddots \\ a_{n1}^{\sigma(t_k)} K_{n1}^{\sigma(t_k)} & \cdots & a_{nn}^{\sigma(t_k)} K_{nn}^{\sigma(t_k)} \end{bmatrix},\\
&\bar{L}_{\sigma(t_k)} = \mathrm{diag}\{L_1^{\sigma(t_k)}, L_2^{\sigma(t_k)}, \ldots, L_n^{\sigma(t_k)}\},
\end{aligned}
$$

and a mapping $\{\rho_1(t_k), \rho_2(t_k), \ldots, \rho_n(t_k)\} \to \rho(t_k)$. With the above notations, the following filtering error system is obtained:

$$
\begin{cases}
\tilde{x}t_{k+1}) = \tilde{A}_{s(t_k)\sigma(t_k)\rho(t_k)}\tilde{x}(t_k) + M_{\sigma(t_k)}\Delta(t_k)N_{\rho(t_k)}\tilde{x}(t_k) + \tilde{B}_{s(t_k)\sigma(t_k)}w(t_k)\\
\quad + \sum_{p=1}^{n}\left(\alpha_p(k) - \bar{\alpha}_p\right)\left[\tilde{A}_{p,\sigma(t_k)\rho(t_k)}\tilde{x}(t_k) + M_{p,\sigma(t_k)}\Delta(t_k)N_{\rho(t_k)}\tilde{x}(t_k)\right],\\
\tilde{e}(t_k) = \tilde{L}_{\sigma(t_k)}\tilde{x}(t_k),
\end{cases}
\tag{7.12}
$$

where

$$
\begin{aligned}
&\tilde{x}(t_k) = \left[\, \bar{x}^T(t_k)\ \hat{x}^T(t_k)\,\right]^T,\ \tilde{e}(t_k) = \bar{z}(t_k) - \hat{z}(t_k),\\
&\tilde{A}_{s(t_k)\sigma(t_k)\rho(t_k)} = \begin{bmatrix} \bar{A}_{s(t_k)} & 0 \\ \bar{H}_{\sigma(t_k)}\mathrm{T}_\alpha\Pi_{\rho(t_k)}\bar{C} & \bar{K}_{\sigma(t_k)} \end{bmatrix},\\
&\tilde{A}_{p,\sigma(t_k)\rho(t_k)} = \begin{bmatrix} 0 & 0 \\ \bar{H}_{\sigma(t_k)}\Phi_p\Pi_{\rho(t_k)}\bar{C} & 0 \end{bmatrix},\\
&\tilde{B}_{s(t_k)\sigma(t_k)} = \begin{bmatrix} \bar{B}_{s(t_k)} \\ \bar{H}_{\sigma(t_k)}\bar{D} \end{bmatrix},\ M_{\sigma(t_k)} = \begin{bmatrix} 0 \\ \bar{H}_{\sigma(t_k)}\mathrm{T}_\alpha \end{bmatrix},\\
&N_{\rho(t_k)} = \left[\, \Pi_{\rho(t_k)}\bar{C}\ 0\,\right],\ M_{p,\sigma(t_k)} = \begin{bmatrix} 0 \\ \bar{H}_{\sigma(t_k)}\Phi_p \end{bmatrix},\\
&\tilde{L}_{\sigma(t_k)} = \left[\, \bar{L}\ -\bar{L}_{\sigma(t_k)}\,\right].
\end{aligned}
$$

Remark 7.2 A unified switched system has now been proposed to model the nonuniform sampling, measurement size reduction and communication rate reduction as well as signal quantization and measurement missing phenomena. A similar modeling has been proposed for the centralized filtering problem in Chap. 4. Here a distributed solution will be given.

It is noted that system (7.12) has three switching signals. It is not easy to find a stability condition for such a hybrid system. Now, we define a mapping: $\{s(t_k), \sigma(t_k), \rho(t_k)\} \to m(t_k)$, where $m(t_k)$ is a new piecewise signal. Then system (7.12) becomes

$$\begin{cases} \tilde{x}(t_{k+1}) = \left[\tilde{A}_{m(t_k)} + M_{m(t_k)}\Delta(t_k)N_{m(t_k)}\right]\tilde{x}(t_k) + \tilde{B}_{m(t_k)}w(t_k) \\ \quad + \sum_{p=1}^{n}\left(\alpha_p(k) - \bar{\alpha}_p\right)\left[\tilde{A}_{p,m(t_k)} + M_{p,m(t_k)}\Delta(t_k)N_{m(t_k)}\right]\tilde{x}(t_k), \\ \tilde{e}(t_k) = \tilde{L}_{m(t_k)}\tilde{x}(t_k). \end{cases} \tag{7.13}$$

According to the definitions of $s(t_k)$, $\sigma(t_k)$ and $\rho(t_k)$, one sees that $m(t_k) \in \Omega = \left\{1, 2, \ldots, t \times \left(\prod_{p=1}^{n} n_p\right) \times N\right\}$ in general. It is seen that system (7.13) is a switched system, and the average dwell time scheme is used to analyze this system.

Definition 7.1 The system (7.13) is called robustly exponentially stable in the mean-square sense, if there exist some scalars $\pi > 0$ and $0 < \chi < 1$, such that the solution $\tilde{x}$ of system (7.13) satisfies $\mathbb{E}\{\|\tilde{x}(t_k)\|\} < \pi\chi^{(k-k_0)}\|\tilde{x}(t_0)\|$, $\forall t_k \geq t_0$.

Definition 7.2 For a given scalar $\gamma > 0$, the system (7.13) is said to be robustly exponentially stable in the mean-square sense and achieves a prescribed H_∞ performance γ, if it is exponentially stable and under zero initial condition, $\sum_{k=0}^{+\infty}\frac{1}{n}\mathbb{E}\{\tilde{e}^T(t_k)\tilde{e}(t_k)\} \leq \sum_{k=0}^{+\infty}\gamma^2 w^T(t_k)w(t_k)$ holds for all nonzero $w(t_k) \in l_2[0, \infty)$.

The filtering problem is now formulated as follows.

Filtering Problem: design the filter in form of (7.11) such that the filtering error system (7.13) is robustly exponentially stable in the mean-square sense and achieves a prescribed H_∞ performance level in the presence of the nonuniform sampling, the measurement size reduction, the signal quantization, the communication rate reduction as well as the measurement losses.

7.3 Filter Analysis and Design

In this section, a sufficient condition is established such that the filtering error system (7.13) is exponentially stable in the mean-square sense with a prescribed H_∞ performance level.

Theorem 7.1 *For some given scalars $\tau > 0, \mu > 1, 0 < \lambda_i < 1, \delta_p > 0$ and $0 < \lambda < 1$, if there exist positive-definite matrices P_i and a positive scale ε such that the following inequalities,*

$$\begin{bmatrix} \Psi_1 & \Psi_2 & \Psi_3 & \Psi_4 & \Psi_5 & 0 \\ * & -P_i^{-1} & 0 & 0 & 0 & M_i \\ * & * & -nI & 0 & 0 & 0 \\ * & * & * & -\bar{P}_i & 0 & \Psi_6 \\ * & * & * & * & -\varepsilon I & 0 \\ * & * & * & * & * & -\varepsilon I \end{bmatrix} < 0, \tag{7.14}$$

$$P_i \leq \mu P_j, i \neq j, \tag{7.15}$$

$$T_a > T_a^* = -\frac{\ln \mu}{\ln \lambda}, \tag{7.16}$$

hold for all $i, j \in \Omega$, then the filtering error system (7.13) is exponentially stable in the mean-square sense with decay rate $\chi = \sqrt{\lambda_b \mu^{1/T_a}}$ and achieves a prescribed H_∞ performance level $\gamma = \tau\sqrt{\frac{(1-\lambda_a)}{1-\lambda_b/\lambda}}$, where, $\lambda_a = \min_{i\in\Omega}\{\lambda_i\}$, $\lambda_b = \max_{i\in\Omega}\{\lambda_i\}$, $\lambda > \lambda_b$, and

$$\Psi_1 = \begin{bmatrix} -\lambda_i P_i & 0 \\ 0 & -\tau^2 I \end{bmatrix}, \Psi_2 = \begin{bmatrix} \tilde{A}_i & \tilde{B}_i \end{bmatrix}^T,$$
$$\Psi_3 = \begin{bmatrix} \tilde{L}_i & 0 \end{bmatrix}^T, \Psi_4 = \begin{bmatrix} \theta_1 \tilde{A}_{1i}^T & \cdots & \theta_n \tilde{A}_{ni}^T \\ 0 & \cdots & 0 \end{bmatrix},$$
$$\Psi_5 = \begin{bmatrix} N_i^T \Lambda\varepsilon \\ 0 \end{bmatrix}, \Psi_6 = \begin{bmatrix} \theta_1 M_{1i} \\ \theta_2 M_{2i} \\ \vdots \\ \theta_n M_{ni} \end{bmatrix}, \bar{P}_i = \text{diag}\{P_i^{-1}, \ldots, P_i^{-1}\},$$
$$\Lambda = \text{diag}\{\delta_1, \delta_2, \ldots, \delta_n\}, \theta_p = \sqrt{\bar{\alpha}_p(1-\bar{\alpha}_p)}, p = 1, 2, \ldots, n.$$

Proof In order to derive the stability condition for system (7.13), we choose the following Lyapunov functional:

$$V_{m(k)}(k) = \tilde{x}^T(k) P_{m(k)} \tilde{x}(k). \tag{7.17}$$

Then for each $m(k) = i$ and $\forall i \in \Omega$, it follows that

$$
\begin{aligned}
&\mathbb{E}\{V_i(k+1)-\lambda_i V_i(k)+\Upsilon(k)\}\\
&=\left[\tilde{A}_i\tilde{x}(t_k)+M_i\Delta(t_k)N_i\tilde{x}(t_k)+\tilde{B}_i w(t_k)\right]^T\\
&\quad\times P_i\left[\tilde{A}_i\tilde{x}(t_k)+M_i\Delta(t_k)N_i\tilde{x}(t_k)+\tilde{B}_i w(t_k)\right]\\
&\quad+\sum_{p=1}^{n}\theta_p^2\left[\tilde{A}_{p,i}\tilde{x}(t_k)+M_{p,i}\Delta(t_k)N_i\tilde{x}(t_k)\right]^T\\
&\quad\times P_i\left[\tilde{A}_{p,i}\tilde{x}(t_k)+M_{p,i}\Delta(t_k)N_i\tilde{x}(t_k)\right]\\
&\quad+\left[\tilde{L}_i\tilde{x}(t_k)\right]^T\left[\tilde{L}_i\tilde{x}(t_k)\right]-\lambda_i^2\tilde{x}^T(t_k)P_i\tilde{x}(t_k)-\tau^2 w^T(t_k)w(t_k),
\end{aligned}
\tag{7.18}
$$

where $\Upsilon(k)=\frac{1}{n}\tilde{e}^T(t_k)\tilde{e}(t_k)-\tau^2 w^T(t_k)w(t_k)$. In the latter development, we use k as t_k for short. By Lemma 2.1, it is easy to see that

$$
\mathbb{E}\{V_i(k+1)-\lambda_i V_i(k)+\Upsilon(k)\}<0 \tag{7.19}
$$

is equivalent to

$$
\Theta_1+\Theta_2\Delta(k)\Theta_3^T+\Theta_3\Delta(k)\Theta_2^T<0, \tag{7.20}
$$

where

$$
\Theta_1=\begin{bmatrix}\Psi_1 & \Psi_2 & \Psi_3 & \Psi_4\\ * & -P_i^{-1} & 0 & 0\\ * & * & -nI & 0\\ * & * & * & -\bar{P}_i\end{bmatrix},\ \Theta_2=\begin{bmatrix}\bar{\Psi}_5\\ 0\\ 0\\ 0\end{bmatrix},\ \Theta_3=\begin{bmatrix}0\\ M_i\\ 0\\ \Psi_6\end{bmatrix},
$$

with

$$
\bar{\Psi}_5=\begin{bmatrix}N_i^T\\ 0\end{bmatrix}.
$$

Equation (7.20) can be rewritten as

$$
\Theta_1+\Theta_2\Lambda\bar{\Delta}(k)\Theta_3^T+\Theta_3^T\Lambda\bar{\Delta}(k)\Theta_2<0, \tag{7.21}
$$

where $\bar{\Delta}(k)=\frac{\Delta(k)}{\Lambda}$. It follows that $\left\|\frac{\Delta(k)}{\Lambda}\right\|\le I$. Based on Lemma 2.2, one sees that (7.21) holds if and only if (7.14) holds. Hence, we have

$$
\mathbb{E}\{V_i(k+1)-\lambda_i V_i(k)+\Upsilon(k)\}<0. \tag{7.22}
$$

For the switching time instant $k_0<k_1<\cdots<k_l<\cdots<k_t, l=1,2,\ldots,t$, let the switching numbers over (k_0,k) be $N_\varpi(k_0,k)$. One has

$$
\mathbb{E}\{V_l(k)\}\le\mathbb{E}\{\lambda_l^{k-k_l}V_l(k_l)\}-\sum_{s=k_l}^{k-1}\lambda_l^{k-s-1}\mathbb{E}\{\Upsilon(s)\}. \tag{7.23}
$$

It follows from (7.15) and (7.23) that

$$\begin{aligned}
&\mathbb{E}\{V_{m(k_l)}(k)\}\\
&\le \lambda_{m(k_l)}^{k-k_l}\mathbb{E}\{V_{m(k_l)}(k_l)\} - \sum_{s=k_l}^{k-1}\lambda_{m(k_l)}^{k-s-1}\mathbb{E}\{\Upsilon(s)\}\\
&\le \lambda_{m(k_l)}^{k-k_l}\mu\mathbb{E}\{V_{m(k_{l-1})}(k_l)\} - \sum_{s=k_l}^{k-1}\lambda_{m(k_l)}^{k-s-1}\mathbb{E}\{\Upsilon(s)\}\\
&\le \lambda_{m(k_l)}^{k-k_l}\mu\left[\lambda_{m(k_{l-1})}^{k_l-k_{l-1}}\mathbb{E}\{V_{m(k_{l-1})}(k_{l-1})\} - \sum_{s=k_{l-1}}^{k_l-1}\lambda_{m(k_{l-1})}^{k-s-1}\mathbb{E}\{\Upsilon(s)\}\right]\\
&\quad - \sum_{s=k_l}^{k-1}\lambda_{m(k_l)}^{k-s-1}\mathbb{E}\{\Upsilon(s)\}\\
&\le \cdots \le \mu^{N_\varpi(k_0,k)}\lambda_{m(k_l)}^{k-k_l}\lambda_{m(k_{l-1})}^{k_l-k_{l-1}}\cdots\lambda_{m(k_0)}^{k_1-k_0}V_{m(k_0)}(k_0) - \Theta(\Upsilon),
\end{aligned} \tag{7.24}$$

where

$$\begin{aligned}
\Theta(\Upsilon) = {}& \mu^{N_\varpi(k_0,k-1)}\lambda_{m(k_l)}^{k-k_l}\prod_{s=1}^{l-1}\lambda_{m(k_s)}^{k_{s+1}-k_s}\textstyle\sum_{s=k_0}^{k_1-1}\lambda_{m(k_0)}^{k_1-1-s}\mathbb{E}\{\Upsilon(s)\}\\
&+\mu^{N_\varpi(k_0,k-1)-1}\lambda_{m(k_l)}^{k-k_l}\prod_{s=2}^{l-1}\lambda_{m(k_j)}^{k_{j+1}-k_j}\textstyle\sum_{s=k_1}^{k_2-1}\lambda_{m(k_1)}^{k_2-1-s}\mathbb{E}\{\Upsilon(s)\}\\
&+\cdots+\mu^0\textstyle\prod_{s=k_l}^{k-1}\lambda_{m(k_l)}^{k-1-s}\mathbb{E}\{\Upsilon(s)\}.
\end{aligned}$$

Now, we consider the exponential stability of system (7.13) with $w(k)=0$. One has

$$\begin{aligned}
&\mathbb{E}\{V_{m(k_l)}(k)\}\\
&\le \mu^{N_\varpi(k_0,k)}\lambda_{m(k_l)}^{k-k_l}\lambda_{m(k_{l-1})}^{k_l-k_{l-1}}\cdots\lambda_{m(k_0)}^{k_1-k_0}V_{m(k_0)}(k_0)\\
&\le \mu^{N_\varpi(k_0,k)}\lambda_b^{k-k_0}V_{m(k_0)}(k_0)\\
&\le \left(\mu^{1/T_a}\lambda_b\right)^{k-k_0}V_{m(k_0)}(k_0)\\
&= \chi^{2(k-k_0)}V_{m(k_0)}(k_0),
\end{aligned} \tag{7.25}$$

which yields $\mathbb{E}\left\{\|\tilde{x}(k)\|^2\right\} \le \frac{\varphi_2}{\varphi_1}\chi^{2(k-k_0)}\|\tilde{x}(k_0)\|^2$, where $\varphi_1 = \min_{i\in\Omega}\sigma_{\min}(P_i)$, $\varphi_2 = \max_{i\in\Omega}\sigma_{\max}(P_i)$, $\chi = \sqrt{\lambda_b\mu^{1/T_a}}$. Therefore, one can readily obtain $\chi<1$ from condition (7.16). According to Definition 7.1, the filtering error system (7.13) is exponentially stable in the mean-square sense with $w(k)=0$.

For the H_∞ performance level, we consider $w(k)\neq 0$. Under the zero initial condition, it follows from (7.23) that

$$\sum_{s=k_0}^{k-1}\mu^{N_\varpi(s,k-1)}\lambda_a^{k-s-1}\mathbb{E}\{\tilde{e}^T(s)\tilde{e}(s)\} \le \tau^2\sum_{s=k_0}^{k-1}\mu^{N_\varpi(s,k-1)}\lambda_b^{k-s-1}w^T(s)w(s). \tag{7.26}$$

Based on the average dwell time condition (7.16), it is easy to see $\frac{N_\varpi(s,k-1)}{k-s-1} < -\frac{\ln\lambda}{\ln\mu}$. Since $\mu>1$, we obtain $\ln\mu^{N_\varpi(s,k-1)} < \ln\lambda^{-(k-s-1)}$, and $1<\mu^{N_\varpi(s,k-1)}<$

$\lambda^{-(k-s-1)}$. Then, it can be readily seen that

$$\sum_{s=k_0}^{k-1}\lambda_a^{k-s-1}\mathbb{E}\{\tilde{e}^T(s)\tilde{e}(s)\} < \tau^2\sum_{s=k_0}^{k-1}\left(\lambda_b/\lambda\right)^{k-s-1}\lambda^{k-s-1}w^T(s)w(s). \tag{7.27}$$

Summing (7.27) from $k = k_0 + 1$ to $k = \infty$ and changing the order of summation yield

$$\sum_{s=k_0}^{+\infty}\mathbb{E}\{\tilde{e}^T(s)\tilde{e}(s)\}\sum_{k=s+1}^{+\infty}\lambda_a^{k-s-1} < \tau^2\sum_{s=k_0}^{+\infty}w^T(s)w(s)\sum_{k=s+1}^{+\infty}\left(\lambda_b/\lambda\right)^{k-s-1}. \tag{7.28}$$

Since $\sum_{k=s+1}^{+\infty}\lambda_a^{k-s-1} = \frac{1}{1-\lambda_a}$ and $\sum_{k=s+1}^{+\infty}\left(\lambda_b/\lambda\right)^{k-s-1} = \frac{1}{1-(\lambda_b/\lambda)}$, we have

$$\sum_{s=k_0}^{+\infty}\mathbb{E}\{\tilde{e}^T(s)\tilde{e}(s)\} < \gamma^2\sum_{s=k_0}^{+\infty}w^T(s)w(s), \tag{7.29}$$

where $\gamma = \tau\sqrt{\frac{1-\lambda_a}{1-\lambda_b/\lambda}}$. It is noted that $\lambda_b < \lambda$, which ensures $\gamma > 0$. With $k_0 = 0$, we can conclude that the filtering error system (7.13) is exponentially stable in the mean-square sense and achieves a prescribed H_∞ performance level γ. This completes the proof.

Unfortunately, even though we can choose some values for μ and λ such that (7.15) and (7.16) have a feasible solution, it is still difficult for us to find the feasible solution of condition (7.14) since it is not a linear matrix inequality due to the co-existence of P_i and P_i^{-1}, so the filter gain parameters $\bar{H}_{\sigma(t_k)}$, $\bar{K}_{\sigma(t_k)}$, and $\bar{L}_{\sigma(t_k)}$ can not be determined from Theorem 7.1. This leads us to present the following result to determine these filter gain parameters.

Theorem 7.2 *For given scalars $\tau > 0$, $\mu > 1$, $0 < \lambda_i < 1$, $\delta_p > 0$, and $0 < \lambda < 1$, if there exist positive-definite matrices P_i, a positive scale ε and any matrices G_i of appropriate dimensions such that the following inequalities,*

$$\begin{bmatrix} \Psi_1 & \tilde{\Psi}_2 & \tilde{\Psi}_3 & \tilde{\Psi}_4 & \tilde{\Psi}_5 & 0 \\ * & T_i & 0 & 0 & 0 & \tilde{\Psi}_6 \\ * & * & -nI & 0 & 0 & 0 \\ * & * & * & \bar{T}_i & 0 & \tilde{\Psi}_7 \\ * & * & * & * & -\varepsilon I & 0 \\ * & * & * & * & * & -\varepsilon I \end{bmatrix} < 0, \tag{7.30}$$

and (7.15), (7.16) hold for all $i, j \in \Omega$, then our filtering problem is solvable, and the filter gains are determined by $\bar{K}_i = G_3^{-T}\tilde{K}_i$, $\bar{H}_i = G_3^{-T}\tilde{H}_i$ and $\bar{L}_i = \tilde{L}_i$, where

$$\tilde{\Psi}_2 = \begin{bmatrix} \tilde{\Psi}_{21} \\ \tilde{\Psi}_{22} \end{bmatrix}, \tilde{\Psi}_3 = \begin{bmatrix} \tilde{\Psi}_{31} \\ 0 \end{bmatrix}, \tilde{\Psi}_4 = \begin{bmatrix} \tilde{\Psi}_{41} & \cdots & \tilde{\Psi}_{4n} \\ 0 & \cdots & 0 \end{bmatrix},$$
$$\tilde{\Psi}_3 = \begin{bmatrix} \tilde{\Psi}_{31} \\ 0 \end{bmatrix}, \tilde{\Psi}_7 = \begin{bmatrix} \tilde{\Psi}_{71} \\ \vdots \\ \tilde{\Psi}_{7n} \end{bmatrix}, T_i = P_i - G_i - G_i^T,$$

with

$$\tilde{\Psi}_{21} = \begin{bmatrix} \tilde{A}_i^T G_{1i} + \bar{C}^T \Pi_i^T \mathrm{T}_\alpha^T \tilde{H}_i^T & \tilde{A}_i^T G_{2i} + \bar{C}^T \Pi_i^T \mathrm{T}_\alpha^T \tilde{H}_i^T \\ \tilde{K}_i^T & \tilde{K}_i^T \end{bmatrix},$$
$$\tilde{\Psi}_{22} = \begin{bmatrix} \bar{B}_i^T G_{1i} + \bar{D}^T \tilde{H}_i^T & \bar{B}_i^T G_{2i} + \bar{D}^T \tilde{H}_i^T \end{bmatrix},$$
$$\tilde{\Psi}_{31} = \begin{bmatrix} \bar{L}^T \\ -\tilde{L}_i^T \end{bmatrix}, \tilde{\Psi}_{4p} = \theta_p \begin{bmatrix} \bar{C}^T \Pi_i^T \Phi_p^T \tilde{H}_i^T & \bar{C}^T \Pi_i^T \Phi_p^T \tilde{H}_i^T \\ 0 & 0 \end{bmatrix},$$
$$\tilde{\Psi}_5 = \begin{bmatrix} \bar{C}^T \Pi_i^T \Lambda \varepsilon \\ 0 \end{bmatrix}, \tilde{\Psi}_6 = \begin{bmatrix} \tilde{H}_i \mathrm{T}_\alpha \\ \tilde{H}_i \mathrm{T}_\alpha \end{bmatrix}, \tilde{\Psi}_{7p} = \theta_p \begin{bmatrix} \tilde{H}_i \Phi_p \\ \tilde{H}_i \Phi_p \end{bmatrix},$$
$$P_i = \begin{bmatrix} P_{1i} & P_{2i} \\ * & P_{3i} \end{bmatrix}, G_i = \begin{bmatrix} G_{1i} & G_{2i} \\ G_3 & G_3 \end{bmatrix}, p = 1, 2, \ldots, n.$$

Proof By left- and right- multiplying (7.14) with $\mathrm{diag}\{I, I, G_i^T, I, G_i^T, \ldots, G_i^T, I, I\}$ and its transpose, respectively, one sees that (7.14) is equivalent to

$$\begin{bmatrix} \Psi_1 & \Psi_2 G & \Psi_3 & \Psi_4 G_i & \Psi_5 & 0 \\ * & -G_i^T P_i^{-1} G_i & 0 & 0 & 0 & G_i^T M_i \\ * & * & -nI & 0 & 0 & 0 \\ * & * & * & \tilde{T}_i & 0 & G_i^T \Psi_6 \\ * & * & * & * & -\varepsilon I & 0 \\ * & * & * & * & * & -\varepsilon I \end{bmatrix} < 0, \tag{7.31}$$

where $\tilde{T}_i = \mathrm{diag}\{-G_i^T P_i^{-1} G_i, \ldots, -G_i^T P_i^{-1} G_i\}$. On the other hand, it is easy to verify that the inequality $-G_i^T P_i^{-1} G_i \le P_i - G_i^T - G_i$, always holds for any matrix G_i. Then, (7.31) holds if

$$\begin{bmatrix} \Psi_1 & \Psi_2 G & \Psi_3 & \Psi_4 G_i & \Psi_5 & 0 \\ * & T_i & 0 & 0 & 0 & G_i^T M_i \\ * & * & -nI & 0 & 0 & 0 \\ * & * & * & \bar{T}_i & 0 & G_i^T \Psi_6 \\ * & * & * & * & -\varepsilon I & 0 \\ * & * & * & * & * & -\varepsilon I \end{bmatrix} < 0, \tag{7.32}$$

which is the same as (7.30) with

$$P_i = \begin{bmatrix} P_{1i} & P_{2i} \\ * & P_{3i} \end{bmatrix}, G_i = \begin{bmatrix} G_{1i} & G_{2i} \\ G_3 & G_3 \end{bmatrix},$$
$$\tilde{K}_i = G_3^T \bar{K}_i, \tilde{H}_i = G_3^T \bar{H}_i, \tilde{L}_i = \bar{L}_i.$$

This completes the proof.

Remark 7.2 In Theorem 7.2, the existence condition for the filters are given in terms of LMIs which is convex in the scalar τ^2. Therefore, one may solve the following optimization problem:

$$\begin{aligned} &\min \rho, \\ &\text{s.t. (7.15), (7.16), and (7.30) with } \rho = \tau^2 \end{aligned} \tag{7.33}$$

to obtain the filter gain parameters such that the H_∞ disturbance attenuation level is minimized. When the optimal ρ is obtained from the above optimization problem, then the designed filters guarantee that the filtering error system is exponentially stable and achieves a prescribed H_∞ performance level $\gamma = \tau\sqrt{\frac{(1-\lambda_a)}{1-\lambda_b/\lambda}}$.

7.4 An Illustrative Example

In this section, a quarter-car suspension system is used to show the effectiveness of the proposed filter design method. The system structure is shown in Fig. 7.2. The sprung mass is m_s, which denotes the car chassis; the unsprung mass is m_u, which represents the wheel assembly; the spring k_s and the damper c_s stand for the stiffness and damping of the uncontrolled suspension that are placed between the car body and the wheel assembly, while the spring k_t serves to the model of the compressibility of the pneumatic tire; the variables x_s; x_u and x_r are the displacements of the car body,

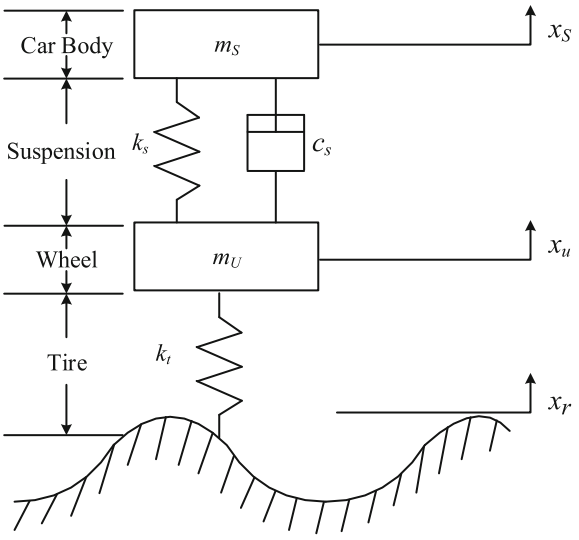

Fig. 7.2 The quarter-car suspension system

the wheel, and the road disturbance input, respectively. The dynamic equations for the sprung and unsprung masses of the quarter-car model are given by

$$\begin{cases} m_s\ddot{x}_s(t) + c_s\dot{x}_{su}(t) + k_s x_{su}(t) = 0, \\ m_u\ddot{x}_u(t) + c_s\dot{x}_{us}(t) + k_s x_{us}(t) + k_t x_{ur}(t) = 0, \end{cases} \tag{7.34}$$

where $x_{su}(t) = x_s(t) - x_u(t)$, $x_{us}(t) = x_u(t) - x_s(t)$ and $x_{sr}(t) = x_s(t) - x_r(t)$. Choose the following set of state variables:

$$\begin{cases} x_1(t) = x_s(t) - x_u(t), \\ x_2(t) = x_u(t) - x_r(t), \\ x_3(t) = \dot{x}_s(t), \\ x_4(t) = \dot{x}_u(t), \end{cases} \tag{7.35}$$

where $x_1(t)$ is the suspension deflection, $x_2(t)$ is the tire deflection, $x_3(t)$ is the sprung mass speed and $x_4(t)$ is the unsprung mass speed. Then, the quarter-car suspension model can be represented as

$$\dot{x}(t) = Ax(t) + Bw(t), \tag{7.36}$$

where

$$A = \begin{bmatrix} 0 & 0 & 1 & -1 \\ 0 & 0 & 0 & 1 \\ -\frac{k_s}{m_s} & 0 & -\frac{c_s}{m_s} & \frac{c_s}{m_s} \\ \frac{k_s}{m_u} & -\frac{k_u}{m_u} & \frac{c_s}{m_u} & -\frac{c_s}{m_u} \end{bmatrix},$$

$$B = \begin{bmatrix} 0 \\ -2\pi q_0\sqrt{G_0 v_0} \\ 0 \\ 0 \end{bmatrix}.$$

The parameters in the quarter-car model matrices are chosen as in [2, 3]:

$$\begin{aligned} &m_s = 973\,\text{kg}, k_s = 42720\,\text{N/m}, \\ &c_s = 3000\,\text{Ns/m}, k_u = 101115\,\text{N/m}, \\ &m_u = 114\,\text{kg}, G_0 = 512 \times 10^{-6}\,\text{m}^3, \\ &q_0 = 0.1\,\text{m}^{-1}, v_0 = 12.5\,\text{m/s}. \end{aligned}$$

In this example, we aim to estimate the sprung mass speed. Hence, $L = \begin{bmatrix} 0 & 0 & 1 & 0 \end{bmatrix}$. A sensor network with three sensors is deployed to achieve this estimation task. The measurements are assumed to be

$$y_p(k) = C_p x(k),\ p = 1, 2, 3, \tag{7.37}$$

where

$$C_1 = \begin{bmatrix} 1\,0\,0\,0 \\ 0\,1\,0\,0 \end{bmatrix}, C_2 = \begin{bmatrix} 0\,0\,0\,1 \end{bmatrix}, C_3 = \begin{bmatrix} 0\,0\,0\,1 \end{bmatrix}.$$

In the example, the three sensors measure the information with a time-varying sampling period $h_k \in \{T_0,\ 2T_0\}$, where $T_0 = 0.06$ s. At each sampling instant, only one element of y_1 is selected for transmission, y_2 and y_3 are always transmitted. In this case, $\Pi_{\rho_{1(t_k)}} \in \left\{\begin{bmatrix} 1\,0 \end{bmatrix}, \begin{bmatrix} 0\,1 \end{bmatrix}\right\}$, $\Pi_{\rho_{2(t_k)}} = 1$, and $\Pi_{\rho_{3(t_k)}} = 1$. Then three measurements are quantized by the logarithmic quantizers with quantization density $\rho_1 = 0.75$, $\rho_2 = 0.8$, and $\rho_3 = 0.6$, respectively. Since the measurement may be lost during the transmission due to the sensor's temporary failure and communication failure, the measurement missing rates are set to be 30, 20, and 40%, respectively. The disturbance weighting matrices are taken as $D_1 = 0.11$, $D_2 = 0.02$, and $D_3 = 0.03$. Now, discretizing the above quarter-car system with period T_0, one obtains

$$A_0 = \begin{bmatrix} 0.5610 & 0.7804 & 0.0447 & 0.0037 \\ 0.3297 & -0.0001 & 0.0436 & 0.0014 \\ -1.9618 & -4.5284 & 0.7529 & 0.0274 \\ -1.3703 & -1.2849 & 0.2335 & -0.2335 \end{bmatrix},$$

$$B_0 = \begin{bmatrix} -0.0024 \\ -0.0023 \\ 0.0110 \\ 0.0503 \end{bmatrix}.$$

By applying the modeling method in Sect. 7.2, the target plant becomes a switched system with two subsystems with $A_i = A_0^i$ and $B_i = B_0^i$, $i = 1, 2$. Moreover, these three sensors share their local information with each other at some time instant, but

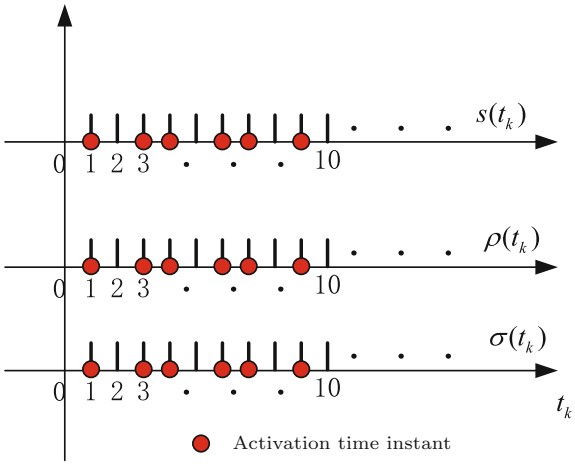

Fig. 7.3 Switching signals

they do not for the energy conservation. In this example, we assume that sensor 1 and 3 have less energy than sensor 2. Hence, at certain time instant, sensor 1 and sensor 3 do not broadcast their information, and this network has the following two topologies:

$$\mathbb{A}^1 = \begin{bmatrix} 1 & 1 & 1 \\ 1 & 1 & 1 \\ 1 & 1 & 1 \end{bmatrix}, \mathbb{A}^2 = \begin{bmatrix} 1 & 1 & 0 \\ 0 & 1 & 0 \\ 0 & 1 & 1 \end{bmatrix}.$$

The measurement size reduction process is modeled as a switched system. For simulation purpose, the activation time instant of three switching signals is assumed to be as in Fig. 7.3, where the signals are varying periodically. We run simulation for 100 time steps. It follows from Fig. 7.3 that $T_a = 1.4925$, and we have two subsystems in total. Choose $\lambda_1 = 0.92$, $\lambda_2 = 0.94$, $\lambda = 0.95$ and $\mu = 1.05$, we have $\lambda_a = 0.92$ and $\lambda_b = 0.94$. It is seen that $T_a^* = 0.9512 < T_a$, which means that (7.16) holds. By solving the optimization problem (7.33), one has the optimal H_∞ performance level of $\gamma^* = 0.2638$. In the simulation setup, the unknown disturbance is taken as $w(k) = 2rand - 1$, where $rand$ is a random function generating a number between [0,1]. Under the zero initial condition, we depict the trajectories of the z and each estimation z_p in Fig. 7.4. The trajectories of the corresponding estimation errors are shown in Fig. 7.5. Since the disturbance in the simulation is randomly generated, we now run additional 100 random simulations on the filtering performance, and the simulation results are exhibited in Fig. 7.6. It is seen that the filtering performance is guaranteed.

We now discuss the impact of the proposed method on the energy consumption. To verify the energy consumption of three sensors, we take energy consumption data

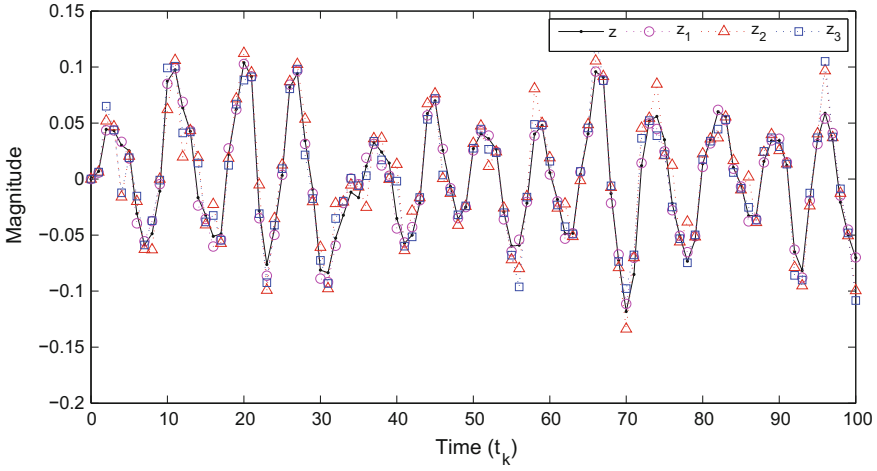

Fig. 7.4 Trajectories of $z(k)$ and its estimates $\hat{z}_p(k)$

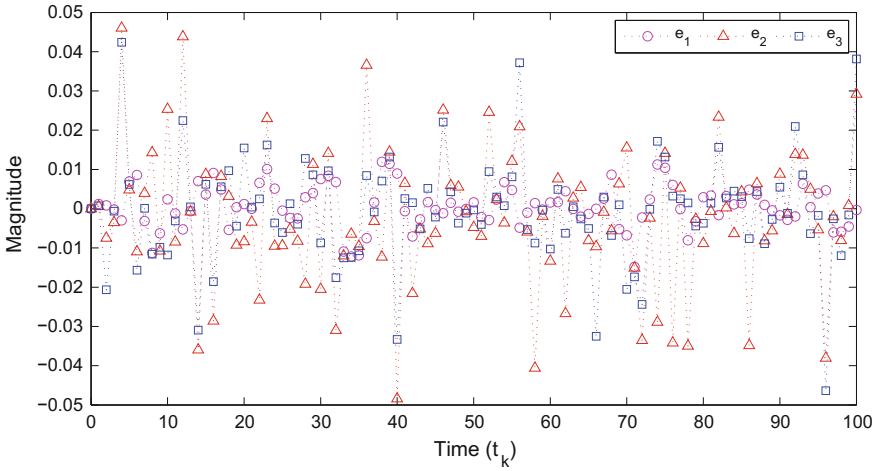

Fig. 7.5 Trajectories of estimation error $\tilde{e}_p(k)$

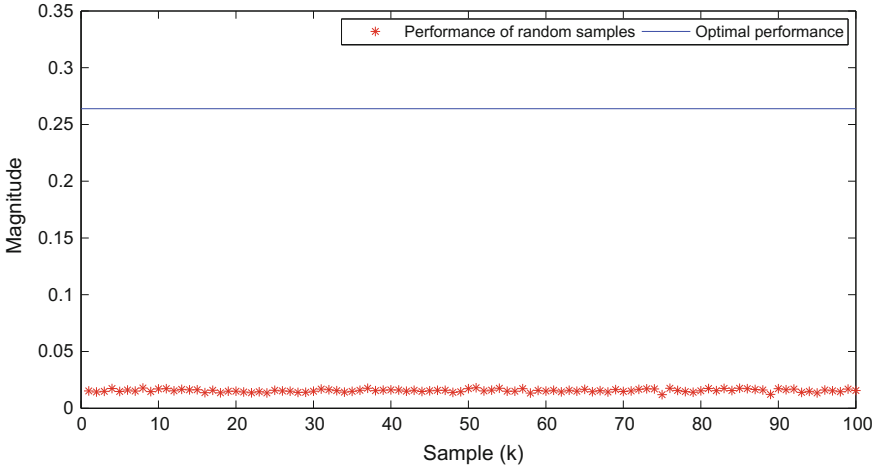

Fig. 7.6 100 samples on the filtering performance

in [4]. The energy consumption is 3.3×10^{-7} [J/bit] to transmit bits, and 1.9×10^{-7} [J/bit] to receive. To measure the energy consumption on the radio in three sensors, we measure the amount of time that the radio on each node has spent in receiving and transmitting modes. The power consumption in measuring, CPU computing, idle listening and sleeping modes will not be taken into account. The following four cases are considered:

- Case 1: sensor networks with only nonuniform sampling;
- Case 2: sensor networks with nonuniform sampling and measurement selection;

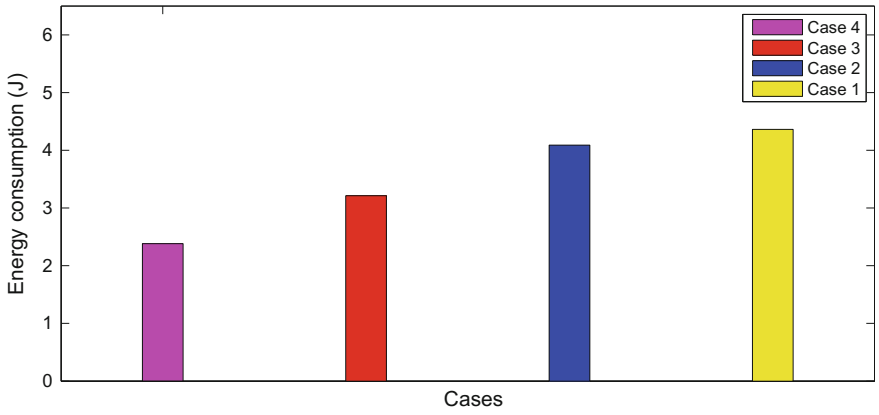

Fig. 7.7 Energy consumption

- Case 3: sensor networks with nonuniform sampling, measurement selection and signal quantization;
- Case 4: sensor networks with nonuniform sampling, measurement selection, signal quantization and communication rate reduction.

Case 4 is the final scheme, which has been used to design the energy-efficient distributed filtering system in sensor networks, and case 4 can be reduced to the above three cases. We run the simulation for 1 hour, and the detailed energy consumption for each case is depicted in Fig. 7.7. It can be seen that each case can save a certain amount of energy in sensor networks, and the case 4 is the most energy-efficient.

7.5 Conclusions

We have studied the distributed filtering in sensor networks from the energy-efficient point of view. A unified switched system approach has been proposed to capture the nonuniform sampling, measurement size reduction and communication rate reduction, all of which help us to save power in sensors. Based on the switched system approach, a sufficient condition has been presented to guarantee that the filtering error system is exponentially stable with a prescribed H_∞ performance level. It has also been shown that the filter gain parameters can be determined by solving an optimization problem. Finally, simulation studies on the quarter-car suspension system have been given to show the effectiveness of the new design method.

References

1. V. Savic, H. Wymeersch, S. Zazo, Belief consensus algorithm for fast distributed tracking in wireless sensor networks. Signal Process. **95**, 149–160 (2014)
2. J. Wu, X. Cen, H. Gao, H_∞ filtering with stochastic sampling. Signal Process. **90**(4), 1131–1145 (2010)
3. H. Du, N. Zhang, H_∞ control of active vehicle suspensions with actuator time delay. J. Sound Vib. **301**(1–2), 236–252 (2007)
4. C. Intanagonwiwat, R. Govindan, D. Estrin, Directed diffusion: A scalable and robust communication paradigm for sensor networks, in *Proceeding of the 6th ACM Annual International Conference on Mobile Computer Networks*, (Boston, MA, USA, 2000), pp. 56–67

Chapter 8
Distributed Filtering with Stochastic Sampling

8.1 Introduction

Some energy-efficient signal sampling and transmission protocols have been discussed in Chap. 7, and the corresponding distributed filter design algorithm is presented. But the scheduling is deterministic. In this chapter, a stochastic sampling scheme is applied to the distributed filtering system. The sampling periods are allowed to vary in a given set, and the transition from one period to another is assumed to satisfy the Markovian process. The network-induced uncertainties, signal quantization and random missing measurements are also considered in the filter design. Based on the Lyapunov stability theory and some stochastic analysis, a sufficient condition is found such that the augmented system is stochastically stable with an average H_∞ performance level. A design procedure is also provided for the optimal distributed filter. An illustrative example is finally given to demonstrate the effectiveness of the proposed design.

8.2 Problem Formulation

The system structure is similar to the one in Fig. 7.1 and shown in Fig. 8.1, where there is no centralized fusion center. The main difference is that a stochastic sampling approach is used rather than the deterministic one in Chap. 7. Meanwhile, the quantization and random measurement missing issues are also addressed as well. As usual, a physical plant is described by the following linear time-invariant model:

$$\begin{cases} \dot{x}(t) = Ax(t) + Bw(t), \\ z(t) = Lx(t), \end{cases} \tag{8.1}$$

where $x(t) \in \mathbb{R}^{n_x}$ is the state variable, $z(t) \in \mathbb{R}^{n_z}$ is the signal to be estimated, $w(t) \in \mathbb{R}^{n_w}$ is the disturbance belonging to $L_2[0, \infty)$.

D. Zhang et al., *Filtering and Control of Wireless Networked Systems*,
Studies in Systems, Decision and Control 97, DOI 10.1007/978-3-319-53123-6_8

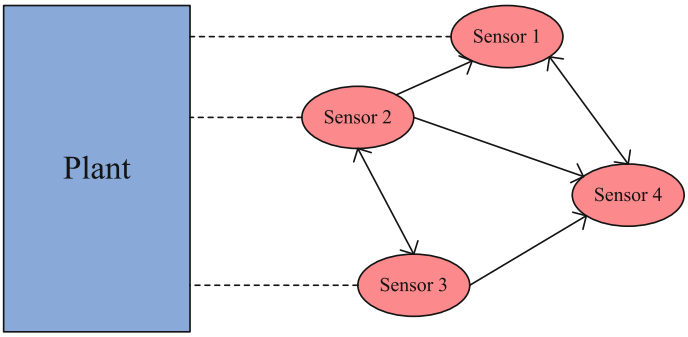

Fig. 8.1 A structure of distributed filtering in sensor networks

As demonstrated in Chap. 7, the time-varying sampling scheme can reduce the power consumption significantly. Here, a stochastic sampling scheme is applied, where the sampling period is time-varying but the variation of the sampling period is assumed to satisfy a Markovian chain. The measurement output is assumed to be sampled at discrete instant t_k, and the sampling period is determined as $h_k = t_{k+1} - t_k$. It is assumed that $h_k = m_k T_0$ and $m_k \in \{i_1, i_2, \ldots, i_s\}$, where T_0 is the basic sampling period. It is easy to see that $h_k \in \{i_1 T_0, i_2 T_0, \ldots, i_s T_0\}$. We now discretize system (8.1) with sampling period h_k to obtain the following discrete-time system:

$$\begin{cases} x(t_{k+1}) = A_k x(t_k) + B_k w(t_k), \\ z(t_k) = L x(t_k), \end{cases} \tag{8.2}$$

where $A_k = e^{Ah_k}$ and $B_k = B\int_0^{h_k} e^{A\tau} d\tau$. Denote $A_0 = e^{AT_0}$ and $B_0 = B\int_0^{T_0} e^{A\tau} d\tau$. By substituting A_0 and B_0 into A_k and B_k, respectively, we obtain $A_k = {A_0}^{m_k}$ and $B_k = \sum_{i=0}^{m_k - 1} {A_0}^i B_0$. It is seen that the values of A_k and B_k are critically dependent on the parameter m_k, which varies within a given set. Based on the above analysis, the system (8.2) can be written as

$$\begin{cases} x(t_{k+1}) = A_{\sigma(k)} x(t_k) + B_{\sigma(k)} w(t_k), \\ z(t_k) = L x(t_k), \end{cases} \tag{8.3}$$

where $\sigma(k)$ is a piecewise signal taking values from $\Gamma = \{1, 2, \ldots, s\}$. Here it is assumed that the transition from one sampling period to another satisfies the Markov process with probabilistic transfer matrix $\Pi = [\sigma_{ij}]$ defined by

$$\begin{cases} \sigma_{ij} = \Pr ob\{\sigma(k+1) = j | \sigma(k) = i\}, \\ \quad \sum_{j=1}^{s} \sigma_{ij} = 1, \forall i, j \in \Gamma. \end{cases} \tag{8.4}$$

The measured output of the i-th sensor is given by

$$y_i(t_k) = C_i x(t_k), i = 1, 2, \ldots, n, \tag{8.5}$$

where $y_i(t_k) \in \mathbb{R}^{n_y}$, C_i is a constant matrix with appropriate dimensions.

It follows from Chap. 7 that the signal quantization is also an effective scheme to reduce the power consumption. In this chapter, the logarithmic quantizer is also applied, and the set of quantization levels is defined by

$$\begin{gathered} U_j = \{\pm u_i^{(j)} : u_{i+1}^{(j)} = \rho_j u_i^{(j)}, i = 1, 2, 3 \ldots\} \cup \{u_0^{(j)}\} \cup \{0\} \\ 0 < \rho_j < 1, u_0^{(j)} > 0. \end{gathered} \tag{8.6}$$

Then the output of the quantizer is described by

$$Q_j(v) = \begin{cases} \rho_j^i u_0^{(j)}, & \text{if } \frac{u_i^{(j)}}{1+\delta_j} < v \leq \frac{u_i^{(j)}}{1-\delta_j}, v > 0, \\ 0, & \text{if } v = 0, \\ -Q_j(-v), & \text{if } v < 0, \end{cases} \tag{8.7}$$

where $\delta_j = \frac{1-\rho_j}{1+\rho_j}$ is the maximum error coefficient of quantizer Q_j, and q_j is the quantization density. The quantization error is defined by

$$e_{Q_j} = Q_j(v) - v = \Delta_j v, \tag{8.8}$$

where $\Delta_j \in [-\delta_j, \delta_j]$. Then the output signal can be written as

$$\tilde{y}_i(t_k) = (I_{n_4} + \Delta^{(i)}(t_k)) C_i x(t_k), i = 1, 2, \ldots, n, \tag{8.9}$$

where $\Delta^{(i)}(t_k) = \text{diag}\{\Delta_1^{(i)}(t_k), \Delta_2^{(i)}(t_k), \ldots, \Delta_{n_4}^{(i)}(t_k)\}$ with $\Delta_k^{(i)} \in [-\delta_i, \delta_i]$, $k = 1, 2, \ldots, n_y$.

In sensor networks, the random loss of measurement may occur due to the interference of the external environment or sensor's temporal failure. A set of independent stochastic variables $\alpha_i(t_k), i = 1, 2, \ldots, n$ are introduced to model this phenomenon, where $\alpha_i(t_k)$ is a binary valuable taking value in $\{0, 1\}$. Specifically, $\alpha_i(t_k) = 1$ means that the measurement is successfully received by the sensor i at t_k, otherwise $\alpha_i(t_k) = 0$. When a sensor does not receive the real time measurement, the measurement arrived in the last time instant will be used to update the filter state. In this chapter, it is assumed that the successful transmission rates are known, i.e., $\Pr ob\{\alpha_i(t_k) = 1\} = \bar{\alpha}_i$ is known.

Now, by taking the measurement loss, quantization and unknown disturbance into account, the input of each filter can be described by

$$\bar{y}_i(t_k) = \alpha_i(t_k)((I + \Delta^{(i)}(t_k))C_i x(t_k) + D_i w(t_k)) + (1 - \alpha_i(t_k))\bar{y}_i(t_{k-1}), \quad (8.10)$$

where D_i is a known constant matrix with appropriate dimensions.

For estimation purpose, we construct the following distributed filter:

$$\begin{cases} \hat{x}_i(t_{k+1}) = \sum\limits_{j\in N_i} a_{ij}K_{ij}\hat{x}_j(t_k) + \sum\limits_{j\in N_i} a_{ij}H_{ij}\bar{y}_j(t_k), \\ \hat{z}_i(t_k) = L_{f_i}\hat{x}_i(t_k), \end{cases} \quad (8.11)$$

where $\hat{x}_i(t_k) \in \mathbb{R}^{n_x}$ is the state estimate, $\hat{z}_i(t_k) \in \mathbb{R}^{n_z}$ is the estimate of $z(k)$ from the filter on node i, K_{ij}, H_{ij} and L_{f_i} are the filter parameter matrices to be designed. $a_i j$ is used to describe the communication topology of sensor network, i.e., $a_{ij} = 1$ if the i-th sensor can receive information from the j-th sensor, otherwise, $a_{ij} = 0$. For easy presentation, we define:

$$\begin{aligned}
&\hat{x}(t_k) = [\,\hat{x}_1^T(t_k)\ \hat{x}_2^T(t_k)\ \cdots\ \hat{x}_n^T(t_k)\,]^T, \\
&\bar{x}(t_k) = [\,\underbrace{x^T(t_k)\ x^T(t_k)\ \cdots\ x^T(t_k)}_{n}\,]^T, \\
&\hat{y}(t_k) = [\,\bar{y}_1^T(t_k)\ \bar{y}_2^T(t_k)\ \cdots\ \bar{y}_n^T(t_k)\,]^T, \\
&\bar{A}_{\sigma(k)} = I_n \otimes A_{\sigma(k)},\ \bar{B}_{\sigma(k)} = [\,\underbrace{B_{\sigma(k)}^T\ B_{\sigma(k)}^T\ \cdots\ B_{\sigma(k)}^T}_{n}\,]^T, \\
&\hat{C} = \mathrm{diag}\left\{\bar{\alpha}_1\Delta^{(1)}(t_k)C_1, \bar{\alpha}_2\Delta^{(2)}(t_k)C_2, \ldots, \bar{\alpha}_n\Delta^{(n)}(t_k)C_n\right\}, \\
&\bar{C} = \mathrm{diag}\left\{\bar{\alpha}_1 C_1, \bar{\alpha}_2 C_2, \ldots, \bar{\alpha}_n C_n\right\}, \bar{C}_i = (e_i e_i^T) \otimes C_i, \\
&\hat{C}_i = (e_i e_i^T) \otimes (\Delta^{(i)}(t_k)C_i), \bar{D} = [\,\bar{\alpha}_1 D_1^T\ \bar{\alpha}_2 D_2^T\ \cdots\ \bar{\alpha}_n D_n^T\,]^T, \\
&\bar{D}_i = e_i \otimes D_i, \bar{L} = I_n \otimes L, \hat{L}_f = \mathrm{diag}\left\{L_{f1}, L_{f2}, \ldots, L_{fn}\right\}.
\end{aligned}$$

Let the estimation error be

$$e(t_k) = [\,(z(t_k) - \hat{z}_1(t_k))^T\ (z(t_k) - \hat{z}_2(t_k))^T\ \cdots\ (z(t_k) - \hat{z}_n(t_k))^T\,]^T.$$

Combining (8.4), (8.10) and (8.11) gives the following augmented system:

$$\begin{cases} \tilde{x}(t_{k+1}) = \tilde{F}_{\sigma(k)}\tilde{x}(t_k) + \tilde{D}_{\sigma(k)}w(t_k) \\ \qquad\qquad + \sum\limits_{i=1}^{n}(\alpha_i(t_k) - \bar{\alpha}_i)(\tilde{G}_i\tilde{x}(t_k) + \tilde{E}_i w(t_k)), \\ e(t_k) = \tilde{L}_f\tilde{x}(t_k), \end{cases} \quad (8.12)$$

where

$$
\begin{aligned}
&\tilde{x}(t_k) = [\,\bar{x}^T(t_k)\ \hat{x}^T(t_k)\ \hat{y}^T(t_{k-1})\,]^T,\\
&\tilde{F}_{\sigma(k)} = \begin{bmatrix} \bar{A}_{\sigma(k)} & 0 & 0 \\ \bar{H}\tilde{C} & \bar{K} & \bar{H}(I-\Lambda) \\ \tilde{C} & 0 & I-\Lambda \end{bmatrix}, \tilde{D}_{\sigma(k)} = \begin{bmatrix} \bar{B}_{\sigma(k)} \\ \bar{H}\bar{D} \\ \bar{D} \end{bmatrix},\\
&\tilde{G}_i = \begin{bmatrix} 0 & 0 & 0 \\ \bar{H}\tilde{C}_i & 0 & -\bar{H}((e_i e_i^T)\otimes I_{n_4}) \\ \tilde{C}_i & 0 & -((e_i e_i^T)\otimes I_{n_4}) \end{bmatrix}, \tilde{E}_i = \begin{bmatrix} 0 \\ \bar{H}\bar{D}_i \\ \bar{D}_i \end{bmatrix},\\
&\tilde{L}_f = \begin{bmatrix} \bar{L} & -\hat{L}_f & 0 \end{bmatrix}, \tilde{C} = \bar{C} + \hat{C}, \tilde{C}_i = \bar{C}_i + \hat{C}_i,\\
&\bar{H} = [\bar{H}_{ij}]_{n\times n}, \text{with}\, \bar{H}_{ij} = \begin{cases} a_{ij}H_{ij}, i = 1,2,\ldots,n;\ j \in N_i \\ 0, i = 1,2,\ldots,n;\ j \notin N_i \end{cases},\\
&\bar{K} = [\bar{K}_{ij}]_{n\times n}, \text{with}\, \bar{K}_{ij} = \begin{cases} a_{ij}K_{ij}, i = 1,2,\ldots,n;\ j \in N_i \\ 0, i = 1,2,\ldots,n;\ j \notin N_i \end{cases},\\
&\Lambda = \text{diag}\,\{\Lambda_1, \Lambda_2, \ldots, \Lambda_n\},\ \text{with}\ \Lambda_i = \text{diag}_{n_4}\{\bar{\alpha}_i\}.
\end{aligned}
$$

The objective of this chapter is to design the distributed filter in the form of (8.11) such that the augmented system (8.12) is stochastically stable and achieves an average H_∞ performance under the stochastic sampling, quantization and measurement missing effects.

Definition 8.1 When the external disturbance $w(t_k) = 0$, $\forall k > 0$, the augmented system (8.12) is said to be stochastically stable if the following inequality,

$$\mathbb{E}\left\{\sum_{k=0}^{\infty} \|\tilde{x}(t_k)\|^2 | \varphi(0)\right\} < \infty, \tag{8.13}$$

holds for any initial condition $\varphi(0) = \{\tilde{x}(t_0), \sigma(0)\}$.

Definition 8.2 For a given scalar $\gamma > 0$, the augmented system (12) is said to be stochastically stable with an average H_∞ performance γ, if it is stochastically stable and the following inequality,

$$\frac{1}{n}\mathbb{E}\left\{\sum_{k=0}^{\infty} e^T(t_k)e(t_k)\right\} \le \gamma^2 \sum_{k=0}^{\infty} w^T(t_k)w(t_k), \tag{8.14}$$

holds for all non-zero $w(t_k) \in l_2[0, \infty)$ under the zero initial condition.

8.3 Filter Analysis and Design

In this section, we aim to solve the distributed H_∞ filtering problem for sensor networks with stochastic sampling and network-induced uncertainties. Theorem 8.1 below guarantees that the augmented system (8.12) is stochastically stable with an average H_∞ performance γ, and Theorem 8.2 proposes the optimal distributed filter design algorithm.

Theorem 8.1 *For the given probabilistic transfer matrix Π and a scalar $\gamma > 0$, the augmented system (8.12) is stochastically stable with an average H_∞ performance γ if there exist symmetric positive matrices $P_i > 0$ and a scalar $\varepsilon > 0$, such that the following inequalities,*

$$\begin{bmatrix} -P_i & 0 & \bar{F}_i^T & \bar{\Phi} & \frac{\sqrt{n}}{n}\tilde{L}^T & \varepsilon N\Delta & 0 \\ * & -\gamma^2 I & \tilde{D}_i^T & \bar{E} & 0 & 0 & 0 \\ * & * & -\bar{P}_i^{-1} & 0 & 0 & 0 & M^T \\ * & * & * & \hat{P}_i & 0 & 0 & \bar{M}^T \\ * & * & * & * & -I & 0 & 0 \\ * & * & * & * & * & -\varepsilon I & 0 \\ * & * & * & * & * & * & -\varepsilon I \end{bmatrix} < 0, \tag{8.15}$$

hold for all $i \in \Gamma$, where

$$\begin{aligned}
&\bar{P}_i = \sum_{j=1}^{s} \sigma_{ij} P_j,\ \hat{P}_i = \mathrm{diag}\{\underbrace{-\bar{P}_i^{-1}, -\bar{P}_i^{-1}, \ldots, -\bar{P}_i^{-1}}_{n}\}, \\
&\bar{\Phi} = \left[\theta_1 \bar{G}_1^T\ \theta_2 \bar{G}_2^T\ \cdots\ \theta_n \bar{G}_n^T\right],\ \bar{E} = \left[\theta_1 \tilde{E}_1^T\ \theta_2 \tilde{E}_2^T\ \cdots\ \theta_n \tilde{E}_n^T\right], \\
&\mathrm{M} = \left[0\ \bar{\mathrm{H}}^T\ I\right],\ \bar{G}_i = \begin{bmatrix} 0 & 0 & 0 \\ \bar{H}\bar{C}_i & 0 & -\bar{H}((e_i e_i^T) \otimes I_{n_4}) \\ \bar{C}_i & 0 & -((e_i e_i^T) \otimes I_{n_4}) \end{bmatrix}, \\
&\bar{F}_i = \begin{bmatrix} \bar{A}_i & 0 & 0 \\ \bar{H}\bar{C} & \bar{K} & \bar{H}(I - \Lambda) \\ \bar{C} & 0 & I - \Lambda \end{bmatrix},\ \mathrm{N} = \begin{bmatrix} \bar{C}^T \\ 0 \\ 0 \end{bmatrix}, \\
&\Delta = \mathrm{diag}\{I_{n_4} \otimes \delta_1, I_{n_4} \otimes \delta_2, \ldots, I_{n_4} \otimes \delta_n\},\ \theta_i = \sqrt{\bar{\alpha}_i(1 - \bar{\alpha}_i)}, \\
&\bar{\mathrm{M}} = \left[\mathrm{M}_1\ \mathrm{M}_2\ \cdots\ \mathrm{M}_n\right], \text{with } \mathrm{M}_i = \theta_i((e_i e_i^T) \otimes I_{n_4})\Lambda^{-1}\mathrm{M}.
\end{aligned}$$

Proof We first consider the stochastic stability of the augmented system (8.12) with $w(t_k) = 0$. To this end, we construct the following Lyapunov function:

$$V(t_k) = \tilde{x}^T(t_k) P_{\sigma(k)} \tilde{x}(t_k). \tag{8.16}$$

Let $\sigma(k) = i$ and $\sigma(k+1) = j$. Then we have

$$\begin{aligned}
\mathbb{E}\{\Delta V(t_k)\} &\triangleq \mathbb{E}\{V(t_{k+1}) - V(t_k)\} \\
&= \mathbb{E}\{[\tilde{x}^T(t_{k+1}) P_j \tilde{x}(t_{k+1}) | \varphi(k)] - \tilde{x}^T(t_k) P_i \tilde{x}(t_k)\} \\
&= \mathrm{E}\left\{\left[\sum_{j=1}^{s} \sigma_{ij} \tilde{x}^T(t_{k+1}) P_j \tilde{x}(t_{k+1})\right] - \tilde{x}^T(t_k) P_i \tilde{x}(t_k)\right\}.
\end{aligned} \tag{8.17}$$

Let $\bar{P}_i = \sum_{j=1}^{s} \sigma_{ij} P_j$. Equation (8.17) can be rewritten as

$$\mathbb{E}\{\Delta V(t_k)\} = \mathbb{E}\{\tilde{x}^T(t_{k+1})\bar{P}_i\tilde{x}(t_{k+1}) - \tilde{x}^T(t_k)P_i\tilde{x}(t_k)\}. \tag{8.18}$$

Since $\tilde{F}_i = \bar{F}_i + \hat{F}$, $\tilde{G}_i = \bar{G}_i + \hat{G}_i$, where

$$\hat{F} = \begin{bmatrix} 0 & 0\,0 \\ \bar{H}\hat{C} & 0\,0 \\ \hat{C} & 0\,0 \end{bmatrix}, \hat{G}_i = \begin{bmatrix} 0 & 0\,0 \\ \bar{H}\hat{C}_i & 0\,0 \\ \hat{C}_i & 0\,0 \end{bmatrix}.$$

We have

$$\mathbb{E}\{\Delta V(t_k)\} = \tilde{x}^{\mathrm{T}}(t_k)\Sigma_i\tilde{x}(t_k), \tag{8.19}$$

where

$$\Sigma_i = (\bar{F}_i + \hat{F}_i)^T\bar{P}_i(\bar{F}_i + \hat{F}_i) + \sum_{j=1}^{n}\theta_j{}^2(\bar{G}_j + \hat{G}_j)^T\bar{P}_i(\bar{G}_j + \hat{G}_j) - P_i.$$

By Lemma 2.1, $\mathbb{E}\{\Delta V(t_k)\} < 0$ is equivalent to

$$\begin{aligned} &\begin{bmatrix} -P_i & \bar{F}_i^T & \bar{\Phi} \\ * & -\bar{P}_i^{-1} & 0 \\ * & * & \hat{P}_i \end{bmatrix} + \begin{bmatrix} N\Delta \\ 0 \\ 0 \end{bmatrix}\Delta^{-1}\Delta(t_k)\begin{bmatrix} 0 & M & \bar{M} \end{bmatrix} \\ &\quad + \begin{bmatrix} 0 \\ M^T \\ \bar{M}^T \end{bmatrix}[\Delta^{-1}\Delta(t_k)]^T\begin{bmatrix} \Delta N^T & 0\,0 \end{bmatrix} < 0, \end{aligned} \tag{8.20}$$

where $\Delta(t_k) = \mathrm{diag}\{\Delta^{(1)}(t_k), \Delta^{(2)}(t_k), \ldots, \Delta^{(n)}(t_k)\}$, and $\left[\frac{\Delta(t_k)}{\Delta}\right]^T\left[\frac{\Delta(t_k)}{\Delta}\right] \le I$. By Lemmas 2.1 and 2.2, we have

$$\begin{bmatrix} -P_i & \bar{F}_i^{\mathrm{T}} & \bar{\Phi} & \varepsilon N\Delta & 0 \\ * & -\bar{P}_i^{-1} & 0 & 0 & M^{\mathrm{T}} \\ * & * & \hat{P}_i & 0 & \bar{M}^{\mathrm{T}} \\ * & * & * & -\varepsilon I & 0 \\ * & * & * & * & -\varepsilon I \end{bmatrix} < 0. \tag{8.21}$$

It can be seen form (8.15) that (8.21) holds, implying

$$\mathbb{E}\{V(t_{k+1})|\varphi(k)\} < V(t_k), \tag{8.22}$$

It is not difficult to find a scalar $0 < \mu < 1$, such that $\mathbb{E}\{V(t_{k+1})|\varphi(k)\} < \mu V(t_k)$ holds. Then, by deduction, we have $\mathbb{E}\{V(t_k)|\varphi(0)\} < \mu^k V(0)$, and consequently,

$$\mathbb{E}\left\{\sum_{k=0}^{h} V(t_k)|\varphi(0)\right\} \le 1+\mu+\cdots+\mu^h V(t_0) = \frac{1-\mu^{h+1}}{1-\mu}V(t_0). \tag{8.23}$$

Let $h \to \infty$, we have the following inequality,

$$\mathbb{E}\left\{\sum_{t_k=0}^{\infty}\|\tilde{x}(t_k)\|^2|\varphi(0)\right\} \leq \frac{1}{(1-\mu)\bar{\lambda}}V(t_0) < \infty, \tag{8.24}$$

where $\bar{\lambda} = \min_{i\in\Gamma}\lambda_{\min}(P_i)$. According to Definition 8.1, the augmented system (8.12) is stochastically stable.

We then consider the average H_∞ performance of the augmented system. Define

$$J \triangleq \mathbb{E}\left\{\frac{1}{n}\sum_{k=0}^{\infty}[e^T(t_k)e(t_k) - \gamma^2 w^T(t_k)w(t_k)]\right\}. \tag{8.25}$$

Under the zero initial conditions, we have

$$J \leq \mathbb{E}\left\{\sum_{k=0}^{\infty}\left[\frac{1}{n}e^T(t_k)e(t_k) - \gamma^2 w^{\mathrm{T}}(t_k)w(t_k) + \Delta V\right]\right\} = \sum_{t_k=0}^{\infty}\eta^T(t_k)\bar{\Sigma}_i\eta(t_k), \tag{8.26}$$

where

$$\bar{\Sigma}_i = \hat{\Sigma}_i + \sum_5\Delta(t_k)\Delta^{-1}\sum_4 + \sum_4{}^T\Delta(t_k)\Delta^{-1}\sum_5{}^T,$$
$$\eta(t_k) = \left[\tilde{x}^T(t_k)\ w^T(t_k)\right]^T, \sum_4 = \left[\begin{array}{cccccc} 0 & 0 & \mathrm{M} & \bar{\mathrm{M}} & 0 \end{array}\right],$$
$$\hat{\Sigma}_i = \begin{bmatrix} -P_i & 0 & \bar{F}_i^T & \bar{\Phi} & \frac{\sqrt{n}}{n}\tilde{L}^T \\ * & -\gamma^2 I & \tilde{D}_i^T & \bar{E} & 0 \\ * & * & -\bar{P}_i^{-1} & 0 & 0 \\ * & * & * & \hat{P}_i & 0 \\ * & * & * & * & -I \end{bmatrix}, \sum_5 = \begin{bmatrix} \mathrm{N}\Delta \\ 0 \\ 0 \\ 0 \\ 0 \end{bmatrix}.$$

By Lemmas 2.1 and 2.2, $\bar{\Sigma}_i < 0$ is equivalent to (8.19). Thus $J < 0$ and the augmented system (8.12) is stochastically stable and achieves an average H_∞ performance γ.

In Theorem 8.1, it is difficult to determine the filter gains due to the coupling between filter parameters and unknown matrices. The procedures on how to design the filter gain parameters is given in the following theorem.

Theorem 8.2 *For the given probabilistic transfer matrix Π and a scalar $\gamma > 0$, the filtering problem is solvable if there exist symmetric positive matrices $P_i = \begin{bmatrix} P_{i11} & P_{i12} & P_{i13} \\ * & P_{i22} & P_{i23} \\ * & * & P_{i33} \end{bmatrix} > 0$, any matrix $\mathrm{T}_i = \begin{bmatrix} \mathrm{T}_{i11} & \mathrm{T}_{i12} & \mathrm{T}_{i13} \\ \mathrm{T}_f & \mathrm{T}_f & 0 \\ \mathrm{T}_{i31} & \mathrm{T}_{i32} & \mathrm{T}_{i33} \end{bmatrix}$ of appropriate dimensions with diagonal matrix T_f, and a scalar $\varepsilon > 0$, such that the following inequalities,*

$$\begin{bmatrix} -P_i & 0 & \bar{\Psi}_i & \sum_{j=1}^{n} e_j^T \otimes \Psi_{ij} & \frac{\sqrt{n}}{n}\mathrm{Z}\ \varepsilon N\Delta & 0 \\ * & -\gamma^2 I & \bar{\Omega}_i & \sum_{j=1}^{n} e_j^T \otimes \Omega_{ij} & 0 & 0 & 0 \\ * & * & \bar{P}_i - \mathrm{T}_i - \mathrm{T}_i{}^T & 0 & 0 & 0 & \bar{\Xi}_i \\ * & * & * & \tilde{P}_i & 0 & 0 & \sum_{j=1}^{n} e_j \otimes \Xi_{ij} \\ * & * & * & * & -I & 0 & 0 \\ * & * & * & * & * & -\varepsilon I & 0 \\ * & * & * & * & * & * & -\varepsilon I \end{bmatrix} < 0, \quad (8.27)$$

hold for all $i \in \Gamma$. *Moreover, the filter gain is determined as follows:*

$$\begin{cases} \bar{\mathrm{H}} = \mathrm{T}_f{}^{-T}\mathrm{H}_F, \bar{\mathrm{K}} = \mathrm{T}_f{}^{-T}\mathrm{K}_F, \\ \bar{L}_f = -L_F{}^T, \end{cases} \quad (8.28)$$

where

$$\Psi_{ij} = \theta_j \begin{bmatrix} \bar{C}_j^T\mathrm{H}_F^T + \tilde{C}_j^T T_{i31} & \bar{C}_j^T\mathrm{H}_F^T + \tilde{C}_j^T T_{i32} & \bar{C}_j^T\mathrm{T}_{i33} \\ 0 & 0 & 0 \\ -\Phi_j(\mathrm{H}_F^T + T_{i31}) & -\Phi_j(\mathrm{H}_F^T + \mathrm{T}_{i32}) & -\Phi_j\mathrm{T}_{i33} \end{bmatrix},$$

$$\bar{\Psi}_i = \begin{bmatrix} \bar{A}_i^{\mathrm{T}}\mathrm{T}_{i11} + \bar{C}^T(\mathrm{H}_F^T + \mathrm{T}_{i31}) \\ \mathrm{K}_F^T \\ (I - \Lambda)(\mathrm{H}_F^T + \mathrm{T}_{i31}) \end{bmatrix}$$

$$\begin{bmatrix} \bar{A}_i^{\mathrm{T}}\mathrm{T}_{i12} + \bar{C}^T(\mathrm{H}_F^T + \mathrm{T}_{i32}) & \bar{A}_i^{\mathrm{T}}\mathrm{T}_{i13} + \bar{C}^T\mathrm{T}_{i33} \\ \mathrm{K}_F^T & 0 \\ (I - \Lambda)(\mathrm{H}_F^T + \mathrm{T}_{i32}) & (I - \Lambda)\mathrm{T}_{i33} \end{bmatrix},$$

$$\bar{\Omega}_i = \begin{bmatrix} \bar{\mathrm{B}}_i^T\mathrm{T}_{i11} + \bar{D}^T(\mathrm{H}_F^T + \mathrm{T}_{i31}) & \bar{\mathrm{B}}_i^T\mathrm{T}_{i12} + \bar{D}^T(\mathrm{H}_F^T + \mathrm{T}_{i32}) & \bar{\mathrm{B}}_i^T\mathrm{T}_{i13} + \bar{D}^T\mathrm{T}_{i33} \end{bmatrix},$$

$$\Omega_{ij} = \theta_j \begin{bmatrix} \bar{D}_j^T\mathrm{H}_F^T + \bar{D}_j^T\mathrm{T}_{i31} & \bar{D}_j^T\mathrm{H}_F^T + \bar{D}_j^T\mathrm{T}_{i32} & \bar{D}_j^T\mathrm{T}_{i33} \end{bmatrix},$$

$$\bar{\Xi}_i = \begin{bmatrix} \mathrm{T}_{i31} + \mathrm{H}_F^T & \mathrm{T}_{i32} + \mathrm{H}_F^T & \mathrm{T}_{i33} \end{bmatrix}^T, \Xi_{ij} = \Phi_j\Lambda^{-1}\bar{\Xi}_i,$$

$$\tilde{P}_i = \mathrm{diag}_n\{\bar{P}_i - \mathrm{T}_i - \mathrm{T}_i{}^T\}, \mathrm{Z} = \begin{bmatrix} \bar{L} & L_F{}^{\mathrm{T}} & 0 \end{bmatrix}^T, \Phi_j = ((e_j^T e_j) \otimes I_{n_4}).$$

Proof Define

$$\mathrm{T}_i = \begin{bmatrix} \mathrm{T}_{i11} & \mathrm{T}_{i12} & \mathrm{T}_{i13} \\ \mathrm{T}_f & \mathrm{T}_f & 0 \\ \mathrm{T}_{i31} & \mathrm{T}_{i32} & \mathrm{T}_{i33} \end{bmatrix}, \mathrm{H}_F = \mathrm{T}_f^T\overline{\mathrm{H}},$$
$$\mathrm{K}_F = \mathrm{T}_f{}^T\overline{\mathrm{K}}, L_F = -\bar{L}_f^T.$$

By Lemmas 2.1 and 2.3, it follows from inequality (8.27) that

$$\begin{bmatrix} -P_i & 0 & \bar{\Psi}_i & \sum_{j=1}^{n} e_j^T \otimes \Psi_{ij} & \frac{\sqrt{n}}{n}\tilde{L}^T & \varepsilon N\Delta & 0 \\ * & -\gamma^2 I & \bar{\Omega}_i & \sum_{j=1}^{n} e_j^T \otimes \Omega_j & 0 & 0 & 0 \\ * & * & -\mathrm{T}_i{}^T \bar{P}_i^{-1}\mathrm{T}_i & 0 & 0 & 0 & \hat{\Xi}_i \\ * & * & * & P_i' & 0 & 0 & \sum_{j=1}^{n} e_j \otimes \Xi_{ij}^T \\ * & * & * & * & -I & 0 & 0 \\ * & * & * & * & * & -\varepsilon I & 0 \\ * & * & * & * & * & * & -\varepsilon I \end{bmatrix} < 0, \quad (8.29)$$

holds, where $P_i' = \mathrm{diag}_n\{-\mathrm{T}_i{}^T \bar{P}_i^{-1}\mathrm{T}_i\}$. Pre- and post-multiplying (8.29) by $\mathrm{diag}\left\{I, I, \underbrace{\mathrm{T}_i{}^{-T}, \ldots, \mathrm{T}_i{}^{-T}}_{n+1}, I, I, I\right\}$ and its transpose respectively, it is easy to have the inequality (8.15). This ends the proof.

Remark 8.3 The optimal H_∞ filter can be obtained by solving the following optimization problem:

$$\begin{aligned} &\min \quad \gamma^2 \\ &\text{s.t.} \quad (8.27). \end{aligned} \quad (8.30)$$

If there exists a solution to the above optimization problem (8.30), the minimum average H_∞ performance $\gamma^* = \sqrt{\gamma^2{}_{\min}}$, and the filter gains are given by (8.28).

8.4 A Simulation Example

In this section, a simulation example of spring-mass system is presented to illustrate the effectiveness of the theoretical results. The spring-mass system can be described by a state space model in the form of system (8.1) with

$$\begin{aligned} x(t) &= \begin{bmatrix} x_1^T(t) & x_2^T(t) & \dot{x}_1^T(t) & \dot{x}_2^T(t) \end{bmatrix}^T, \\ A &= \begin{bmatrix} 0 & 0 & 1 & 0 \\ 0 & 0 & 0 & 1 \\ -2 & 1 & -0.5 & 0 \\ 2 & -2 & 0 & -1 \end{bmatrix}, \; B = \begin{bmatrix} 0 & 0 \\ 0 & 0 \\ 1 & 0 \\ 2 & 0 \end{bmatrix}, \\ L &= \begin{bmatrix} 1 & 0 & 0 & 0 \end{bmatrix}. \end{aligned}$$

where x_1 and x_2 are the displacement of masses m_1 and m_2, respectively. x_3 and x_4 are the velocities of masses m_1 and m_2, respectively. More discussions on the spring-mass system can be found in the last few chapters. To estimate the displacement of mass 1, we deploy a sensor network consisting of three sensors. The measurement matrices are taken as

$$C_i = \begin{bmatrix} 1\ 0\ 0\ 0 \\ 0\ 1\ 0\ 0 \end{bmatrix}, D_i = \begin{bmatrix} 0\ 0.1 \\ 0\ 0.1 \end{bmatrix}, i = 1, 2, 3.$$

Suppose that the basic sampling period is T_0=0.1s, the sampling periods vary in $\Gamma = \{T_0, 2T_0, 3T_0\}$, the transition probability matrix is

$$\Pi = \begin{bmatrix} 0.5\ 0.3\ 0.2 \\ 0.6\ 0.2\ 0.2 \\ 0.7\ 0.2\ 0.1 \end{bmatrix},$$

and the weighted adjacency matrix

$$\mathbb{A} = \begin{bmatrix} 1\ 0\ 1 \\ 1\ 1\ 0 \\ 0\ 1\ 1 \end{bmatrix}.$$

The quantization densities of three sensors are $\rho_1 = 0.9$, $\rho_2 = 0.8$, $\rho_3 = 0.7$, and the measurement missing rates are 10, 20, 30% respectively, i.e., $\bar{\alpha}_1 = 0.9$, $\bar{\alpha}_2 = 0.8$, $\bar{\alpha}_3 = 0.7$. The Markovian system in the form of (8.4) is obtained with

$$A_1 = \begin{bmatrix} 0.9902 & 0.0049 & 0.0972 & 0.0002 \\ 0.0096 & 0.9903 & 0.0003 & 0.0948 \\ -0.1941 & 0.0969 & 0.9416 & 0.0047 \\ 0.1891 & -01894 & 00095 & 0.8955 \end{bmatrix}, B_1 = \begin{bmatrix} 0.0049\ 0 \\ 0.0097\ 0 \\ 0.0975\ 0 \\ 0.1900\ 0 \end{bmatrix},$$

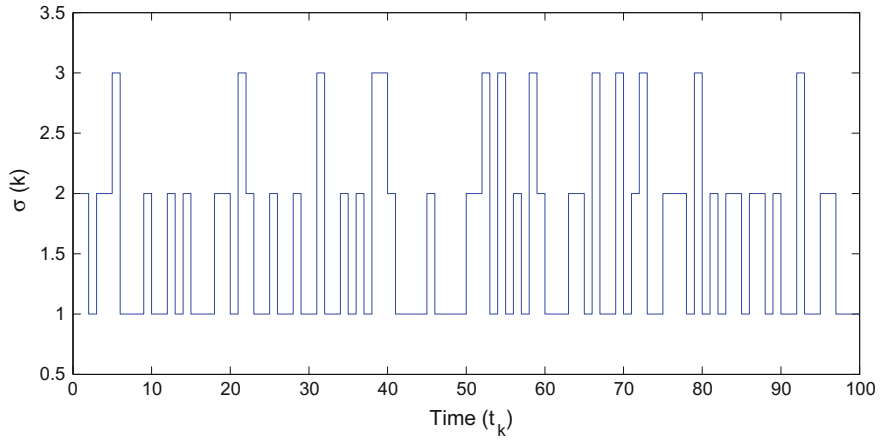

Fig. 8.2 Evolution of the Markovian chain

$$A_2=\begin{bmatrix} 0.9617 & 0.0191 & 0.1878 & 0.0012 \\ 0.0370 & 0.9629 & 0.0025 & 0.1789 \\ -0.3732 & 0.1853 & 0.8678 & 0.0179 \\ 0.3528 & -0.3553 & 0.0357 & 0.7840 \end{bmatrix}, B_2=\begin{bmatrix} 0.0193 & 0 \\ 0.0373 & 0 \\ 0.1903 & 0 \\ 0.3602 & 0 \end{bmatrix},$$

$$A_3=\begin{bmatrix} 0.9162 & 0.0416 & 0.2703 & 0.0040 \\ 0.0792 & 0.9202 & 0.0079 & 0.2515 \\ -0.5328 & 0.2624 & 0.7810 & 0.0376 \\ 0.4872 & -0.4951 & 0.0753 & 0.6686 \end{bmatrix}, B_3=\begin{bmatrix} 0.0428 & 0 \\ 0.0811 & 0 \\ 0.2783 & 0 \\ 0.5110 & 0 \end{bmatrix}.$$

By solving the optimization problem (8.30), the optimal average H_∞ performance is obtained as $\gamma^* = 0.4127$. In order to evaluate the performance of the filtering network, we assume that the disturbances of w_1 and w_2 are randomly varying for $k \in [0, 20]$ and zero elsewhere. According to the given probability transfer matrix, the Markovian chain is generated and shown in Fig. 8.2. The state trajectories of z and its estimates $\hat{z}_1$, $\hat{z}_2$, $\hat{z}_3$ are shown in Fig. 8.3. The trajectories of filtering errors are given in Fig. 8.4. Through the comparison among three filters on hundred sets of repetitive tests, it is shown that filter 2 has the least average error and filter 3 yields the largest one.

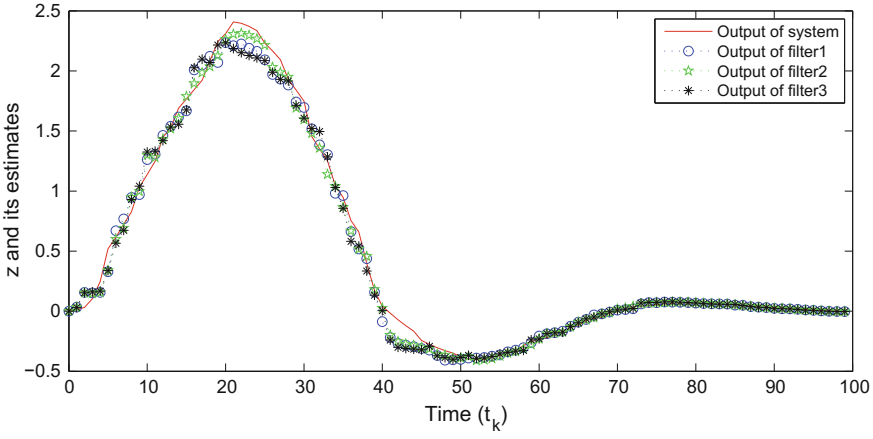

Fig. 8.3 Trajectories of estimation

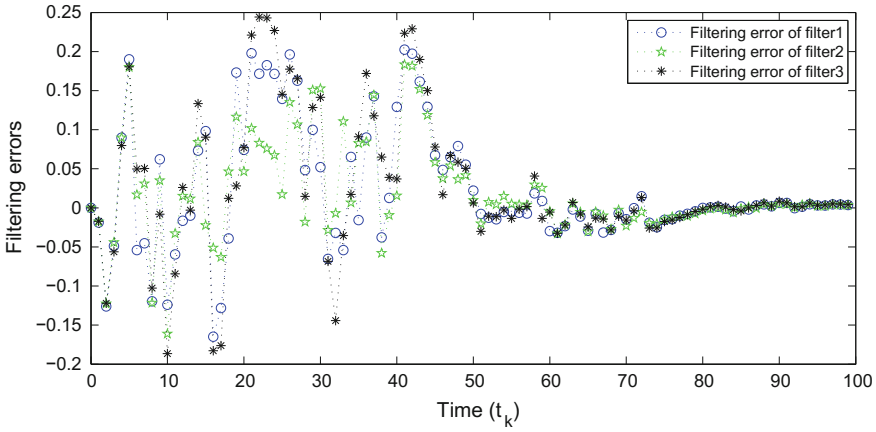

Fig. 8.4 Trajectories of estimation error

8.5 Conclusions

The distributed H_∞ filtering problem for a class of sensor networks has been studied. Issues such as stochastic sampling, signal quantization and random measurement missing are treated in a unified work. A sufficient condition has been presented such that the augmented system is stochastically stable with an average H_∞ performance. The optimal filter design method has also been provided. A numerical example has been given to show the effectiveness of the proposed method. It is worth pointing out that the transition probability of the sampling periods may be partially unknown, the H_∞ filtering problem for a class of sensor networks with stochastic sampling, but with partially unknown transition probability of the sampling periods will be an interesting work to be further done.

Chapter 9
Distributed Filtering with Random Filter Gain Variations

9.1 Introduction

When WSNs are deployed in a vast region, they often do not work as expected. There is environmental influence which may lead to malfunction of the sensors, and most of time it is of non-deterministic. In other words, filters may not be implemented exactly and suffers the random filter gain variation problem. In this chapter, we are concerned with the distributed filtering for a class of sensor networks with random filter gain variations, where the additive norm-bounded filter gain variations is addressed. Though the non-fragile filtering problem has been studied in [1, 2], the filter is designed in a centralized way and the occurrence of the gain variations is deterministic. In reality, uncertainties may occur in some random time instant. How to cope with the random gain variations in the filter gains is a challenging work, especially in the distributed filtering problem. Two fundamental difficulties are identified as follows: (1) For a sensor network, each filter is designed based on the information from a sensor that communicates with its neighbors according to certain network topology, so the first difficulty is how to handle the complicated couplings between one sensor and its neighboring sensors in the presence of multiple random uncertainties. (2) The second one is how to deal with the stochastic uncertainties by quantifying their impacts on the global filtering performance in terms of the occurrence probabilities and the variation bounds.

To handle the above challenges, attention of this chapter is focused on designing a set of distributed filters such that the filtering error system is asymptotically stable in the mean-square sense and achieves a prescribed H_∞ filtering performance in the presence of random variations in filter gains. Firstly, a set of stochastic variables are introduced to capture the random uncertainties in the filter gains. Then, based on the stochastic system analysis, the robust control technique and the Lyapunov stability theory, a new sufficient condition is obtained for the solvability of the filtering problem. Finally, a numerical example is given to show the effectiveness of the proposed design. In our result, relations between the occurrence probability of the gain variations, the uncertain bound and the filtering performance are established.

D. Zhang et al., *Filtering and Control of Wireless Networked Systems*,
Studies in Systems, Decision and Control 97, DOI 10.1007/978-3-319-53123-6_9

9.2 Problem Formulation

The WSN in Fig. 9.1 is a peer-to-peer network and there is no centralized fusion center. Each sensor has a sensing unit, a transmission unit and a computation unit. Based on the local measurement and the neighbor's information, each sensor is able to provide an estimate of the plant. Fundamentals on the sensor networks have been discussed in Chap. 7.

In this chapter, the plant model is described by the following linear discrete-time system:

$$\begin{cases} x(k+1) = Ax(k) + Bw(k), \\ z(k) = Lx(k), \end{cases} \tag{9.1}$$

where $x(k) \in \mathbb{R}^{n_x}$ is the state vector, $z(k) \in \mathbb{R}^{n_z}$ is the signal to be estimated and $w(k) \in \mathbb{R}^{n_w}$ is the unknown disturbance belonging to $l_2[0, \infty)$. The matrices A, B and L in system (9.1) are known constant matrices with appropriate dimensions. The local measurement in sensor i is given by

$$y_i(k) = C_i x(k) + D_i w(k), \tag{9.2}$$

where $y_i(k) \in \mathbb{R}^{n_y}$ is the output of measuring device in the i-th sensor. The matrices C_i and D_i are known constant matrices with appropriate dimensions. Due to the fact that uncertainties exist in real WSNs, exact implementation of the filter is impossible. We now propose the following filter at each sensor:

$$\begin{cases} \hat{x}_i(k+1) = \sum\limits_{j \in N_i} a_{ij}(K_{ij} + \alpha_i(k)\Delta K_{ij})\hat{x}_j(k) \\ \qquad\quad + \sum\limits_{j \in N_i} a_{ij}(H_{ij} + \alpha_i(k)\Delta H_{ij})y_j(k), \\ z_{fi}(k) = (L_{ii} + \alpha_i(k)\Delta L_{ii})\hat{x}_i(k), \end{cases} \tag{9.3}$$

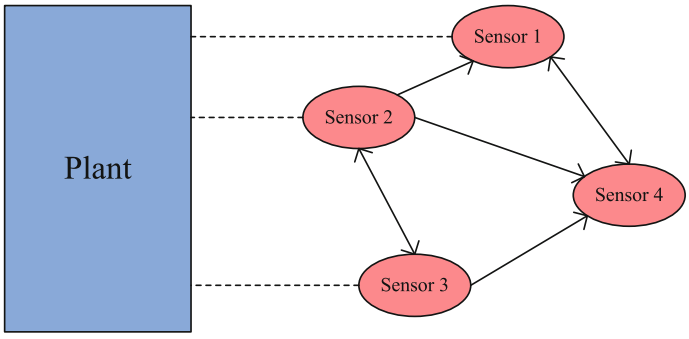

Fig. 9.1 A structure of distributed filtering in sensor networks

where $\hat{x}_i(k) \in \mathbb{R}^{n_x}$ is the sensor's state at node i and $z_{fi}(k) \in \mathbb{R}^{n_z}$ is the estimate of $z(k)$ from the filter at sensor i. K_{ij}, H_{ij} and L_{ii} are the filter parameters to be designed. A set of binary valuables, $\alpha_i(k) \in \{0, 1\}$, are used to describe the random gain variation phenomenon occurring in each sensor. We assume that the occurrence probabilities, $\mathbb{E}\{\alpha_i(k) = 1\} = \bar{\alpha}_i$ are known. $\Delta H_{ij} = M_1 \Delta_{1i}(k) F_{ij}$, $\Delta K_{ij} = M_2 \Delta_{2i}(k) E_{ij}$ and $\Delta L_{ii} = M_3 \Delta_{3i}(k) Q_{ii}$ are the uncertainty sizes in the sensor filter gains. The uncertainties $\Delta_{1i}(k)$, $\Delta_{2i}(k)$ and $\Delta_{3i}(k)$ in each sensor are assumed to be energy bounded, i.e., $\Delta_{si}^T(k)\Delta_{si}(k) \leq \delta_{si} I$, $s = 1, 2, 3$, where the scalars δ_{si} are the magnitude of perturbations. The matrices, M_1, M_2, M_3, E_{ij}, F_{ij} and Q_{ii}, are known constant matrices.

Remark 9.1 The filter gain variation occurs in real systems due to the non-deterministic behavior of malfunction of the filters. In this chapter, a set of stochastic variables $\alpha_i(k)$ is introduced to describe the random gain variation problem. One may conjecture that the filtering performance becomes much worse when uncertainty occurs more frequently and the gain perturbations are larger. We will verify the relation between the variables $\bar{\alpha}_i$, δ_{1i}, δ_{2i}, δ_{3i} and the filtering performance in the simulation part.

For easy reference, we define

$$\hat{x}(k) = [\,\hat{x}_1^T(k)\ \hat{x}_2^T(k)\ \cdots\ \hat{x}_n^T(k)\,]^T, \bar{x}(k) = [\underbrace{x^T(k)\ x^T(k)\ \cdots\ x^T(k)}_{n}]^T,$$

$$e(k) = [\,(z(k) - z_{f1}(k))^T\ \cdots\ (z(k) - z_{fn}(k))^T\,]^T,$$

$$\bar{C} = \mathrm{diag}\{C_1, C_2, \ldots, C_n\}, \bar{A} = I_n \otimes A,$$

$$\bar{B} = [\underbrace{B^T\ B^T\ \cdots\ B^T}_{n}]^T, \bar{D} = [\,D_1^T\ D_2^T\ \cdots\ D_n^T\,]^T,$$

$$\bar{L} = I_n \otimes L, \hat{L} = \mathrm{diag}\{L_{11}, L_{22}, \ldots, L_{nn}\},$$

$$\bar{M}_1 = I_n \otimes M_1, \bar{M}_2 = I_n \otimes M_2, \bar{M}_3 = I_n \otimes M_3,$$

$$\Phi_i = \mathrm{diag}\{\underbrace{0, 0, \ldots, 0}_{i-1}, I_{n_1}, \ldots, 0\},$$

$$\bar{\Phi}_i = \mathrm{diag}\{\underbrace{0, 0, \ldots, 0}_{i-1}, I_{n_4}, \ldots, 0\},$$

$$\Pi = \mathrm{diag}\{\bar{\alpha}_1 I_{n_1}, \bar{\alpha}_2 I_{n_1}, \ldots, \bar{\alpha}_n I_{n_1}\},$$

$$\bar{\Pi} = \mathrm{diag}\{\bar{\alpha}_1 I_{n_2}, \bar{\alpha}_2 I_{n_2}, \ldots, \bar{\alpha}_n I_{n_2}\},$$

$$\bar{\Delta}_1(k) = \mathrm{diag}\{\underbrace{\Delta_{11}(k), \Delta_{12}(k), \ldots, \Delta_{1n}(k)}_{n}\},$$

$$\bar{\Delta}_2(k) = \mathrm{diag}\{\underbrace{\Delta_{21}(k), \Delta_{22}(k), \ldots, \Delta_{2n}(k)}_{n}\},$$

$$\bar{\Delta}_3(k) = \mathrm{diag}\{\underbrace{\Delta_{31}(k), \Delta_{32}(k), \ldots, \Delta_{3n}(k)}_{n}\},$$

$$Q = \mathrm{diag}\{Q_{11}, Q_{22}, \ldots, Q_{nn}\},$$

$$E = \left[\bar{E}_{ij}\right]_{n\times n}, \text{ with}$$

$$\bar{E}_{ij} = \begin{cases} a_{ij} E_{ij}, & i = 1, 2, ..., n;\ j \in N_i, \\ 0, & i = 1, 2, ..., n;\ j \notin N_i, \end{cases}$$

$$
\begin{aligned}
&F = \left[\bar{F}_{ij}\right]_{n\times n} \text{ with}\\
&\bar{F}_{ij} = \begin{cases} a_{ij}F_{ij}, & i = 1, 2, ..., n;\ j \in N_i,\\ 0, & i = 1, 2, ..., n;\ j \notin N_i, \end{cases}\\
&\bar{K} = \left[\bar{K}_{ij}\right]_{n\times n} \text{ with}\\
&\bar{K}_{ij} = \begin{cases} a_{ij}K_{ij}, & i = 1, 2, ..., n;\ j \in N_i,\\ 0, & i = 1, 2, ..., n;\ j \notin N_i, \end{cases}\\
&\bar{H} = \left[\bar{H}_{ij}\right]_{n\times n} \text{ with}\\
&\bar{H}_{ij} = \begin{cases} a_{ij}H_{ij}, & i = 1, 2, ..., n;\ j \in N_i,\\ 0, & i = 1, 2, ..., n;\ j \notin N_i. \end{cases}
\end{aligned}
$$

Based on the above analysis, we have the following filtering error system:

$$
\begin{cases}
\tilde{x}(k+1)\\
\quad = \left(\tilde{A} + \tilde{\Pi}\tilde{M}_1\tilde{\Delta}_1(k)\bar{F}\right)\tilde{x}(k) + \left(\tilde{B} + \tilde{\Pi}\tilde{M}_1\tilde{\Delta}_1(k)\tilde{F}\right)w(k)\\
\quad + \sum_{i=1}^{n}(\alpha_i(k) - \bar{\alpha}_i)\left\{\tilde{\Phi}_i\tilde{M}_1\tilde{\Delta}_1(k)\bar{F}\tilde{x}(k) + \tilde{\Phi}_i\tilde{M}_1\tilde{\Delta}_1(k)\tilde{F}w(k)\right\},\\
e(k) = \left(\tilde{L} - \bar{\Pi}\bar{M}_3\bar{\Delta}_3(k)\bar{Q}\right)\tilde{x}(k)\\
\quad + \sum_{i=1}^{n}(\alpha_i(k) - \bar{\alpha}_i)\left\{-\bar{\Phi}_i\bar{M}_3\bar{\Delta}_3(k)\bar{Q}\right\}\tilde{x}(k),
\end{cases}
\tag{9.4}
$$

where

$$
\begin{aligned}
&\tilde{x}(k) = \left[\bar{x}^T(k)\ \hat{x}^T(k)\right]^T,\\
&\tilde{A} = \begin{bmatrix} \bar{A} & 0\\ \bar{H}\bar{C} & \bar{K} \end{bmatrix}, \tilde{B} = \begin{bmatrix} \bar{B}\\ \bar{H}\bar{D} \end{bmatrix},\\
&\tilde{\Pi} = \begin{bmatrix} 0 & 0\\ \Pi & \Pi \end{bmatrix}, \tilde{M}_1 = \begin{bmatrix} \bar{M}_1 & 0\\ 0 & \bar{M}_2 \end{bmatrix},\\
&\tilde{\Delta}_1(k) = \begin{bmatrix} \bar{\Delta}_1(k) & 0\\ 0 & \bar{\Delta}_2(k) \end{bmatrix}, \bar{F} = \begin{bmatrix} F\bar{C} & 0\\ 0 & E \end{bmatrix},\\
&\tilde{F} = \begin{bmatrix} F\bar{D}\\ 0 \end{bmatrix}, \tilde{\Phi}_i = \begin{bmatrix} 0 & 0\\ \Phi_i & \Phi_i \end{bmatrix},\\
&\tilde{L} = \left[\bar{L}\ -\hat{L}\right], \bar{Q} = \left[0\ Q\right].
\end{aligned}
$$

The filtering problem is formulated as follows.

Filtering Problem: design a set of distributed filters such that the filtering error system is mean-square asymptotically stable and achieves a prescribed H_∞ performance level γ in the presence of randomly occurring uncertainties in the filter gains.

Our later development makes use of the following definitions.

Definition 9.1 The system (9.4) with $w(k) = 0$ is said to be asymptotically stable in the mean-square sense, if the solution $\tilde{x}(k)$ of system (9.4) satisfies $\lim_{k\to\infty} \mathbb{E}\{\|\tilde{x}(k)\|\} = \tilde{x}(k_0)$, where $\tilde{x}(k_0)$ is the initial condition.

Definition 9.2 For a given scalar $\gamma > 0$, the system (9.4) is said to be asymptotically stable in the mean-square sense with an average H_∞ performance γ, if it is asymptotically stable and $\frac{1}{n}\sum_{s=k_0}^{\infty}\mathbb{E}\{e^T(s)e(s)\} \le \gamma^2\sum_{s=k_0}^{\infty} w^T(s)w(s)$ holds for all nonzero $w(k) \in l_2[0,\infty)$ under zero initial conditions.

9.3 Filter Analysis and Design

In this section, we aim to solve the distributed filtering problem.

Theorem 9.1 *The filtering error system (9.4) is asymptotically stable in the mean-square sense and achieves a prescribed H_∞ performance γ if there exist positive-definite matrix P and a positive scale ε such that the following inequality hold:*

$$\begin{bmatrix} \Xi_1 & \Xi_2 & \Xi_3 & 0 & 0 & \Xi_4 & 0 \\ * & -P^{-1} & 0 & 0 & 0 & 0 & \Xi_5 \\ * & * & -nI & 0 & 0 & 0 & \Xi_6 \\ * & * & * & -\bar{P}^{-1} & 0 & 0 & \Xi_7 \\ * & * & * & * & -\phi & 0 & \Xi_8 \\ * & * & * & * & * & -\bar{\varepsilon}I & 0 \\ * & * & * & * & * & * & -\bar{\varepsilon}I \end{bmatrix} < 0, \tag{9.5}$$

where

$$\begin{aligned}
&\Xi_1 = \begin{bmatrix} -P & 0 \\ * & -\gamma^2 I \end{bmatrix}, \Xi_2 = \begin{bmatrix} \tilde{A}^T \\ \tilde{B}^T \end{bmatrix}, \Xi_3 = \begin{bmatrix} \tilde{L}^T \\ 0 \end{bmatrix}, \\
&\Xi_4 = \begin{bmatrix} \varepsilon\bar{F}^T\bar{\Lambda}_1 & \varepsilon\bar{Q}^T\Lambda_3 \\ \varepsilon\tilde{F}^T\bar{\Lambda}_1 & 0 \end{bmatrix}, \Xi_5 = \begin{bmatrix} \bar{\Pi}\tilde{M}_1 & 0 \end{bmatrix}, \\
&\Xi_6 = \begin{bmatrix} 0 & -\Pi\bar{M}_3 \end{bmatrix}, \Xi_7 = \begin{bmatrix} \Omega_1 & 0 \end{bmatrix}, \\
&\Xi_8 = \begin{bmatrix} 0 & \Omega_2 \end{bmatrix}, \bar{P}^{-1} = \mathrm{diag}\{P^{-1}, \ldots, P^{-1}\}, \\
&\phi = \mathrm{diag}\{nI, \ldots, nI\}, \bar{\varepsilon}_1 I = \mathrm{diag}\{\varepsilon I, \varepsilon I\}, \\
&\bar{\Lambda}_1 = \mathrm{diag}\{\underbrace{\delta_1 I, \ldots \delta_1 I}_{n}, \underbrace{\delta_2 I, \ldots \delta_2 I}_{n}\}, \Lambda_3 = \mathrm{diag}\{\underbrace{\delta_3 I, \ldots \delta_3 I}_{n}\},
\end{aligned}$$

with

$$\begin{aligned}
&\Omega_1 = \begin{bmatrix} \theta_1\tilde{\Phi}_1\tilde{M}_1 \\ \theta_2\tilde{\Phi}_2\tilde{M}_1 \\ \vdots \\ \theta_n\tilde{\Phi}_n\tilde{M}_1 \end{bmatrix}, \Omega_2 = \begin{bmatrix} \theta_1\Phi_1\bar{M}_3 \\ \theta_2\Phi_2\bar{M}_3 \\ \vdots \\ \theta_n\Phi_n\bar{M}_3 \end{bmatrix}, \\
&\theta_i = \sqrt{\alpha_i(1-\alpha_i)}.
\end{aligned}$$

Proof Consider the exponential stability of the filtering error system (9.4) with $w(k) = 0$. We define the Lyapunov functional, $V(k) = \tilde{x}^T(k)P\tilde{x}(k)$. Thus, one sees

$$\begin{aligned}
&\mathbb{E}\{V(k+1) - V(k)\} \\
&= \tilde{x}^T(k)(\tilde{A} + \tilde{\Pi}\tilde{M}_1\tilde{\Delta}_1(k)\bar{F})^T P(\tilde{A} + \tilde{\Pi}\tilde{M}_1\tilde{\Delta}_1(k)\bar{F})\tilde{x}(k) \\
&+ \sum_{i=1}^{n} \theta_i^2 \tilde{x}^T(k)(\tilde{\Phi}_i\tilde{M}_1\tilde{\Delta}_1(k)\bar{F})^T P(\tilde{\Phi}_i\tilde{M}_1\tilde{\Delta}_1(k)\bar{F})\tilde{x}(k) \\
&- \tilde{x}^T(k)^T P\tilde{x}(k).
\end{aligned} \tag{9.6}$$

It is easy to know that $\mathbb{E}\{V(k+1) - V(k)\} < 0$ is equivalent to

$$\begin{bmatrix}
-P & (\tilde{A} + \tilde{\Pi}\tilde{M}_1\tilde{\Delta}_1(k)\bar{F})^T & \Theta_1 & \cdots & \Theta_n \\
* & -P^{-1} & 0 & 0 & 0 \\
* & * & -P^{-1} & 0 & 0 \\
* & * & * & \ddots & \vdots \\
* & * & * & * & -P^{-1}
\end{bmatrix} < 0, \tag{9.7}$$

where $\Theta_i = \theta_i(\tilde{\Phi}_i\tilde{M}_1\tilde{\Delta}_1(k)\bar{F})^T$, that is,

$$\Psi_1 + \Psi_2\tilde{\Delta}_1(k)\Psi_3 + \Psi_3^T\tilde{\Delta}_1(k)\Psi_2^T < 0, \tag{9.8}$$

where

$$\Psi_1 = \begin{bmatrix}
-P & \tilde{A} & 0 & \cdots & 0 \\
* & -P^{-1} & 0 & 0 & 0 \\
* & * & -P^{-1} & 0 & 0 \\
* & * & * & \ddots & \vdots \\
* & * & * & * & -P^{-1}
\end{bmatrix},$$

$$\Psi_2 = \begin{bmatrix} \bar{F}^T \\ 0 \\ 0 \\ \vdots \\ 0 \end{bmatrix}, \Psi_3 = \begin{bmatrix} 0 \\ \tilde{\Pi}\tilde{M}_1 \\ \theta_1\tilde{\Phi}_1\tilde{M}_1 \\ \vdots \\ \theta_n\tilde{\Phi}_n\tilde{M}_1 \end{bmatrix}^T.$$

By Lemma 2.2, (9.8) holds if and only if

$$\begin{bmatrix}
\Psi_1 & \varepsilon\Psi_2\bar{\Lambda}_1 & \Psi_3^T \\
* & -\varepsilon I & 0 \\
* & * & \varepsilon I
\end{bmatrix} < 0. \tag{9.9}$$

Clearly, condition (9.5) guarantees (9.9), which indicates that the filtering error system (9.4) is mean-square stable. Now we consider the H_∞ performance. We construct the same Lyapunov function $V(k) = \tilde{x}^T(k)P\tilde{x}(k)$. It follows that

$$\begin{aligned}
&\mathbb{E}\left\{V(k+1)-V(k)+\tfrac{1}{n}e^T(k)e(k)-\gamma^2 w^T(k)w(k)\right\}\\
&\quad=\left[\mathbb{A}\tilde{x}(k)+\mathbb{B}w(k)\right]^T P\left[\mathbb{A}\tilde{x}(k)+\mathbb{B}w(k)\right]\\
&\quad+\sum_{i=1}^{n}\theta_i^2\left[\mathbb{S}_i\tilde{x}(k)+\mathbb{R}_i w(k)\right]^T P\left[\mathbb{S}_i\tilde{x}(k)+\mathbb{R}_i w(k)\right]\\
&\quad+\tfrac{1}{n}\left[\mathbb{W}\tilde{x}(k)\right]^T\left[\mathbb{W}\tilde{x}(k)\right]\\
&\quad+\tfrac{1}{n}\sum_{i=1}^{n}\theta_i^2\left[\mathbb{Z}_i\tilde{x}(k)\right]^T\left[\mathbb{Z}_i\tilde{x}(k)\right],
\end{aligned}\tag{9.10}$$

where

$$\begin{aligned}
&\mathbb{A}=\tilde{A}+\tilde{\Pi}\tilde{M}_1\tilde{\Delta}_1(k)\bar{F},\mathbb{B}=\tilde{B}+\tilde{\Pi}\tilde{M}_1\tilde{\Delta}_1(k)\tilde{F},\\
&\mathbb{S}_i=\tilde{\Phi}_i\tilde{M}_1\tilde{\Delta}_1(k)\bar{F},\mathbb{R}_i=\tilde{\Phi}_i\tilde{M}_1\tilde{\Delta}_1(k)\tilde{F},\\
&\mathbb{W}=\tilde{L}-\bar{\Pi}\bar{M}_3\bar{\Delta}_3(k)\bar{Q},\mathbb{Z}_i=-\bar{\Phi}_i\bar{M}_3\bar{\Delta}_3(k)\bar{Q}.
\end{aligned}$$

Following the similar analysis method as before, we have

$$\mathbb{E}\left\{V(k+1)-V(k)+\frac{1}{n}e^T(k)e(k)-\gamma^2 w^T(k)w(k)\right\}<0.\tag{9.11}$$

Under the zero initial condition, it is easy to obtain $\frac{1}{n}\sum_{s=k_0}^{\infty}\mathbb{E}\{e^T(s)e(s)\}\le\gamma^2\sum_{s=k_0}^{\infty}w^T(s)w(s)$ by following the methods in the last few chapters. This completes the proof.

Remark 9.2 Theorem 9.1 provides a sufficient stability condition for the filtering error system (9.4), where the parameters $\bar{\alpha}_i, i=1,2,\ldots,n$, and δ_{1i}, δ_{2i} and δ_{3i} are included in this theorem. The impacts of the occurrence probability and the uncertain bounds of perturbations on the global filtering performance have been established.

It should be noted that we can not obtain filter gains by solving the matrix inequality (9.5) due to the existence of the term P^{-1}. The gains are determined in the following theorem.

Theorem 9.2 *The filtering problem is solvable if there exist a positive-definite matrix* $P=\begin{bmatrix}P_1 & P_2\\ * & P_3\end{bmatrix}$, *a positive scale* ε *and any matrix* $G=\begin{bmatrix}G_1 & G_2\\ G_3 & G_3\end{bmatrix}$ *with appropriate dimensions, such that the following inequality,*

$$\begin{bmatrix}
\Xi_1 & \bar{\Xi}_2 & \Xi_3 & 0 & 0 & \Xi_4 & 0\\
* & T & 0 & 0 & 0 & 0 & \bar{\Xi}_5\\
* & * & -nI & 0 & 0 & 0 & \Xi_6\\
* & * & * & \bar{T} & 0 & 0 & \bar{\Xi}_7\\
* & * & * & * & -\phi & 0 & \Xi_8\\
* & * & * & * & * & -\bar{\varepsilon}I & 0\\
* & * & * & * & * & * & -\bar{\varepsilon}I
\end{bmatrix}<0\tag{9.12}$$

holds. Then the filter gains are given by $\bar{H}=G_3^{-T}\tilde{H}$, $\bar{K}=G_3^{-T}\tilde{K}$ *and* $\hat{L}=\breve{L}$. *where*

$$\bar{\Xi}_2 = \begin{bmatrix} \bar{\Xi}_{21} \\ \bar{\Xi}_{22} \end{bmatrix}, \bar{\Xi}_5 = \begin{bmatrix} \bar{\Xi}_{51} & 0 \end{bmatrix}, \bar{\Xi}_7 = \begin{bmatrix} \bar{\Omega}_1 & 0 \end{bmatrix},$$

with

$$\bar{\Omega}_1 = \begin{bmatrix} \bar{\Omega}_{11} \\ \bar{\Omega}_{12} \\ \vdots \\ \bar{\Omega}_{1n} \end{bmatrix},$$

and

$$\begin{aligned}
\bar{\Xi}_{21} &= \begin{bmatrix} \bar{A}^T G_1 + \bar{C}^T \tilde{H}^T & \bar{A}^T G_2 + \bar{C}^T \tilde{H}^T \\ \tilde{K}^T & \tilde{K}^T \end{bmatrix}, \\
\bar{\Xi}_{22} &= \begin{bmatrix} \bar{B}^T G_1 + \bar{D}^T \tilde{H}^T & \bar{B}^T G_2 + \bar{D}^T \tilde{H}^T \end{bmatrix}, \\
\bar{\Xi}_{51} &= \begin{bmatrix} G_3^T \Pi \bar{M}_1 & G_3^T \Pi \bar{M}_2 \\ G_3^T \Pi \bar{M}_1 & G_3^T \Pi \bar{M}_2 \end{bmatrix}, \\
\bar{\Omega}_{1i} &= \theta_i \begin{bmatrix} G_3^T \Phi_i \bar{M}_1 & G_3^T \Phi_i \bar{M}_2 \\ G_3^T \Phi_i \bar{M}_1 & G_3^T \Phi_i \bar{M}_2 \end{bmatrix}, \\
T &= P - G - G^T, \bar{T} = \operatorname{diag}\{\underbrace{T, T, \ldots, T}_{n}\}, \\
G_3 &= \operatorname{diag}\{G_{31}, G_{32}, \ldots, G_{3n}\}.
\end{aligned}$$

Proof For a matrix G, one has the following fact

$$-G^T P^{-1} G \le P - G - G^T. \tag{9.13}$$

Suppose that the inequality

$$\begin{bmatrix}
\Xi_1 & \bar{\Xi}_2 & \Xi_3 & 0 & 0 & \Xi_4 & 0 \\
* & -G^T P^{-1} G & 0 & 0 & 0 & 0 & \bar{\Xi}_5 \\
* & * & -nI & 0 & 0 & 0 & \Xi_6 \\
* & * & * & \hat{T} & 0 & 0 & \bar{\Xi}_7 \\
* & * & * & * & -\phi & 0 & \Xi_8 \\
* & * & * & * & * & -\bar{\varepsilon} I & 0 \\
* & * & * & * & * & * & -\bar{\varepsilon} I
\end{bmatrix} < 0 \tag{9.14}$$

holds, where $\hat{T} = \operatorname{diag}\{\underbrace{-G^T P^{-1} G, \ldots, -G^T P^{-1} G}_{n}\}$. Then, left- and right-multiplying (9.14) by $\operatorname{diag}\{I, I, G^{-T}, I, \underbrace{G^{-T}, \ldots, G^{-T}}_{n}, \underbrace{I, \ldots, I}_{n}, I, I, I, I\}$ and its transpose, respectively, gives (9.5). By (9.13), one sees that inequality (9.12) guarantees (9.14). This completes the proof.

Remark 9.3 In order to obtain the minimum H_∞ performance γ^*, one can solve the following optimization problem with linear matrix inequality constraint:

$$\begin{array}{c} \min \quad \rho \\ \text{s.t. (9.12) with } \rho{=}\gamma \end{array} \tag{9.15}$$

and obtain the minimum H_∞ performance γ^* by $\gamma^* = \rho$.

9.4 A Simulation Example

We consider a mechanical system with two masses and two springs. A similar example has been studied in Chaps. 3–8, but here a small modification is made, i.e., Mass 2 is not affected by disturbance. For simplicity but without loss of generality, a wireless sensor network with two sensors is deployed to monitor the spring-mass system. The structure of the distributed filtering for spring-mass system is depicted in Fig. 9.2. The mechanical system is represented by its state-space model:

$$\dot{x}(t) = \begin{bmatrix} 0 & 0 & 1 & 0 \\ 0 & 0 & 0 & 1 \\ -\frac{k_1+k_2}{m_1} & \frac{k_2}{m_1} & -\frac{c}{m_1} & 0 \\ \frac{k_2}{m_2} & -\frac{k_2}{m_2} & 0 & -\frac{c}{m_2} \end{bmatrix} x(t) + \begin{bmatrix} 0 \\ 0 \\ \frac{1}{m_1} \\ 0 \end{bmatrix} w(t), \tag{9.16}$$

where x_1 and x_2 are the positions of masses m_1 and m_2, respectively. k_1 and k_2 are the spring constants. The viscous friction coefficient between the masses and the horizontal surface is denoted by c. Suppose that x_2 is to be estimated by the filters, and x_1 is measured by two sensors with noise $w(t)$ via the broadcasting of the wireless module in mass 1. We have $z(t) = [0\ 1\ 0\ 0]x(t)$, $C_1 = C_2 = \begin{bmatrix} 1\ 0\ 0\ 0 \end{bmatrix}$, $D_1 = 1$ and $D_3 = 0.6$.

The discrete version of the system (9.17) with sampling period $T = 0.3$ s is given by

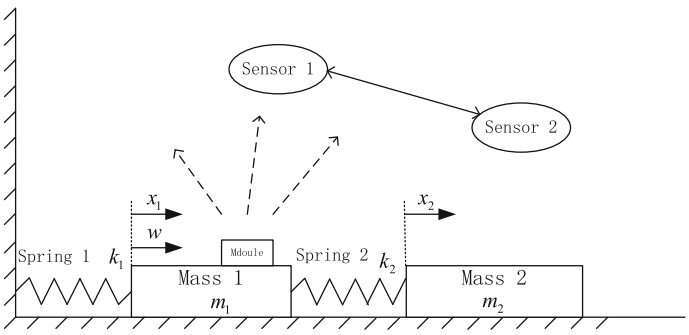

Fig. 9.2 Structure of the spring-mass system

$$A = \begin{bmatrix} 0.9162 & 0.0416 & 0.2703 & 0.0040 \\ 0.0792 & 0.9202 & 0.0079 & 0.2515 \\ -0.5328 & 0.2624 & 0.7810 & 0.0376 \\ 0.4872 & -0.4951 & 0.0753 & 0.6686 \end{bmatrix}, B = \begin{bmatrix} 0.0422 \\ 0.0006 \\ 0.2703 \\ 0.0079 \end{bmatrix}.$$

In this example, two sensors share their local estimate and measurement with each other. Suppose that the occurrence probabilities of the filter gain variation are $\bar{\alpha}_1 = 0.8$ and $\bar{\alpha}_2 = 0.6$, respectively, and the variation bounds are $\delta_{1i} = \delta_{2i} = \delta_{3i} = 1$. The related uncertain matrices are

$$\begin{aligned} &M_1 = \begin{bmatrix} 0.1 & 0.1 & 0.1 & 0.1 \end{bmatrix}^T, \\ &M_2 = \begin{bmatrix} 0.1 & 0.2 & 0.1 & 0.1 \end{bmatrix}^T, M_3 = 0.1, \\ &E_{11} = E_{12} = E_{21} = E_{22} = \begin{bmatrix} 0.1 & 0.1 & 0.1 & 0.1 \end{bmatrix}, \\ &F_{11} = 0.2, F_{12} = 0.2, F_{21} = -0.1, F_{22} = 0.1, \\ &Q_{11} = Q_{22} = \begin{bmatrix} 0.1 & 0.1 & 0.1 & 0.1 \end{bmatrix}. \end{aligned}$$

By solving the optimization problem (9.16), we obtain the optimal performance $\gamma^* = 0.3774$. To further investigate the filtering performance, we assume that the uncertainties in gains are $\Delta_1(k) = \sin(k)$, $\Delta_2(k) = rand[-1, 1]$, $\Delta_3(k) = \cos(k)$. The noise $w(k)$ is assumed to be

$$w(k) = \begin{cases} rand[-1, 1], & k \in [1, 50]; \\ 0, & k = (50, 100]. \end{cases} \tag{9.17}$$

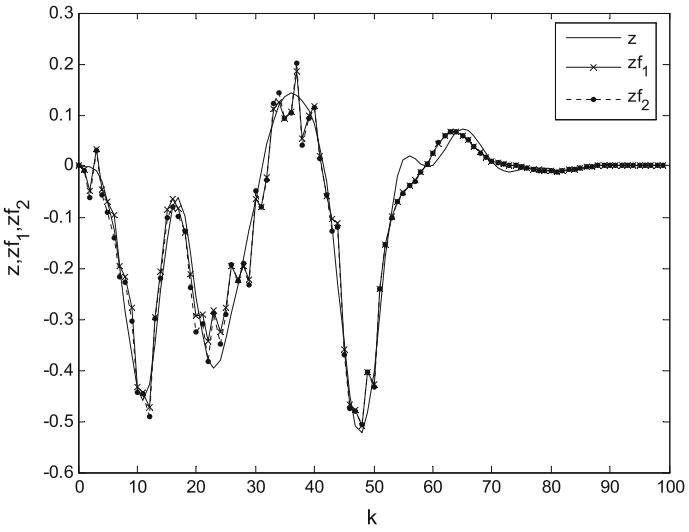

Fig. 9.3 Trajectories of estimated signals

The trajectories of the estimated signals are shown in Fig. 9.3. The actual H_∞ performance levels and the optimal one are shown in Fig. 9.4 after 100 Monte Carol simulations.

Next, the relations between the occurrence probability of the gain variation and the filtering performance are found and shown in Table 9.1 when we set $\bar{\alpha}_1 = 0.8$. The relation between the uncertain bound δ_{1i} and the γ^* is given in Table 9.2 when we choose $\delta_{2i} = \delta_{3i} = 1$ and $\delta_{11} = \delta_{12}$. It is seen that the more frequently the uncertainty occurs, the worse filtering performance result is. In addition, the filtering performance is worse when the larger perturbation occurs.

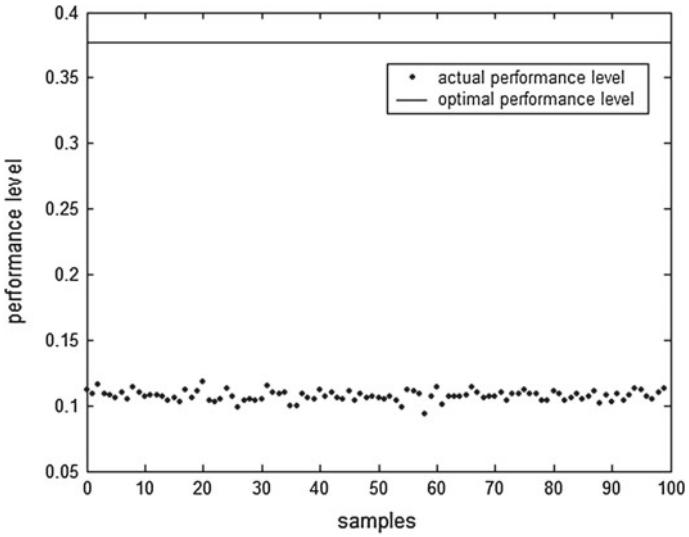

Fig. 9.4 Actual performance level and optimal performance level

Table 9.1 Relation between $\bar{\alpha}_2$ and γ^*

$\bar{\alpha}_2$	0.4	0.5	0.6	0.7	0.8
γ^*	0.3506	0.3658	0.3774	0.3865	0.3937

Table 9.2 Relation between δ_{1i} and γ^*

δ_{1i}	0.4	0.6	0.8	1.0	1.2
γ^*	0.3660	0.3689	0.3727	0.3774	0.3826

9.5 Conclusions

We have investigated the distributed filtering for a class of sensor networks with filter gain variations, in which a set of stochastic random variables are introduced to model the so-called random filter gain variation phenomenon. Based on the Lyapunov stability theory, the solvability condition of the considered filtering problem is presented. The relations between the occurrence probability of uncertainty, uncertain bound and the filtering performance are established. A numerical example has been given to show the effectiveness of the proposed design.

References

1. X. Chang, Robust nonfragile H_∞ filtering for fuzzy systems with linear fractional parameteric uncertainties. IEEE Trans. Fuzzy Syst. **20**(6), 1001–1011 (2012)
2. X. Chang, G. Yang, Non-fragile H_∞ filter design for discrete-time fuzzy systems with multiplicative gain variations. Inf. Sci. **266**, 171–185 (2014)

Chapter 10
Distributed Filtering with Measurement Size Reduction and Filter Gain Variations

10.1 Introduction

We have mentioned two practical problems, i.e., energy constraint and filter gain variations are commonly encountered in WSNs. In this chapter, the distributed filtering for a class of discrete-time systems in sensor networks with these two problems is discussed in a unified framework. The strategies of reducing the packet size and the transmission rate are proposed to save sensor's power. Firstly, the local measurement size is reduced by using an effective measurement selection protocol, and then the selected measurement is transmitted stochastically to its neighboring sensors. In order to capture the filter implementation uncertainties, the additive gain variation problem is also considered. Based on the switched system approach and some stochastic system analysis methods, a new sufficient condition is obtained such that the filtering error system is exponentially stable in the mean-square sense and achieves a prescribed H_∞ performance level. As usual, the filter parameters are determined by solving a set of linear matrix inequalities. A simulation example is finally presented to show the effectiveness of the proposed results.

10.2 Problem Statement

The sensor network is deployed to monitor the plant, and there is no centralized fusion center in this network. In this chapter, each sensor collects a local measurement and shares the information with its' neighboring ones, see Fig. 10.1 for illustration.

In this chapter, the plant is described by the following discrete-time state space model:

$$\begin{cases} x(k+1) = Ax(k) + Bw(k), \\ z(k) = Lx(k), \end{cases} \tag{10.1}$$

D. Zhang et al., *Filtering and Control of Wireless Networked Systems*,
Studies in Systems, Decision and Control 97, DOI 10.1007/978-3-319-53123-6_10

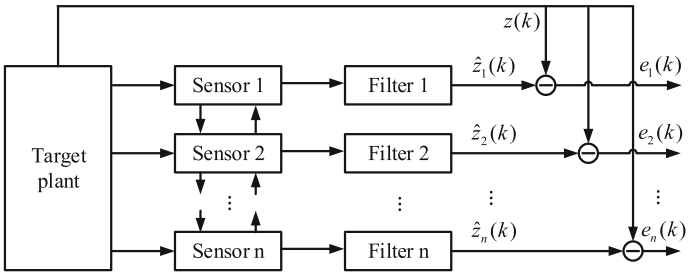

Fig. 10.1 A structure of distributed filtering in sensor networks

where $x(k) \in \mathbb{R}^{n_x}$ is the state vector. $z(k) \in \mathbb{R}^{n_z}$ is the signal to be estimated. $w(k) \in \mathbb{R}^{n_w}$ is the noise vector, belonging to $l_2[0, \infty)$. A, B and L are some known constant matrices with appropriate dimensions.

The local measurement of the i-th sensor is given by

$$y_i(k) = C_i x(k) + D_i w(k), \tag{10.2}$$

where $y_i(k) \in \mathbb{R}^{p_i}$ is the measured output from the i-th sensor. The matrices C_i and D_i are some known matrices with appropriate dimensions.

Due to the power limitation, not all local measurements are allowed to be transmitted. Only one element of measurement signal is selected and then encapsulated into a packet for transmission as this is the most energy-efficient. The measurement selection scheme is achieved by introducing the following matrix:

$$\Pi_{\rho_i(k)} = \left[0 \cdots \underbrace{1}_{i} \cdots 0 \right], \tag{10.3}$$

where $\rho_i(k) \in \{1, 2, \ldots, p_i\}$ is a time-varying signal describing which element of the measurement is selected. For example, when the first element of y_i is selected for transmission, we have $\rho_i(k) = 1$ and $\Pi_{\rho_i(k)} = \left[1 \cdots 0 \cdots 0 \right]$. When the second element of y_i is selected for transmission, we have $\rho_i(k) = 2$ and $\Pi_{\rho_i(k)} = \left[0\ 1 \cdots 0 \cdots 0 \right]$. Based on the similar idea, one may also select more elements for transmission. Then, the measurement after selection is

$$\bar{y}_i(k) = \Pi_{\rho_i(k)} \left[C_i x(k) + D_i w(k) \right]. \tag{10.4}$$

Compared with the original measurement signal, the size of measurement has been reduced and fewer packets are needed to transmit required information. In order to save more sensor power, the transmission rate reduction scheme is also applied.

Here, a stochastic transmission protocol is introduced, that is, the sensor transmits the measurement signal according to a given probability. Moreover, the zero input scheme is applied when no current measurement is received. In this scenario, the sensor does not need an additional unit to store the last received measurement. Then, the input of filter is described as

$$\tilde{y}_i(k) = \alpha_i(k)\Pi_{\rho_i(k)}\left[C_i x(k) + D_i w(k)\right], \tag{10.5}$$

where $\alpha_i(k)$ is a binary stochastic variable, taking the values in $\{0, 1\}$. In this chapter, $\Pr ob\{\alpha_i(k) = 1\} = \mathbb{E}\{\alpha_i(k)\} = \bar{\alpha}_i$ is the transmission rate of the i-th sensor. The transmission rate can be set to a certain value based on the trade-off between the filtering performance and the energy consumption.

In order to capture the filter implementation uncertainties, the additive filter gain variation problem is taken into account when we design the filter. Hence, the following filter structure is adopted:

$$\begin{cases} \hat{x}_i(k+1) = (K_{ii} + \Delta K_{ii})\hat{x}_i(k) + \sum\limits_{j \in N_i} a_{ij}(H_{ij} + \Delta H_{ij})\tilde{y}_j(k), \\ \hat{z}_i(k) = (L_{fi} + \Delta L_{fi})\hat{x}_i(k), \end{cases} \tag{10.6}$$

where $\hat{x}_i(k) \in \mathbb{R}^{n_x}$ is the state of the i-th filter, and $\hat{z}_i(k) \in \mathbb{R}^{n_z}$ is the estimate of $z(k)$ from the filter in sensor i. K_{ii}, H_{ij} and L_{fi} are the filter parameters to be determined. The uncertainties in the filter gains are described as follows:

$$\begin{cases} \Delta H_{ij} = W_{ij}\bar{\Delta}_{ij}(k)V_{ij}, \\ \Delta K_{ii} = M_{ii}\Delta_{ii}(k)N_{ii}, \\ \Delta L_{fi} = S_i\tilde{\Delta}_i(k)T_i, \end{cases} \tag{10.7}$$

where $\|\Delta_{ii}(k)\| \leq \delta_{ii}I$, $\left\|\bar{\Delta}_{ij}(k)\right\| \leq \bar{\delta}_{ij}I$, $\left\|\tilde{\Delta}_i(k)\right\| \leq \tilde{\delta}_i I$ with some known scalars δ_{ii}, $\bar{\delta}_{ij}$ and $\tilde{\Delta}_i$. These scalars are regarded as the bounds of the uncertainties. W_{ij}, V_{ij}, M_{ii}, N_{ii}, S_i and T_i are the known matrices with appropriate dimensions.

For easy presentation, we define the following notations:

$$
\begin{aligned}
&\bar{x}(k) = [\, x^T(k)\; x^T(k) \cdots x^T(k)\,]^T, \hat{x}(k) = [\, \hat{x}_1^T(k)\; \hat{x}_2^T(k) \cdots \hat{x}_n^T(k)\,]^T,\\
&\hat{z}(k) = [\, \hat{z}_1^T(k) \cdots \hat{z}_n^T(k)\,]^T, \bar{z}(k) = [\, z^T(k) \cdots z^T(k)\,]^T,\\
&\Pi_\alpha = \mathrm{diag}\{\alpha_1 I, \alpha_2 I, \ldots, \alpha_n I\}, \Pi_{\rho(k)} = \mathrm{diag}\{\Pi_{\rho_1(k)}, \ldots, \Pi_{\rho_n(k)}\},\\
&\bar{A} = \mathrm{diag}\{A, \ldots, A\}, \bar{B} = [\, B^T \cdots B^T\,]^T,\\
&\bar{C} = \mathrm{diag}\{C_1, \ldots, C_n\}, \bar{D} = [\, D_1^T \cdots D_n^T\,]^T,\\
&\bar{L} = \mathrm{diag}\{L, L, \ldots, L\}, W_i = \mathrm{diag}\{W_{1i}, \ldots, W_{ni}\},\\
&\bar{\Delta}_i(k) = \mathrm{diag}\{\bar{\Delta}_{1i}(k), \ldots, \bar{\Delta}_{ni}(k)\}, \Delta_1(k) = \mathrm{diag}\{\Delta_{11}(k), \ldots, \Delta_{nn}(k)\},\\
&\bar{\Lambda} = \mathrm{diag}\{\bar{\Lambda}_1, \ldots, \bar{\Lambda}_n\}, \Lambda = \mathrm{diag}\{\delta_{11} I, \ldots, \delta_{nn} I\},\\
&\tilde{\Lambda} = \mathrm{diag}\{\tilde{\Delta}_{11} I, \ldots, \tilde{\Delta}_{nn} I\}, \bar{\Lambda}_i = \mathrm{diag}\{\bar{\delta}_{1i} I, \ldots, \bar{\delta}_{ni} I\},\\
&\bar{M} = \mathrm{diag}\{M_{11}, M_{22}, \ldots, M_{nn}\}, \bar{N} = \mathrm{diag}\{N_{11}, N_{22}, \ldots, N_{nn}\},\\
&\tilde{S} = \mathrm{diag}\{S_1, S_2, \ldots, S_n\}, \bar{T} = \mathrm{diag}\{T_1, T_2, \ldots, T_n\},\\
&\bar{K} = \mathrm{diag}\{K_{11}, K_{22}, \ldots, K_{nn}\}, \bar{L}_f = \mathrm{diag}\{L_{f1}, L_{f2}, \ldots, L_{fn}\},\\
&\bar{H} = \begin{bmatrix} a_{11}H_{11} & \cdots & a_{1n}H_{1n} \\ \vdots & \ddots & \vdots \\ a_{n1}H_{n1} & \cdots & a_{nn}H_{nn} \end{bmatrix}, \bar{V} = \begin{bmatrix} a_{11}V_{11} & \cdots & a_{1n}V_{1n} \\ \vdots & \ddots & \vdots \\ a_{n1}V_{n1} & \cdots & a_{nn}V_{nn} \end{bmatrix},\\
&\Phi_i = \mathrm{diag}\{\delta(i-1), \ldots, \delta(i-t), \ldots, \delta(i-n)\},
\end{aligned}
$$

where $\delta(i) \in \{0, 1\}$ is the Kronecker delta function, and $\rho(k)$ is a mapping from $\{\rho_1(k), \rho_2(k), \ldots \rho_n(k)\}$. It follows from the above definition of $\rho_i(k)$, one sees that $\rho(k)$ takes the values from the set: $\Psi = \left\{1, 2, \ldots, \prod_{i=1}^{n} p_i\right\}$.

Remark 10.1 It is noted that we have introduced several switching signals $\rho_i(k)$ to model the measurement selection process. By using one-to-one mapping above, we can use only one switching signal $\rho(k)$ to describe all the switching cases. Due to the fact that we only select one element at each time instant, we have $\rho_i(k) \in \{1, 2, \ldots, p_i\}$. Then, for the switching signal $\rho(k)$, the maximal possible number is $p_1 \times p_2 \times \cdots \times p_n$, and $\rho(k)$ takes the values from the set: $\Psi = \left\{1, 2, \ldots, \prod_{i=1}^{n} p_i\right\}$, where $\prod_{i=1}^{n} p_i = p_1 \times p_2 \times \cdots \times p_n$.

Based on the above notations we have the following filtering error system:

$$
\begin{cases}
\tilde{x}(k+1) = \left(\tilde{A}_{\rho(k)} + \tilde{M}\Delta(k)\bar{N}_1\right)\tilde{x}(k) + \left(\tilde{B}_{\rho(k)} + \tilde{M}\Delta(k)\bar{N}_2\right)w(k)\\
\quad + \sum_{s=1}^{n} (\alpha_s(k) - \bar{\alpha}_s)\begin{bmatrix} \left(\tilde{A}_{s,\rho(k)} + \tilde{M}_s\Delta(k)\bar{N}_1\right)\tilde{x}(k) \\ + \left(\tilde{B}_{s,\rho(k)} + \tilde{M}_s\Delta(k)\bar{N}_2\right)w(k) \end{bmatrix},\\
e(k) = \left(\tilde{L} + \tilde{S}\tilde{\Delta}(k)\tilde{T}\right)\tilde{x}(k),
\end{cases}
\tag{10.8}
$$

where

$$
\begin{aligned}
&\tilde{x}(k) = [\,\tilde{x}^T(k)\ \hat{x}^T(k)\,]^T, e(k) = \hat{z}(k) - \bar{z}(k),\\
&\tilde{A}_{\rho(k)} = \begin{bmatrix} \bar{A} & 0 \\ \bar{H}\Pi_\alpha \Pi_{\rho(k)}\bar{C} & \bar{K} \end{bmatrix}, \tilde{B}_{\rho(k)} = \begin{bmatrix} \bar{B} \\ \bar{H}\Pi_\alpha \Pi_{\rho(k)}\bar{D} \end{bmatrix},\\
&\tilde{A}_{s,\rho(k)} = \begin{bmatrix} 0 & 0 \\ \bar{H}\Phi_s \Pi_{\rho(k)}\bar{C} & 0 \end{bmatrix}, \tilde{B}_{s,\rho(k)} = \begin{bmatrix} 0 \\ \bar{H}\Phi_i \Pi_{\rho(k)}\bar{D} \end{bmatrix},\\
&\tilde{M} = \begin{bmatrix} 0 & \cdots & 0 & 0 \\ \alpha_1 W_1 & \cdots & \alpha_n W_n & \bar{M} \end{bmatrix},\\
&\bar{N}_1 = \begin{bmatrix} \bar{V}\Phi_1 \Pi_{\rho(k)}\bar{C} & 0 \\ \vdots & \vdots \\ \bar{V}\Phi_n \Pi_{\rho(k)}\bar{C} & 0 \\ 0 & \bar{N} \end{bmatrix}, \bar{N}_2 = \begin{bmatrix} \bar{V}\Phi_1 \Pi_{\rho(k)}\bar{D} \\ \vdots \\ \bar{V}\Phi_n \Pi_{\rho(k)}\bar{D} \\ 0 \end{bmatrix},\\
&\tilde{M}_i = \begin{bmatrix} 0 \cdots 0 & \cdots 0\ 0 \\ 0 \cdots W_i & \cdots 0\ 0 \end{bmatrix}, \Delta(k) = \mathrm{diag}\{\bar{\Delta}_1(k), \ldots, \bar{\Delta}_n(k), \Delta_1(k)\}\\
&\tilde{L} = [\,-\bar{L}\ \bar{L}_f\,].
\end{aligned}
$$

The system (10.8) is a switched system, and the average dwell time approach is utilized to derive the main results.

Definition 10.1 The system (10.8) is called robustly exponentially stable in the mean-square sense, if there exist some scalars $\pi > 0$ and $0 < \chi < 1$, such that the solution $\tilde{x}$ of system (10.8) satisfies $\mathbb{E}\{\|\tilde{x}(k)\|\} < \pi\chi^{(k-k_0)}\|\tilde{x}(k_0)\|, \forall k \geq k_0$.

Definition 10.2 For a given scalar $\gamma > 0$, the system (10.8) is said to be robustly exponentially stable in the mean-square sense and achieves a prescribed H_∞ performance γ, if it is exponentially stable and under zero initial condition, $\sum_{k=0}^{+\infty} \mathbb{E}\frac{1}{n}\{e^T(k)e(k)\} \leq \sum_{k=0}^{+\infty} \gamma^2 w^T(k)w(k)$ holds for all nonzero $w(k) \in l_2[0, \infty)$.

Our filtering problem is stated as follows.

Filtering Problem: design a filter in form of (10.6) such that the filtering error system (10.8) is robustly exponentially stable in the mean-square sense and achieves a prescribed H_∞ performance level in the presence of measurement size and transmission rate reduction and uncertain filter gain variation.

10.3 Filter Analysis and Design

In this section, a sufficient condition is first established to guarantee the exponential stability of the filtering error system (10.8) with a prescribed H_∞ performance level.

Theorem 10.1 *For given scalars $\tau > 0, \mu > 1, 0 < \lambda_i < 1$, and $0 < \lambda < 1$, if there exist positive-definite matrices P_i and a positive scalar $\varepsilon > 0$ such that the following inequalities,*

$$\begin{bmatrix} \Xi_1 & \Xi_2 & \Xi_3 & \Xi_4 & \Xi_5 & 0 \\ * & -P_i^{-1} & 0 & 0 & 0 & \Xi_6 \\ * & * & -nI & 0 & 0 & \Xi_7 \\ * & * & * & -\bar{P}_i & 0 & \Xi_8 \\ * & * & * & * & -\bar{\varepsilon} & 0 \\ * & * & * & * & * & -\bar{\varepsilon} \end{bmatrix} < 0, \tag{10.9}$$

$$P_i \leq \mu P_j, i \neq j, \tag{10.10}$$

$$T_a > T_a^* = -\frac{\ln \mu}{\ln \lambda}, \tag{10.11}$$

hold for all $i, j \in \Psi$, then the filtering error system (10.8) is exponentially stable in the mean-square sense with decay rate $\chi = \sqrt{\lambda_b \mu^{1/T_a}}$ and achieves a prescribed H_∞ performance level $\gamma = \tau\sqrt{\frac{(1-\lambda_a)}{1-\lambda_b/\lambda}}$, where $\lambda_a = \min_{i\in\Psi}\{\lambda_i\}$, $\lambda_b = \max_{i\in\Psi}\{\lambda_i\}$, $\lambda > \lambda_b$, and

$$\Xi_1 = \begin{bmatrix} -\lambda_i P_i & 0 \\ 0 & -\tau^2 I \end{bmatrix}, \Xi_2 = \begin{bmatrix} \tilde{A}_i & \tilde{B}_i \end{bmatrix}^T, \Xi_3 = \begin{bmatrix} \tilde{L} & 0 \end{bmatrix}^T,$$
$$\Xi_4 = \begin{bmatrix} \theta_1 \tilde{A}_{1i}^T & \cdots & \theta_n \tilde{A}_{ni}^T \\ \theta_1 \tilde{B}_{1i}^T & \cdots & \theta_n \tilde{B}_{ni}^T \end{bmatrix}, \Xi_5 = \begin{bmatrix} \bar{N}_1^T \hat{\Lambda}\varepsilon & \tilde{T}^T \tilde{\Lambda}\varepsilon \\ \bar{N}_2^T \hat{\Lambda}\varepsilon & 0 \end{bmatrix},$$
$$\Xi_6 = \begin{bmatrix} \tilde{M} & 0 \end{bmatrix}, \Xi_7 = \begin{bmatrix} 0 & \tilde{S} \end{bmatrix}, \Xi_8 = \begin{bmatrix} \theta_1 \tilde{M}_1 & 0 \\ \vdots & \vdots \\ \theta_n \tilde{M}_n & 0 \end{bmatrix}, \hat{\Lambda} = \begin{bmatrix} \Lambda & 0 \\ 0 & \tilde{\Lambda} \end{bmatrix},$$
$$\bar{P}_i = \text{diag}\{P_i^{-1}, \ldots, P_i^{-1}\}, \bar{\varepsilon} = \text{diag}\{\varepsilon I, \varepsilon I\}.$$

Proof We choose the following Lyapunov functional:

$$V_{\rho(k)}(k) = \tilde{x}^T(k) P_{\rho(k)} \tilde{x}(k). \tag{10.12}$$

Then for each $\rho(k) = i$, it follows that $\forall i \in \Psi$,

$$\begin{aligned} &\mathbb{E}\{V_i(k+1) - \lambda_i V_i(k) + \Upsilon(k)\} \\ &= \left[\left(\tilde{A}_{\rho(k)} + \tilde{M}\Delta(k)\bar{N}_1\right)\tilde{x}(k) + \left(\tilde{B}_{\rho(k)} + \tilde{M}\Delta(k)\bar{N}_2\right)w(k)\right]^T \\ &\quad \times P_i \left[\left(\tilde{A}_{\rho(k)} + \tilde{M}\Delta(k)\bar{N}_1\right)\tilde{x}(k) + \left(\tilde{B}_{\rho(k)} + \tilde{M}\Delta(k)\bar{N}_2\right)w(k)\right] \\ &\quad + \sum_{i=1}^{n} \theta_i^2 \left[\left(\tilde{A}_{i,\rho(k)} + \tilde{M}_i\Delta(k)\bar{N}_1\right)\tilde{x}(k) + \left(\tilde{B}_{i,\rho(k)} + \tilde{M}_i\Delta(k)\bar{N}_2\right)w(k)\right]^T \\ &\quad \times P_i \left[\left(\tilde{A}_{i,\rho(k)} + \tilde{M}_i\Delta(k)\bar{N}_1\right)\tilde{x}(k) + \left(\tilde{B}_{i,\rho(k)} + \tilde{M}_i\Delta(k)\bar{N}_2\right)w(k)\right] \\ &\quad + \tfrac{1}{n}\left[\left(\tilde{L} + \tilde{S}\tilde{\Delta}(k)\tilde{T}\right)\tilde{x}(k)\right]^T \left[\left(\tilde{L} + \tilde{S}\tilde{\Delta}(k)\tilde{T}\right)\tilde{x}(k)\right] \\ &\quad - \lambda_i \eta^T(k) P_i \eta(k) - \tau^2 w^T(k) w(k), \end{aligned} \tag{10.13}$$

where $\Upsilon(k) = \frac{1}{n}e^T(k)e(k) - \tau^2 w^T(k)w(k)$. By some arrangement, it is easy to see that $\mathbb{E}\{V_i(k+1) - \lambda_i V_i(k) + \Upsilon(k)\} < 0$ is equivalent to

$$\Omega_1 + \Omega_2 \Delta(k) \Omega_3^T + \Omega_3 \Delta(k) \Omega_2^T < 0, \tag{10.14}$$

where

$$\Omega_1 = \begin{bmatrix} \Xi_1 & \Xi_2 & \Xi_3 & \Xi_4 \\ * & -P_i^{-1} & 0 & 0 \\ * & * & -nI & 0 \\ * & * & * & -\bar{P}_i \end{bmatrix}, \Omega_2 = \begin{bmatrix} \bar{\Xi}_5 \\ 0 \\ 0 \\ 0 \end{bmatrix},$$
$$\Omega_3 = \begin{bmatrix} 0 \\ \Xi_6 \\ \Xi_7 \\ \Xi_8 \end{bmatrix}, \hat{\Delta}(k) = \begin{bmatrix} \Delta(k) & 0 \\ 0 & \tilde{\Delta}(k) \end{bmatrix},$$

with

$$\bar{\Xi}_5 = \begin{bmatrix} \bar{N}_1^T & \tilde{T}^T \\ \bar{N}_2^T & 0 \end{bmatrix}.$$

By some manipulation, (10.14) is written as

$$\Omega_1 + \Omega_2 \bar{\Lambda} \bar{\Delta}(k) \Omega_3^T + \Omega_3^T \bar{\Lambda} \bar{\Delta}(k) \Omega_2 < 0, \tag{10.15}$$

where $\bar{\Lambda} = \text{diag}\{\Lambda, \tilde{\Lambda}\}$, and $\bar{\Delta}(k) = \begin{bmatrix} \frac{\Delta(k)}{\Lambda} & 0 \\ 0 & \frac{\tilde{\Delta}(k)}{\tilde{\Lambda}} \end{bmatrix}$. It follows that $\left\| \frac{\Delta(k)}{\Lambda} \right\| \leq I$, $\left\| \frac{\tilde{\Delta}(k)}{\tilde{\Lambda}} \right\| < I$. Based on Lemma 2.2, one sees that (10.15) holds if and only if (10.9) holds. Hence,

$$\mathbb{E}\{V_i(k+1) - \lambda_i V_i(k) + \Upsilon(k)\} < 0. \tag{10.16}$$

For the switching time instant $k_0 < k_1 < \cdots < k_i < \cdots < k_s$, we define the switching number of $\rho(k)$ over (k_0, k) as $N_\rho(k_0, k)$. One has

$$\mathbb{E}\{V_i(k)\} \leq \mathbb{E}\{\lambda_i^{k-k_i} V_i(k_i)\} - \sum_{s=k_i}^{k-1} \lambda_i^{k-s-1} \mathbb{E}\{\Upsilon(s)\}. \tag{10.17}$$

It follows from (10.10) and (10.17) that

$$
\begin{aligned}
&\mathbb{E}\{V_{\rho(k_l)}(k)\} \\
&\le \lambda_{\rho(k_l)}^{k-k_l}\mathbb{E}\{V_{\rho(k_l)}(k_l)\} - \sum_{s=k_l}^{k-1}\lambda_{\rho(k_l)}^{k-s-1}\mathbb{E}\{\Upsilon(s)\} \\
&\le \lambda_{\rho(k_l)}^{k-k_l}\mu\mathbb{E}\{V_{\rho(k_{l-1})}(k_l)\} - \sum_{s=k_l}^{k-1}\lambda_{\rho(k_l)}^{k-s-1}\mathbb{E}\{\Upsilon(s)\} \\
&\le \lambda_{\rho(k_l)}^{k-k_l}\mu\left[\lambda_{\rho(k_{l-1})}^{k_l-k_{l-1}}\mathbb{E}\{V_{\rho(k_{l-1})}(k_{l-1})\} - \sum_{s=k_{l-1}}^{k_l-1}\lambda_{\rho(k_{l-1})}^{k-s-1}\mathbb{E}\{\Upsilon(s)\}\right] \\
&\quad - \sum_{s=k_l}^{k-1}\lambda_{\rho(k_l)}^{k-s-1}\mathbb{E}\{\Upsilon(s)\} \\
&\le \cdots \le \mu^{N_\rho(k_0,k)}\lambda_{\rho(k_l)}^{k-k_l}\lambda_{\rho(k_{l-1})}^{k_l-k_{l-1}}\cdots\lambda_{\rho(k_0)}^{k_1-k_0}V_{\rho(k_0)}(k_0) - \Theta(\Upsilon),
\end{aligned}
\tag{10.18}
$$

where

$$
\begin{aligned}
\Theta(\Upsilon) &= \mu^{N_\rho(k_0,k-1)}\lambda_{\rho(k_l)}^{k-k_l}\prod_{s=1}^{l-1}\lambda_{\rho(k_s)}^{k_{s+1}-k_s}\sum_{s=k_0}^{k_1-1}\lambda_{\rho(k_0)}^{k_1-1-s}\mathbb{E}\{\Upsilon(s)\} \\
&\quad + \mu^{N_\rho(k_0,k-1)-1}\lambda_{\rho(k_l)}^{k-k_l}\prod_{s=2}^{l-1}\lambda_{\rho(k_j)}^{k_{j+1}-k_j}\sum_{s=k_1}^{k_2-1}\lambda_{\rho(k_1)}^{k_2-1-s}\mathbb{E}\{\Upsilon(s)\} \\
&\quad + \cdots + \mu^0\prod_{s=k_l}^{k-1}\lambda_{\rho(k_l)}^{k-1-s}\mathbb{E}\{\Upsilon(s)\}.
\end{aligned}
$$

Now, we consider the exponential stability of system (10.8) with $w(k) = 0$. One has

$$
\begin{aligned}
&\mathbb{E}\{V_{\rho(k_l)}(k)\} \\
&\le \mu^{N_\rho(k_0,k)}\lambda_{\rho(k_l)}^{k-k_l}\lambda_{\rho(k_{l-1})}^{k_l-k_{l-1}}\cdots\lambda_{\rho(k_0)}^{k_1-k_0}V_{\rho(k_0)}(k_0) \\
&\le \mu^{N_\rho(k_0,k)}\lambda_b^{k-k_0}V_{\rho(k_0)}(k_0) \\
&\le \left(\mu^{1/T_a}\lambda_b\right)^{k-k_0}V_{\rho(k_0)}(k_0) = \chi^{2(k-k_0)}V_{\rho(k_0)}(k_0),
\end{aligned}
\tag{10.19}
$$

which yields $\mathbb{E}\left\{\|\tilde{x}(k)(k)\|^2\right\} \le \frac{\varphi_2}{\varphi_1}\chi^{2(k-k_0)}\|\tilde{x}(k_0)\|^2$, where $\varphi_1 = \min_{i\in\Psi}\sigma_{\min}(P_i)$, $\varphi_2 = \max_{i\in\Psi}\sigma_{\max}(P_i)$, $\chi = \sqrt{\lambda_b\mu^{1/T_a}}$. Therefore, one can readily obtain $\chi < 1$ from (10.11). According to Definition 10.1, the filtering error system (10.8) is exponentially stable in the mean-square sense with $w(k) = 0$.

For the H_∞ performance level, we consider $w(k) \neq 0$. Under zero initial condition, it follows from (10.18) that

$$
\sum_{s=k_0}^{k-1}\mu^{N_\rho(s,k-1)}\lambda_a^{k-s-1}\mathbb{E}\{e^T(s)e(s)\} \le \tau^2\sum_{s=k_0}^{k-1}\mu^{N_\rho(s,k-1)}\lambda_b^{k-s-1}w^T(s)w(s). \tag{10.20}
$$

With the average dwell time condition (10.11), it is easy to see $\frac{N_\rho(s,k-1)}{k-s-1} < -\frac{\ln\lambda}{\ln\mu}$. Since $\mu > 1$, we obtain $\ln\mu^{N_\rho(s,k-1)} < \ln\lambda^{-(k-s-1)}$, and $1 < \mu^{N_\rho(s,k-1)} < \lambda^{-(k-s-1)}$. Then, it can be readily seen that

$$\sum_{s=k_0}^{k-1} \lambda_a^{k-s-1} \mathbb{E}\{e^T(s)e(s)\} < \tau^2 \sum_{s=k_0}^{k-1} \left(\lambda_b/\lambda\right)^{k-s-1} \lambda^{k-s-1} w^T(s)w(s). \tag{10.21}$$

Summing (10.21) from $k = k_0 + 1$ to $k = \infty$ and changing the order of summation yield

$$\sum_{s=k_0}^{+\infty} \mathbb{E}\{e^T(s)e(s)\} \sum_{k=s+1}^{+\infty} \lambda_a^{k-s-1} < \tau^2 \sum_{s=k_0}^{+\infty} w^T(s)w(s) \sum_{k=s+1}^{+\infty} \left(\lambda_b/\lambda\right)^{k-s-1}. \tag{10.22}$$

Since $\sum\limits_{k=s+1}^{+\infty} \lambda_a^{k-s-1} = \frac{1}{1-\lambda_a}$ and $\sum\limits_{k=s+1}^{+\infty} \left(\lambda_b/\lambda\right)^{k-s-1} = \frac{1}{1-(\lambda_b/\lambda)}$, we have

$$\sum_{s=k_0}^{+\infty} \mathbb{E}\{e^T(s)e(s)\} < \gamma^2 \sum_{s=k_0}^{+\infty} w^T(s)w(s), \tag{10.23}$$

where $\gamma = \tau\sqrt{\frac{1-\lambda_a}{1-\lambda_b/\lambda}}$. It is noted that $\lambda_b < \lambda$, which ensures $\gamma > 0$. Let $k_0 = 0$, one sees that the filtering error system (10.8) is exponentially stable in the mean-square sense and achieves a prescribed H_∞ performance level γ. This completes the proof.

Theorem 10.1 does not give the filter gains directly. The filter gains are determined in the following theorem.

Theorem 10.2 *For given scalars $\tau > 0, \mu > 1, 0 < \lambda_i < 1$, and $0 < \lambda < 1$, if there exist positive-definite matrices P_i, a positive scalar $\varepsilon > 0$, and any matrices G_i of appropriate dimensions such that the following inequality,*

$$\begin{bmatrix} \Xi_1 & \tilde{\Xi}_2 & \tilde{\Xi}_3 & \tilde{\Xi}_4 & \Xi_5 & 0 \\ * & T_i & 0 & 0 & 0 & \tilde{\Xi}_6 \\ * & * & -nI & 0 & 0 & \Xi_7 \\ * & * & * & \bar{T}_i & 0 & \tilde{\Xi}_8 \\ * & * & * & * & -\bar{\varepsilon} & 0 \\ * & * & * & * & * & -\bar{\varepsilon} \end{bmatrix} < 0, \tag{10.24}$$

(10.10) and (10.11) hold for all $i, j \in \Psi$, then the filtering problem is solvable, and the filter gains are determined by $\bar{K} = G_3^{-T}\tilde{K}$, $\bar{H} = G_3^{-T}\tilde{H}$ and $\bar{L}_f = \tilde{L}_f$, where

$$\tilde{\Xi}_2 = \begin{bmatrix} \tilde{\Xi}_{21} \\ \tilde{\Xi}_{22} \end{bmatrix}, \tilde{\Xi}_3 = \begin{bmatrix} \tilde{\Xi}_{31} \\ 0 \end{bmatrix}, \tilde{\Xi}_4 = \begin{bmatrix} \tilde{\Xi}_{41} & \cdots & \tilde{\Xi}_{4n} \\ \tilde{\Xi}_{41} & \cdots & \tilde{\Xi}_{4n} \end{bmatrix},$$

$$\tilde{\Xi}_6 = \begin{bmatrix} \bar{\alpha}_1 G_3^T W_1 & \cdots & \bar{\alpha}_n G_3^T W_n & G_3^T \bar{M} \\ \bar{\alpha}_1 G_3^T W_1 & \cdots & \bar{\alpha}_n G_3^T W_n & G_3^T \bar{M} \end{bmatrix}, \tilde{\Xi}_8 = \begin{bmatrix} \tilde{\Xi}_{81} \\ \vdots \\ \tilde{\Xi}_{8n} \end{bmatrix},$$

$$T_i = P_i - G_i - G_i^T,$$

with

$$\tilde{\Xi}_{21} = \begin{bmatrix} A^T G_{1i} + \bar{C}^T \Pi_i^T \Pi_\alpha^T \tilde{H}^T & A^T G_{2i} + \bar{C}^T \Pi_i^T \Pi_\alpha^T \tilde{H}^T \\ \tilde{K}^T & \tilde{K}^T \end{bmatrix},$$

$$\tilde{\Xi}_{22} = \begin{bmatrix} B^T G_{1i} + \bar{D}^T \Pi_i^T \Pi_\alpha^T \tilde{H}^T & B^T G_{2i} + \bar{D}^T \Pi_i^T \Pi_\alpha^T \tilde{H}^T \end{bmatrix},$$

$$\tilde{\Xi}_{31} = \begin{bmatrix} -\bar{L}^T \\ \tilde{L}_f^T \end{bmatrix}, \tilde{\Xi}_{4s} = \theta_s \begin{bmatrix} \bar{C}^T \Pi_i^T \Phi_s^T \tilde{H}^T & \bar{C}^T \Pi_i^T \Phi_s^T \tilde{H}^T \\ 0 & 0 \end{bmatrix},$$

$$\bar{\Xi}_{4s} = \theta_s \begin{bmatrix} \bar{D}^T \Pi_i^T \Phi_s^T \tilde{H}^T & \bar{D}^T \Pi_i^T \Phi_s^T \tilde{H}^T \end{bmatrix},$$

$$\tilde{\Xi}_{81} = \begin{bmatrix} \theta_1 G_3^T W_1 \cdots 0\ 0 \\ \theta_1 G_3^T W_1 \cdots 0\ 0 \end{bmatrix}, \tilde{\Xi}_{8s} = \begin{bmatrix} 0 \cdots \theta_s G_3^T W_s \cdots 0\ 0 \\ 0 \cdots \theta_s G_3^T W_s \cdots 0\ 0 \end{bmatrix},$$

$$\tilde{\Xi}_{8n} = \begin{bmatrix} 0 \cdots \theta_n G_3^T W_n\ 0 \\ 0 \cdots \theta_n G_3^T W_n\ 0 \end{bmatrix}, P_i = \begin{bmatrix} P_{1i} & P_{2i} \\ * & P_{3i} \end{bmatrix}, G_i = \begin{bmatrix} G_{1i} & G_{2i} \\ G_3 & G_3 \end{bmatrix},$$

and G_3 is a diagonal matrix.

Proof It is seen that (10.24) holds if there exists a matrix G_i such that

$$\begin{bmatrix} \Xi_1 & \tilde{\Xi}_2 & \tilde{\Xi}_3 & \tilde{\Xi}_4 & \Xi_5 & 0 \\ * & -G_i^T P_i^{-1} G_i & 0 & 0 & 0 & \tilde{\Xi}_6 \\ * & * & -nI & 0 & 0 & \Xi_7 \\ * & * & * & \tilde{T}_i & 0 & \tilde{\Xi}_8 \\ * & * & * & * & -\bar{\varepsilon} & 0 \\ * & * & * & * & * & -\bar{\varepsilon} \end{bmatrix} < 0, \tag{10.25}$$

where $\tilde{T}_i = \text{diag}\{-G_i^T P_i^{-1} G_i, \ldots, -G_i^T P_i^{-1} G_i\}$. Then by left- and right- multiplying (10.25) with $\text{diag}\{I, I, G_i^{-T}, I, G_i^{-T}, \ldots, G_i^{-T}, I, I, I, I\}$ and its transpose, respectively, it is easy to see that (10.9) guarantees (10.25). This completes the proof.

Remark 10.2 In Theorem 10.2, the existence condition for the filters is given in terms of LMIs which is convex in the scalar τ^2. Therefore, one may solve the following optimization problem:

$$\begin{aligned} &\min \rho, \\ &\text{s.t. (10.10), (10.11), (10.24) with } \rho = \tau^2. \end{aligned} \tag{10.26}$$

to obtain the filter gain parameters such that the H_∞ disturbance attenuation level is minimized. When the optimal ρ is obtained from the above optimization problem, then the designed filters guarantee that the filtering error system is exponentially stable and achieves a prescribed H_∞ performance level $\gamma = \tau\sqrt{\frac{(1-\lambda_a)}{1-\lambda_b/\lambda}}$.

10.4 An Illustrative Example

Consider a spring-mass system, which has been studied in Chap. 9. The dynamics of spring-mass system can be modeled as the following LTI system under sampling period $T = 0.3s$:

$$x(k+1) = Ax(k) + Bw(k), \tag{10.27}$$

where

$$A = \begin{bmatrix} 0.9162 & 0.0416 & 0.2703 & 0.0040 \\ 0.0792 & 0.9202 & 0.0079 & 0.2515 \\ -0.5328 & 0.2624 & 0.7810 & 0.0376 \\ 0.4872 & -0.4951 & 0.0753 & 0.6686 \end{bmatrix}, B = \begin{bmatrix} 0.0422 \\ 0.0006 \\ 0.2703 \\ 0.0079 \end{bmatrix}.$$

More discussions on modeling of spring-mass system can be found in Chap. 9. As in Chap. 9, two sensors are deployed to monitor the spring-mass system. In this example, the local measurements are assumed to be

$$\begin{cases} y_1(k) = C_1 x(k) + D_1 w(k), \\ y_2(k) = C_2 x(k) + D_2 w(k), \end{cases} \tag{10.28}$$

with $C_1 = \begin{bmatrix} 1 & 0 & 0 & 0 \\ 0 & 1 & 0 & 0 \end{bmatrix}$, $D_1 = \begin{bmatrix} 0.5 \\ 0.6 \end{bmatrix}$, $C_2 = \begin{bmatrix} 1 & 0 & 0 & 0 \end{bmatrix}$, $D_2 = 0.6$.

Due to the energy constraints of the sensor network, the size of measurement y_1 should be reduced before transmission, and y_2 is transmitted directly. In this example, $\Pi_{\rho_1(k)} \in \left\{ \begin{bmatrix} 1 & 0 \end{bmatrix}, \begin{bmatrix} 0 & 1 \end{bmatrix} \right\}$, and each element of y_1 is designed to be transmitted for 5 time steps. The transmission rate of each sensor is set to be 10, and 20%, i.e., $\bar{\alpha}_1 = 0.9$, and $\bar{\alpha}_2 = 0.8$. The signal to be estimated is $z(k) = \begin{bmatrix} 1 & 1 & 0 & 0 \end{bmatrix} x(k)$. In this estimation task, these two sensors share their measurements with each other. The matrices in (10.7) is assumed to be

$$\begin{aligned} &M_{11} = [0.1\ 0.1\ 0.2\ 0.1]^T, M_{22} = [0.05\ 0.1\ 0.1\ 0.1]^T, \\ &N_{11} = [0.1\ 0.1\ 0.1\ 0.1], N_{22} = [0.1\ 0\ 0.1\ 0.1], \\ &W_{11} = [0.1\ 0.1\ 0.2\ 0.1]^T, W_{12} = [0.1\ 0.1\ 0.1\ 0.1]^T, \\ &W_{21} = [-0.1\ 0.1\ 0.2\ 0.1]^T, W_{22} = [0.1\ 0.1\ 0\ 0.1]^T, \\ &V_{11} = 0.1, V_{12} = 0.08, V_{21} = 0.05, V_{22} = 0.03, \\ &S_1 = 0.1, S_2 = 0.1, T_1 = [0.1\ 0.1\ 0.1\ 0.1], \\ &T_2 = [-0.1\ 0.1\ -0.1\ 0.1]. \end{aligned}$$

The uncertainties in (10.7) are $\Delta_{ii}(k) = rand[0, 1]$, $\bar{\Delta}_{ij}(k) = rand[0, 1]$ and $\tilde{\Delta}_i(k) = rand[0, 1]$, where $rand$ is a random function. Choosing $\lambda_1 = 0.92$, $\lambda_2 = 0.95$, $\lambda = 0.96$ and $\mu = 1.1$, we have $\lambda_a = 0.92$ and $\lambda_b = 0.95$. By solving optimization (10.26), we obtain the optimal H_∞ performance level is $\gamma^* = 4.1783$. The corresponding filter gain parameters are

$$K_{11} = \begin{bmatrix} 0.6891 & -0.0971 & 0.1101 & 0.0083 \\ -0.2865 & 0.1683 & -0.4210 & 0.0573 \\ -0.7598 & 0.3223 & 0.6706 & -0.0293 \\ -0.3400 & -0.2475 & -0.3959 & -0.3505 \end{bmatrix},$$

$$H_{11} = \begin{bmatrix} -0.0892 \\ -0.3558 \\ -0.2611 \\ 0.6194 \end{bmatrix}, H_{12} = \begin{bmatrix} -0.1947 \\ -0.4891 \\ 0.2026 \\ 0.5422 \end{bmatrix},$$

$$K_{22} = \begin{bmatrix} 0.7180 & -0.0796 & 0.1209 & 0.0058 \\ -0.1849 & 0.1194 & -0.3842 & 0.0882 \\ -0.7449 & 0.2355 & 0.7267 & 0.0025 \\ -0.2168 & -0.0014 & 0.2172 & -0.3073 \end{bmatrix},$$

$$H_{21} = \begin{bmatrix} -0.0912 \\ -0.4202 \\ -0.3471 \\ 0.1254 \end{bmatrix}, H_{22} = \begin{bmatrix} -0.1715 \\ -0.5076 \\ 0.1314 \\ 0.2889 \end{bmatrix},$$

$$L_{f1} = \begin{bmatrix} -1.3752 & -0.7531 & 0.0810 & 0.0263 \end{bmatrix},$$

$$L_{f2} = \begin{bmatrix} -1.4260 & -0.7532 & 0.1011 & 0.0165 \end{bmatrix}.$$

In the simulation setup, the unknown disturbance is taken as $w(k) = e^{-0.5k} \sin(0.05k)$. Under the zero initial conditions, the filtering performance is shown in Figs. 10.2 and 10.3. It follows from Fig. 10.3 that the true H_∞ performance level is 0.7623, which is smaller than $\gamma^* = 4.1783$. Due to the fact that there are many stochastic uncertainties in the simulation, we run 100 simulations on the H_∞ perfor-

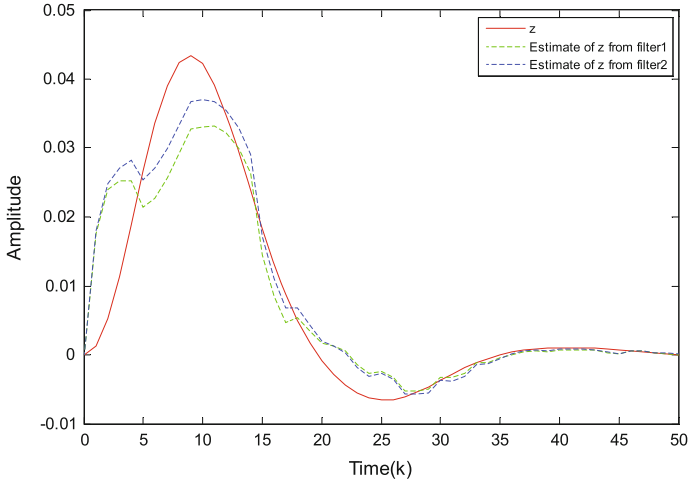

Fig. 10.2 Trajectories of $z(k)$ and its estimates $\hat{z}_i(k)$

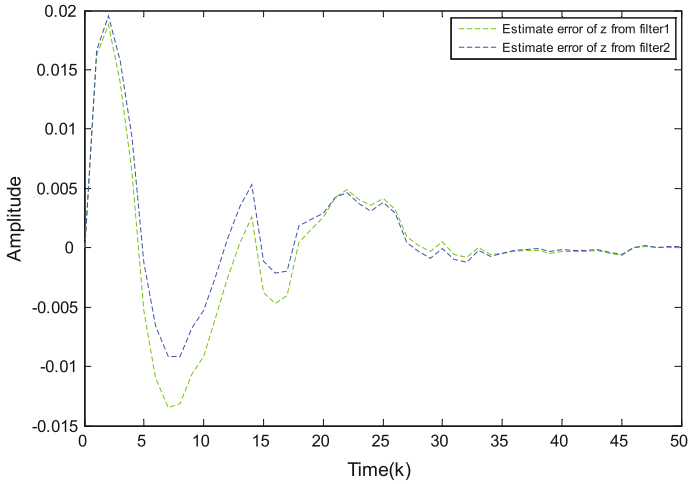

Fig. 10.3 Trajectories of estimation error $e_i(k)$

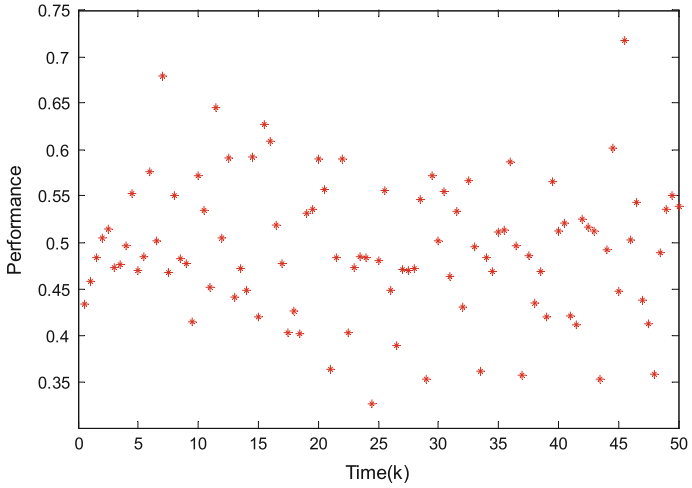

Fig. 10.4 One hundred samples without packet losses

mance level and the results are depicted in Fig. 10.4. It is seen that our filter design method is very effective. In order to see that our filtering result is also robust to packet losses, we depict the 100 simulations on the filtering performance with 20% packet dropout in each channel, see Fig. 10.5. Compared with Fig. 10.4, the estimation performance becomes worse, but the overall performance is still guaranteed.

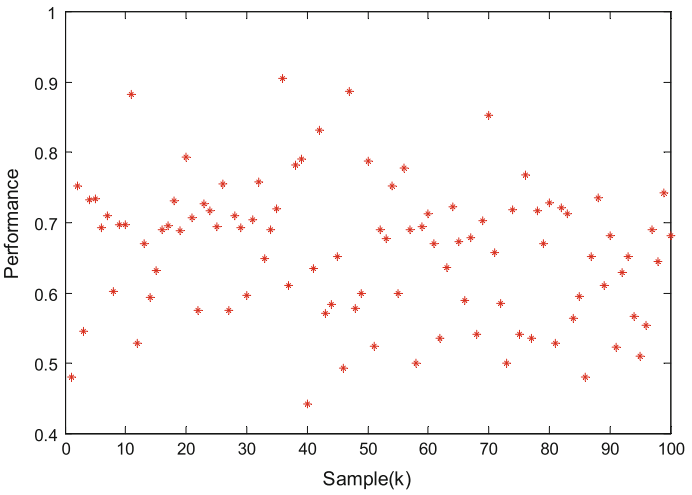

Fig. 10.5 One hundred samples with packet losses

10.5 Conclusions

We have studied the distributed non-fragile filtering for a class of discrete-time systems in sensor networks with energy constraints. Measurement size reduction and stochastic transmission techniques are used in a unified framework to overcome power constraints in sensors. Moreover, the practical issue, i.e., the filter gain variation problem, is also taken into account in the filter design. Based on the switched system approach and some stochastic system analysis, the filter gain parameters can be found by solving a set of LMIs, which is numerically efficient. Finally, a simulation example has been given to show the effectiveness of the proposed design.

Chapter 11
Distributed Control with Controller Gain Variations

11.1 Introduction

In the last few chapters, we have addressed the filtering problem of wireless networks with energy constraints and filter gain variations. From this chapter onwards, we turn to discuss the stabilization problem. In this chapter, the attention is focused on the non-fragile distributed stabilization of large-scale system, in which the controller gain variation and random controller failure are taken into account. Specifically, a set of stochastic variables are introduced to model the random controller failure phenomenon, then the additive controller gain variation problem is considered in the controller design. Based on the Lyapunov stability theory and some stochastic system analysis, a sufficient condition is obtained to guarantee that the closed-loop system is asymptotically stable in the mean-square sense with a prescribed H_∞ disturbance attenuation level. The optimal controller gain design algorithm is presented by solving an optimization problem. A simulation example is finally given to show the effectiveness of the proposed design.

11.2 Problem Formulation

The problem under consideration is to stabilize the interconnected systems by deploying a group of controllers. The system structure is shown in Fig. 11.1, where each controller is able to communicate with its neighbors via networked communication. The multiple controllers act as a controller network with a certain topology.

Standard definitions for the controller network are given as follows. Let the topology of a given controller network be represented by a direct graph $\pi(k) = (\upsilon, \chi, \mathbb{A})$ of order n with the set of controllers $\upsilon = \{1, 2, \ldots, n\}$, set of edges $\chi \subseteq \upsilon \times \upsilon$, and a weighted adjacency matrix $\mathbb{A} = [a_{ij}]$ with nonnegative adjacency elements a_{ij}. The edge of π is denoted by (i, j). The adjacency elements associated with the edges of the graph are $a_{ij} = 1 \Leftrightarrow (i, j) \in \upsilon$, when controller i can receive information

D. Zhang et al., *Filtering and Control of Wireless Networked Systems*,
Studies in Systems, Decision and Control 97, DOI 10.1007/978-3-319-53123-6_11

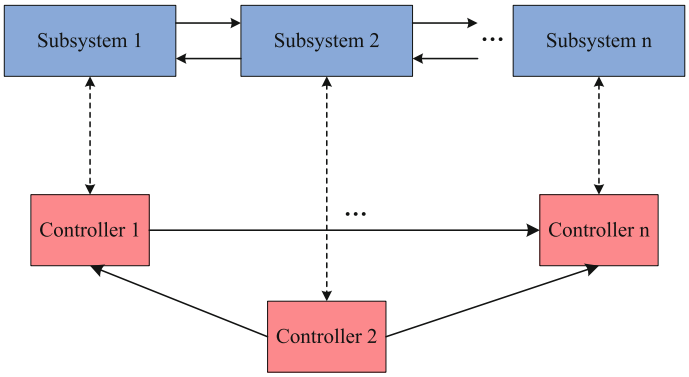

Fig. 11.1 The structure of distributed control systems

from sensor j. On the other hand, $a_{ij} = 0$ if controller i can not receive information from controller j, which may be out of communication range or the j-th controller does not transmit information. Moreover, we assume $a_{ii} = 1$ for all $i \in \upsilon$. The set of neighbors of node $i \in \upsilon$ plus the node itself are denoted by $N_i = \{j \in \upsilon : (i, j) \in \upsilon\}$. $\mathbb{A} = [a_{ij}]$ is a square matrix representing the topology of the controller network.

The plant to be controlled is represented by the following discrete-time large-scale systems:

$$\begin{cases} x_i(k+1) = A_{ii}x_i(k) + \sum\limits_{j=1, j\neq i}^{n} A_{ij}x_j(k) + B_i u_i(k) + E_i v_i(k), \\ z_i(k) = L_i x_i(k), \end{cases} \tag{11.1}$$

where $x_i(k) \in \mathbb{R}^{n_i}$ is the system state, $z_i(k) \in \mathbb{R}^{m_i}$ is the performance output vector, $u_i(k) \in \mathbb{R}^{p_i}$ is the control input vector and $v_i(k) \in \mathbb{R}^{q_i}$ is the unknown disturbance belonging to $l_2[0, \infty)$. A_{ij} is the couplings of the j-th subsystem onto i-th subsystem. A_{ij}, B_i, E_i and L_i are known matrices with appropriate dimensions.

Remark 11.1 The analysis and synthesis of the above large-scale system (11.1) has been widely studied in the literature. Specifically, the above large-scale system has been used to model various practical plants, such as process network [1] and inverted pendulum system [2]. But so far, no results have been reported on the distributed non-fragile control problem.

Due to the implementation uncertainties in the controller and the occurrence of controller failure, we design the following controllers:

$$u_i(k) = \sum_{j \in N_i} \alpha_i(k) a_{ij}(K_{ij} + \Delta K_{ij}) x_j(k), \tag{11.2}$$

where the stochastic variables, $\alpha_i(k) \in \{0, 1\}$ are introduced to model the random controller failures. In this chapter, the probabilities, $\Pr ob\{\alpha_i(k) = 1\} = \bar{\alpha}_i$, are

assumed to be available for our controller design, and $\Pr ob\{\alpha_i(k) = 0\} = 1 - \bar{\alpha}_i$ is known as the failure rate of the i-th controller. K_{ij} is the controller gains to be determined. The controller gain variations are assumed to be $\Delta K_{ij} = M_{ij}\Delta_{ij}(k)N_{ij}$, where $\|\Delta_{ij}(k)\| \leq \delta_{ij}$ are the upper bounds of the variation. M_{ij} and N_{ij} are some constant matrices with appropriate dimensions.

The topology of controller network may not be the same as the plant network due to the fact that the controllers are communicating with each other via the networked communication. The controller network is a sparse network, which will bring us many difficulties on modeling of the closed-loop system. Specifically, when the random controller failure problem is taken into account, the problem is more complicated since the controller gains will be coupled with random variables and multiple uncertainties. In order to model the closed-loop system, we define the following notations:

$$
\begin{aligned}
&x(k) = \begin{bmatrix} x_1^T & \cdots & x_n^T \end{bmatrix}^T, z(k) = \begin{bmatrix} z_1^T & \cdots & z_n^T \end{bmatrix}^T,\\
&u(k) = \begin{bmatrix} u_1^T & \cdots & u_n^T \end{bmatrix}^T, v(k) = \begin{bmatrix} v_1^T & \cdots & v_n^T \end{bmatrix}^T,\\
&K = \begin{bmatrix} a_{11}K_{11} & \cdots & a_{1n}K_{1n} \\ \vdots & \ddots & \vdots \\ a_{n1}K_{N1} & \cdots & a_{nn}K_{nn} \end{bmatrix}, A = \begin{bmatrix} A_{11} & \cdots & A_{1n} \\ \vdots & \ddots & \vdots \\ A_{n1} & \cdots & A_{nn} \end{bmatrix}, \bar{N} = \begin{bmatrix} N_1 \\ \vdots \\ N_n \end{bmatrix},\\
&B = \operatorname{diag}\{B_1, \ldots, B_n\}, E = \operatorname{diag}\{E_1, \ldots, E_n\}, L = \operatorname{diag}\{L_1, \ldots, L_n\},\\
&\bar{\Pi} = \operatorname{diag}\{\bar{\alpha}_1 I, \ldots, \bar{\alpha}_n I\}, \Phi_i = \operatorname{diag}\{\rho(i-1)I, \ldots, \rho(i-n)I\},\\
&M_\alpha = \begin{bmatrix} \alpha_1\Phi_1 M & \cdots & \alpha_n\Phi_n M \end{bmatrix}, \Delta(k) = \operatorname{diag}\{\Delta_1(k), \ldots, \Delta_n(k)\},\\
&\bar{M}_i = \operatorname{diag}\{\rho(i-1)\Phi_1 M, \ldots, \rho(i-n)\Phi_n M\}, \Lambda = \operatorname{diag}\{\delta_1, \ldots, \delta_n\},
\end{aligned}
$$

with

$$
\begin{aligned}
&N_i = \operatorname{diag}\{N_{i1}, \ldots, N_{in}\}, \Delta_i(k) = \operatorname{diag}\{\Delta_{i1}(k), \ldots, \Delta_{in}(k)\},\\
&\delta_i = \operatorname{diag}\{\delta_{i1}I, \ldots, \delta_{in}I\}.
\end{aligned}
$$

where $\rho(i)$ is the Kreonecker function. Therefore, we have the following closed-loop system,

$$
\begin{cases}
x(k+1) = \left[A + B(\bar{\Pi}K + M_\alpha\Delta(k)\bar{N})\right]x(k) + Ev(k) \\
\qquad\quad + \sum_{i=1}^{n}(\alpha_i(k) - \bar{\alpha}_i)\left[B(\Phi_i K + \bar{M}_i\Delta(k)\bar{N})x(k)\right], \\
z(k) = Lx(k),
\end{cases}
\tag{11.3}
$$

The control problem is formulated as follows: design the controller in form of (11.2) such that the closed-loop system (11.3) is asymptotically stable in the mean-square sense and achieves a prescribed H_∞ performance level in the presence of controller gain variation and random controller failure. We need the following definition in the subsequent analysis and development.

Definition 11.1 For a given scalar $\gamma > 0$, the system (11.3) is said to be asymptotically stable in the mean-square sense and achieves a prescribed H_∞ performance

γ, if it is asymptotically stable, and under zero initial condition, $\sum_{s=0}^{+\infty} \mathbb{E}\{z^T(s)z(s)\} \leq \sum_{s=0}^{+\infty} \gamma^2 v^T(s)v(s)$ holds for all nonzero $v(k) \in l_2[0, \infty)$.

11.3 Main Results

In this section, a sufficient condition is firstly established such that the closed-loop system (11.3) is asymptotically stable in the mean-square sense with a prescribed H_∞ performance level.

Theorem 11.1 *For given scalars δ_{ij}, $\bar{\alpha}_i > 0$, $\gamma > 0$ and the controller gain K, if there exist a positive definite matrix $P > 0$ and a positive scalar $\varepsilon > 0$ such that the following inequality,*

$$\begin{bmatrix} \Xi & \Omega_1 & \Omega_2 & \Omega_3 & \varepsilon\Omega_4 & 0 \\ * & -P^{-1} & 0 & 0 & 0 & BM_\alpha \\ * & * & -I & 0 & 0 & 0 \\ * & * & * & -\bar{P} & 0 & \Omega_5 \\ * & * & * & * & -\varepsilon I & 0 \\ * & * & * & * & * & -\varepsilon I \end{bmatrix} < 0, \tag{11.4}$$

holds, then the closed-loop system (11.3) is asymptotically stable in the mean-square sense and achieves a prescribed H_∞ performance level γ, where

$$\begin{aligned} &\Xi = \begin{bmatrix} -P & 0 \\ 0 & -\gamma^2 I \end{bmatrix}, \Omega_1 = \begin{bmatrix} A + B\bar{\Pi}K & E \end{bmatrix}^T, \\ &\Omega_2 = \begin{bmatrix} L & 0 \end{bmatrix}^T, \Omega_3 = \begin{bmatrix} \Omega_{31} & \cdots & \Omega_{3n} \end{bmatrix}, \\ &\Omega_4 = \begin{bmatrix} \Lambda\bar{N} & 0 \end{bmatrix}^T, \Omega_5 = \begin{bmatrix} \Omega_{51}^T & \cdots & \Omega_{5n}^T \end{bmatrix}^T, \\ &\bar{P} = \mathrm{diag}\{-P^{-1}, \ldots, -P^{-1}\}, \theta_i = \sqrt{\bar{\alpha}_i(1-\bar{\alpha}_i)}, \end{aligned}$$

with

$$\Omega_{3i} = \begin{bmatrix} \theta_i B\Phi_i K & 0 \end{bmatrix}^T, \Omega_{5i} = \theta_i B\bar{M}_i.$$

Proof We construct the following Lyapunov functional:

$$V(k) = x^T(k)Px(k). \tag{11.5}$$

Then, one sees

$$
\begin{aligned}
&\mathbb{E}\left\{V(k+1)-V(k)+z^T(k)z(k)-\gamma^2 v^T(k)v(k)\right\}\\
&=\mathbb{E}\left\{x^T(k+1)Px(k+1)-x^T(k)Px(k)+z^T(k)z(k)-\gamma^2 v^T(k)v(k)\right\}\\
&=\left\{\left[A+B(\bar{\Pi}K+M_\alpha\Delta(k)\bar{N})\right]x(k)+Ev(k)\right\}^T\\
&\quad\times P\left\{\left[A+B(\bar{\Pi}K+M_\alpha\Delta(k)\bar{N})\right]x(k)+Ev(k)\right\}\\
&+\sum_{i=1}^{N}\theta_i^2\left[B(\Phi_i K+\bar{M}_i\Delta(k)\bar{N})x(k)\right]^T P\left[B(\Phi_i K+\bar{M}_i\Delta(k)\bar{N})x(k)\right]\\
&-x^T(k)Px(k)+[Lx(k)]^T[Lx(k)]-\gamma^2 v^T(k)v(k)\\
&=\eta^T(k)\left(\Xi+\bar{\Omega}_1^T\bar{\Omega}_1+\bar{\Omega}_2^T\bar{\Omega}_2+\sum_{i=1}^{n}\bar{\Omega}_{3i}^T\bar{\Omega}_{3i}\right)\eta(k),
\end{aligned}
\tag{11.6}
$$

where

$$
\begin{aligned}
&\eta(k)=\left[x^T(k)\ v^T(k)\right]^T,\ \bar{\Omega}_1=\left[A+B(\bar{\Pi}K+M_\alpha\Delta(k)\bar{N})\ E\right],\\
&\bar{\Omega}_{3i}=\left[B(\Phi_i K+\bar{M}_i\Delta(k)\bar{N})\ 0\right].
\end{aligned}
$$

It is seen $\Xi+\bar{\Omega}_1^T P\bar{\Omega}_1+\Omega_2^T\Omega_2+\sum_{i=1}^{n}\bar{\Omega}_{3i}^T\bar{\Omega}_{3i}<0$ is equivalent to

$$
\begin{aligned}
&\begin{bmatrix}\Xi & \Omega_1 & \Omega_2 & \Omega_3\\ * & -P^{-1} & 0 & 0\\ * & * & -I & 0\\ * & * & * & -\bar{P}\end{bmatrix}+\begin{bmatrix}\Omega_4\\0\\0\\0\end{bmatrix}\frac{\Delta(k)}{\Lambda}\begin{bmatrix}0\\BM_\alpha\\0\\\Omega_5\end{bmatrix}^T\\
&\quad+\begin{bmatrix}0\\BM_\alpha\\0\\\Omega_5\end{bmatrix}\frac{\Delta(k)}{\Lambda}\begin{bmatrix}\Omega_4\\0\\0\\0\end{bmatrix}^T<0
\end{aligned}
\tag{11.7}
$$

It follows from Lemma 2.2 that (11.7) holds if and only if there exists a positive scalar $\varepsilon>0$ such that

$$
\begin{bmatrix}\Xi & \Omega_1 & \Omega_2 & \Omega_3\\ * & -P^{-1} & 0 & 0\\ * & * & -I & 0\\ * & * & * & -\bar{P}\end{bmatrix}+\varepsilon\begin{bmatrix}\Omega_4\\0\\0\\0\end{bmatrix}\begin{bmatrix}\Omega_4\\0\\0\\0\end{bmatrix}^T+\varepsilon^{-1}\begin{bmatrix}0\\BM_\alpha\\0\\\Omega_5\end{bmatrix}\begin{bmatrix}0\\BM_\alpha\\0\\\Omega_5\end{bmatrix}^T<0.
\tag{11.8}
$$

By using the Lemma 2.2, (11.8) is equivalent to (11.4). Then, we have

$$
\mathbb{E}\left\{V(k+1)-V(k)+z^T(k)z(k)-\gamma^2 v^T(k)v(k)\right\}<0.
\tag{11.9}
$$

It follows from Chap. 2, the system (11.3) is asymptotically stable in the mean-square sense and achieves a prescribed H_∞ performance level γ. This completes the proof.

Remark 11.2 It is noted that the uncertain bounds on the gain variation have been included in the above theorem. One may establish the relation between these gain variation bounds and the control performance, e.g., the H_∞ performance level.

Due to the co-existence of P and P^{-1}, we can not obtain the controller gain directly from Theorem 11.1. The controller design is given in the following theorem.

Theorem 11.2 *For given scalars δ_{ij}, $\bar{\alpha}_i > 0$ and $\gamma > 0$, if there exist a diagonal matrix Q and a positive scalar $\bar{\varepsilon} > 0$ such that the following inequality,*

$$\begin{bmatrix} \tilde{\Xi} & \tilde{\Omega}_1 & \tilde{\Omega}_2 & \tilde{\Omega}_3 & \tilde{\Omega}_4 & 0 \\ * & -Q & 0 & 0 & 0 & BM_\alpha\bar{\varepsilon} \\ * & * & -I & 0 & 0 & 0 \\ * & * & * & -\bar{Q} & 0 & \tilde{\Omega}_5 \\ * & * & * & * & -\bar{\varepsilon}I & 0 \\ * & * & * & * & * & -\bar{\varepsilon}I \end{bmatrix} < 0, \tag{11.10}$$

holds, then the closed-loop system (11.3) is asymptotically stable in the mean-square sense and achieves a prescribed H_∞ performance level γ. Moreover the controller gain is determined by $K = \bar{K}Q^{-1}$, where,

$$\begin{aligned} &\tilde{\Xi} = \begin{bmatrix} -Q & 0 \\ 0 & -\gamma^2 I \end{bmatrix}, \tilde{\Omega}_1 = \begin{bmatrix} AQ + B\bar{\Pi}\bar{K} & E \end{bmatrix}^T, \\ &\tilde{\Omega}_2 = \begin{bmatrix} LQ & 0 \end{bmatrix}^T, \tilde{\Omega}_3 = \begin{bmatrix} \tilde{\Omega}_{31} & \cdots & \tilde{\Omega}_{3N} \end{bmatrix}, \\ &\tilde{\Omega}_4 = \begin{bmatrix} \Lambda\bar{N}Q & 0 \end{bmatrix}^T, \tilde{\Omega}_5 = \begin{bmatrix} \tilde{\Omega}_{51}^T & \cdots & \tilde{\Omega}_{5n}^T \end{bmatrix}^T, \\ &\bar{Q} = \mathrm{diag}\{-Q, \ldots, -Q\}, \end{aligned}$$

with

$$\tilde{\Omega}_{3i} = \begin{bmatrix} \theta_i B\Phi_i\bar{K} & 0 \end{bmatrix}^T, \tilde{\Omega}_{5i} = \theta_i\bar{\varepsilon}B\bar{M}_i.$$

Proof By left- and right-multiplying (11.4) by $\mathrm{diag}\{P^{-1}, I, I, I, \underbrace{I, \ldots, I}_{n},\}$ $\{\varepsilon^{-1}I, \varepsilon^{-1}I\}$ and its transpose, (11.4) becomes

$$\begin{bmatrix} \hat{\Xi} & \hat{\Omega}_1 & \hat{\Omega}_2 & \hat{\Omega}_3 & \hat{\Omega}_4 & 0 \\ * & -Q & 0 & 0 & 0 & BM_\alpha\varepsilon^{-1} \\ * & * & -I & 0 & 0 & 0 \\ * & * & * & -\hat{Q} & 0 & \tilde{\Omega}_5\varepsilon^{-1} \\ * & * & * & * & -\varepsilon^{-1}I & 0 \\ * & * & * & * & * & -\varepsilon^{-1}I \end{bmatrix} < 0, \tag{11.11}$$

where

$$\hat{\Xi} = \begin{bmatrix} -P^{-1} & 0 \\ 0 & -\gamma^2 I \end{bmatrix}, \hat{\Omega}_1 = \begin{bmatrix} AP^{-1} + B\bar{\Pi}KP^{-1} & E \end{bmatrix}^T,$$
$$\hat{\Omega}_2 = \begin{bmatrix} LP^{-1} & 0 \end{bmatrix}^T, \hat{\Omega}_3 = \begin{bmatrix} \hat{\Omega}_{31} & \cdots & \hat{\Omega}_{3n} \end{bmatrix},$$
$$\hat{\Omega}_4 = \begin{bmatrix} \Lambda\bar{N}P^{-1} & 0 \end{bmatrix}^T,$$
$$\hat{Q} = \text{diag}\{-P^{-1}, \ldots, -P^{-1}\},$$

with

$$\hat{\Omega}_{3i} = \begin{bmatrix} \theta_i B\Phi_i K P^{-1} & 0 \end{bmatrix}^T.$$

Let P be a diagonal matrix, $Q = P^{-1}$, $\bar{K} = KP^{-1}$, and $\bar{\varepsilon} = \varepsilon^{-1}$. One sees that (11.11) is the same as (11.10), which indicates that the closed-loop system is asymptotically stable in the mean-square sense and achieves a prescribed H_∞ performance level under the controller (11.2). The proof is completed.

Remark 11.3 A diagonal matrix Q is introduced to obtain the control gain parameters due to the sparse restriction on the controller gain K. The similar method has been recently used in [3], where the distributed filtering in sensor networks with missing measurement was studied. Such a choice may introduce some design conservatism. An alternative algorithm is to use the well-known cone complementarity linearization algorithm (CCL) method in [4]. Nevertheless, the CCL method needs a lot of iterations, which may not be easy to be applied to a system with large dimensions.

Remark 11.4 In Theorem 11.2, the existence condition for the controllers are given in terms of LMIs which is convex in the scalar γ^2. Therefore, one may solve the following optimization problem:

$$\begin{aligned} &\min \rho, \\ &\text{s.t. (11.10)} \quad \text{with} \quad \rho = \gamma^2. \end{aligned} \tag{11.12}$$

to obtain the controller gain parameters such that the H_∞ disturbance attenuation level is minimized. When the optimal ρ is obtained from the above optimization problem, the designed controllers guarantee that the closed-loop system is asymptotically stable and achieves a prescribed H_∞ performance level ρ.

11.4 An Illustrative Example

In this section, a large-scale system with two identical inverted pendulums is given to verify the effectiveness of our results. The inverted pendulums are coupled by springs and subject to two distinct inputs. The structure is seen in Fig. 11.2.

The position, a, of the spring can be changed along the full length l, of the pendulums. The objective is to design two distributed controllers for the individual masses, m. Two controllers are sharing their local measurement with each other, i.e., $a_{ij} = 1$ for all $i, j = 1, 2$. Let k and g denote the spring constant and gravity

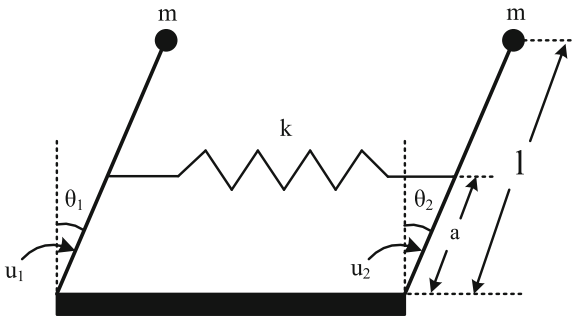

Fig. 11.2 The interconnected inverted pendulum system

acceleration, respectively. Then the motion equation for the i-th inverted pendulum is given in [2] by

$$\dot{x}_i(t) = \begin{bmatrix} 0 & l \\ \frac{g}{l} - \frac{2ka^2}{ml^2} & 0 \end{bmatrix} x_i(t) + \begin{bmatrix} 0 \\ \frac{1}{ml^2} \end{bmatrix} u_i(t) + \sum_{j=1, j\neq i}^{2} \begin{bmatrix} 0 & 0 \\ \frac{ka^2}{ml^2} & 0 \end{bmatrix} x_j(t), \quad (11.13)$$

where $x_i(t) = \begin{bmatrix} \theta_i(t) & \dot{\theta}_i(t) \end{bmatrix}^T$.

We set $k = 1, l = 1, m = 1$ and $a = 0.1$. For the sampling period of $T = 0.02s$, the following discrete-time model is obtained:

$$x_i(k+1) = \begin{bmatrix} 1.002 & 0.02 \\ 0.1957 & 1.002 \end{bmatrix} x_i(k) + \begin{bmatrix} 0.0002 \\ 0.02 \end{bmatrix} u_i(k) + \sum_{j=1, j\neq i}^{2} \begin{bmatrix} 0 & 0 \\ 0.002 & 0 \end{bmatrix} x_j(k). \quad (11.14)$$

For the disturbance on the inverted pendulum, we assume that the disturbance weighting matrices are $E_1 = E_2 = \begin{bmatrix} 0.1 & 0.2 \end{bmatrix}$, and disturbance signals are given by

$$v_i(k) = \begin{cases} rand, & 1 \leq k \leq 20, \\ 0, & 20 < k \leq 200. \end{cases} \quad (11.15)$$

where $rand$ is a random function generating a value between [0, 1]. It follows from Fig. 11.3 that the inverted pendulum system is open-loop unstable as the state diverges from the equilibrium point. Before the controller design, the performance related matrices are taken as $L_1 = L_2 = \begin{bmatrix} 0.5 & 0.5 \end{bmatrix}$. The gain variation related matrices are assumed to be

$$\begin{aligned} &M_{11} = 0.1, M_{12} = 0.1, M_{21} = 0.05, M_{22} = 0.08, \\ &N_{11} = \begin{bmatrix} 0.1 & 0.1 \end{bmatrix}, N_{12} = \begin{bmatrix} 0.1 & 0.03 \end{bmatrix}, \\ &N_{21} = \begin{bmatrix} 0.1 & -0.1 \end{bmatrix}, N_{22} = \begin{bmatrix} 0.05 & 0.1 \end{bmatrix}, \\ &\Delta_{ij}(k) = rand, i, j = 1, 2. \end{aligned}$$

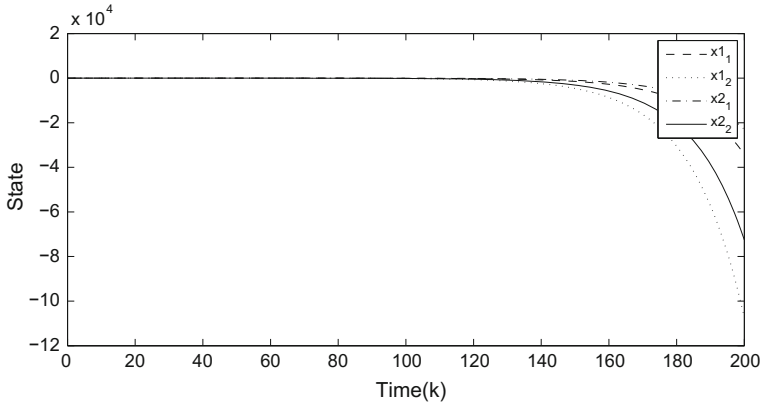

Fig. 11.3 The state trajectories of open-loop system

It follows from the above assumptions, the uncertain bounds on the controller gain variation are $\delta_{ij} = 1, i, j = 1, 2$. Suppos that the controller failure probabilities are 20 and 10%, respectively, i.e., $\bar{\alpha}_1 = 0.8$, and $\bar{\alpha}_2 = 0.9$. Then, by solving the optimization problem (11.12), we have $\gamma^* = 0.3279$, and the controller gain is

$$K = \begin{bmatrix} -69.2272 & -53.7477 & -0.1993 & -0.0020 \\ -0.1720 & -0.0033 & -62.4480 & -51.8637 \end{bmatrix}.$$

Under the zero initial condition, the state-trajectories of closed-loop system are depicted in Fig. 11.4. It is seen that states tend to zero, which means that the closed-loop system is asymptotically stable. To verify the H_∞ performance level, we depict the performance output signals in Fig. 11.5. It is seen that the controlled performance state tends to zero when the disturbance signal disappear. We compute $\gamma = \sqrt{\frac{\sum_{s=0}^{200} z^T(s)z(s)}{\sum_{s=0}^{200} v^T(s)v(s)}} = 0.1631$. 100 samples on the true performance level are shown in Fig. 11.6. The minimal performance level is 0.13, and the maximal performance level is 0.24, which is smaller than the optimal one. We thus conclude that our controller design algorithm is effective.

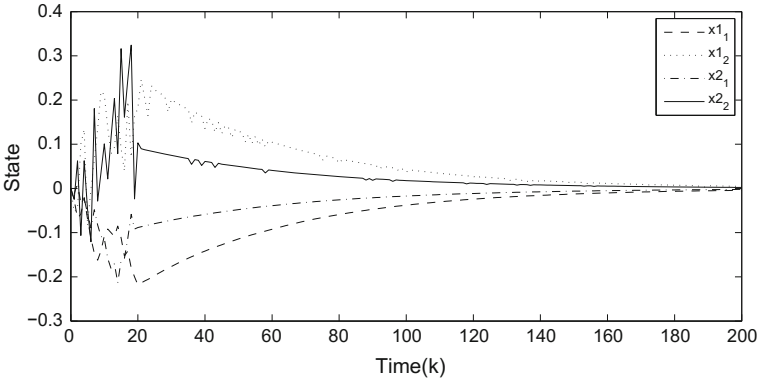

Fig. 11.4 The state trajectories of closed-loop system

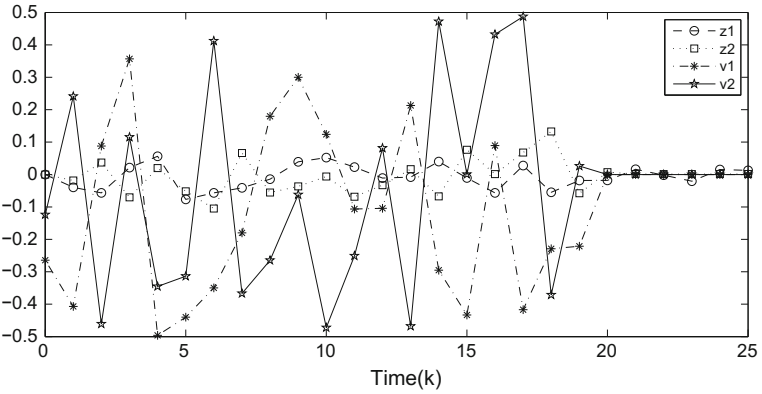

Fig. 11.5 The trajectories of performance output signal and disturbance

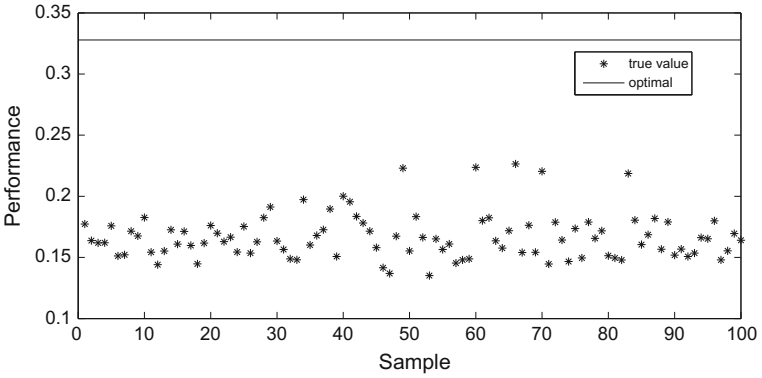

Fig. 11.6 100 samples on the performance level γ

11.5 Conclusions

We have investigated the non-fragile distributed stabilization of large-scale systems with random controller failure. The additive gain variation and the random controller failure are simultaneously considered in the controller design. Based on the Lyapunov stability theory and the stochastic system approach, a sufficient condition has been obtained such that the closed-loop system is asymptotically stable in the mean-square sense and guarantees a prescribed H_∞ disturbance attenuation level. Finally, a simulation study has been given to show the effectiveness of the new design method. In the next chapter, the energy constraint problem will be addressed.

References

1. J.H. Park, On design of dynamic output feedback controller for GCS of large-scale systems with delays in interconnections: LMI optimization approach. Appl. Math. Comput. **161**(2), 423–432 (2005)
2. Y. Wang, L. Xie, C. de. Souza, Robust decentralized control of interconnected uncertain linear systems, in *In Porceeding of the 34th Conference on Decision and Control* (New Orleans, LA, 1995), pp. 2653–2658
3. B. Shen, Z. Wang, Y.S. Hung, Distributed H_∞ consensus filtering in sensor networks with multiple missing measurements: the finite horizon case. Automatica **46**(10), 1682–1688 (2010)
4. L.E. Ghaoui, F. Oustry, M. AitRami, A cone complementarity linearization algorithm for static output-feedback and related problems. IEEE Trans. Autom. Control **42**(8), 1171–1176 (1997)

Chapter 12
Distributed Control with Measurement Size Reduction and Random Fault

12.1 Introduction

This chapter is concerned with the design of energy-efficient and reliable distributed controllers for a class of nonlinear large-scale systems. Techniques such as reducing the packet size and the communication times are used to save the energy consumption of the sensors, and thereby extend the lifetime of the networks. The signal quantization technique is used to reduce the transmitted packet size, and a communication sequence is introduced to reduce the communication times. A set of stochastic variables are employed to model the random sensor failure phenomenon. Based on the switched system theory and the Lyapunov stability technique, a sufficient condition is proposed such that the closed-loop system is exponentially stable in the mean-square sense and achieves a prescribed H_∞ disturbance attenuation level. The controller gain design algorithm is presented by resorting to the cone complementarity linearization (CCL) method. A numerical example is finally given to show the effectiveness of the proposed design.

12.2 Problem Formulation

The system under consideration is shown in Fig. 12.1, where each sensor is able to communicate with its neighbouring ones via wireless communication. In this chapter, each sensor is equipped with a *measuring* unit, a *quantization* unit, a *processing* unit and a *communication* unit. The sensor network acts as a control network.

The plant to be controlled is represented by the following discrete-time nonlinear large-scale system:

D. Zhang et al., *Filtering and Control of Wireless Networked Systems*,
Studies in Systems, Decision and Control 97, DOI 10.1007/978-3-319-53123-6_12

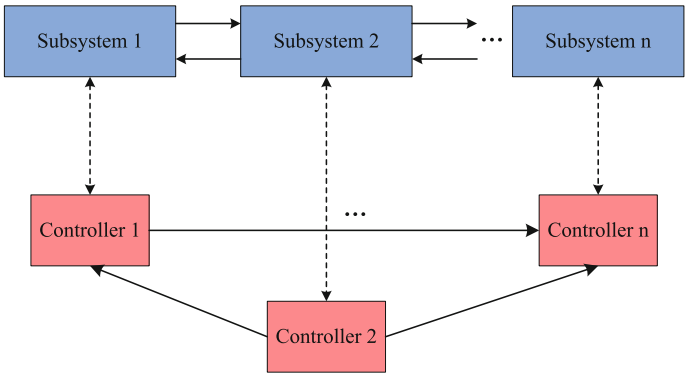

Fig. 12.1 The sensor-network-based control system

$$\begin{cases} x_i(k+1) = A_{ii}x_i(k) + W_{0i}g(x_i(k)) + W_{1i}g(x_i(k-d_i(k))) \\ \qquad\quad + \sum\limits_{j=1,j\neq i}^{N} A_{ij}x_j(k) + B_i u_i(k) + E_i v_i(k), \\ z_i(k) = L_i x_i(k), \\ x_i(s) = \psi_i(s), \quad s = -d_{2i}, \ldots, 0, \end{cases} \tag{12.1}$$

where $x_i(k) \in \mathbb{R}^{n_i}$ is the state vector, $u_i(k) \in \mathbb{R}^{p_i}$ is the control input vector, and $v_i(k) \in \mathbb{R}^{q_i}$ is the unknown disturbance, belonging to $l_2[0,\infty)$. $g(x_i(k))$ is the nonlinear perturbation on the i-th subsystem and is assumed to satisfy $\|g(x_i(k))\| \leq \|Ux_i(k)\|$ with a known matrix U. It is seen that the matrix U represents the bound of the nonlinear perturbation. $\psi_i(s)$ is the initial condition. $z_i(k) \in \mathbb{R}^{m_i}$ is the performance output vector. A_{ij}, $j \neq i$, is the couplings of the j-th subsystem onto i-th subsystem. $d_i(k)$ is the time-varying delay and it is assumed to be bounded by $d_{1i} \leq d_i(k) \leq d_{2i}$, where d_{1i} and d_{2i} are some positive scalars. A_{ii}, A_{ij}, W_{0i}, W_{1i}, B_i, E_i and L_i are known matrices with appropriate dimensions.

In order to reduce the communication between the local sensors, the local measurement signal is quantized and scheduled before transmission to other sensors. In this scenario, less information is transmitted but the topology of sensor network becomes time-varying. We now use the following controller:

$$u_i(k) = \sum_{j=1}^{N} a_{ij}^{\sigma(k)} K_{ij}^{\sigma(k)} \alpha_j(k) Q_j(x_j(k)), \tag{12.2}$$

where $Q_i(\bullet)$ is the i-th quantizer with the quantization density $0 < \rho_i < 1$ and it is assumed to be symmetric and time-invariant, i.e., $Q_i(-\tau_i) = -Q_i(-\tau_i)$. For any $i, i = 1, 2, \ldots, N$, the set of quantization levels are described as

$$\begin{aligned} U_i = &\left\{\pm\kappa_i^s, \kappa_i^s = \rho_i^s\kappa_i^0, s = \pm1, \pm2, \ldots\right\} \\ &\cup \left\{\pm\kappa_i^0\right\} \cup \{0\}, 0 < \rho_i < 1, \kappa_i^0 > 0. \end{aligned} \tag{12.3}$$

The quantized output $Q_i(\bullet)$ is given by

$$Q_i(\tau_i) = \begin{cases} \kappa_i^s, & \text{if } \frac{1}{1+\delta_i}\kappa_i^s < \tau_i \leq \frac{1}{1-\delta_i}\kappa_i^s, \tau_i > 0, \\ 0, & \text{if } \tau_i = 0, \\ -Q_i(-\tau_i), & \text{if } \tau_i < 0, \end{cases} \tag{12.4}$$

where $\delta_i = \frac{1-\rho_i}{1+\rho_i} < 1$. Define the quantization error

$$e_i = Q_i(\tau_i) - \tau_i = \Delta_i(k)\tau_i, \tag{12.5}$$

the signal after quantization can be described as

$$\tilde{x}_i(k) = (I + \Delta_i(k))x_i(k), \tag{12.6}$$

where $\|\Delta_i(k)\| \leq \delta_i I$. The stochastic variables $\alpha_i(k) \in \{0, 1\}$, are introduced to model the random sensor failures, with $\alpha_i(k) = 1$ if a sensor is working normally, $\alpha_i(k) = 0$, otherwise. In this chapter, $\Pr ob\{\alpha_i(k) = 1\} = \mathbb{E}\{\alpha_i(k)\} = \bar{\alpha}_i$ is assumed to be known. The scalar $a_{ij}^{\sigma(k)}$, $j \neq i$ is the interconnection of the sensors, which is different from that of the plant networks, where $a_{ij}^{\sigma(k)} = 1$, if i-th sensor receives information from the j-th subsystem, whereas $a_{ij}^{\sigma(k)} = 0$ if the i-th sensor cannot receive information from the j-th subsystem. Suppose we have M scheduled communication sequences, then $\sigma(k) \in \Gamma = \{1, 2, \ldots, M\}$, and it is viewed as a switching signal. Clearly, different topologies represent different energy consumption. $K_{ij}^{\sigma(k)}$ is the controller gains in the i-th subsystem under the switching signal $\sigma(k)$, which will be determined later.

Remark 12.1 Unlike the fixed topology assumptions that were made on the distributed control of large-scale systems in [2–6], the topologies of the sensor network here are dynamical, which provides a tradeoff between the energy consumption and control performance. In order to achieve this, one may design two topologies, one is for the energy-efficiency, e.g., local sensor does not communicate with the neighbouring ones, while the other one is for the control performance improvement, i.e., local sensor communicates with the neighbouring ones in a fully connected manner. It is interesting to see that the controller design is completely different from the existing decentralized and distributed frameworks. Here, we have built a bridge between the decentralized control methodology and the distributed one.

Due to the couplings of the system state variables and also the couplings of local controllers, we define the following notations for easy presentation:

$$x(k) = \left[x_1^T \cdots x_N^T \right]^T, z(k) = \left[z_1^T \cdots z_N^T \right]^T, \ u(k) = \left[u_1^T \cdots u_N^T \right]^T,$$
$$v(k) = \left[v_1^T \cdots v_N^T \right]^T, \ g(x(k)) = \left[g^T(x_1(k)) \cdots g^T(x_N(k)) \right]^T,$$
$$g(x(k - d(k))) = \left[g^T(x_1(k - d_1(k))) \cdots g^T(x_N(k - d_N(k))) \right]^T,$$

$$K_{\sigma(k)} = \begin{bmatrix} a_{11}^{\sigma(k)} K_{11}^{\sigma(k)} & \cdots & a_{1N}^{\sigma(k)} K_{1N}^{\sigma(k)} \\ \vdots & \ddots & \vdots \\ a_{N1}^{\sigma(k)} K_{N1}^{\sigma(k)} & \cdots & a_{NN}^{\sigma(k)} K_{NN}^{\sigma(k)} \end{bmatrix}, \ A = \begin{bmatrix} A_{11} & \cdots & A_{1N} \\ \vdots & \ddots & \vdots \\ A_{N1} & \cdots & A_{NN} \end{bmatrix},$$
$W_0 = \text{diag}\{W_{01}, \ldots, W_{0N}\}$, $W_1 = \text{diag}\{W_{11}, \ldots, W_{1N}\}$,
$B = \text{diag}\{B_1, \ldots, B_N\}$, $E = \text{diag}\{E_1, \ldots, E_N\}$,
$L = \text{diag}\{L_1, \ldots, L_N\}$, $\bar{U} = \text{diag}\{U, \ldots, U\}$, $\bar{\Pi} = \text{diag}\{\bar{\alpha}_1 I, \ldots, \bar{\alpha}_N I\}$,
$\Phi_i = \text{diag}\{\rho(i-1)I, \ldots, \rho(i-N)I\}$, $\Delta(k) = \text{diag}\{\Delta_1(k), \ldots, \Delta_N(k)\}$,
$\Lambda = \text{diag}\{\delta_1 I, \ldots, \delta_N I\}$, $d_1 = \min\{d_{1i}\}$, $d_2 = \max\{d_{2i}\}$.

where $\rho(i)$ is the Kreonecker function. With the above notations, we have the following closed-loop system,

$$\begin{cases} x(k+1) = \left[A + BK_{\sigma(k)}\bar{\Pi}(I + \Delta(k))\right] x(k) \\ \qquad + W_0 g(x(k)) + W_1 g(x(k - d(k))) + Ev(k) \\ \qquad + \sum_{i=1}^{N} (\alpha_i(k) - \bar{\alpha}_i) \left[BK_{\sigma(k)}\Phi_i(I + \Delta(k))x(k)\right], \\ z(k) = Lx(k), \end{cases} \tag{12.7}$$

where $d_1 \leq d(k) \leq d_2$. The System (12.5) is a switched system and the average dwell time approach is also be utilized to analyze the closed-loop system.

The distributed control problem in this chapter is formulated as follows: design a set of controllers in form of (12.2) such that the closed-loop system (12.5) is exponentially stable in the mean-square sense and achieves a prescribed H_∞ performance level in the presence of reduced communications and random sensor fault.

Definition 12.1 The closed-loop system (12.5) is said to be exponentially stable in the mean-square sense, if there exist some scalars $\pi > 0$ and $0 < \chi < 1$, such that the solution $x(k)$ of system (12.5) satisfies $\mathbb{E}\{\|x(k)\|\} < \pi\chi^{(k-k_0)} \sup_{k_0 - d_2 \leq s \leq k_0} \|\psi(s)\|$, $\forall k \geq k_0$.

Definition 12.2 For given scalars $\gamma > 0$, system (12.5) is said to be exponentially stable in the mean-square sense and achieves a prescribed H_∞ performance γ, if it is exponentially stable and under zero initial condition, $\sum_{s=0}^{+\infty} \mathbb{E}z^T(s)z(s)\} \leq \sum_{s=0}^{+\infty} \gamma^2 v^T(s)v(s)$ holds for all nonzero $v(k) \in l_2[0, \infty)$.

12.3 Main Results

Theorem 12.1 *For given scalars $\tau > 0$, $\mu > 1$, $0 < \lambda_l < 1$, $\bar{\alpha}_i > 0$ and $0 < \lambda < 1$, if there exist positive definite matrix $P_l > 0$, positive scalars $\varepsilon > 0$, $\beta_1 > 0$ and $\beta_2 > 0$ such that the following inequalities*

$$\begin{bmatrix} \Xi & \Omega_1^T & \Omega_2^T & \Omega_3 & \Omega_4^T & 0 \\ * & -P_l^{-1} & 0 & 0 & 0 & BK_l\bar{\Pi} \\ * & * & -I & 0 & 0 & 0 \\ * & * & * & -\bar{P}_l & 0 & \Omega_5^T \\ * & * & * & * & -\varepsilon I & 0 \\ * & * & * & * & * & -\varepsilon I \end{bmatrix} < 0, \tag{12.8}$$

$$P_l \le \mu P_v, l \ne v, \tag{12.9}$$

$$T_a > T_a^* = -\frac{\ln \mu}{\ln \lambda}, \tag{12.10}$$

hold for all $l, v \in \Gamma$*, then the closed-loop system* (12.5) *is exponentially stable in the mean-square sense and achieves a prescribed* H_∞ *performance level* $\gamma = \tau\sqrt{\frac{(1-\lambda_a)}{1-\lambda_b/\lambda}}$*, where*

$$\begin{aligned}
&\Xi = \Xi_{5\times 5}, \\
&\Omega_1 = \begin{bmatrix} A + BK_l\bar{\Pi} & 0 & W_0 & W_1 & E \end{bmatrix}, \\
&\Omega_2 = \begin{bmatrix} L & 0 & 0 & 0 & 0 \end{bmatrix}, \Omega_3 = \begin{bmatrix} \Omega_{31} & \cdots & \Omega_{3N} \end{bmatrix}, \\
&\Omega_4 = \begin{bmatrix} \Lambda\varepsilon & 0 & 0 & 0 & 0 \end{bmatrix}, \Omega_5 = \begin{bmatrix} \Omega_{51} & \cdots & \Omega_{5N} \end{bmatrix}, \\
&\bar{P}_l = \text{diag}\{P_l^{-1}, \ldots, P_l^{-1}\}, \theta_i = \sqrt{\bar{\alpha}_i(1-\bar{\alpha}_i)}, \\
&\lambda_a = \min_{l\in\Gamma}\{\lambda_l\}, \lambda_b = \max_{l\in\Gamma}\{\lambda_l\}, \lambda > \lambda_b, d_{12} = d_2 - d_1.
\end{aligned}$$

with

$$\begin{aligned}
&\Xi_{11} = -\lambda_l P_l + \beta_1 \bar{U}^T \bar{U} + (d_{12}+1)Q_l, \\
&\Xi_{22} = -\lambda_l^{d_2} Q_l + \beta_2 \bar{U}^T \bar{U}, \\
&\Xi_{33} = -\beta_1 I, \Xi_{44} = -\beta_2 I, \Xi_{55} = -\tau^2 I, \\
&\Omega_{3i} = \begin{bmatrix} \theta_i BK_l\Phi_i & 0 & 0 & 0 & 0 \end{bmatrix}^T, \Omega_{5i} = \theta_i (BK_l\Phi_i)^T.
\end{aligned}$$

Proof We construct the following Lyapunov functional for each $l \in \Gamma$:

$$V(k) = \sum_{i=1}^{3} V_i(k), \tag{12.11}$$

where

$$\begin{aligned}
V_1(k) &= x^T(k) P_l x(k), \\
V_2(k) &= \sum_{s=k-d(k)}^{k-1} x^T(s) \lambda_l^{k-s-1} Q_l x(s), \\
V_3(k) &= \sum_{t=k-d_2+1}^{k-d_1} \sum_{s=t}^{k-1} x^T(s) \lambda_l^{k-s-1} Q_l x(s).
\end{aligned}$$

Then, one has

$$
\begin{aligned}
&\mathbb{E}\{V_1(k+1)-\lambda_l V_1(k)\}\\
&=\mathbb{E}\left\{x^T(k+1)P_l x(k+1)-\lambda_l x^T(k)P_l x(k)\right\}\\
&=\left\{\begin{array}{l}\left[A+BK_l\bar{\Pi}(I+\Delta(k))\right]x(k)+W_0 g(x(k))\\ \quad +W_1 g(x(k-d(k)))+Ev(k)\end{array}\right\}^T P_l\\
&\quad\times\left\{\begin{array}{l}\left[A+BK_l\bar{\Pi}(I+\Delta(k))\right]x(k)+W_0 g(x(k))\\ \quad +W_1 g(x(k-d(k)))+Ev(k)\end{array}\right\}\\
&\quad+\sum_{i=1}^{N}\theta_i^2\left[BK_l\Phi_i(I+\Delta(k))x(k)\right]^T P_l\left[BK_l\Phi_i(I+\Delta(k))x(k)\right]\\
&\quad-\lambda_l x^T(k)P_l x(k)\\
&=\eta^T(k)\left(\bar{\Omega}_1^T P_l\bar{\Omega}_1+\sum_{i=1}^{N}\bar{\Omega}_{3i}^T\bar{\Omega}_{3i}\right)\eta(k)-\lambda_l x^T(k)P_l x(k),
\end{aligned}
\tag{12.12}
$$

where

$$
\begin{aligned}
\bar{\Omega}_1&=\left[A+BK_l\bar{\Pi}(I+\Delta(k))\ 0\ W_0\ W_1\ E\right],\\
\bar{\Omega}_{3i}&=\left[\theta_i BK_l\Phi_i(I+\Delta(k))\ 0\ 0\ 0\ 0\right],\\
\eta(k)&=\left[x^T(k)\ x^T(k-d(k))\ g^T(x(k))\right.\\
&\qquad\left.g^T(x(k-d(k)))\ v^T(k)\right]^T.
\end{aligned}
$$

In addition, we have

$$
\begin{aligned}
&\mathbb{E}\{V_2(k+1)-\lambda_l V_2(k)\}\\
&=\sum_{s=k-d(k+1)+1}^{k}x^T(s)\lambda_l^{k-s}Q_l x(s)-\sum_{s=k-d(k)}^{k-1}x^T(s)\lambda_l^{k-s}Q_l x(s)\\
&=x^T(k)Q_l x(k)-\lambda_l^{d(k)}x^T(k-d(k))Q_l x(k-d(k))\\
&\quad+\sum_{s=k-d(k+1)+1}^{k-1}x^T(s)\lambda_l^{k-s}Q_l x(s)-\sum_{s=k-d(k)+1}^{k-1}x^T(s)\lambda_l^{k-s}Q_l x(s)\\
&\le x^T(k)Q_l x(k)-x^T(k-d(k))\lambda_l^{d_2}x(k-d(k))\\
&\quad+\sum_{s=k-d(k+1)+1}^{k-d_1}x^T(s)\lambda_l^{k-s}Q_l x(s)+\sum_{s=k-d_1+1}^{k-1}x^T(s)\lambda_l^{k-s}Q_l x(s)\\
&\quad-\sum_{s=k-d(k)+1}^{k-1}x^T(s)\lambda_l^{k-s}Q_l x(s).
\end{aligned}
\tag{12.13}
$$

Note that

$$
\begin{aligned}
&\sum_{s=k-d(k+1)+1}^{k-d_1}x^T(s)\lambda_l^{k-s}Q_l x(s)+\sum_{s=k-d_1+1}^{k-1}x^T(s)\lambda_l^{k-s}Q_l x(s)\\
&\quad\le\sum_{s=k-d_2+1}^{k-d_1}x^T(s)\lambda_l^{k-s}Q_l x(s)+\sum_{s=k-d(k)+1}^{k-1}x^T(s)\lambda_l^{k-s}Q_l x(s).
\end{aligned}
\tag{12.14}
$$

Then, it follows that

$$\begin{aligned}&\mathbb{E}\{V_2(k+1)-\lambda_l V_2(k)\}\\&\quad\le x^T(k)Q_l x(k)-x^T(k-d(k))\lambda_l^{d_2}x(k-d(k))\\&\quad+\sum_{s=k-d_2+1}^{k-d_1}x^T(s)\lambda_l^{k-s}Q_l x(s).\end{aligned}\tag{12.15}$$

Furthermore, we see

$$\begin{aligned}&\mathbb{E}\{V_3(k+1)-\lambda_l V_3(k)\}\\&=\sum_{t=k-d_2+2}^{k-d_1+1}\sum_{s=t}^{k}x^T(s)\lambda_l^{k-s}Q_l x(s)-\sum_{t=k-d_2+1}^{k-d_1}\sum_{s=t}^{k-1}x^T(s)\lambda_l^{k-s}Q_l x(s)\\&=d_{12}x^T(k)Q_l x(k)-\sum_{s=k-d_2+1}^{k-d_1}x^T(s)\lambda_l^{k-s}Q_l x(s).\end{aligned}\tag{12.16}$$

According to the assumptions on the nonlinear function $g(x(k))$, the following inequalities are true for positive scalars $\beta_1>0$ and $\beta_2>0$:

$$\beta_1 x^T(k)\bar{U}^T\bar{U}x(k)-\beta_1 g^T(x(k))g(x(k))\ge 0,\tag{12.17}$$

$$\begin{aligned}&\beta_2 x^T(k-d(k))\bar{U}^T\bar{U}x(k-d(k))\\&\quad-\beta_2 g^T(x(k-d(k))g(x(k-d(k))\ge 0.\end{aligned}\tag{12.18}$$

It follows from the above analysis that

$$\begin{aligned}&\mathbb{E}\left\{V(k+1)-\lambda_l V(k)+z^T(k)z(k)-\tau^2 v^T(k)v(k)\right\}\\&\le\eta^T(k)\left[\Xi+\bar{\Omega}_1^T P_l\bar{\Omega}_1+\Omega_2^T\Omega_2+\sum_{i=1}^{N}\bar{\Omega}_{3i}^T\bar{\Omega}_{3i}\right]\eta(k).\end{aligned}\tag{12.19}$$

By some manipulation, it is seen that $\Xi+\bar{\Omega}_1^T P_l\bar{\Omega}_1+\Omega_2^T\Omega_2+\sum_{i=1}^{N}\bar{\Omega}_{3i}^T\bar{\Omega}_{3i}<0$ is equivalent to

$$\begin{aligned}&\begin{bmatrix}\Xi & \Omega_1^T & \Omega_2^T & \Omega_3\\ * & -P_l^{-1} & 0 & 0\\ * & * & -I & 0\\ * & * & * & -\bar{P}_l\end{bmatrix}+\begin{bmatrix}\bar{\Omega}_4^T\\0\\0\\0\end{bmatrix}\frac{\Delta(k)}{\Lambda}\begin{bmatrix}0\\BK_l\bar{\Pi}\\0\\\Omega_5\end{bmatrix}^T\\&+\begin{bmatrix}0\\BK_l\bar{\Pi}\\0\\\Omega_5\end{bmatrix}\frac{\Delta(k)}{\Lambda}\begin{bmatrix}\bar{\Omega}_4^T\\0\\0\\0\end{bmatrix}^T<0.\end{aligned}\tag{12.20}$$

By Lemma 2.2, it is seen that (12.18) holds if (12.8) holds. Then, we have

$$\mathbb{E}\left\{V_l(k+1)-\lambda_l V(k)+z^T(k)z(k)-\tau^2 v^T(k)v(k)\right\}<0.\tag{12.21}$$

For the switching time instant $k_0 < k_1 < \cdots < k_l < \cdots < k_s$, we define the switching numbers of $\sigma(k)$ over (k_0, k) as $N_\sigma(k_0, k)$. One has

$$\mathbb{E}\{V_l(k)\} \le \mathbb{E}\{\lambda_l^{k-k_l} V_l(k_l)\} - \sum_{s=k_l}^{k-1} \lambda_l^{k-s-1} \mathbb{E}\{\Upsilon(s)\}, \tag{12.22}$$

where $\Upsilon(k) = z^T(k)z(k) - \tau^2 v^T(k)v(k)$. It follows from (12.9) and (12.20) that

$$\begin{aligned}
&\mathbb{E}\{V_{\sigma(k_l)}(k)\} \\
&\le \lambda_{\sigma(k_l)}^{k-k_l} \mathbb{E}\{V_{\sigma(k_l)}(k_l)\} - \sum_{s=k_l}^{k-1} \lambda_{\sigma(k_l)}^{k-s-1} \mathbb{E}\{\Upsilon(s)\} \\
&\le \lambda_{\sigma(k_l)}^{k-k_l} \mu \mathbb{E}\{V_{\sigma(k_{l-1})}(k_l)\} - \sum_{s=k_l}^{k-1} \lambda_{\sigma(k_l)}^{k-s-1} \mathbb{E}\{\Upsilon(s)\} \\
&\le \lambda_{\sigma(k_l)}^{k-k_l} \mu \left[\lambda_{\sigma(k_{l-1})}^{k_l-k_{l-1}} \mathbb{E}\{V_{\sigma(k_{l-1})}(k_{l-1})\} - \sum_{s=k_{l-1}}^{k_l-1} \lambda_{\sigma(k_{l-1})}^{k-s-1} \mathbb{E}\{\Upsilon(s)\} \right] \\
&\quad - \sum_{s=k_l}^{k-1} \lambda_{\sigma(k_l)}^{k-s-1} \mathbb{E}\{\Upsilon(s)\} \\
&\le \cdots \le \mu^{N_\sigma(k_0,k)} \lambda_{\sigma(k_l)}^{k-k_l} \lambda_{\sigma(k_{l-1})}^{k_l-k_{l-1}} \cdots \lambda_{\sigma(k_0)}^{k_1-k_0} V_{\sigma(k_0)}(k_0) - \Theta(\Upsilon),
\end{aligned} \tag{12.23}$$

where

$$\begin{aligned}
\Theta(\Upsilon) = {} & \mu^{N_\sigma(k_0,k-1)} \lambda_{\sigma(k_l)}^{k-k_l} \prod_{s=1}^{l-1} \lambda_{\sigma(k_s)}^{k_{s+1}-k_s} \sum_{s=k_0}^{k_1-1} \lambda_{\sigma(k_0)}^{k_1-1-s} \mathbb{E}\{\Upsilon(s)\} \\
& + \mu^{N_\sigma(k_0,k-1)-1} \lambda_{\sigma(k_l)}^{k-k_l} \prod_{s=2}^{l-1} \lambda_{\sigma(k_j)}^{k_{j+1}-k_j} \sum_{s=k_1}^{k_2-1} \lambda_{\sigma(k_1)}^{k_2-1-s} \mathbb{E}\{\Upsilon(s)\} \\
& + \cdots + \mu^0 \prod_{s=k_l}^{k-1} \lambda_{\sigma(k_l)}^{k-1-s} \mathbb{E}\{\Upsilon(s)\}.
\end{aligned}$$

Now, we consider the exponential stability of the system (12.5) with $v(k) = 0$. By choosing $N_0 = 0$, one has

$$\begin{aligned}
&\mathbb{E}\{V_{\sigma(k_l)}(k)\} \\
&\le \mu^{N_\sigma(k_0,k)} \lambda_{\sigma(k_l)}^{k-k_l} \lambda_{\sigma(k_{l-1})}^{k_l-k_{l-1}} \cdots \lambda_{\sigma(k_0)}^{k_1-k_0} V_{\sigma(k_0)}(k_0) \\
&\le \mu^{N_\sigma(k_0,k)} \lambda_b^{k-k_0} V_{\sigma(k_0)}(k_0) \\
&\le \left(\mu^{1/T_a} \lambda_b\right)^{k-k_0} V_{\sigma(k_0)}(k_0) = \chi^{2(k-k_0)} V_{\sigma(k_0)}(k_0),
\end{aligned} \tag{12.24}$$

where $\chi = \sqrt{\lambda_b \mu^{1/T_a}}$. It follows from (12.9) that there exist two positive scalars $\varphi_1 > 0$ and $\varphi_2 > 0$ such that

$$\mathbb{E}\left\{\|x(k)\|^2\right\} \le \frac{\varphi_2}{\varphi_1} \chi^{2(k-k_0)} \sup_{k_0-d_2 \le s \le k_0} \|\psi(s)\|. \tag{12.25}$$

According to condition (12.8), one can readily obtain $\chi < 1$. Hence, the closed-loop system (12.5) is exponentially stable in the mean-square sense.

We now consider the H_∞ performance level. Under zero initial condition, it follows from (12.21) that

$$\sum_{s=k_0}^{k-1} \mu^{N_\sigma(s,k-1)} \lambda_a^{k-s-1} \mathbb{E}\{z^T(s)z(s)\} \le \tau^2 \sum_{s=k_0}^{k-1} \mu^{N(s,k-1)} \lambda_b^{k-s-1} v^T(s)v(s). \quad (12.26)$$

With the average dwell time condition (12.8), it is easy to see $\frac{N_\sigma(s,k-1)}{k-s-1} < -\frac{\ln\lambda}{\ln\mu}$. Since $\mu > 1$, we obtain $\ln \mu^{N_\sigma(s,k-1)} < \ln \lambda^{-(k-s-1)}$, and $1 < \mu^{N_\sigma(s,k-1)} < \lambda^{-(k-s-1)}$. Then, it can be readily seen that

$$\sum_{s=k_0}^{k-1} \lambda_a^{k-s-1} \mathbb{E}\{z^T(s)z(s)\} < \tau^2 \sum_{s=k_0}^{k-1} \left(\lambda_b/\lambda\right)^{k-s-1} \lambda^{k-s-1} v^T(s)v(s). \quad (12.27)$$

Summing (12.27) from $k = k_0 + 1$ to $k = \infty$ and changing the order of summation yield

$$\sum_{s=k_0}^{+\infty} \mathbb{E}\{z^T(s)z(s)\} \sum_{k=s+1}^{+\infty} \lambda_a^{k-s-1} < \tau^2 \sum_{s=k_0}^{+\infty} v^T(s)v(s) \sum_{k=s+1}^{+\infty} \left(\lambda_b/\lambda\right)^{k-s-1}. \quad (12.28)$$

Since $\sum_{k=s+1}^{+\infty} \lambda_a^{k-s-1} = \frac{1}{1-\lambda_a}$ and $\sum_{k=s+1}^{+\infty} \left(\lambda_b/\lambda\right)^{k-s-1} = \frac{1}{1-(\lambda_b/\lambda)}$, we have

$$\sum_{s=k_0}^{+\infty} \mathbb{E}\{z^T(s)z(s)\} < \gamma^2 \sum_{s=k_0}^{+\infty} v^T(s)v(s), \quad (12.29)$$

where $\gamma = \tau\sqrt{\frac{1-\lambda_a}{1-\lambda_b/\lambda}}$. According to Definition 12.2, the closed-loop system (12.5) is exponentially stable in the mean-square sense and achieves a prescribed H_∞ performance level. This completes the proof.

Due to the co-existence of P_l and P_l^{-1}, we can not obtain the controller gain directly from Theorem 12.1. We now present the following theorem for the gain calculation.

Theorem 12.2 *For given scalars $\tau > 0$, $\mu > 1$, $0 < \lambda_l < 1$, $\bar{\alpha}_i > 0$ and $0 < \lambda < 1$, the control problem is solvable if there exist positive definite matrices $P_l > 0$, $T_l > 0$, and positive scalars $\varepsilon > 0$, $\beta_1 > 0$, $\beta_2 > 0$ such that the following inequalities,*

$$\begin{bmatrix} \Xi & \Omega_1^T & \Omega_2^T & \Omega_3 & \Omega_4^T & 0 \\ * & -T_l & 0 & 0 & 0 & BK_l\bar{\Pi} \\ * & * & -I & 0 & 0 & 0 \\ * & * & * & -\bar{T}_l & 0 & \Omega_5^T \\ * & * & * & * & -\varepsilon I & 0 \\ * & * & * & * & * & -\varepsilon I \end{bmatrix} < 0, \tag{12.30}$$

$$T_l P_l = I, \tag{12.31}$$

and (12.7) *hold for all* $l, v \in \Gamma$, *where* $\bar{T}_l = \text{diag}\{T_l, \ldots, T_l\}$.

Proof The proof is trivial by letting $T_l = P_l^{-1}$, and thus it is omitted.

We can see from Theorem 12.2 that the conditions (12.7) and (12.30) are linear matrix inequalities which can be solved efficiently by available software. The challenge lies in the condition (12.31), which is a bilinear matrix equation and it is non-convex. Over the past decades, much work has been done to solve this kind of problems, among which the cone complementarity linearization (CCL) algorithm [1] was shown to be efficient by many numerical implementations. In this chapter, the CCL algorithm is used to solve the above non-convex problem, and the controller gain parameter can be obtained by solving the following optimization problem:

Controller design:

$$\min \ \text{Tr}\left(\sum_{l=1}^{M} (T_l \times P_l)\right), \tag{12.32}$$

s.t. (12.7), (12.30) and

$$\begin{bmatrix} T_l & I \\ I & P_l \end{bmatrix} \geq 0. \tag{12.33}$$

Remark 12.2 In solving the optimization problem (12.32), the control performance related parameter τ should be given first. Thus, the minimal H_∞ performance level may not be obtained. In order to obtain the minimal H_∞ performance, one may initially choose a large τ, and then solve the optimization problem. If no solution is found, one reduces a larger τ until the the optimization problem is feasible. On the other hand, if the optimization problem admits a solution for the chosen τ, then one decreases τ by a small $\Delta\tau$ and solve the optimization problem.

12.4 An Illustrative Example

In this section, a practical example is given to show the effectiveness of the proposed design. The example under consideration is the interconnected chemical reactors composing of two non-isothermal continuous stirred-tank reactors (CSTRs) with

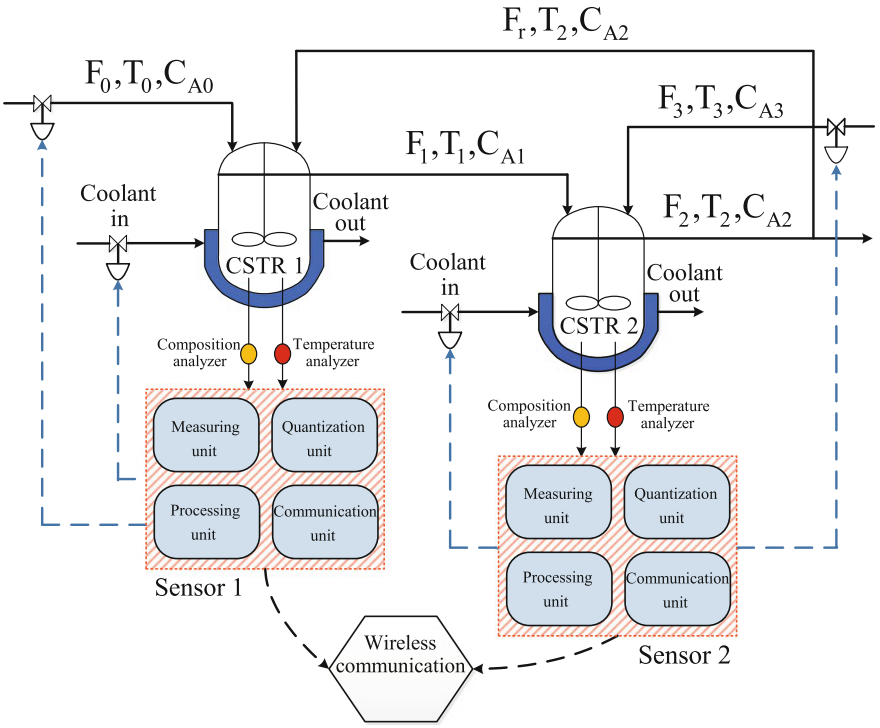

Fig. 12.2 Process flow diagram of two interconnected CSTR systems

interconnections between reactors. Figure 12.2 shows the process flow diagram of two interconnected CSTR units. It follows from Fig. 12.2 that the feed to CSTR 1 consists of two streams, one containing fresh flow at rate F_0, molar concentration C_{A0}, and temperature T_0; the second stream contains recycled flow from CSTR 2 at rate F_r, molar concentration C_{A2}, and temperature T_2. The feed to CSTR 2 consists of the output of CSTR 1, and an additional fresh stream at flow rate F_3, molar concentration C_{A03}, and temperature T_{03}. The plant model is given [4] by

$$\begin{cases} \dot{T}_1 = \frac{F_0}{V_1}(T_0 - T_1) + \frac{F_r}{V_1}(T_2 - T_1) + \sum_{i=1}^{3} G_i(T_1)C_{A1} + \frac{Q_1}{\rho c_p V_1}, \\ \dot{C}_{A1} = \frac{F_0}{V_1}(C_{A0} - C_{A1}) + \frac{F_r}{V_1}(C_{A2} - C_{A1}) + \sum_{i=1}^{3} R_i(T_1)C_{A1}, \\ \dot{T}_2 = \frac{F_1}{V_2}(T_1 - T_2) + \frac{F_3}{V_2}(T_{03} - T_2) + \sum_{i=1}^{3} G_i(T_2)C_{A2} + \frac{Q_2}{\rho c_p V_2}, \\ \dot{C}_{A2} = \frac{F_1}{V_2}(C_{A1} - C_{A2}) + \frac{F_3}{V_2}(C_{A03} - C_{A2}) - \sum_{i=1}^{3} R_i(T_2)C_{A2}, \end{cases} \tag{12.34}$$

where $G_i(T_j) = \left(-(\Delta H_i)/\rho c_p\right) R_i(T_j)$ and $R_i(T_j) = k_{i0} \exp\left((-E_i)/RT_i\right)$ for $j = 1, 2$. $\Delta H_i, k_{i0}, E_i, i = 1, 2, 3$, denote the enthalpies, pre-exponential constants and activation energies of the reactions, respectively; Also, c_p and ρ denote the heat capacity and density of fluid in the reactor, respectively. The open-loop plant is unstable at the desired operating point $((T_1^s, C_{A1}^s, T_2^s, C_{A2}^s) = 457.9\,\text{K}, 1.77\,\text{kmol/m}^3, 415.5\,\text{K}, 1.75\,\text{kmol/m}^3)$. By linearizing the plant equations (12.34) around the given operating point, the following system is obtained:

$$\begin{cases} \dot{x}_1(t) = A_{11}^c x_1(t) + \bar{B}_1^c u_1(t) + A_{12}^c x_2(t), \\ \dot{x}_2(t) = A_{22}^c x_2(t) + \bar{B}_2^c u_2(t) + A_{21}^c x_1(t), \end{cases} \tag{12.35}$$

where x_i and u_i are the state and input vectors for the i-th subsystem, respectively, and they are defined by

$$x_1 = \begin{bmatrix} \frac{T_1 - T_1^s}{T_1^s} \\ \frac{CA_1 - C_{A1}^s}{C_{A1}^s} \end{bmatrix}, x_2 = \begin{bmatrix} \frac{T_2 - T_2^s}{T_2^s} \\ \frac{CA_2 - C_{A2}^s}{C_{A2}^s} \end{bmatrix},$$
$$u_1 = \begin{bmatrix} Q_1 \\ C_{A0} - C_{A0}^s \end{bmatrix}, u_2 = \begin{bmatrix} Q_2 \\ C_{A03} - C_{A03}^s \end{bmatrix}.$$

Based on the values of the process parameters given in Table 12.1 (taken from [4]), the matrices in (12.35) are obtained as:

Table 12.1 Parameters and steady-state values for the chemical reactors

$F_0 = 4.998\,\text{m}^3/\text{h}$	$R = 8.314\,\text{kJ/kmol K}$
$F_1 = 39.996\,\text{m}^3/\text{h}$	$E_1 = 5.0 \times 10^4\,\text{kJ/kmol}$
$F_3 = 30.0\,\text{m}^3/\text{h}$	$E_2 = 7.53 \times 10^4\,\text{kJ/kmol}$
$F_r = 34.998\,\text{m}^3/\text{h}$	$E_3 = 7.53 \times 10^4\,\text{kJ/kmol}$
$V_1 = 1.0\,\text{m}^3$	$\rho = 1000.0\,\text{kg/m}^3$
$V_2 = 3.0\,\text{m}^3$	$C_p = 0.231\,\text{kJ/kmol K}$
$T_0 = 300.0\,\text{K}$	$T_1^s = 457.9\,\text{K}$
$T_{03} = 300.0\,\text{K}$	$T_2^s = 415.5\,\text{K}$
$C_{A0}^S = 4.0\,\text{kmol/m}^3$	$C_{A1}^s = 1.77\,\text{kmol/ m}^3$
$C_{A03}^S = 2.0\,\text{kmol/m}^3$	$C_{A2}^2 = 1.75\,\text{kmol/ m}^3$
$\Delta H_1 = -5.0 \times 10^4\,\text{kJ/kmol}$	$k_{10} = 3.0 \times 10^5\,\text{h}^{-1}$
$\Delta H_2 = -5.2 \times 10^4\,\text{kJ/kmol}$	$k_{20} = 3.0 \times 10^5\,\text{h}^{-1}$
$\Delta H_3 = -5.4 \times 10^4\,\text{kJ/kmol}$	$k_{30} = 3.0 \times 10^5\,\text{h}^{-1}$

$$A_{11}^c = \begin{bmatrix} 25.2914 & 4.9707 \\ -78.028 & -45.9368 \end{bmatrix}, A_{12}^c = \begin{bmatrix} 31.7512 & 0 \\ 0 & 34.6421 \end{bmatrix},$$
$$\bar{B}_1^c = \begin{bmatrix} 9.45 \times 10^{-6} & 0 \\ 0 & 2.8234 \end{bmatrix},$$
$$A_{22}^c = \begin{bmatrix} -2.8370 & 1.4157 \\ -22.4506 & -24.8828 \end{bmatrix}, A_{21}^c = \begin{bmatrix} 14.6953 & 0 \\ 0 & 13.4690 \end{bmatrix},$$
$$\bar{B}_2^c = \begin{bmatrix} 3.47 \times 10^{-6} & 0 \\ 0 & 5.7071 \end{bmatrix}.$$

With a sampling time of $T_s = 0.0025$ h, the above process system is transformed to the following discrete-time interconnected system:

$$\begin{cases} x_1(k+1) = A_{11}^d x_1(k) + \bar{B}_1^d u_1(k) + A_{12}^d x_2(k), \\ x_2(k+1) = A_{22}^d x_2(k) + \bar{B}_2^d u_2(k) + A_{21}^d x_1(k), \end{cases} \tag{12.36}$$

where

$$A_{11}^d = \begin{bmatrix} 1.0632 & 0.0124 \\ -0.1951 & 0.8852 \end{bmatrix}, A_{12}^d = \begin{bmatrix} 0.0794 & 0 \\ 0 & 0.0866 \end{bmatrix},$$
$$\bar{B}_1^d = \begin{bmatrix} 9.45 \times 10^{-7} & 0 \\ 0 & 0.0071 \end{bmatrix},$$
$$A_{22}^d = \begin{bmatrix} 0.9929 & 0.0035 \\ -0.0561 & 0.9378 \end{bmatrix}, A_{21}^d = \begin{bmatrix} 0.0367 & 0 \\ 0 & 0.0337 \end{bmatrix},$$
$$\bar{B}_2^d = \begin{bmatrix} 3.47 \times 10^{-7} & 0 \\ 0 & 0.0143 \end{bmatrix}.$$

It follows from [7] that the nonlinear perturbation, time-delay and disturbance occur in CSTR systems. Then, we model the interconnected CSTR system by

$$\begin{cases} x_i(k+1) = A_{ii} x_i(k) + W_{0i} g(x_i(k)) + W_{1i} g(x_i(k - d_i(k))) \\ \qquad\qquad + \sum_{j=1, j\neq i}^{2} A_{ij} x_j(k) + B_i u_i(k) + E_i v_i(k), \\ z_i(k) = L_i x_i(k). \end{cases} \tag{12.37}$$

The parameters of each subsystem are given as follows.
Subsystem 1:

$$A_{11} = \begin{bmatrix} 1.0632 & 0.0124 \\ -0.1951 & 0.8852 \end{bmatrix}, A_{12} = \begin{bmatrix} 0.0794 & 0 \\ 0 & 0.0866 \end{bmatrix},$$
$$W_{01} = W_{11} = \begin{bmatrix} 0.1 & 0 \\ 0.1 & 0.01 \end{bmatrix}, B_1 = \begin{bmatrix} 9.45 \times 10^{-7} & 0 \\ 0 & 0.0071 \end{bmatrix},$$
$$E_1 = \begin{bmatrix} 0.7 \\ 0.3 \end{bmatrix}, L_1 = \begin{bmatrix} 0.5 & 0.5 \end{bmatrix}.$$

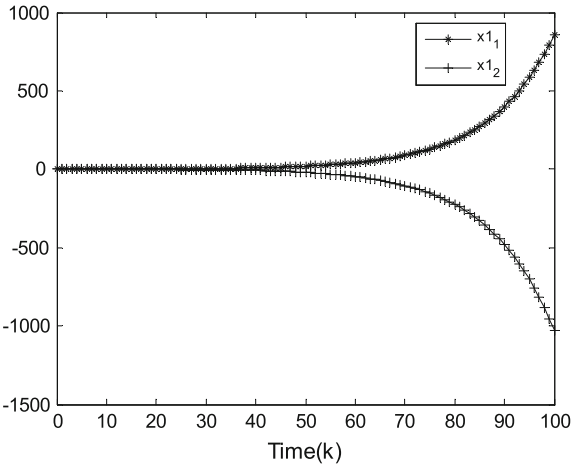

Fig. 12.3 State trajectories of subsystem 1 without control

Subsystem 2:

$$A_{22} = \begin{bmatrix} 0.9929 & 0.0035 \\ -0.0561 & 0.9378 \end{bmatrix}, A_{21} = \begin{bmatrix} 0.0367 & 0 \\ 0 & 0.0337 \end{bmatrix},$$
$$W_{02} = W_{12} = \begin{bmatrix} -0.1 & 0 \\ -0.1 & 0.1 \end{bmatrix}, B_2 = \begin{bmatrix} 3.47 \times 10^{-7} & 0 \\ 0 & 0.0143 \end{bmatrix},$$
$$E_2 = \begin{bmatrix} 0.5 \\ 0.3 \end{bmatrix}, L_2 = \begin{bmatrix} 0.1 & 0.8 \end{bmatrix}.$$

The nonlinear disturbance is assumed to be $g(x_i(k)) = \begin{bmatrix} \tanh(0.2x_{1i}) \\ \tanh(0.2x_{2i}) \end{bmatrix}$. Then we have $U = \text{diag}\{0.2, 0.2\}$. The time-varying delays are assumed to be $1 \leq d_1(k) \leq 3$ and $2 \leq d_2(k) \leq 4$, respectively. Then, $d_1 = 1$, and $d_2 = 4$. Choosing initial conditions as $\psi_1 = \psi_2 = \begin{bmatrix} 0.1 & 0.1 \end{bmatrix}^T$, random delays for $d_1(k)$ and $d_2(k)$, and $v_1 = v_2 = 0$, then the state trajectories of these two systems are shown in Figs. 12.3 and 12.4, respectively. One can see that this system is open-loop unstable.

In this example, we use two wireless sensors to perform the control task and all state variables are assumed to be available for controller design. In order to save energy in sensors, signal is quantized before transmission and the communication between these two sensors is scheduled to be intermittent. The quantization densities are set to be $\rho_1 = 0.9$, $\rho_2 = 0.7$. In addition, we choose $a_{ij}^1 = 1$ and $a_{ij}^2 = 0$ for $i, j = 1, 2, i \neq j$. The communication sequence is scheduled to be the following periodical signal,

$$\sigma(k) = \begin{cases} 1, 1 \leq k \leq 5, \\ 2, 6 \leq k \leq 10. \end{cases} \tag{12.38}$$

It is seen that the entire system works in the centralized framework under topology 1 and the decentralized control one under topology 2. The sensor faulty rates in this

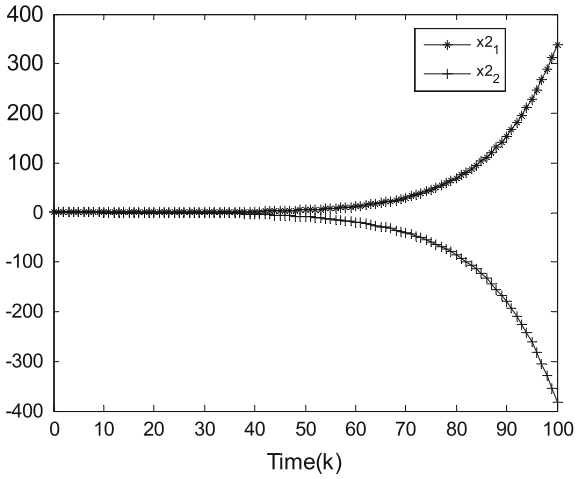

Fig. 12.4 State trajectories of subsystem 2 without control

example are assumed to be 20, 30%, that is $\bar{\alpha}_1 = 0.8$, $\bar{\alpha}_2 = 0.7$. By choosing $\lambda_1 = 0.95$, $\lambda_2 = 0.98$, $\lambda = 0.99$ and $\mu = 1.05$, we have $T_a^* = 4.8546 < 5$, hence the condition (12.8) is satisfied. Solving the optimization problem (12.32), we obtain the minial H_∞ performance level $\gamma^* = 0.7141$. The corresponding controller gains are

$$K_1 = \begin{bmatrix} -1.2724 \times 10^6 & -0.1511 \times 10^6 & -0.1636 \times 10^6 & -420.0542 \\ 14.7123 & -126.5612 & 8.9966 & -17.5228 \\ -0.0944 \times 10^6 & -0.0868 \times 10^6 & -3.2858 \times 10^6 & -0.6258 \times 10^6 \\ -0.6780 & -1.2824 & -3.9407 & -76.4545 \end{bmatrix},$$

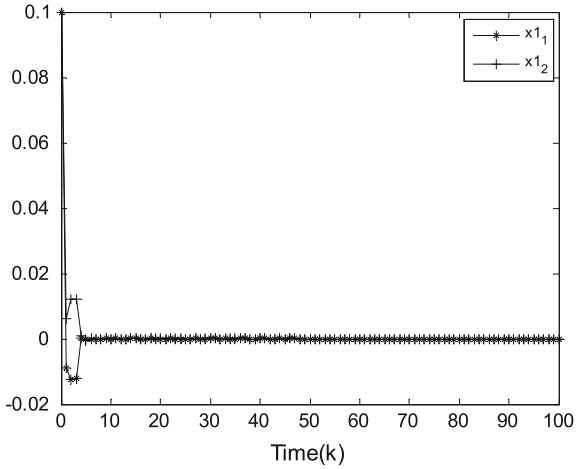

Fig. 12.5 State trajectories of subsystem 1 with control

$$K_2 = \begin{bmatrix} -1.2791 \times 10^6 & -0.0859 \times 10^6 & 0 & 0 \\ 11.8000 & -127.1985 & 0 & 0 \\ 0 & 0 & -3.3545 \times 10^6 & -0.4665 \times 10^6 \\ 0 & 0 & -5.1766 & -75.3818 \end{bmatrix}.$$

Under the same initial conditions as before, the state trajectories of these two systems are depicted in Figs. 12.5 and 12.6, respectively. One sees that the closed-loop system is stable based on our design. We now evaluate the H_∞ performance level. For simulation purpose, we choose $v_1(k) = \sin(0.2k)$ and $v_2(k) = \cos(0.2k)$.

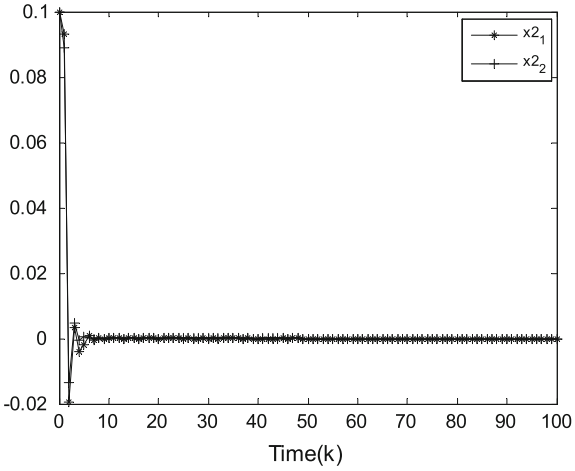

Fig. 12.6 State trajectories of subsystem 2 with control

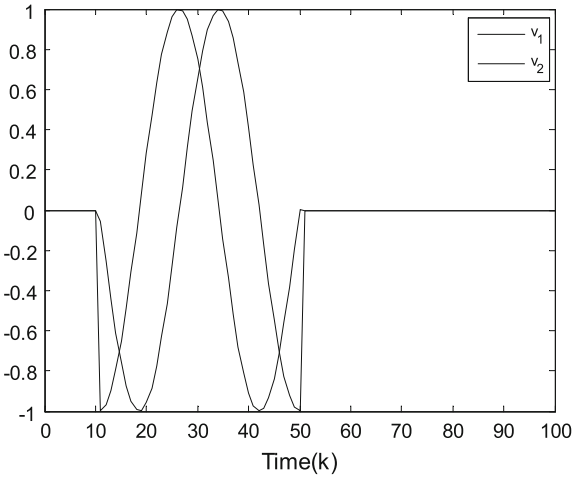

Fig. 12.7 Trajectories of noise

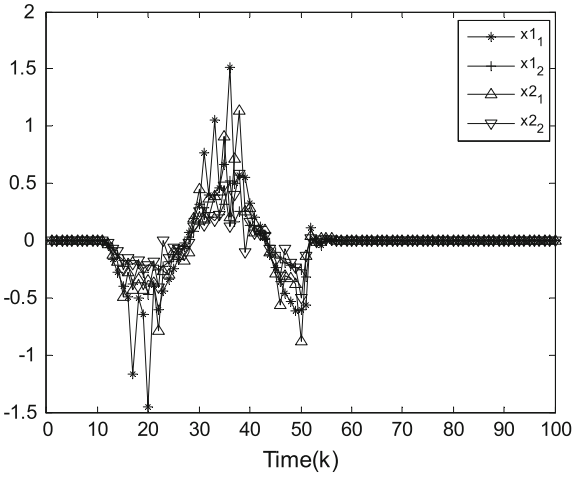

Fig. 12.8 State trajectories of two subsystems

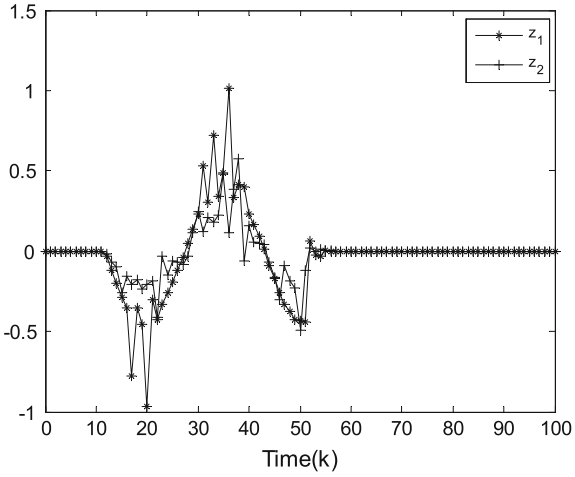

Fig. 12.9 Trajectories of performance output

The trajectories are shown in Fig. 12.7. Choosing the zero initial conditions for the two subsystems, the state trajectories are depicted in Fig. 12.8. Figure 12.9 depicts the trajectories of performance output. By simple calculation, we have $\sqrt{\sum_{s=0}^{100} z^T(s)z(s) \Big/ \sum_{s=0}^{100} v^T(s)v(s)} = 0.5678 < \gamma^*$.

12.5 Conclusions

We have studied the distributed stabilization of large-scale systems in a sensor network with energy constraint and random sensor faults. In order to save limited energy in sensors, techniques such as reducing the packet size reduction and the communication frequency reduction have been used. A set of binary variables has been introduced to model the random sensor fault phenomenon. Based on the switched system theory, Lyapunov stability technique and some stochastic system analysis, a sufficient condition has been obtained such the closed-loop system is exponentially stable in the mean-square sense and achieves a prescribed disturbance attenuation level in the H_∞ sense. Controller gains is designed based on the CCL method. A numerical example has been given to show the effectiveness of the proposed design.

In this chapter, we only use the signal quantization and transmission rate reduction schemes to reduce the transmission power. As we have mentioned that some other methods such as aperiodic sampling and measurement size reduction schemes can also help reduce the transmission power. Now, the problem is if we can simultaneously use these schemes to achieve the energy-efficiency goal? The similar problem has been discussed in the distributed filtering system. We will discuss the distributed control problem in the next chapter.

References

1. L.E. Ghaoui, F. Oustry, M. AitRami, A cone complementarity linearization algorithm for static output-feedback and related problems. IEEE Trans. Autom. Control **42**(8), 1171–1176 (1997)
2. S.C. Xu, J. Bao, Plantwide process control with asynchronous sampling and communications. J. Process Control **21**(6), 927–948 (2011)
3. S.C. Xu, J. Bao, Distributed control of plant-wide chemical processes with uncertain time-delays. Chem. Eng. Sci. **84**, 512–532 (2012)
4. F. Kazempour, J. Ghaisari, Stability analysis of model-based networked distributed control systems. J. Process Control **23**, 444–452 (2013)
5. M. Pajic, S. Sundaram, G.J. Pappas, R. Mangharam, The wireless control network: a new approach for control over networks. IEEE Trans. Autom. Control **56**(10), 2305–2318 (2011)
6. P. Millan, L. Orihuela, C. Vivas, F.R. Rubio, D.V. Dimarogonas, K.H. Johansson, Sensor-network-based robust distributed control and estimation. Control Eng. Pract. **21**(9), 1238–1249 (2013)
7. C.S. Bildea, A.C. Dimian, P.D. Iedema, Nonlinear behavior of reactor-separator-recycle systems. Comput. Chem. Eng. **24**, 209–215 (2000)

Chapter 13
Distributed Control with Communication Reduction

13.1 Introduction

In this chapter, we revisit the sensor-network-based control problem for a class of large-scale systems, and the energy constraint is still our main concern. To achieve the energy-efficiency goal, the measurement size reduction technique and communication rate reduction method are introduced in the control system design. Firstly, a time-varying sampling scheme is used in the sampling process, and only one element of the sampled data is then chosen and quantized for transmission. Then, an intermittent communication between the local sensors with their neighbours are used to reduce the communication rate. A unified switched system approach is proposed to model the nonuniform sampling, the measurement size reduction, and the communication rate reduction phenomenon. A sufficient condition is presented such that the closed-loop system is exponentially stable in the mean-square sense and achieves a prescribed H_∞ performance level. The controller gains are determined by using the cone complementarity linearization (CCL) algorithm subject to certain LMI constraint. Finally, a case study on the interconnected CSTR system is given to show the effectiveness of the proposed new design.

13.2 Problem Formulation

The problem under consideration is to stabilize the large-scale system by the distributed control. The target plant is firstly sampled under time-varying periods. Then, we select one element of state measurement, and quantize this measurement for transmission. It is known that the controller failure may occur in the control system. Our system is shown in Fig. 13.1.

Consider the following continuous-time linear time-invariant (LTI) system:

D. Zhang et al., *Filtering and Control of Wireless Networked Systems*,
Studies in Systems, Decision and Control 97, DOI 10.1007/978-3-319-53123-6_13

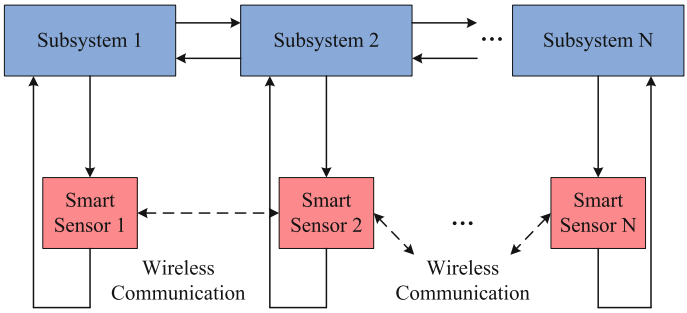

Fig. 13.1 Sensor-network-based control system

$$\begin{cases} \dot{x}(t) = Ax(t) + Bu(t) + Ev(t), \\ z(t) = Lx(t), \end{cases} \tag{13.1}$$

where $x(t) \in \mathbb{R}^n$ is the state vector, $z(t) \in \mathbb{R}^m$ is the performance output vector, $u(t) \in \mathbb{R}^p$ is the control input vector and $v(t) \in \mathbb{R}^q$ is the unknown disturbance belonging to $L_2[0, +\infty)$. A, B, E and L are some constant matrices with appropriate dimensions. To control a large-scale system, the first step is to partition it into some small subsystems. These subsystems are interconnected under certain topology, hence the system (13.1) is sparse. Let $G = (v, \varepsilon)$ be the direct graph associated with the matrix $\mathbb{A} = [a_{ij}]$, that is, the node set is $v = \{1, 2, \ldots, N\}$ and there exists a directed edge $(i, j) \in \varepsilon \subseteq v \times v$ if and only if $a_{ij} \neq 0$. Let v be partitioned into N disjoint sets, $v = \{v_1, v_2, \ldots, v_N\}$, and let $G_i = (v_i, \varepsilon_i)$ be the i-th subgraph of G with vertices v_i and edges $\varepsilon_i = \varepsilon \cap (v_i \times v_i)$. According to this partition, the matrix A us given by

$$A = \begin{bmatrix} A_{11} & A_{12} & \cdots & A_{1N} \\ A_{21} & A_{22} & \cdots & A_{2N} \\ \vdots & \vdots & \ddots & \vdots \\ A_{N1} & A_{N2} & \cdots & A_{NN} \end{bmatrix} = A_D + A_C,$$

where $A_{ii} \in \mathbb{R}^{n_i \times n_i}$, $A_{ij} \in \mathbb{R}^{n_i \times n_j}$, A_D is block-diagonal, and $A_C = A - A_D$. It is noted that if $A_D = \text{diag}\{A_{11}, \ldots, A_{NN}\}$ then A_D represents the decoupled diagonal subsystems and A_C describes their interconnections. Specifically, if A is sparse, then several blocks in A_C are zero. In this chapter, we assume that the interconnection of the plant only occurs in the state variables. Then, we have

$$B = \text{diag}\{B_1, B_2, \ldots, B_N\}, E = \text{diag}\{E_1, E_2, \ldots, E_N\},$$
$$L = \text{diag}\{L_1, L_2, \ldots, L_N\}.$$

With the above structure, the system (13.1) becomes an interconnected system and the dynamics of each subsystem is given by

$$\begin{cases} x_i(t) = A_{ii}x(t) + \sum\limits_{j=1,j\neq i}^{N} A_{ij}x_j(t) + B_i u_i(t) + E_i v_i(t), \\ z_i(t) = L_i x(t). \end{cases} \tag{13.2}$$

We are now in the position to discuss the issues with networked control.

13.2.1 Sampling

In the networked control system, a signal is usually sampled and only its value at the sampling time instant is available for controller design. In this chapter, the sampling period of each sensor is set to be the same, and all the sensors work in an synchronous mode. For each sensor, the sampling period is allow to vary, i.e., each sensor has a time-varying sampling period. Define the measurement sampling period as $h_k = t_{k+1} - t_k$, where, t_k is the sampling time instant. In this chapter, we assume that h_k takes a value from a given set. Specifically, let $h_k = n_k T_0$, where $n_k \in \{l_1, l_2, \ldots, l_{N_1}\}$, l_j, $j = 1, 2, \ldots, N_1$ are positive integers, and T_0 is the basic sampling period.

We now discretize the system (13.2) with the sampling period h_k and applying a zero-order-holder, we obtain the following discrete-time system:

$$\begin{cases} x_i(t_{k+1}) = A_{ii}(k)x(t_k) + \sum\limits_{j=1,j\neq i}^{N} A_{ij}(k)x_j(t_k) \\ \qquad\qquad +B_i(k)u_i(t_k) + E_i(k)v_i(t_k), \\ z_i(t_k) = L_i x(t_k), \end{cases} \tag{13.3}$$

where $A_{ii}(k) = e^{A_{ii}h_k}$, $A_{ij}(k) = \left(\int_0^{h_k} e^{A_{ii}\tau}d\tau\right) A_{ij}$, $B_i(k) = \left(\int_0^{h_k} e^{A_{ii}\tau}d\tau\right) B_i$ and $E_i(k) = \left(\int_0^{h_k} e^{A_{ii}\tau}d\tau\right) E_i$. Let $A_{ii0} = e^{A_{ii}T_0}$, $A_{ij0} = \left(\int_0^{T_0} e^{A_{ii}\tau}d\tau\right) A_{ij}$, $B_{i0} = \left(\int_0^{T_0} e^{A_{ii}\tau}d\tau\right) B_i$, $E_{i0} = \left(\int_0^{T_0} e^{A_{ii}\tau}d\tau\right) E_i$. Then, we have $A_{ii}(k) = {A_0}^{n_k}$, $A_{ij}(k) = \sum\limits_{t=0}^{n_k-1} {A_{ii0}}^t A_{ij0}$, $B_i(k) = \sum\limits_{t=0}^{n_k-1} {A_{ii0}}^t B_{i0}$, $E_i(k) = \sum\limits_{t=0}^{n_k-1} {A_{ii0}}^t E_{i0}$. It is seen that the values of $A_{ij}(k)$, $B_i(k)$ and $E_i(k)$ are determined by the sampling period h_k. Define a piecewise constant signal, $s(k) \in \Omega_1 = \{1, 2, \ldots, N_1\}$. Then, we have the following switching system model for (13.3):

$$\begin{cases} x_i(t_{k+1}) = A^{ii}_{s(t_k)}x(t_k) + \sum\limits_{j=1,j\neq i}^{N} A^{ij}_{s(t_k)}x_j(t_k) \\ \qquad\qquad +B^i_{s(t_k)}u_i(t_k) + E^i_{s(t_k)}v_i(t_k), \\ z_i(t_k) = L_i x(t_k), \end{cases} \tag{13.4}$$

where $A^{ii}_{s(t_k)} = A_{ii0}{}^{l_{s(t_k)}}$, $A^{ij}_{s(t_k)} = \sum_{t=1}^{l_{s(t_k)}} A^{t-1}_{ii0} A_{ij0}$, $B^{i}_{s(t_k)} = \sum_{t=1}^{l_{s(t_k)}} A^{t-1}_{ii0} B_{i0}$, $E^{i}_{s(t_k)} = \sum_{t=1}^{l_{s(t_k)}} A^{t-1}_{ii0} E_{i0}$.

13.2.2 Measurement Size Reduction

It follows from the simulation results in Chap. 10 that reducing the packet size and transmission rate are efficient methods to save the sensor power. Since the size of the original measurement may be large, we introduce a measurement selection scheme. Only one element is selected and quantized for transmission. The selected measurement signal is described as

$$\tilde{x}_p(t_k) = \Pi_{\rho_i(t_k)} x_p(t_k), \tag{13.5}$$

where $\Pi_{\rho_{p(t_k)}}$ is a matrix introduced to choose one element for transmission, and $\rho_{p(t_k)}$, $p = 1, 2, \ldots, N$, are piecewise signals, which belongs to $\Omega_{p2} = \{1, 2, \ldots, n_p\}$. Specifically, when the first element is selected, then $\Pi_{\rho_{p(t_k)}} = [\,1\ 0\ \cdots\ 0\,]$; the second element is selected, then $\Pi_{\rho_{p(t_k)}} = [\,0\ 1\ \cdots\ 0\,]$, and so on. It is seen that $\Pi_{\rho_{p(t_k)}}$ are a set of switching signals.

The selected measurement is then quantized for transmission. In this chapter, the logarithmic quantizer is used. The quantizer $Q^p(\bullet)$ is assumed to be symmetric and time-invariant, i.e., $Q^p(-v_p) = -Q^p(-v_p)$. For any $p = 1, 2, \ldots, n$, the set of quantization levels are described as

$$\begin{aligned} U^p = &\left\{\pm\kappa_i^p, \kappa_i^p = \rho_i^p \kappa_0^p, i = 0, \pm1, \pm2, \ldots\right\} \\ &\cup \left\{\pm\kappa_0^p\right\} \cup \{0\}, 0 < \rho^p < 1, \kappa_0^p > 0. \end{aligned} \tag{13.6}$$

The quantized output of $Q^p(\bullet)$ is given by

$$Q^p(v_p) = \begin{cases} \kappa_i^p, & \text{if } \frac{1}{1+\delta^p}\kappa_i^p < v_p < \frac{1}{1-\delta^p}\kappa_i^p,\ v_p > 0, \\ 0, & \text{if } v_p = 0, \\ -Q^p(-v_p), & \text{if } v_p < 0, \end{cases} \tag{13.7}$$

where $\delta_p = \frac{1-\rho_p}{1+\rho_p} < 1$, with the quantization density $0 < \rho_p < 1$. The quantized measurement is described by

$$\hat{x}_p(t_k) = Q_p(\bar{x}_p(t_k)). \tag{13.8}$$

Define the quantization error $e_p = \hat{x}_p(t_k) - \bar{x}_p(t_k)$, then $\hat{x}_p(t_k) = (I + \Delta_p(t_k))\bar{x}_p(t_k)$, where $\left\|\Delta_p(t_k)\right\| \le \delta_p$.

It has been shown that reducing the communication rate is also an effective method to save sensor power. The most energy-efficient case is no communication among different smart sensors, but the control performance is known to be the worst. So, we introduce a time-varying communication scheme for our system, which can also

affect the sensor network's structure. Basis on sensor networks is given as follows. Let the topology of a given sensor network be represented by a direct graph $\pi(k) = (\xi, \chi, \mathbb{B}^{\sigma(k)})$ of order n with the set of sensors $\upsilon = \{1, 2, \ldots, N\}$, set of edges $\chi \subseteq \xi \times \xi$, and a weighted adjacency matrix $\mathbb{B}^{\sigma(k)} = [b_{pq}^{\sigma(k)}]$ with nonnegative adjacency elements $b_{pq}^{\sigma(k)}$. The edge of π is denoted by (p, q). The adjacency elements associated with the edges of the graph are $b_{pq}^{\sigma(k)} = 1 \Leftrightarrow (p, q) \in \xi$, when the sensor p can receive information from controller q. On the other hand, $b_{pq}^{\sigma(k)} = 0$ if sensor p can not receive information from controller q, which may be out of communication range or the q-th sensor does not broadcast information. Moreover, it is seen that $b_{pp}^{\sigma(k)} = 1$ for all $p \in \xi$. The set of neighbors of node $p \in \xi$ plus the node itself are denoted by $N_p = \{q \in \xi : (p, q) \in \xi\}$. $\sigma(k) : [0, \infty) \to \Omega_3 = \{1, 2, \ldots, N_3\}$ is a switching signal. For each $l \in \Omega_3$, $\mathbb{B}^l = [b_{ij}^l]$ is a square matrix representing the topology of the sensor network. The number of the topologies is determined directly by how one regulates the working mode of the sensor network.

With the controller failure, the controller is described as

$$u_p(t_k) = \sum\nolimits_{p \in N_p} \alpha_p(t_k) b_{pq}^{\sigma(t_k)} K_{pq}^{\sigma(t_k)} \hat{x}_q(t_k), \tag{13.9}$$

where $\alpha_p(t_k) \in \{0, 1\}$ is a binary value, indicating whether the controller has failure or not. When $\alpha_p(t_k) = 1$, it means that the controller is working normally, while the controller has fault if $\alpha_p(t_k) = 0$. This value is not known in advance, but the statistic value is known, i.e., $\mathbb{E}\left\{\alpha_p(t_k) = 1\right\} = \bar{\alpha}_p$ is known for controller design. In implementation of the controller, the actuator will receive zero control input signal when the controller has failure.

To simplify the presentation, we define the following notations:

$$x(t_k) = \left[x_1^T(t_k)\ x_2^T(t_k) \cdots x_N^T(t_k) \right]^T, u(t_k) = \left[u_1^T(t_k)\ u_2^T(t_k) \cdots u_N^T(t_k) \right]^T,$$
$$v(t_k) = \left[v_1^T(t_k)\ v_2^T(t_k) \cdots v_N^T(t_k) \right]^T, z(t_k) = \left[z_1^T(t_k)\ z_2^T(t_k) \cdots z_N^T(t_k) \right]^T,$$
$$\Pi_\alpha = \mathrm{diag}\{\bar{\alpha}_1 I, \bar{\alpha}_2 I, \ldots, \bar{\alpha}_N I\}, \Pi_{\rho(t_k)} = \mathrm{diag}\{\Pi_{\rho_1(t_k)}, \Pi_{\rho_2(t_k)}, \ldots, \Pi_{\rho_N(t_k)}\},$$
$$A_{s(t_k)} = \begin{bmatrix} A_{s(t_k)}^{11} & A_{s(t_k)}^{12} & \cdots & A_{s(t_k)}^{1N} \\ A_{s(t_k)}^{21} & A_{s(t_k)}^{22} & \cdots & A_{s(t_k)}^{2N} \\ \vdots & \vdots & \ddots & \vdots \\ A_{s(t_k)}^{N1} & A_{s(t_k)}^{N2} & \cdots & A_{s(t_k)}^{NN} \end{bmatrix}, B_{s(t_k)} = \mathrm{diag}\{B_{s(t_k)}^1, B_{s(t_k)}^2, \ldots, B_{s(t_k)}^N\},$$
$$E_{s(t_k)} = \mathrm{diag}\{E_{s(t_k)}^1, E_{s(t_k)}^2, \ldots, E_{s(t_k)}^N\},\ L = \mathrm{diag}\{L_1, L_2, \ldots, L_N\},$$
$$\Phi_p = \mathrm{diag}\{0, \ldots, \underbrace{I}_{p-th}, \ldots, 0\}, \Delta(t_k) = \mathrm{diag}\{\Delta_1(t_k), \Delta_2(t_k), \ldots, \Delta_N(t_k)\},$$
$$K_{\sigma(t_k)} = \begin{bmatrix} b_{11}^{\sigma(t_k)} K_{11}^{\sigma(t_k)} & b_{12}^{\sigma(t_k)} K_{12}^{\sigma(t_k)} & \cdots & b_{1N}^{\sigma(t_k)} K_{1N}^{\sigma(t_k)} \\ b_{21}^{\sigma(t_k)} K_{21}^{\sigma(t_k)} & b_{22}^{\sigma(t_k)} K_{22}^{\sigma(t_k)} & \cdots & b_{2N}^{\sigma(t_k)} K_{2N}^{\sigma(t_k)} \\ \vdots & \vdots & \ddots & \vdots \\ b_{N1}^{\sigma(t_k)} K_{N1}^{\sigma(t_k)} & b_{N2}^{\sigma(t_k)} K_{N2}^{\sigma(t_k)} & \cdots & b_{NN}^{\sigma(t_k)} K_{NN}^{\sigma(t_k)} \end{bmatrix}.$$

Then, we have the following closed-loop system,

$$\begin{cases} x(t_{k+1}) = \left[A_{s(t_k)} + B_{s(t_k)}\Pi_\alpha K_{\sigma(t_k)}\left(I + \Delta(t_k)\right)\Pi_{\rho(t_k)}\right]x(t_k) \\ \quad + E_{s(t_k)}v(t_k) + \sum\limits_{p=1}^{N}\theta_p(t_k)\left[B_{s(t_k)}\Phi_p K_{\sigma(t_k)}\left(I + \Delta(t_k)\right)\Pi_{\rho(t_k)}\right]x(t_k), \\ z(t_k) = Lx(t_k), \end{cases} \tag{13.10}$$

where $\theta_p(t_k) = \alpha_p(t_k) - \bar{\alpha}_p$. The system (13.10) has three switching signals, and analysis of such a complex system is difficult. Here, we define a mapping: $\{\sigma(t_k), \rho(t_k), s(t_k)\} \to \delta(t_k)$, then for each $\delta(t_k) = i$, we have

$$\begin{cases} x(t_{k+1}) = \left[A_i x(t_k) + B_i\Pi_\alpha K_i\left(I + \Delta(t_k)\right)\Pi_i\right]x(t_k) + E_i v(t_k) \\ \qquad + \sum\limits_{p=1}^{N}\theta_p(t_k)\left[B_i\Phi_p K_i\left(I + \Delta(t_k)\right)\Pi_i\right]x(t_k), \\ z(t_k) = Lx(t_k). \end{cases} \tag{13.11}$$

One sees that the system (13.11) is a switched system, and $\delta(t_k) \in \Omega = \left\{1, 2, \ldots, M \times N_3 \times \prod\limits_{p=1}^{N} n_p\right\}$. As in the last few chapters, we will also use the average dwell time approach to analyze (13.11).

The control problem is now formulated as follows: design the controller in form of (13.9) such that the closed-loop system (13.11) is robustly exponentially stable in the mean-square sense and achieves a prescribed H_∞ performance level in the presence of nonuniform sampling, the measurement size reduction, the communication rate reduction as well as the controller failure.

Definition 13.1 The system (13.11) is called robustly exponentially stable in the mean-square sense, if there exist some scalars $\pi > 0$ and $0 < \chi < 1$, such that the solution $\tilde{x}$ of system (13.11) satisfies $\mathbb{E}\{\|x(t_k)\|\} < \pi\chi^{(k-k_0)}\|x(t_0)\|, \forall t_k \geq t_0$.

Definition 13.2 For a given scalar $\gamma > 0$, the system (13.11) is said to be robustly exponentially stable in the mean-square sense and achieves a prescribed H_∞ performance γ, if it is exponentially stable and under zero initial condition, $\sum\limits_{k=0}^{+\infty}\mathbb{E}\{z^T(t_k)z(t_k)\} \leq \sum\limits_{k=0}^{+\infty}\gamma^2 v^T(t_k)v(t_k)$ holds for all nonzero $v(t_k) \in l_2[0, \infty)$.

13.3 Main Results

In this section, a sufficient condition is firstly presented such that the closed-loop system (13.11) is exponentially stable in the mean-square sense with a prescribed H_∞ performance level.

Theorem 13.1 *For some given scalars $\tau > 0, \mu > 1, 0 < \lambda_i < 1, \delta_p > 0$, $0 < \lambda < 1$, and controller gains K_i, if there exist positive-definite matrices P_i, and a positive scale ε such that the following inequalities,*

$$\begin{bmatrix} \Sigma_1 & \Sigma_2 & \Sigma_3 & \Sigma_4 & \Sigma_5 & 0 \\ * & -P_i^{-1} & 0 & 0 & 0 & \Sigma_6 \\ * & * & -I & 0 & 0 & 0 \\ * & * & * & \bar{P}_i & 0 & \Sigma_7 \\ * & * & * & * & -\varepsilon I & 0 \\ * & * & * & * & * & -\varepsilon I \end{bmatrix} < 0, \tag{13.12}$$

$$P_i \le \mu P_j, i \ne j, \tag{13.13}$$

$$T_a > T_a^* = -\frac{\ln \mu}{\ln \lambda}, \tag{13.14}$$

hold for all $i, j \in \Omega$, then the closed-loop system (13.11) is exponentially stable in the mean-square sense with decay rate $\chi = \sqrt{\lambda_b \mu^{1/T_a}}$ and achieves a prescribed H_∞ performance level $\gamma = \tau\sqrt{\frac{(1-\lambda_a)}{1-\lambda_b/\lambda}}$, where $\lambda_a = \min_{i\in\Omega}\{\lambda_i\}$, $\lambda_b = \max_{i\in\Omega}\{\lambda_i\}$, $\lambda > \lambda_b$, and

$$\Sigma_1 = \begin{bmatrix} -\lambda_i P_i & 0 \\ 0 & -\tau^2 I \end{bmatrix}, \Sigma_2 = \begin{bmatrix} A_i^T + \Pi_i^T K_i^T \Pi_\alpha^T B_i^T \\ E_i^T \end{bmatrix}, \Sigma_3 = \begin{bmatrix} L^T \\ 0 \end{bmatrix},$$

$$\Sigma_4 = \begin{bmatrix} \theta_1 \Pi_i^T K_i^T \Phi_1^T B_i^T & \theta_2 \Pi_i^T K_i^T \Phi_2^T B_i^T & \cdots & \theta_N \Pi_i^T K_i^T \Phi_N^T B_i^T \\ 0 & 0 & \cdots & 0 \\ \vdots & \vdots & \ddots & \vdots \\ 0 & 0 & \cdots & 0 \end{bmatrix},$$

$$\Sigma_5 = \begin{bmatrix} \Pi_i^T \Lambda\varepsilon \\ 0 \end{bmatrix}, \Sigma_6 = B_i \Pi_\alpha K_i, \Sigma_7 = \begin{bmatrix} \theta_1 B_i \Phi_1 K_i \\ \theta_2 B_i \Phi_2 K_i \\ \vdots \\ \theta_N B_i \Phi_N K_i \end{bmatrix},$$

$\Lambda = \text{diag}\{\delta_1, \delta_2, \ldots, \delta_n\}$, $\theta_p = \sqrt{\bar{\alpha}_p(1-\bar{\alpha}_p)}$, $p = 1, 2, \ldots, n$,
$\bar{P}_i = \text{diag}\{-P_i, -P_i, \ldots, -P_i\}$.

Proof Choose the following Lyapunov functional:

$$V_{\delta(k)}(k) = x^T(k) P_{\delta(k)} x(k). \tag{13.15}$$

Then for each $\delta(k) = i$ and $\forall i \in \Omega$, it follows that

$$
\begin{aligned}
&\mathbb{E}\left\{V_i(k+1)-\lambda_i V_i(k)+\Upsilon(k)\right\}\\
&=\left(\left[A_i x(t_k)+B_i\Pi_\alpha K_i\left(I+\Delta(t_k)\right)\Pi_i\right]x(t_k)+E_i v(t_k)\right)^T\\
&\times P_i\left(\left[A_i x(t_k)+B_i\Pi_\alpha K_i\left(I+\Delta(t_k)\right)\Pi_i\right]x(t_k)+E_i v(t_k)\right)\\
&+\sum_{p=1}^{N}\theta_p^2\left(\left[B_i\Phi_p K_i\left(I+\Delta(t_k)\right)\Pi_i\right]x(t_k)\right)^T P_i\left(\left[B_i\Phi_p K_i\left(I+\Delta(t_k)\right)\Pi_i\right]x(t_k)\right)\\
&+[Lx(t_k)]^T\left[Lx(t_k)\right]-\tau^2 v^T(t_k)v(t_k),
\end{aligned}
\tag{13.16}
$$

where $\Upsilon(k)=z^T(k)z(k)-\tau^2 v^T(k)v(k)$. By using Lemma 2.1, it is easy to see that

$$
\mathbb{E}\left\{V_i(k+1)-\lambda_i V_i(k)+\Upsilon(k)\right\}<0 \tag{13.17}
$$

is equivalent to

$$
\Theta_1+\Theta_2\Delta(k)\Theta_3^T+\Theta_3\Delta(k)\Theta_2^T<0, \tag{13.18}
$$

where

$$
\Theta_1=\begin{bmatrix}\Sigma_1 & \Sigma_2 & \Sigma_3 & \Sigma_4\\ * & -P_i^{-1} & 0 & 0\\ * & * & -I & 0\\ * & * & * & -P_i\end{bmatrix},\ \Theta_2=\begin{bmatrix}\bar{\Sigma}_5\\ 0\\ 0\\ 0\end{bmatrix},\ \Theta_3=\begin{bmatrix}0\\ \Sigma_6\\ 0\\ \Sigma_7\end{bmatrix},
$$

with

$$
\bar{\Sigma}_5=\begin{bmatrix}\Pi_i^T\\ 0\end{bmatrix}.
$$

By some manipulations, (13.18) can be rewritten as

$$
\Theta_1+\Theta_2\Lambda\bar{\Delta}(k)\Theta_3^T+\Theta_3^T\Lambda\bar{\Delta}(k)\Theta_2<0, \tag{13.19}
$$

where $\bar{\Delta}(k)=\frac{\Delta(k)}{\Lambda}$. It follows that $\left\|\frac{\Delta(k)}{\Lambda}\right\|\le I$. Based on Lemma 2.2, one sees that (13.19) holds if and only if (13.12) holds. Hence, we see

$$
\mathbb{E}\left\{V_i(k+1)-\lambda_i V_i(k)+\Upsilon(k)\right\}<0. \tag{13.20}
$$

For the switching time instant $k_0<k_1<\cdots<k_l<\cdots<k_t$, $l=1,2,\ldots,t$, we define the switching numbers of $\delta(k)$ over (k_0,k) as $N_\delta(k_0,k)$, then one has

$$
\mathbb{E}\{V_l(k)\}\le\mathbb{E}\{\lambda_l^{k-k_l}V_l(k_l)\}-\sum_{s=k_l}^{k-1}\lambda_l^{k-s-1}\mathbb{E}\{\Upsilon(s)\}. \tag{13.21}
$$

It follows from (13.13) and (13.21) that

$$
\begin{aligned}
&\mathbb{E}\{V_{\delta(k_l)}(k)\}\\
&\le \lambda_{\delta(k_l)}^{k-k_l}\mathbb{E}\{V_{\delta(k_l)}(k_l)\} - \sum_{s=k_l}^{k-1}\lambda_{\delta(k_l)}^{k-s-1}\mathbb{E}\{\Upsilon(s)\}\\
&\le \lambda_{\delta(k_l)}^{k-k_l}\mu\mathbb{E}\{V_{\delta(k_{l-1})}(k_l)\} - \sum_{s=k_l}^{k-1}\lambda_{\delta(k_l)}^{k-s-1}\mathbb{E}\{\Upsilon(s)\}\\
&\le \lambda_{\delta(k_l)}^{k-k_l}\mu\left[\lambda_{\delta(k_{l-1})}^{k_l-k_{l-1}}\mathbb{E}\{V_{\delta(k_{l-1})}(k_{l-1})\} - \sum_{s=k_{l-1}}^{k_l-1}\lambda_{\delta(k_{l-1})}^{k-s-1}\mathbb{E}\{\Upsilon(s)\}\right]\\
&\quad - \sum_{s=k_l}^{k-1}\lambda_{\delta(k_l)}^{k-s-1}\mathbb{E}\{\Upsilon(s)\}\\
&\le \cdots \le \mu^{N_\delta(k_0,k)}\lambda_{\delta(k_l)}^{k-k_l}\lambda_{\delta(k_{l-1})}^{k_l-k_{l-1}}\cdots\lambda_{\delta(k_0)}^{k_1-k_0}V_{\delta(k_0)}(k_0) - \Theta(\Upsilon),
\end{aligned}
\tag{13.22}
$$

where

$$
\begin{aligned}
\Theta(\Upsilon) &= \mu^{N_\delta(k_0,k-1)}\lambda_{\sigma(k_l)}^{k-k_l}\prod_{s=1}^{l-1}\lambda_{\sigma(k_s)}^{k_{s+1}-k_s}\sum_{s=k_0}^{k_1-1}\lambda_{\sigma(k_0)}^{k_1-1-s}\mathbb{E}\{\Upsilon(s)\}\\
&\quad + \mu^{N_\delta(k_0,k-1)-1}\lambda_{\sigma(k_l)}^{k-k_l}\prod_{s=2}^{l-1}\lambda_{\sigma(k_j)}^{k_{j+1}-k_j}\sum_{s=k_1}^{k_2-1}\lambda_{\sigma(k_1)}^{k_2-1-s}\mathbb{E}\{\Upsilon(s)\}\\
&\quad + \cdots + \mu^0\prod_{s=k_l}^{k-1}\lambda_{\sigma(k_l)}^{k-1-s}\mathbb{E}\{\Upsilon(s)\}.
\end{aligned}
$$

Now, we consider the exponential stability of the system (13.11) with $v(k) = 0$. One has

$$
\begin{aligned}
&\mathbb{E}\{V_{\delta(k_l)}(k)\}\\
&\le \mu^{N_\delta(k_0,k)}\lambda_{\sigma(k_l)}^{k-k_l}\lambda_{\rho(k_{l-1})}^{k_l-k_{l-1}}\cdots\lambda_{\rho(k_0)}^{k_1-k_0}V_{\rho(k_0)}(k_0)\\
&\le \mu^{N_\delta(k_0,k)}\lambda_b^{k-k_0}V_{\delta(k_0)}(k_0)\\
&\le \left(\mu^{1/T_a}\lambda_b\right)^{k-k_0}V_{\delta(k_0)}(k_0) = \chi^{2(k-k_0)}V_{\delta(k_0)}(k_0),
\end{aligned}
\tag{13.23}
$$

which yields $\mathbb{E}\left\{\|x(k)\|^2\right\} \le \frac{\varphi_2}{\varphi_1}\chi^{2(k-k_0)}\|x(k_0)\|^2$, where $\varphi_1 = \min_{i\in\Omega}\sigma_{\min}(P_i)$, $\varphi_2 = \max_{i\in\Omega}\sigma_{\max}(P_i)$, $\chi = \sqrt{\lambda_b\mu^{1/T_a}}$. Therefore, one can readily obtain $\chi < 1$ from condition (13.14). According to Definition 13.1, the closed-loop system (13.11) is exponentially stable in the mean-square sense with $v(k) = 0$.

For the H_∞ performance level, we consider $v(k) \neq 0$. Under the zero initial condition, it follows from (13.22) that

$$
\sum_{s=k_0}^{k-1}\mu^{N_\delta(s,k-1)}\lambda_a^{k-s-1}\mathbb{E}\{z^T(s)z(s)\} \le \tau^2\sum_{s=k_0}^{k-1}\mu^{N_\delta(s,k-1)}\lambda_b^{k-s-1}v^T(s)v(s). \tag{13.24}
$$

With the average dwell time condition (13.14), it is easy to see $\frac{N_\delta(s,k-1)}{k-s-1} < -\frac{\ln\lambda}{\ln\mu}$. Since $\mu > 1$, we obtain $\ln\mu^{N_\delta(s,k-1)} < \ln\lambda^{-(k-s-1)}$, and $1 < \mu^{N_\varpi(s,k-1)} < \lambda^{-(k-s-1)}$. Then, it can be readily seen that

$$
\sum_{s=k_0}^{k-1}\lambda_a^{k-s-1}\mathbb{E}\{z^T(s)z(s)\} < \tau^2\sum_{s=k_0}^{k-1}(\lambda_b/\lambda)^{k-s-1}\lambda^{k-s-1}v^T(s)v(s). \tag{13.25}
$$

Summing (13.25) from $k = k_0 + 1$ to $k = \infty$ and changing the order of summation yield

$$\sum_{s=k_0}^{+\infty} \mathbb{E}\{z^T(s)z(s)\} \sum_{k=s+1}^{+\infty} \lambda_a^{k-s-1} < \tau^2 \sum_{s=k_0}^{+\infty} v^T(s)v(s) \sum_{k=s+1}^{+\infty} (\lambda_b/\lambda)^{k-s-1}. \quad (13.26)$$

Since $\sum_{k=s+1}^{+\infty} \lambda_a^{k-s-1} = \frac{1}{1-\lambda_a}$ and $\sum_{k=s+1}^{+\infty} (\lambda_b/\lambda)^{k-s-1} = \frac{1}{1-(\lambda_b/\lambda)}$, we have

$$\sum_{s=k_0}^{+\infty} \mathbb{E}\{z^T(s)z(s)\} < \gamma^2 \sum_{s=k_0}^{+\infty} v^T(s)v(s), \quad (13.27)$$

where $\gamma = \tau\sqrt{\frac{1-\lambda_a}{1-\lambda_b/\lambda}}$. It is noted that $\lambda_b < \lambda$, which ensures $\gamma > 0$. Let $k_0 = 0$, the system (13.11) is exponentially stable in the mean-square sense and achieves a prescribed H_∞ performance level γ. This completes the proof.

We see from Theorem 13.1 that the conditions (13.13) and (13.14) are linear matrix inequalities which can be solved efficiently by available software toolboxes. The challenge lies in the condition (13.12), where we have P_i and P_i^{-1}. This condition is known to be a nonlinear matrix inequality. The CCL algorithm is employed to determine the controller gains.

Theorem 13.2 *For some given scalars $\tau > 0, \mu > 1, 0 < \lambda_i < 1, \delta_p > 0$, and $0 < \lambda < 1$, if there exist positive-definite matrices P_i, T_i, and a positive scale ε such that the following optimization problem has a feasible solution, then the control problem is solvable.*

Optimization problem:

$$\min \ \mathrm{Tr}\left(\sum_{i=1}^{\mathrm{Z}} (T_i \times P_i)\right) \quad (13.28)$$

s.t. (13.13), (13.14) and

$$\begin{bmatrix} T_i & I \\ I & P_i \end{bmatrix} \geq 0, \quad (13.29)$$

$$\begin{bmatrix} \Sigma_1 & \Sigma_2 & \Sigma_3 & \Sigma_4 & \Sigma_5 & 0 \\ * & -T_i & 0 & 0 & 0 & \Sigma_6 \\ * & * & -I & 0 & 0 & 0 \\ * & * & * & \bar{T}_i & 0 & \Sigma_7 \\ * & * & * & * & -\varepsilon I & 0 \\ * & * & * & * & * & -\varepsilon I \end{bmatrix} < 0, \quad (13.30)$$

where $\bar{T}_i = \text{diag}\{\underbrace{T_i, T_i, \ldots, T_i}_{N}\}$, and $\mathrm{Z} = M \times N_3 \times \prod_{l=1}^{N} n_l$.

Remark 13.1 To solve the above optimization problem, the H_∞ performance related parameter τ should be given first. Then in order to obtain the minimal H_∞ performance level, one may first choose a relative large value for τ, and decrease this value until the above optimization has no solution. Eventually, one has the minimal τ, we obtain the minimal H_∞ performance level as $\gamma = \tau\sqrt{\frac{(1-\lambda_a)}{1-\lambda_b/\lambda}}$.

13.4 An Illustrative Example

In this section, a real-world example is given to show the effectiveness of the proposed design. The example under consideration is the interconnected chemical reactors composing of two non-isothermal continuous stirred-tank reactors (CSTRs) with interconnections between reactors. System structure is depicted in Fig. 13.2. The

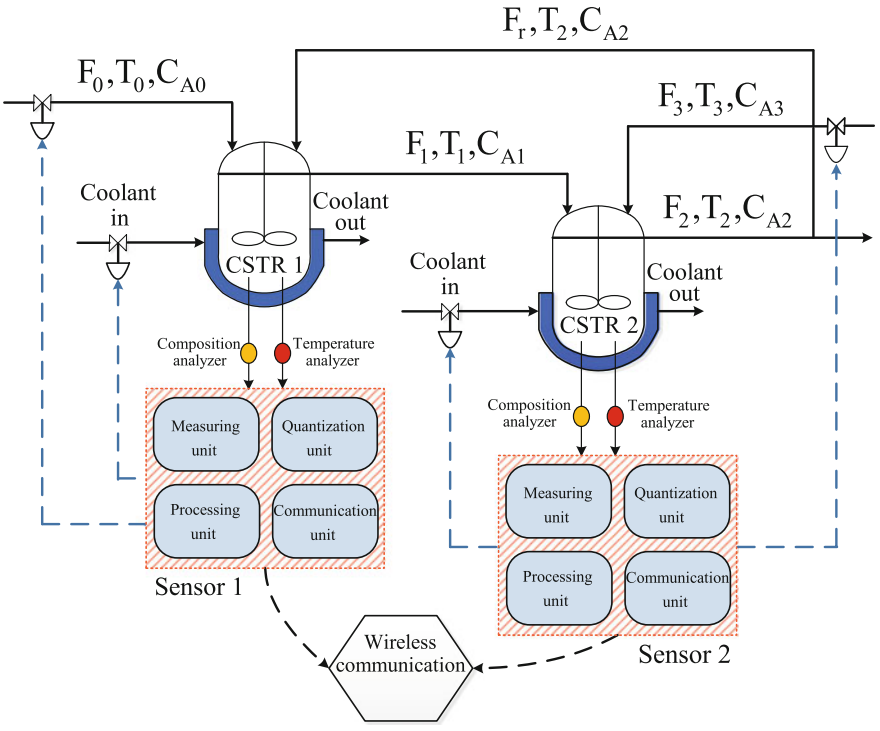

Fig. 13.2 Process flow diagram of two interconnected CSTR systems

CSTR system can be described by the following LTI system when it is linearized around the point of $((T_1^s, C_{A1}^s, T_2^s, C_{A2}^s) = 457.9\,\text{K}, 1.77\,\text{kmol/m}^3, 415.5\,\text{K}, 1.75\,\text{kmol/m}^3)$:

$$\begin{cases} \dot{x}_1(t) = A_{11}^c x_1(t) + \bar{B}_1^c u_1(t) + A_{12}^c x_2(t), \\ \dot{x}_2(t) = A_{22}^c x_2(t) + \bar{B}_2^c u_2(t) + A_{21}^c x_1(t), \end{cases} \tag{13.31}$$

where x_i and u_i are the state and input vector for the i-th subsystem, respectively, and they are defined by

$$x_1 = \begin{bmatrix} \frac{T_1 - T_1^s}{T_1^s} \\ \frac{CA_1 - C_{A1}^s}{C_{A1}^s} \end{bmatrix}, x_2 = \begin{bmatrix} \frac{T_2 - T_2^s}{T_2^s} \\ \frac{CA_2 - C_{A2}^s}{C_{A2}^s} \end{bmatrix},$$
$$u_1 = \begin{bmatrix} Q_1 \\ C_{A0} - C_{A0}^s \end{bmatrix}, u_2 = \begin{bmatrix} Q_2 \\ C_{A03} - C_{A03}^s \end{bmatrix}.$$

With the values of the process parameters given in Table 12.1, the matrices in (13.32) are obtained as

$$A_{11}^c = \begin{bmatrix} 25.2914 & 4.9707 \\ -78.028 & -45.9368 \end{bmatrix}, A_{12}^c = \begin{bmatrix} 31.7512 & 0 \\ 0 & 34.6421 \end{bmatrix},$$
$$\bar{B}_1^c = \begin{bmatrix} 9.45 \times 10^{-6} & 0 \\ 0 & 2.8234 \end{bmatrix},$$
$$A_{22}^c = \begin{bmatrix} -2.8370 & 1.4157 \\ -22.4506 & -24.8828 \end{bmatrix}, A_{21}^c = \begin{bmatrix} 14.6953 & 0 \\ 0 & 13.4690 \end{bmatrix},$$
$$\bar{B}_2^c = \begin{bmatrix} 3.47 \times 10^{-6} & 0 \\ 0 & 5.7071 \end{bmatrix}.$$

In this example, the disturbance weight matrices are taken as $E_1 = \begin{bmatrix} 0 \\ 1 \end{bmatrix}$, and $E_2 = \begin{bmatrix} 1 \\ 0 \end{bmatrix}$. We now discrete the above system by using two sampling periods, i.e., $h_k \in \{T_0, 2T_0\}$, with $T_0 = 0.0025\,\text{h}$. Then, based on our sampling approach, a discrete-time interconnected system with two subsystems is obtained as

$$x_i(t_{k+1}) = A_{s(t_k)}^{ii} x(t_k) + \sum_{j=1, j\neq i}^{2} A_{s(t_k)}^{ij} x_j(t_k) + B_{s(t_k)}^{i} u_i(t_k) + E_{s(t_k)}^{i} v_i(t_k), \tag{13.32}$$

where $s(t_k) \in \Omega_1 = \{1, 2\}$, and other matrices are not given for presentation brevity.

In this example, we aim to design two distributed smart controllers to stabilize this plant. Due to the power constraint, at each sampling time instant, only one element of the state $x_i(t_k)$ is chosen and this element is then quantized for transmission. Hence, $\Pi_{\rho_1(t_k)} \in \{[1\ 0], [0\ 1]\}$, and $\Pi_{\rho_2(t_k)} \in \{[1\ 0], [0\ 1]\}$. The quantization density is taken as $\rho_1 = 0.9$, and $\rho_1 = 0.8$. In the distributed control system, two smart sensors

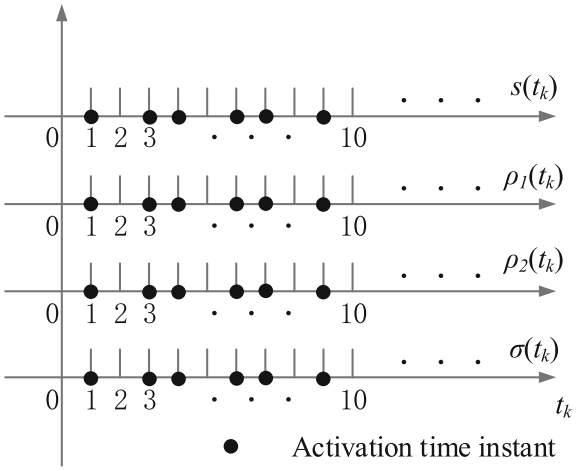

Fig. 13.3 Switching signals

are allowed to communicate with each other to improve the control performance. But as we know, the communication will consume much energy. Hence, in this example, controller 2 does not transmit its information to controller 1, and controller 1 transmits its information to the controller 2 intermittently. The topologies are $\mathbb{B}^1 = \begin{bmatrix} 1 & 0 \\ 0 & 1 \end{bmatrix}$, and $\mathbb{B}^2 = \begin{bmatrix} 1 & 0 \\ 1 & 1 \end{bmatrix}$.

The controller failure rates are taken as 10, and 20%, respectively, that is $\bar{\alpha}_1 = 0.9$, and $\bar{\alpha}_2 = 0.8$. For simulation purpose, the activation time instant of the switching signals is assumed to be as in Fig. 13.3, where the signals are varying periodically. According to the activation process in Fig. 13.3, we have $\Pi_{\rho(t_k)} \in \left\{ \begin{bmatrix} 1 & 0 \\ 1 & 0 \end{bmatrix}, \begin{bmatrix} 0 & 1 \\ 0 & 1 \end{bmatrix} \right\}$. Moreover, one also sees from Fig. 13.3 that the closed-loop system (13.33) can be modeled as a switched system with two subsystems. In this simulation, we run experiment for 100 time steps. The disturbance signals are taken as

$$v_1(k) = v_2(k) = \begin{cases} \text{rand} - 0.5, & 1 \le k \le 50, \\ 0, & \text{others}, \end{cases} \tag{13.33}$$

where rand is random function generating a value between 0 to 1. Figure 13.4 shows the evolution of the above disturbance signal. Under this signal, Fig. 13.5 shows the state evolution of system (13.33) without control. It is seen that the original system is unstable. It follows from Fig. 13.3 that $T_a = 1.4925$. Choosing $\lambda_1 = 0.92$, $\lambda_2 = 0.94$, $\lambda = 0.95$ and $\mu = 1.05$, we have $\lambda_a = 0.92$ and $\lambda_b = 0.94$. It is seen that $T_a^* = 0.9512 < T_a$, which means that (13.13) holds. To illustrate the performance against the unknown disturbance, we take $L_1 = L_2 = \begin{bmatrix} 0.5 & 0.5 \end{bmatrix}$. By solving the optimization problem (13.28), we have the H_∞ performance level $\gamma = 0.0357$. With

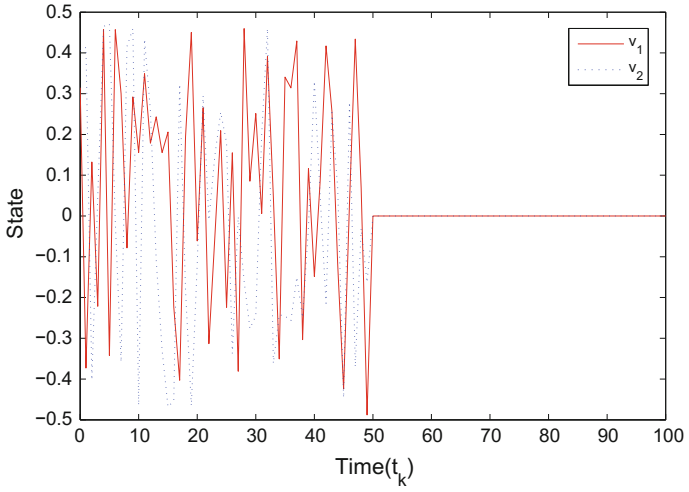

Fig. 13.4 The trajectories of the disturbance

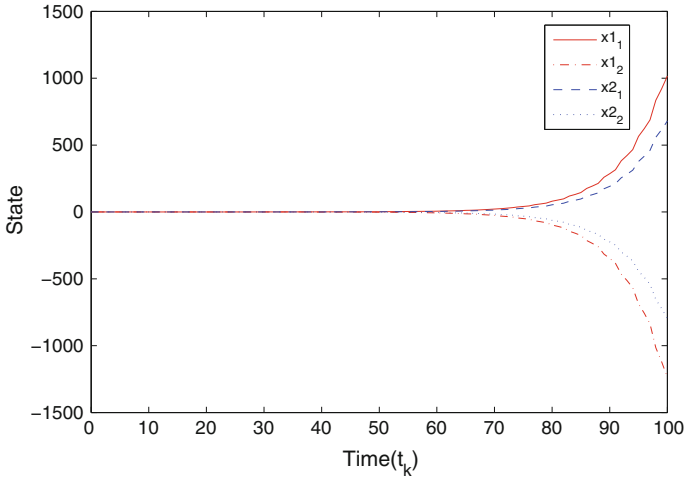

Fig. 13.5 The trajectories of the open-loop system

the controller, we depict the state trajectories in Fig. 13.6. It is seen that when the disturbance turns to be zero, the state will also becomes zero. One hundred samples on the H_∞ performance level are shown in Fig. 13.7. It is clear that our control design can guarantee the control performance.

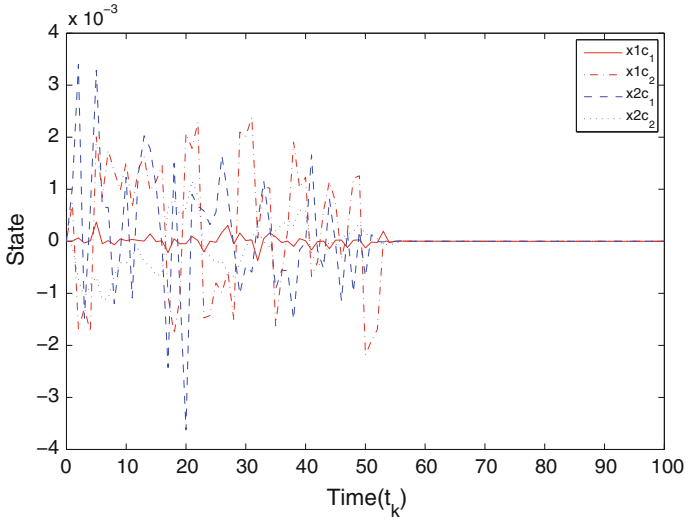

Fig. 13.6 The trajectories of the closed-loop system

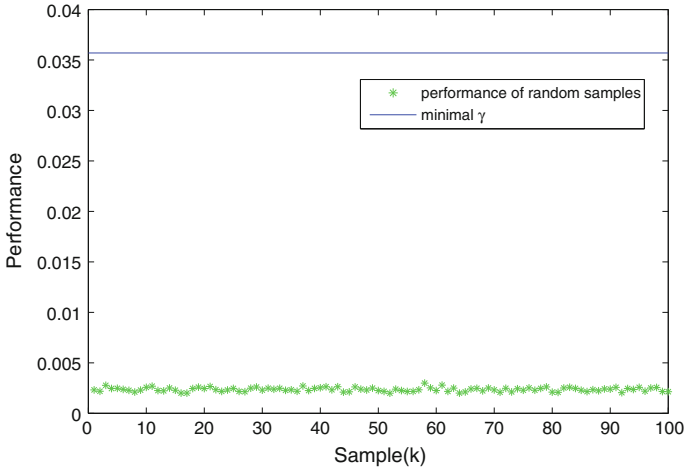

Fig. 13.7 On hundred samples on the H_∞ performance level

13.5 Conclusions

We have studied the distributed stabilization of a class of large-scale systems with power constraint. The techniques such as reducing the measurement size and communication rates are introduced to achieve the energy-efficiency goal. Based on the switched system theory, a sufficient condition has been proposed such that the filtering error system is exponentially stable in the mean-square sense and also achieves a

prescribed H_∞ performance level. The controller gains are determined by using the CCL algorithm. Finally, the effectiveness of the proposed design is illustrated by the CSTR system.

It should be noted that in many complex networks, the interconnection of a target control plant may change due to possible disturbances, fault or attack. Then, how to handle the topology switching of plant network is the topic in the next chapter.

Chapter 14
Distributed Control with Event-Based Communication and Topology Switching

14.1 Introduction

In Chaps. 11–13, the connectivity of topology in plant network is assumed to be fixed. However, such an assumption may not hold in many practical systems. Take the smart grid system as an example, the transmission control has been identified as a valuable mechanism for a variety of benefits, e.g., improving the system reliability and the market surplus. However, the use of transmission as a controllable asset will inevitably lead to the topology switching of a power grid [1]. Another example is the possible cyber or physical attacks on the modern industrial systems, in which the topology may be changed by such attacks, see [2] for more details. The robust distributed control of large-scale systems under the uncertain topology was discussed in [3], and the novelty is that they give the robustness analysis under the topology uncertainty and look for some appropriate control rules for the desired H_∞ robust performance. However, no topology switching is taken into account. Very recently in [4], the state estimation for a class of complex networks with topology switching was investigated. An asynchronous estimator was designed to overcome the difficulty that the estimator can not access to the topology information instantly. But they only considered the decentralized state estimation problem, and the topology switching is assumed to satisfy a Markovian process. How to design a distributed control algorithm for a class of large-scale networked control systems with a general topology switching phenomenon is a challenging work.

Motivated by the above discussions, we pay our attention on the distributed control for a class of large-scale networked control systems with energy constraints and topology switching. First, the event-based communication protocol is employed to reduce the unnecessary communications between the plant network and controller network. Such an on-line scheduling not only alleviates the communication constraint problem, but also achieves a better control performance. The selected measurement signal is then quantized by a logarithmic quantizer for transmission. A group of asynchronous controllers are designed when the real time information about the topology is not available in such a networked environment. A stochastic switched system

D. Zhang et al., *Filtering and Control of Wireless Networked Systems*,
Studies in Systems, Decision and Control 97, DOI 10.1007/978-3-319-53123-6_14

model with sector bound uncertainties is proposed to capture the communication constraints and topology switching phenomena. A sufficient condition is developed that guarantees the globally exponential stability of the overall system by using the Lyapunov direct method and the controller gains are determined by using the cone complementarity linearization (CCL) algorithm. Finally, a simulation study on the CSTR systems is performed and the effectiveness of controller design algorithm is verified.

14.2 Problem Formulation

In this chapter, we suppose that a networked control system consists of a number of subsystems, each comprising of a plant and a controller, coupled together in a networked structure. The interaction of plants with each other forms the *plant network*. Control signals are exchanged using the *control network*. The system is depicted in Fig. 14.1. In the following, each component is described in detail.

Consider a discrete-time large-scale system with N subsystems with the p-th subsystem described as

$$\begin{cases} x_p(k+1) = A_p x_p(k) + \sum\limits_{q=1,q\neq p}^{N} W_{pq}^{\sigma(k)} x_q(k) \\ \qquad\qquad +F_p g(x_p(k)) + E_p u_p(k) + B_p w_p(k), \\ z_p(k) = L_p x_p(k),\ p = 1, 2, \ldots, N, \end{cases} \tag{14.1}$$

where $x_p(k) \in \mathbb{R}^{n_p}$ is the state vector, $u_p(k) \in \mathbb{R}^{m_p}$ is the control input vector, $g(x_p(k))$ is the nonlinear perturbation on the p-th subsystem and it is assumed to satisfy $\|g(x_p(k))\| \leq \|Ux_p(k)\|$, in which U is a bounding matrix. $w_p(k) \in \mathbb{R}^{n_p}$ is the unknown disturbance, which belongs to $l_2[0, \infty)$. $z_p(k) \in \mathbb{R}^{l_p}$ is the output vector. $W_{pq}^{\rho(k)}$ is the coupling matrix of the plant network under a certain topology and $\rho(k) \in \Upsilon_1 = \{1, 2, 3, \ldots, M\}$ is a piecewise signal describing which topology is activated. A_p, $W_{pq}^{\sigma(k)}$, F_p, E_p, B_p and L_p are known matrices with appropriate dimensions. We assume that the pair (A_p, E_p) is controllable. For the switching signal $\rho(k)$, we define

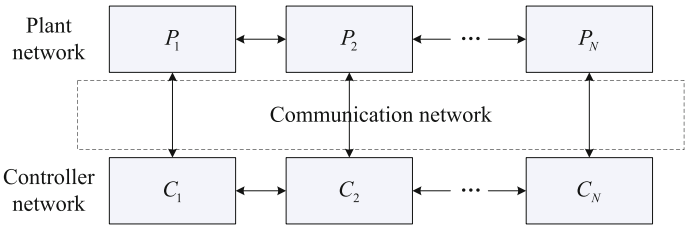

Fig. 14.1 Structure of the considered distributed control system

the switching sequence $\{(i_1, k_1), (i_2, k_2), \ldots, (i_t, k_t), \ldots, |i_t \in \Upsilon_1, l = 1, 2, \ldots\}$. It indicates that the i_l-th topology is activated when $k \in [k_l, k_{l+1})$.

Our purpose is to design a state feedback based controller to manage the plant, but due to the communication constraint, the state measurement might not be allowed to be transmitted for controller network design. In this chapter, the event-based communication protocol is first employed such that the transmission only occurs if it changes a lot. The event generation function is taken as $f_p(\omega_p(k), \tau_p) = \varpi_p^T(k)\Sigma_p\varpi_p(k) - \tau_p x_p^T(k)\Sigma_p x_p(k)$, where $\varpi_p(k)$ is the error between two successive transmissions, i.e., $\varpi_p(k) = x_p(k_l) - x_p(k)$, $x_p(k_l)$ is the next possible transmitted state measurement and $x_p(k)$ is the last transmitted one. $\Sigma_p > 0$ is a weighting matrix and $\tau_p \in [0, 1)$ is a slack variable, which can be tuned in the design. In this chapter, the transmission only occurs when the following event happens:

$$f_p(\varpi_p(k), \tau_p) > 0. \tag{14.2}$$

The event-triggered time instant can be determined by

$$k_{l+1}^p = \inf\left\{k \in \mathrm{N} | \, k > k_l^p, \, f_p(\varpi_p(k), \tau_p) > 0\right\},$$

which might not be equal to the current sampling time k.

The transmitted measurement can be described as $\tilde{x}_p(k) = x_p(k_l)$, which is then quantized by a logarithmic quantizer. Note that the logarithmic quantizer is static and time-invariant, and it has been widely used in many digital and networked control systems. For any $p = 1, 2, \ldots, N$, we define the following set of quantization levels:

$$\begin{aligned} U_p = &\left\{\pm\kappa_i^{(p)}, \kappa_i^{(p)} = \rho_p^i \kappa_0^{(p)}, i = 0, \pm 1, \pm 2, \ldots\right\} \\ &\cup \left\{\pm\kappa_0^{(p)}\right\} \cup \{0\}, 0 < \rho_p < 1, \kappa_0^{(p)} > 0. \end{aligned} \tag{14.3}$$

The quantized output of $Q_p(\bullet)$ is then given by

$$Q_p(v_p) = \begin{cases} \kappa_i^{(p)}, & \text{if } \frac{1}{1+\delta_p}\kappa_i^{(p)} < v_p < \frac{1}{1-\delta_p}\kappa_i^{(p)}, v_p > 0, \\ 0, & \text{if } v_p = 0, \\ -Q_p(-v_p), & \text{if } v_p < 0, \end{cases} \tag{14.4}$$

where $\delta_p = \frac{1-\rho_p}{1+\rho_p} < 1$, and the quantization density is $0 < \rho_p < 1$. The quantized state is described by

$$\bar{x}_p(k) = Q_p\left(\tilde{x}_p(k)\right). \tag{14.5}$$

Let the quantization error be $e_p(k) = \bar{x}_p(k) - \tilde{x}_p(k)$. We have $\bar{x}_p(k) = (I + \Delta_p(k))\tilde{x}_p(k)$, where $\left\|\Delta_p(k)\right\| \leq \delta_p I$.

In the networked control system, the transmitted packet may be lost due to the unreliability nature of a communication channel. When the packet dropout occurs,

the zero input mechanism is applied when the packet is lost. With the packet dropout, the control input signal is described by

$$u_p(k) = \alpha_p(k) \sum_{q \in N_p} a_{pq} K_{pq}^{\rho(k)} \bar{x}_q(k), \tag{14.6}$$

where $\alpha_p(k) \in \{0, 1\}$ is a binary variable, indicating whether the control input signal is lost or not. As in the last chapters, $\Pr ob\{\alpha_p(k) = 1\} = \mathbb{E}\{\alpha_p(k)\} = \bar{\alpha}_p$ is known as the successful transmission rate, which is assumed to be a known scalar. $\rho(k) \in \Upsilon_1$ is the switching signal obtained by the controller, and it may not be the same as the plant's topology due to remote transmission. In this chapter, we assume that the maximal transmission delay is bounded by π, where π is a positive integer. a_{pq} is the connection variable of the controller network, and $a_{pq} = 1$ if the q-th controller is the neighbor of the p-th controller, otherwise, $a_{pq} = 0$. $K_{pq}^{\rho(k)}$ is the controller gains to be determined. Define the asynchronous time lag by l_t, and $l_t \leq \pi$. Then the switching sequence of $\rho(k)$ is given by

$$\{(i_1, k_1 + l_1), (i_2, k_2 + l_2), \ldots, (i_t, k_t + l_t), \ldots, | p_t \in \Upsilon_1, l = 1, 2, \ldots\},$$

which means that i_t-th controller mode is activated when $k \in [k_t + l_t, k_{t+1} + l_{t+1})$.

Remark 14.1 $\rho(k)$ is actually a delayed switching signal of $\sigma(k)$. In particularly, $\rho(k) = \sigma(k - l_t)$, where l_t is the transmission delay, and it is also regarded as the asynchronous switching time. We use two switching signals only for analysis simplicity.

For easy presentation, we first define the following notations:

$$\begin{aligned}
&x(k) = \left[x_1^T(k)\ x_2^T(k) \cdots x_N^T(k) \right]^T, u(k) = \left[u_1^T(k)\ u_2^T(k) \cdots u_N^T(k) \right]^T,\\
&w(k) = \left[w_1^T(k)\ w_2^T(k) \cdots w_N^T(k) \right]^T, v(k) = \left[\varpi_1^T(k)\ \varpi_2^T(k) \cdots \varpi_N^T(k) \right]^T,\\
&G(x(k)) = \left[g^T(x_1(k))\ g^T(x_2(k)) \cdots g^T(x_N(k)) \right]^T,\\
&z(k) = \left[z_1^T(k)\ z_2^T(k) \cdots z_N^T(k) \right]^T, A = \text{diag}\{A_1, A_2, \ldots, A_N\},\\
&F = \text{diag}\{F_1, F_2, \ldots, F_N\}, E = \text{diag}\{E_1, E_2, \ldots, E_N\},\\
&B = \text{diag}\{B_1, B_2, \ldots, B_N\}, L = \text{diag}\{L_1, L_2, \ldots, L_N\},\\
&\Delta(k) = \text{diag}\{\Delta_1(k), \Delta_2(k), \ldots, \Delta_N(k)\},\\
&W_{\rho(k)} = \left[w_{pq}^{\sigma(k)} \right]_{N \times N}, K_{\rho(k)} = \left[a_{pq} K_{pq}^{\rho(k)} \right]_{N \times N},\\
&\bar{\Pi} = \text{diag}\{\bar{\alpha}_1 I, \bar{\alpha}_2 I, \ldots, \bar{\alpha}_N I\}, \Phi_p = \text{diag}\{0, \ldots, \underbrace{I}_{p-th}, \ldots 0\},\\
&\Lambda = \text{diag}\{\delta_1 I, \delta_2 I, \ldots, \delta_N I\}, \Psi = \text{diag}\{\Sigma_1, \Sigma_2, \ldots, \Sigma_N\},\\
&\tilde{\Psi} = \text{diag}\{\tau_1 \Sigma_1, \tau_2 \Sigma_2, \ldots, \tau_N \Sigma_N\}.
\end{aligned}$$

The closed-loop system is obtained as

$$\begin{cases} x(k+1) = A_{\sigma(k),\rho(k)}x(k) + FG(x(k)) \\ \quad + E\bar{\Pi}K_{\rho(k)}(I + \Delta(k))v(k) + Bw(k) \\ \quad + \sum_{p=1}^{N} \theta_p(k)\left[E\Phi_p K_{\rho(k)}(I + \Delta(k))x(k) + E\Phi_p K_{\rho(k)}(I + \Delta(k))v(k)\right], \\ z(k) = Lx(k), \end{cases} \tag{14.7}$$

where $A_{\sigma(k),\rho(k)} = A + W_{\sigma(k)} + E\bar{\Pi}K_{\rho(k)}(I + \Delta(k))$, $\theta_p(k) = \alpha_p(k) - \bar{\alpha}_p$.

It follows from the switching sequences of $\rho(k)$ and $\sigma(k)$ that for each $\sigma(k) = i, \rho(k) = j; i, j \in \Upsilon_1$, when $k \in [k_t + l_t, k_{t+1})$, system (14.7) can be written as

$$\begin{cases} x(k+1) = A_i x(k) + FG(x(k)) + E\bar{\Pi}K_i(I + \Delta(k))v(k) + Bw(k) \\ + \sum_{p=1}^{N} \theta_p(k)\left[E\Phi_p K_i(I + \Delta(k))x(k) + E\Phi_p K_i(I + \Delta(k))v(k)\right], \\ z(k) = Lx(k), \end{cases} \tag{14.8}$$

When $k \in [k_t, k_t + l_t)$, $t = 1, 2, \ldots$, we have

$$\begin{cases} x(k+1) = A_{ij}x(k) + FG(x(k)) + E\bar{\Pi}K_j(I + \Delta(k))v(k) + Bw(k) \\ + \sum_{p=1}^{N} \theta_p(k)\left[E\Phi_p K_j(I + \Delta(k))x(k) + E\Phi_p K_j(I + \Delta(k))v(k)\right], \\ z(k) = Lx(k). \end{cases} \tag{14.9}$$

Note that the system described by (14.8)–(14.9) is a very complicated dynamic system as it has asynchronous and synchronous motions. In this chapter, the average dwell time approach will be utilized to obtain the main results. The basic idea is that each subsystem should be activated for some time and the average activating time should be larger than a certain value.

For simplicity, we assume $N_0 = 0$. We want to design the sparse controller $K_{\rho(k)}$ such that the closed-loop system (14.8)–(14.9) is exponentially stable in the mean-square sense and a prescribed H_∞ disturbance attenuation level is also guaranteed.

Definition 14.1 The system described by (14.8)–(14.9) is said to be mean-square exponentially stable, if there exist some scalars $\delta > 0$ and $0 < \chi < 1$, such that the trajectory $x(k)$ of system (14.8)–(14.9) satisfies $\mathbb{E}\left\{\|x(k)\|^2\right\} < \delta\chi^{k-k_0}\|x(k_0)\|^2$, $k \geq 0$, where χ is called the decay rate and $x(k_0)$ is the initial condition.

Definition 14.2 For a given scalar $\gamma > 0$, system described by (14.8)–(14.9) is said to be mean-square exponentially stable and achieves a prescribed H_∞ performance γ, if it is mean-square exponentially stable and under zero initial condition, $\sum_{k=0}^{+\infty} \mathbb{E}\{z^T(k)z(k)\} \leq \sum_{k=0}^{+\infty} \gamma^2 w^T(k)w(k)$ holds for all nonzero $w(k) \in l_2[0, \infty)$.

14.3 Main Results

By the aid of the switched system theory, we find a sufficient condition such that the closed-loop system is exponentially stable with a prescribed H_∞ disturbance attenuation level.

Theorem 14.1 *For some given scalars* $0 < a < 1, b \geq 1, 1 < c < 1/a$, *and* $\mu \geq 1$, *the closed-loop system (14.8)–(14.9) is exponentially stable in the mean-square sense with a prescribed* H_∞ *performance level* $\gamma = \sqrt{\frac{1-a}{1-ac}}\lambda$, *if there exist positive-definite matrices* P_i, P_{ij} *and scalars* $\lambda_1, \lambda_2, \varepsilon$ *such that the following inequalities,*

$$\begin{bmatrix} \Omega_{1i} & \Omega_{2i} & \Omega_3 & \Omega_{4i} & \Omega_5 & 0 \\ * & -P_i^{-1} & 0 & 0 & 0 & E\bar{\Pi}K_i \\ * & * & -I & 0 & 0 & 0 \\ * & * & * & \Omega_{6i} & 0 & \Omega_{7i} \\ * & * & * & * & -\varepsilon I & 0 \\ * & * & * & * & * & -\varepsilon I \end{bmatrix} < 0, \tag{14.10}$$

$$\begin{bmatrix} \Omega_{1ij} & \Omega_{2ij} & \Omega_3 & \Omega_{4j} & \Omega_5 & 0 \\ * & -P_{ij}^{-1} & 0 & 0 & 0 & E\bar{\Pi}K_j \\ * & * & -I & 0 & 0 & 0 \\ * & * & * & \Omega_{6ij} & 0 & \Omega_{7j} \\ * & * & * & * & -\varepsilon I & 0 \\ * & * & * & * & * & -\varepsilon I \end{bmatrix} < 0, \tag{14.11}$$

$$P_i \leq \mu P_{ij}, \tag{14.12}$$

$$P_{ij} \leq \mu P_j, \tag{14.13}$$

$$T_a > T_a^* = \frac{\ln\left[(b/a)^\pi \mu^2\right]}{\ln c}, \tag{14.14}$$

hold for all $i, j \in \Upsilon_1$ *and* $i \neq j$,, *where*

$$\Omega_{1i} = \begin{bmatrix} -aP_i + \lambda_1 \bar{U}^T \bar{U} + \lambda_2 \tilde{\Psi} & 0 & 0 & 0 \\ * & -\lambda_1 I & 0 & 0 \\ * & * & -\lambda_2 \Psi & 0 \\ * & * & * & -\lambda^2 I \end{bmatrix},$$

$$\Omega_{2i} = \begin{bmatrix} (A + W_i + E\bar{\Pi}K_i) & F & (E\bar{\Pi}K_i) & B \end{bmatrix}^T, \Omega_3 = \begin{bmatrix} L & 0 & 0 & 0 \end{bmatrix}^T,$$

$$\Omega_{4i} = \begin{bmatrix} \theta_1 K_i^T \Phi_1^T E & \theta_2 K_i^T \Phi_2^T E & \cdots & \theta_N K_i^T \Phi_N^T E \\ 0 & 0 & \cdots & 0 \\ \theta_1 K_i^T \Phi_1^T E & \theta_2 K_i^T \Phi_2^T E & \cdots & \theta_N K_i^T \Phi_N^T E \\ 0 & 0 & \cdots & 0 \end{bmatrix},$$

$$
\begin{aligned}
&\Omega_5 = \left[\varepsilon\Lambda\ 0\ \varepsilon\Lambda\ 0\right]^T, \Omega_{6i} = \operatorname{diag}\left\{-P_i^{-1}, -P_i^{-1}, \ldots, -P_i^{-1}\right\},\\
&\Omega_{7i} = \left[(\theta_1 K_i \Phi_1 E)^T\ (\theta_2 K_i \Phi_2 E)^T \cdots (\theta_N K_i \Phi_N E)^T\right]^T,\\
&\Omega_{1ij} = \begin{bmatrix} -bP_{ij} + \lambda_1 \bar{U}^T \bar{U} + \lambda_2 \tilde{\Psi} & 0 & 0 & 0\\ * & -\lambda_1 I & 0 & 0\\ * & * & -\lambda_2 \Psi & 0\\ * & * & * & -\lambda^2 I \end{bmatrix},\\
&\Omega_{2ij} = \left[\left(A + W_i + E\bar{\Pi} K_j\right)\ F\ \left(E\bar{\Pi} K_j\right)\ B\right]^T,\\
&\Omega_{4j} = \begin{bmatrix} \theta_1 K_j^T \Phi_1^T E & \theta_2 K_j^T \Phi_2^T E & \cdots & \theta_N K_j^T \Phi_N^T E\\ 0 & 0 & \cdots & 0\\ \theta_1 K_j^T \Phi_1^T E & \theta_2 K_j^T \Phi_2^T E & \cdots & \theta_N K_j^T \Phi_N^T E\\ 0 & 0 & \cdots & 0 \end{bmatrix},\\
&\Omega_{6ij} = \operatorname{diag}\left\{-P_{ij}^{-1}, -P_{ij}^{-1}, \ldots, -P_{ij}^{-1}\right\},\\
&\Omega_{7j} = \left[\left(\theta_1 K_j \Phi_1 E\right)^T\ \left(\theta_2 K_j \Phi_2 E\right)^T \cdots \left(\theta_N K_j \Phi_N E\right)^T\right]^T.
\end{aligned}
$$

Proof Since the closed-loop system (14.7) consists of two different dynamics, (14.8) and (14.9), it is reasonable to construct two different Lyapunov functional for such a complex system. To do so, for each $\sigma(k) = i$, $\rho(k) = j; i, j \in \Upsilon_1$, we propose the following Lyapunov functional:

$$
\begin{cases} V_i = x^T(k) P_i x(k), & k \in [k_0, k_1) \cup [k_t + l_t, k_{t+1}),\\ V_{ij} = x^T(k) P_{ij} x(k), & k \in [k_t, k_t + l_t), \end{cases} \tag{14.15}
$$

We now consider the case where $k \in [k_0, k_1) \cup [k_t + l_t, k_{t+1})$ and check the stability of $x(k)$. Then we have

$$
\begin{aligned}
&\mathbb{E}\left\{V_i(k+1) - aV_i(k) + \Gamma(k)\right\}\\
&= \mathbb{E}\left\{x^T(k+1) P_i x(k+1) - a x^T(k) P_i x(k) + \Gamma(k)\right\}\\
&= \left[A_i x(k) + FG(x(k)) + E\bar{\Pi} K_i (I + \Delta(k)) v(k) + B w(k)\right]^T\\
&\quad \times \left[A_i x(k) + FG(x(k)) + E\bar{\Pi} K_i (I + \Delta(k)) v(k) + B w(k)\right]\\
&\quad + \sum_{p=1}^{N} \bar{\theta}_p^2 \left[E\Phi_p K_i (I + \Delta(k)) x(k) + E\Phi_p K_i (I + \Delta(k)) v(k)\right]^T\\
&\quad \times \left[E\Phi_p K_i (I + \Delta(k)) x(k) + E\Phi_p K_i (I + \Delta(k)) v(k)\right]\\
&\quad + [Lx(k)]^T [Lx(k)] - \lambda^2 w^T(k) w(k),
\end{aligned} \tag{14.16}
$$

where $\Gamma(k) = z^T(k) z(k) - \lambda^2 w^T(k) w(k)$. It follows from the assumption of nonlinear function $g(x_p(k))$ that there exists a positive scalar $\lambda_1 > 0$ such that

$$
-\lambda_1 G^T(x(k)) G(x(k)) + \lambda_1 x^T(k) x(k) > 0. \tag{14.17}
$$

On the other hand, the event condition (14.2) implies that the following inequality is true:

$$
-\lambda_2 v^T(k) \Psi v(k) + \lambda_2 x^T(k) \tilde{\Psi} x(k) > 0, \tag{14.18}
$$

where λ_2 is a positive scalar. Let $\chi_1 = -\lambda_1 G^T(x(k))G(x(k)) + \lambda_1 x^T(k)x(k)$, and $\chi_2 = -\lambda_2 v^T(k)\Psi v(k) + \lambda_2 x^T(k)\tilde{\Psi}x(k)$. It follows from (14.16) that

$$\begin{aligned}
&\mathbb{E}\{V_i(k+1) - aV_i(k) + \Gamma(k)\} \\
&\quad \le \mathbb{E}\{V_i(k+1) - aV_i(k) + \Gamma(k)\} + \chi_1 + \chi_2 \\
&\quad = \eta^T(k)\left[\Omega_{1i} + \bar{\Omega}_{2i}P_i\bar{\Omega}_{2i}^T + \Omega_3\Omega_3^T + \sum_{p=1}^{N}\bar{\theta}_p^2\bar{\Omega}_{4i}^p P_i\left(\bar{\Omega}_{4i}^p\right)^T\right]\eta(k),
\end{aligned} \tag{14.19}$$

where

$$\begin{aligned}
\eta(k) &= \left[x^T(k)\ G^T(x(k))\ v^T(k)\ w^T(k)\right]^T, \\
\bar{\Omega}_{2i} &= \left[\left(A + W_i + E\bar{\Pi}K_i\left(I + \Delta(k)\right)\right)\ F\ \left(E\bar{\Pi}K_i\left(I + \Delta(k)\right)\right)\ B\right]^T, \\
\bar{\Omega}_{4i}^p &= \left[E\Phi_p K_i\left(I + \Delta(k)\right)\ 0\ E\Phi_p K_i\left(I + \Delta(k)\right)\ 0\right]^T.
\end{aligned}$$

It is seen that $\mathbb{E}\{V_i(k+1) - aV_i(k) + \Gamma(k)\} < 0$ if

$$\Omega_{1i} + \bar{\Omega}_{2i}P_i\bar{\Omega}_{2i}^T + \Omega_3\Omega_3^T + \sum_{p=1}^{N}\bar{\theta}_p^2\bar{\Omega}_{4i}^p P_i\left(\bar{\Omega}_{4i}^p\right)^T < 0 \tag{14.20}$$

is true. By Lemma 2.1, (14.20) is equivalent to

$$\begin{bmatrix} \Omega_{1i} & \bar{\Omega}_{2i} & \Omega_3 & \bar{\Omega}_{4i} \\ * & -P_i^{-1} & 0 & 0 \\ * & * & -I & 0 \\ * & * & * & \Omega_{6i} \end{bmatrix} < 0, \tag{14.21}$$

where $\bar{\Omega}_{4i} = \left[\bar{\Omega}_{4i}^1\ \bar{\Omega}_{4i}^2\ \cdots\ \bar{\Omega}_{4i}^N\right]$. By some manipulations, (14.21) can be written as

$$\begin{bmatrix} \Omega_{1i} & \Omega_{2i} & \Omega_3 & \Omega_{4i} \\ * & -P_i^{-1} & 0 & 0 \\ * & * & -I & 0 \\ * & * & * & \Omega_{6i} \end{bmatrix} + \begin{bmatrix} \Lambda \\ 0 \\ \Lambda \\ 0 \end{bmatrix} \frac{\Delta}{\Lambda} \begin{bmatrix} 0 \\ E\bar{\Pi}K \\ 0 \\ \Omega_{7i} \end{bmatrix}^T + \begin{bmatrix} 0 \\ E\bar{\Pi}K \\ 0 \\ \Omega_{7i} \end{bmatrix} \frac{\Delta}{\Lambda} \begin{bmatrix} \Lambda \\ 0 \\ \Lambda \\ 0 \end{bmatrix}^T < 0. \tag{14.22}$$

Since $\left\|\frac{\Delta}{\Lambda}\right\| \le I$, it is easy to see that (14.22) holds if and only if (14.10) is true. Then, we can infer

$$\mathbb{E}\{V_i(k+1) - aV_i(k) + \Gamma(k)\} < 0, \tag{14.23}$$

that is,

$$\mathbb{E}\{V_i(k)\} < a^{k-l_t-k_t}\mathbb{E}\{V_i(k_t + l_t)\} + \sum_{s=k_t+l_t}^{k-1} a^{k-s-1}\mathbb{E}\{\Gamma(s)\}, \tag{14.24}$$

Similarly, we have

$$\mathbb{E}\{V_i(k)\} < a^{k-k_0}\mathbb{E}\{V_i(k_0)\} + \sum_{s=k_0}^{k-1} a^{k-s-1}\mathbb{E}\{\Gamma(s)\}. \tag{14.25}$$

For the scenario where $k \in [k_t, k_t + l_t)$, the following statement holds,

$$\mathbb{E}\left\{V_{ij}(k)\right\} < b^{k-k_t}\mathbb{E}\left\{V_{ij}(k_t)\right\} + \sum_{s=k_t}^{k-1} b^{k-s-1}\mathbb{E}\{\Gamma(s)\}. \tag{14.26}$$

We are now on the stage to consider the exponential stability of the closed-loop system (14.8)–(14.9) with $w(k) = 0$. Since the state could either be operated under the asynchronous control mode or the synchronous control one, we first discuss the first case, i.e., for $k \in [k_t, k_t + l_t)$. It follows from (14.26) that $\mathbb{E}\left\{V_{ij}(k)\right\} < b^{k-k_t}\mathbb{E}\left\{V_{ij}(k_t)\right\}$. By resorting to (14.12) and (14.13), we eventually obtain

$$\begin{aligned}
&\mathbb{E}\left\{V_{\sigma(k)\rho(k)}(k)\right\}\\
&\quad\le b^{k-k_t}\mathbb{E}\left\{V_{\sigma(k_t)\rho(k_t)}(k_t)\right\}\\
&\quad= b^{k-k_t}\mathbb{E}\left\{V_{\sigma(k_t)\rho(k_{t-1}+l_{t-1})}(k_t)\right\}\\
&\quad\le b^{k-k_t}\mu\mathbb{E}\left\{V_{\sigma(k_t-1)}(k_t)\right\}\\
&\quad= b^{k-k_t}\mu\mathbb{E}\left\{V_{\sigma(k_{t-1})}(k_t)\right\}\\
&\quad\le b^{k-k_t}\mu a^{k_t-k_{t-1}-l_{t-1}}\mathbb{E}\left\{V_{\sigma(k_{t-1})}(k_{t-1}+l_{t-1})\right\}\\
&\quad= b^{k-k_t}\mu a^{k_t-k_{t-1}-l_{t-1}}\mu\mathbb{E}\left\{V_{\sigma(k_{t-1})\rho(k_{t-2}+l_{t-2})}(k_{t-1}+l_{t-1})\right\}\\
&\quad\vdots\\
&\quad\le \mu^{N_\sigma(k_0,k)}\mu^{N_\rho(k_0,k)}a^{\mathbb{T}^{\downarrow(k_0,k)}}b^{\mathbb{T}^{\uparrow(k_0,k)}}V_{\sigma(k_0)}(k_0),
\end{aligned} \tag{14.27}$$

where $N_\rho(k_0, k)$ is the switching numbers of $\rho(\tau)$ over time-interval (k_0, k), $\mathbb{T}^{\downarrow(k_0,k)} = k_t - k_0 - (l_{t-1} + \cdots l_1)$, and $\mathbb{T}^{\uparrow(k_0,k)} = k - k_t + (l_{t-1} + \cdots l_1)$. Due to the fact that $\rho(k)$ is a delayed signal of $\sigma(k)$, $N_\rho(k_0, k) \le N_\sigma(k_0, k)$ must hold. With $\mu \ge 1$, it follows that

$$\begin{aligned}
&\mathbb{E}\left\{V_{\sigma(k)\rho(k)}(k)\right\}\\
&\quad\le (\mu^2)^{N_\sigma(k_0,k)}a^{\mathbb{T}^{\downarrow(k_0,k)}}b^{\mathbb{T}^{\uparrow(k_0,k)}}V_{\sigma(k_0)}(k_0)\\
&\quad= (\mu^2)^{N_\sigma(k_0,k)}a^{(k-k_0)}\left(b/a\right)^{\mathbb{T}^{\uparrow(k_0,k)}}V_{\sigma(k_0)}(k_0)\\
&\quad\le (\mu^2)^{N_\sigma(k_0,k)}a^{(k-k_0)}\left(b/a\right)^{\pi\times N_\sigma(k_0,k)}V_{\sigma(k_0)}(k_0).
\end{aligned} \tag{14.28}$$

By the average dwell time condition (14.14), and the relation $N_\sigma(k_0, k) \le \frac{k-k_0}{T_a}$, we have

$$\mathbb{E}\left\{V_{\sigma(k)\rho(k)}(k)\right\} \le (ca)^{(k-k_0)}V_{\sigma(k_0)}(k_0). \tag{14.29}$$

On the other hand, it follows from the Lyapunov function (14.15) that there exist two scalars $\hbar_1 > 0$ and $\hbar_2 > 0$ such that

$$\hbar_1\mathbb{E}\left\{\|x(k)\|^2\right\} \le \mathbb{E}\left\{V_{\sigma(k)\rho(k)}(k)\right\} \le \hbar_2(ca)^{(k-k_0)}\|x(k_0)\|^2, \tag{14.30}$$

where $\hbar_1 = \min_{i,j\in\Upsilon_1; i\neq j} \lambda_{\min}(P_{ij})$, $\hbar_2 = \max_{i\in\Upsilon_1} \lambda_{\max}(P_i)$. Since $1 < c < \frac{1}{a}$, (14.30) implies that the system (14.8)–(14.9) is mean-square exponentially stable when $k \in [k_t, k_t + l_t)$.

By a similar analysis for $k \in [k_t + l_t, k_{t+1})$, we obtain

$$\begin{aligned}
&\mathbb{E}\left\{V_{\sigma(k)}(k)\right\} \\
&\leq a^{k-k_t-l_t}\mathbb{E}\left\{V_{\sigma(k)}(k_t+l_t)\right\} \\
&= a^{k-k_t-l_t}\mathbb{E}\left\{V_{\sigma(k_t+l_t)}(k_t+l_t)\right\} \\
&\vdots \\
&\leq \mu^{N_\sigma(k_0,k)}\mu^{N_\rho(k_0,k)}a^{\mathbb{T}^{\downarrow}(k_0,k)}b^{\mathbb{T}^{\uparrow}(k_0,k)}V_{\sigma(k_0)}(k_0) \\
&\vdots \\
&\leq (ca)^{(k-k_0)}V_{\sigma(k_0)}(k_0).
\end{aligned} \tag{14.31}$$

There also exist two scalars $\bar{\hbar}_1 > 0$ and $\hbar_2 > 0$ such that

$$\bar{\hbar}_1\mathbb{E}\left\{\|x(k)\|^2\right\} \leq \mathbb{E}\left\{V_{\sigma(k)}(k)\right\} \leq \hbar_2(ca)^{(k-k_0)}\|x(k_0)\|^2. \tag{14.32}$$

One has

$$\mathbb{E}\left\{\|x(k)\|^2\right\} \leq \frac{\hbar_2}{\bar{\hbar}_1}(ca)^{(k-k_0)}\|x(k_0)\|^2. \tag{14.33}$$

Let $\tilde{\hbar}_1 = \min\{\hbar_1, \bar{\hbar}_1\}$. We finally have

$$\mathbb{E}\left\{\|x(k)\|^2\right\} \leq \frac{\hbar_2}{\tilde{\hbar}_1}(ca)^{(k-k_0)}\|x(k_0)\|^2. \tag{14.34}$$

According to Definition 14.1, system (14.8)–(14.9) is exponentially stable in the mean-square sense when $w(k) = 0$.

We now address the H_∞ disturbance attenuation level of the closed-loop system. Based on the above analysis, it is easy to see that

$$\begin{aligned}
\mathbb{E}\left\{V_{ij}(k)\right\} \leq\ &(\mu^2)^{N_\sigma(k_0,k)}a^{\mathbb{T}^{\downarrow}(k_0,k)}b^{\mathbb{T}^{\uparrow}(k_0,k)}V_{\sigma(k_0)}(k_0) \\
&-\textstyle\sum_{s=k_0}^{k-1}\mu^{N_{\sigma,\rho}(s,k-1)}a^{\mathbb{T}^{\downarrow}(s,k-1)}b^{\mathbb{T}^{\uparrow}(s,k-1)}\mathbb{E}\left\{\Gamma(s)\right\},
\end{aligned} \tag{14.35}$$

for $k \in [k_t, k_t + l_t)$, where $N_{\sigma,\rho}(s, k-1) = N_\rho(s, k-1) + N_\sigma(s, k-1)$. Under the zero initial condition, i.e., $V_{\sigma(k_0)}(k_0) = 0$, and $V_{ij}(k) \geq 0$, we have

$$\sum_{s=k_0}^{k-1}\mu^{N_{\sigma,\rho}(s,k-1)}a^{\mathbb{T}^{\downarrow}(s,k-1)}b^{\mathbb{T}^{\uparrow}(s,k-1)}\mathbb{E}\left\{\Gamma(s)\right\} \leq 0, \tag{14.36}$$

i.e.,

$$\begin{aligned}&\sum_{s=k_0}^{k-1}\mu^{N_{\sigma,\rho}(s,k-1)}a^{\mathbb{T}^{\downarrow(s,k-1)}}b^{\mathbb{T}^{\uparrow(s,k-1)}}\mathbb{E}\{z^T(s)z(s)\}\\&\quad\le\lambda^2\sum_{s=k_0}^{k-1}\mu^{N_{\sigma,\rho}(s,k-1)}a^{\mathbb{T}^{\downarrow(s,k-1)}}b^{\mathbb{T}^{\uparrow(s,k-1)}}w^T(s)w(s).\end{aligned}\tag{14.37}$$

Note that

$$\begin{aligned}&\sum_{s=k_0}^{k-1}\mu^{N_{\sigma,\rho}(s,k-1)}a^{\mathbb{T}^{\downarrow(s,k-1)}}b^{\mathbb{T}^{\uparrow(s,k-1)}}\mathbb{E}\{z^T(s)z(s)\}\\&=\sum_{s=k_0}^{k-1}\mu^{N_{\sigma,\rho}(s,k-1)}a^{k-1-s}\left(b/a\right)^{\mathbb{T}^{\uparrow(s,k-1)}}\mathbb{E}\{z^T(s)z(s)\}\\&\ge\sum_{s=k_0}^{k-1}a^{k-1-s}\mathbb{E}\{z^T(s)z(s)\},\end{aligned}\tag{14.38}$$

and

$$\begin{aligned}&\sum_{s=k_0}^{k-1}\mu^{N_\sigma(s,k-1)}\mu^{N_\rho(s,k-1)}a^{\mathbb{T}^{\downarrow(s,k-1)}}b^{\mathbb{T}^{\uparrow(s,k-1)}}w^T(s)w(s)\\&\le\sum_{s=k_0}^{k-1}\mu^{2N_\sigma(s,k-1)}a^{k-1-s}\left(b/a\right)^{\mathbb{T}^{\uparrow(s,k-1)}}w^T(s)w(s)\\&\le\sum_{s=k_0}^{k-1}\mu^{2N_\sigma(s,k-1)}a^{k-1-s}\left(b/a\right)^{\pi\times N_\sigma(s,k-1)}w^T(s)w(s)\\&\le\sum_{s=k_0}^{k-1}\left[\mu^2\left(b/a\right)^{\pi}\right]^{\frac{k-s-1}{T_a}}a^{k-1-s}w^T(s)w(s).\end{aligned}\tag{14.39}$$

By (14.14), we obtain

$$\begin{aligned}&\sum_{s=k_0}^{k-1}\mu^{N_\sigma(s,k-1)}\mu^{N_\rho(s,k-1)}a^{\mathbb{T}^{\downarrow(s,k-1)}}b^{\mathbb{T}^{\uparrow(s,k-1)}}w^T(s)w(s)\\&\quad\le\sum_{s=k_0}^{k-1}c^{k-s-1}a^{k-1-s}w^T(s)w(s)\\&\quad=\sum_{s=k_0}^{k-1}(ca)^{k-1-s}w^T(s)w(s).\end{aligned}\tag{14.40}$$

Then, the following inequality,

$$\begin{aligned}&\sum_{s=k_0}^{k-1}a^{k-1-s}\mathbb{E}\{z^T(s)z(s)\}\\&\qquad\le\lambda^2\sum_{s=k_0}^{k-1}(ca)^{k-1-s}w^T(s)w(s),\end{aligned}\tag{14.41}$$

is true. Summing both sides of (14.41) from $k=1$ to $k=+\infty$ and changing the order of summation yield

$$\sum_{s=k_0}^{+\infty}\mathbb{E}\{z^T(s)z(s)\}\le\frac{1-a}{1-ca}\lambda^2\sum_{s=k_0}^{+\infty}w^T(s)w(s).\tag{14.42}$$

By following a similar analysis for $k\in[k_t+l_t,k_{t+1})$, we can also have the same result. Thus, the system (14.8)–(14.9) is exponentially stable in the mean-square sense with a prescribed H_∞ disturbance attenuation level $\gamma=\sqrt{\frac{1-a}{(1-ca)}}\lambda$. The proof is now completed.

One can see from Theorem 14.1 that we have P_i, P_{ij} and their inverses in Eqs. (14.10) and (14.11), it is impossible for us to determine the controller gain at this stage. To overcome this problem, we present the following theorem.

Theorem 14.2 *For some given scalars* $0<a<1$, $b\ge1$, $1<c<1/a$, *and* $\mu\ge1$, *the control problem is solvable if there exist positive-definite matrices* P_i, P_{ij}, Q_i, Q_{ij}, *and positive scalars* $\lambda_1,\lambda_2,\varepsilon$ *such that the conditions (14.12)–(14.14) and*

$$\begin{bmatrix} \Omega_{1i} & \Omega_{2i} & \Omega_3 & \Omega_{4i} & \Omega_5 & 0 \\ * & -Q_i & 0 & 0 & 0 & E\bar{\Pi}K_i \\ * & * & -I & 0 & 0 & 0 \\ * & * & * & \bar{\Omega}_{6i} & 0 & \Omega_{7i} \\ * & * & * & * & -\varepsilon I & 0 \\ * & * & * & * & * & -\varepsilon I \end{bmatrix} < 0, \tag{14.43}$$

$$\begin{bmatrix} \Omega_{1ij} & \Omega_{2ij} & \Omega_3 & \Omega_{4j} & \Omega_5 & 0 \\ * & -Q_{ij} & 0 & 0 & 0 & E\bar{\Pi}K_j \\ * & * & -I & 0 & 0 & 0 \\ * & * & * & \bar{\Omega}_{6ij} & 0 & \Omega_{7j} \\ * & * & * & * & -\varepsilon I & 0 \\ * & * & * & * & * & -\varepsilon I \end{bmatrix} < 0, \tag{14.44}$$

$$Q_i P_i = I, \tag{14.45}$$

$$Q_{ij} P_{ij} = I, \tag{14.46}$$

are all satisfied for $i, j \in \Upsilon_1$, *where* $\bar{\Omega}_{6i} = \text{diag}\{-Q_i, -Q_i, \ldots, -Q_i\}$ *and* $\bar{\Omega}_{6ij} = \text{diag}\{-Q_{ij}, -Q_{ij}, \ldots, -Q_{ij}\}$.

Proof it is easy to see that Theorem 14.2 reduces to Theorem 14.1 by $Q_i = P_i^{-1}$ and $Q_{ij} = P_{ij}^{-1}$.

It should be pointed out that (14.43) and (14.44) in Theorem 14.2 have become a set of linear matrix inequalities, which can be easily solved by some standard software, but (14.45) and (14.46) are two bilinear matrix equations. It is still not an easy task to use Theorem 14.2 directly to calculate the controller gains K_i. To conquer this problem, we resort to the cone complementarity linearization algorithm, and the controller gain K_i can now be calculated by solving the following optimization problem:

$$\begin{aligned} \min \quad & \text{Tr}\left\{\sum_{i=1}^{\Upsilon_1} Q_i P_i + \sum_{i=1}^{\Upsilon_1}\sum_{j=1}^{\Upsilon_1} Q_{ij} P_{ij}\right\} \\ \text{s.t. } & (14.12) - (14.14), (14.43), (14.44) \text{ and} \\ & \begin{bmatrix} Q_i & I \\ * & P_i \end{bmatrix} \geq 0, \quad \begin{bmatrix} Q_{ij} & I \\ * & P_{ij} \end{bmatrix} \geq 0. \end{aligned} \tag{14.47}$$

14.4 A Simulation Study

In this section, a simulation study on the network-based chemical reactors consisting of two non-isothermal continuous stirred-tank reactors (CSTRs) with interconnections between reactors is presented. The system is depicted in Fig. 14.2. It follows from Chap. 12 that the dynamics of CSTR can be modeled as the following LTI system when the original nonlinear system is linearized around the operating point:

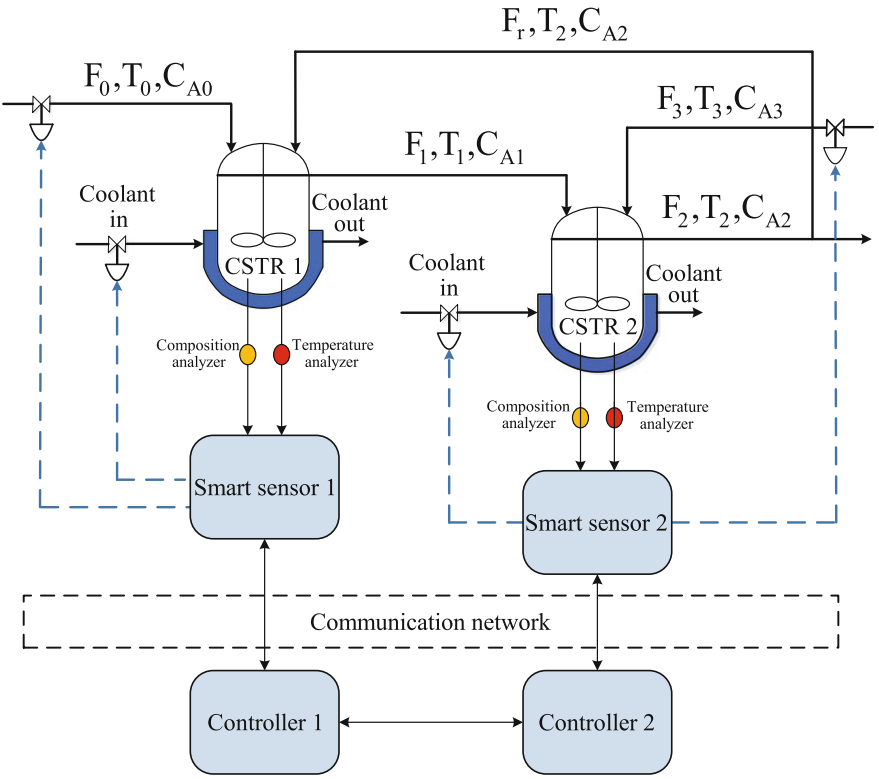

Fig. 14.2 Process flow diagram of two interconnected CSTR systems

$$\begin{cases} \dot{x}_1(t) = A_{11}^c x_1(t) + \bar{B}_1^c u_1(t) + A_{12}^c x_2(t), \\ \dot{x}_2(t) = A_{22}^c x_2(t) + \bar{B}_2^c u_2(t) + A_{21}^c x_1(t), \end{cases} \tag{14.48}$$

where x_i and u_i are the state and input vectors for the i-th subsystem, respectively, and they are defined by

$$x_1 = \begin{bmatrix} \frac{T_1 - T_1^s}{T_1^s} \\ \frac{CA_1 - C_{A1}^s}{C_{A1}^s} \end{bmatrix}, x_2 = \begin{bmatrix} \frac{T_2 - T_2^s}{T_2^s} \\ \frac{CA_2 - C_{A2}^s}{C_{A2}^s} \end{bmatrix},$$
$$u_1 = \begin{bmatrix} Q_1 \\ C_{A0} - C_{A0}^s \end{bmatrix}, u_2 = \begin{bmatrix} Q_2 \\ C_{A03} - C_{A03}^s \end{bmatrix}.$$

With the parameters in Table 12.1, the matrices in (14.49) are calculated as

$$A_{11}^c = \begin{bmatrix} 25.2914 & 4.9707 \\ -78.028 & -45.9368 \end{bmatrix}, A_{12}^c = \begin{bmatrix} 31.7512 & 0 \\ 0 & 34.6421 \end{bmatrix},$$
$$\bar{B}_1^c = \begin{bmatrix} 9.45 \times 10^{-6} & 0 \\ 0 & 2.8234 \end{bmatrix},$$
$$A_{22}^c = \begin{bmatrix} -2.8370 & 1.4157 \\ -22.4506 & -24.8828 \end{bmatrix}, A_{21}^c = \begin{bmatrix} 14.6953 & 0 \\ 0 & 13.4690 \end{bmatrix},$$
$$\bar{B}_2^c = \begin{bmatrix} 3.47 \times 10^{-6} & 0 \\ 0 & 5.7071 \end{bmatrix}.$$

Discretizing system (14.48) under a sampling time of $T_s = 0.0025$ h gives following discrete-time interconnected systems:

$$\begin{cases} x_1(k+1) = A_{11}^d x_1(k) + \bar{B}_1^d u_1(k) + A_{12}^d x_2(k), \\ x_2(k+1) = A_{22}^d x_2(k) + \bar{B}_2^d u_2(k) + A_{21}^d x_1(k), \end{cases} \tag{14.49}$$

where

$$A_{11}^d = \begin{bmatrix} 1.0632 & 0.0124 \\ -0.1951 & 0.8852 \end{bmatrix}, A_{12}^d = \begin{bmatrix} 0.0794 & 0 \\ 0 & 0.0866 \end{bmatrix},$$
$$\bar{B}_1^d = \begin{bmatrix} 9.45 \times 10^{-7} & 0 \\ 0 & 0.0071 \end{bmatrix}, A_{22}^d = \begin{bmatrix} 0.9929 & 0.0035 \\ -0.0561 & 0.9378 \end{bmatrix},$$
$$A_{21}^d = \begin{bmatrix} 0.0367 & 0 \\ 0 & 0.0337 \end{bmatrix}, \bar{B}_2^d = \begin{bmatrix} 3.47 \times 10^{-7} & 0 \\ 0 & 0.0143 \end{bmatrix}.$$

In a practical CSTR system, the feed to CSTR 1 and CSTR 2 may be changing due to different operation tasks, which result in a time-varying connection configuration of CSTR 1 and CSTR 2. Hence the topology switching problem is taken into account to reflect a more practical CSTR system. In addition, note that the nonlinear perturbation and the unknown disturbance usually occur in CSTR systems. Therefore, a practical CSTR system can be modeled by system (1) with two subsystems, and the parameters of each subsystem are listed as follows.

Subsystem 1:

$$A_1 = \begin{bmatrix} 1.0632 & 0.0124 \\ -0.1951 & 0.8852 \end{bmatrix}, W_{12}^1 = \begin{bmatrix} 0.0794 & 0 \\ 0 & 0.0866 \end{bmatrix}, W_{12}^2 = 0.5 W_{12}^1,$$
$$F_1 = \begin{bmatrix} 0.1 & 0 \\ 0.1 & 0.01 \end{bmatrix}, E_1 = \begin{bmatrix} 9.45 \times 10^{-7} & 0 \\ 0 & 0.0071 \end{bmatrix}, B_1 = \begin{bmatrix} 0.7 \\ 0.3 \end{bmatrix}, L_1 = \begin{bmatrix} 0.5 & 0.5 \end{bmatrix};$$

Subsystem 2:

$$A_2 = \begin{bmatrix} 0.9929 & 0.0035 \\ -0.0561 & 0.9378 \end{bmatrix}, W_{21}^1 = \begin{bmatrix} 0.0367 & 0 \\ 0 & 0.0337 \end{bmatrix}, W_{21}^2 = 0.5 W_{21}^1,$$

$$F_2 = \begin{bmatrix} 0.1 & 0 \\ 0.1 & 0.01 \end{bmatrix},\ E_2 = \begin{bmatrix} 3.47 \times 10^{-7} & 0 \\ 0 & 0.0143 \end{bmatrix},\ B_2 = \begin{bmatrix} 0.5 \\ 0.3 \end{bmatrix},\ L_2 = \begin{bmatrix} 0.1 & 0.8 \end{bmatrix}.$$

The nonlinear disturbance is assumed to be $g(x_p(k)) = \begin{bmatrix} \tanh(0.2x_{1i}) \\ \tanh(0.2x_{2i}) \end{bmatrix}$, and then $U = \text{diag}\{0.2, 0.2\}$.

It has been shown in the last few chapters that the above CSTR system is open-loop unstable. In this example, we use two controllers to perform the control task and all states are assumed to be measurable. To handle the communication constraint problem, the state measurement is transmitted only a pre-designed event condition (14.2) is satisfied. The weighting matrices and tuning parameters of the event function are chosen to be $\Sigma_1 = \Sigma_2 = I$, $\tau_1 = 0.95$, and $\tau_2 = 0.9$. The selected measurement signals are then quantized by two logarithmic quantizers with quantization densities $\rho_1 = 0.9$ and $\rho_2 = 0.8$. As we mentioned above, the transmission in a networked environment is not always reliable and the packet dropout may occur. We assume that the packet dropout rates are 10 and 20%. Then $\bar{\alpha}_1 = 0.9$ and $\bar{\alpha}_2 = 0.8$. Suppose that the topology switching is periodical with the period $T = 5$, which is unknown to the controller side. The transmission of real-time topology switching information to the controller network is through a communication network and it suffers some time delay and the maximal delay bound is assumed to $\pi = 2$. Choosing $a = 0.95$, $b = 1.01$, $c = 1.05$ and $\mu = 1.01$, we have $T_a^* = 4.8171$, which means that condition (14.14) holds. Now solving the optimization problem (14.47), we have $\gamma^* = 4.5750$, and the controller gains

$$K_1 = \begin{bmatrix} -631750 & 17.4059 & -56796 & -0.0144 \\ 18.1060 & -54.3548 & -2.5585 & -0.9495 \\ -29965 & -0.4728 & -1614900 & 0.2100 \\ -0.4626 & -2.3728 & 0.5786 & -18.7411 \end{bmatrix},$$

$$K_2 = \begin{bmatrix} -629800 & 17.4578 & -50356 & 0.0275 \\ 16.9747 & -54.5540 & -1.0162 & 0.5902 \\ -2821.4 & -0.4287 & -1620200 & 0.1752 \\ -0.9302 & 0.5184 & -0.1141 & -18.7036 \end{bmatrix}.$$

To verify control performance, we first consider the case where $w(k) = 0$. Choosing the initial conditions as $x_1(0) = \begin{bmatrix} 0.3 \\ 0.8 \end{bmatrix}$, $x_2(0) = \begin{bmatrix} 1.2 \\ 0.4 \end{bmatrix}$, we depict the state response trajectories in Figs. 14.3 and 14.4. It is seen that closed-loop system is stable. We now consider the scenario that $w_1(k) = w_2(k) = \sin(0.1k) * e^{-0.1k}$, and the initial conditions of the CSTR are zero. The simulation results are depicted in Figs. 14.5, 14.6, 14.7 and 14.8. Specifically, Figs. 14.5 and 14.6 illustrate the state response trajectories and Figs. 14.7 and 14.8 show the performance trajectories. The above simulation results have demonstrated the effectiveness of the proposed control algorithm.

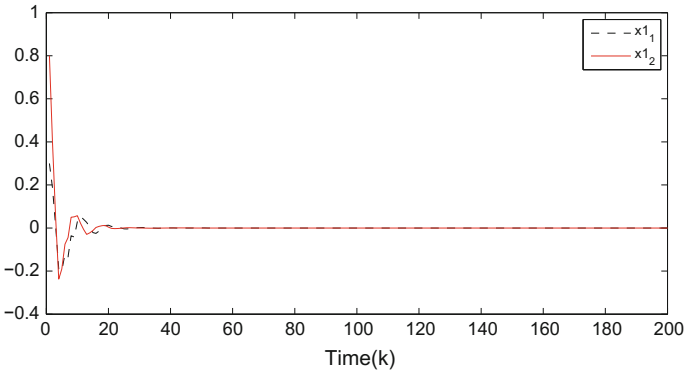

Fig. 14.3 State trajectories of subsystem 1

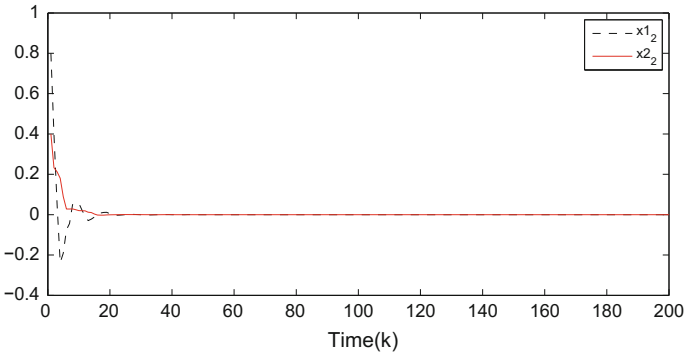

Fig. 14.4 State trajectories of subsystem 2

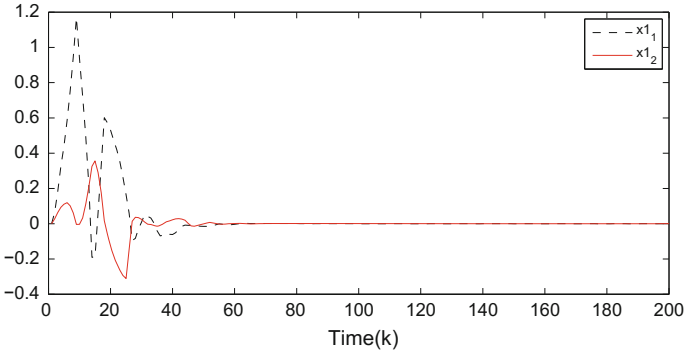

Fig. 14.5 State trajectories of subsystem 1

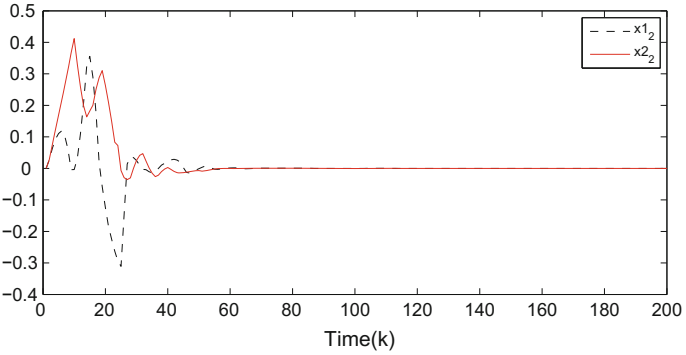

Fig. 14.6 State trajectories of subsystem 2

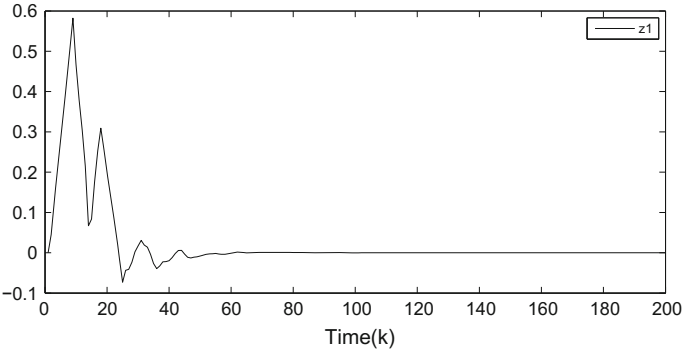

Fig. 14.7 Trajectories of performance output 1

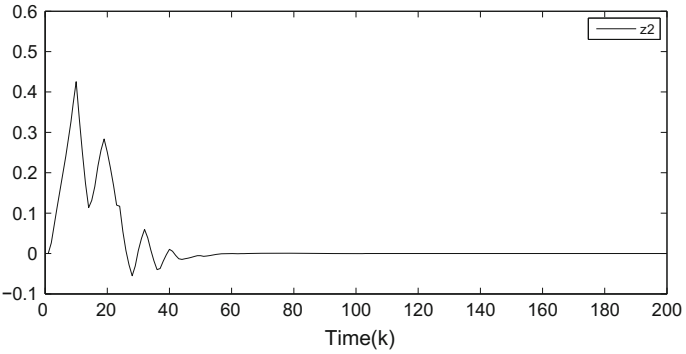

Fig. 14.8 Trajectories of performance output 2

14.5 Conclusions

We have investigated the distributed control problem for a class of large-scale system with communication constraints and topology switching. Strategies such as event-based communication and logarithmic quantization have introduced to reduce the transmitted information. A set of asynchronous controllers have been designed to deal with the difficulty that the topology information can not be accessed in time by the controller. Based on the Lyapunov direct method and the switched system approach, a sufficient condition has been proposed such that the closed-loop system is exponentially stable in the mean-square sense and achieves a prescribed H_∞ disturbance attenuation level. The well-known CCL algorithm has been borrowed for the controller gain design. Finally, a simulation study has been given to demonstrated the effectiveness of the proposed controller design algorithm.

References

1. K.W. Hedman, S.S. Oren, R.P. Neill, A review of transmission switching and network topology optimization, in *Proceeding of the IEEE Power and Energy Society General Meeting* (2011), pp. 1–7
2. Y.W. Wang, H.O. Wang, H.W. Xiao, Z.H. Guan, Synchronization of complex dynamical networks under recoverable attacks. Automatica **46**(1), 197–203 (2010)
3. D. Xue, A. Gusrialdi, S. Hirche, Robust distributed control design for interconnected systems under topology uncertainty, in *Proceeding of the American Control Conference* (2013), pp. 6541–6546
4. Y. Xu, R.Q. Lu, H. Peng, K. Xie, A.K. Xue, Asynchronous dissipative state estimation for stochastic complex networks with quantized jumping coupling and uncertain measurements, in *IEEE Transactions on Neural Networks and Learning Systems*. doi:10.1109/TNNLS.2015.2503772